FACILE CHEMICAL STRATEGIES FOR THE PREPARATION OF MULTIWALLED CARBON NANOTUBE-BASED COMPOSITE ELECTRODES FOR SENSING APPLICATIONS

Thesis submitted to the University of Calicut in partial fulfilment of the requirements for the degree of

DOCTOR OF PHILOSOPHY IN CHEMISTRY

in the Faculty of Science

By

RESHMA M.

Under the guidance of

Dr. MANU R.

Research and PG Department of Chemistry

Sri Vyasa N.S.S. College, Wadakkanchery

(Affiliated to the University of Calicut)

Thrissur, Kerala, 680623

February 2024

SRI VYASA N.S.S COLLEGE

Affiliated to University of Calicut and Reaccredited by NAAC with B Grade

VYASAGIRI P.O, WADAKKANCHERY THRISSUR, KERALA - 680623

OFFICE: 04884-237249, PRINCIPAL : 6238139722

Website: www.srivyasanss.ac.in, Email: mail@srivyasanss.ac.in

30/08/2024

CERTIFICATE

Certified that the thesis entitled **"FACILE CHEMICAL STRATEGIES FOR THE PREPARATION OF MULTIWALLED CARBON NANOTUBE-BASED COMPOSITE ELECTRODES FOR SENSING APPLICATIONS"**, submitted by **Ms. Reshma M.** is an authentic record of research work carried out by her under my direct supervision and guidance at the Research and Post Graduate Department of Chemistry, Sri Vyasa N.S.S. College, Wadakkanchery, in fulfillment of the requirements for the award of degree of Doctor of Philosophy in Chemistry of the University of Calicut. I also certify that no corrections/modifications have been recommended by the adjudicators in the thesis and the content of the thesis in both hard copy and soft copy are one and same.

Wadakkanchery

Dr. Manu R.
(Research guide)
Assistant Professor and HOD
Research and PG Department
of Chemistry
Sri Vyasa N.S.S. College
Wadakkanchery

SRI VYASA N.S.S COLLEGE
No.....
Date.....
VYASAGIRI

Dr. MANU.R
PEN: 748132
Assistant Professor & Head
PG & Research Department of Chemistry
Sri Vyasa NSS College,
Wadakkanchery, Thrissur-680 623

SRI VYASA N.S.S COLLEGE

Affiliated to University of Calicut and Reaccredited by NAAC with B Grade

VYASAGIRI P.O, WADAKKANCHERY THRISSUR, KERALA - 680623

OFFICE: 04884-237249, PRINCIPAL : 6238139722

Website: www.srivyasanss.ac.in, Email: mail@srivyasanss.ac.in

12-02-2024

CERTIFICATE

Certified that the thesis entitled **"FACILE CHEMICAL STRATEGIES FOR THE PREPARATION OF MULTIWALLED CARBON NANOTUBE-BASED COMPOSITE ELECTRODES FOR SENSING APPLICATIONS"**, submitted by **Ms. Reshma M.** is an authentic record of research work carried out by her under my direct supervision and guidance at the Research and Post Graduate Department of Chemistry, Sri Vyasa N.S.S. College, Wadakkanchery, in fulfillment of the requirements for the award of degree of Doctor of Philosophy in Chemistry of the University of Calicut, and further that no part of the same has been submitted anywhere for the award of any degree or diploma.

Wadakkanchery

Dr. Manu R.
(Research guide)
Assistant Professor and HOD
Research and PG Department
of Chemistry
Sri Vyasa N.S.S. College
Wadakkanchery

SRI VYASA N.S.S COLLEGE
No.....
Date.....
VYASAGIRI

Dr. MANU.R
PEN: 748132
Assistant Professor & Head
PG & Research Department of Chemistry
Sri Vyasa NSS College,
Wadakkanchery, Thrissur-680 623

DECLARATION

I hereby declare that the work presented in the thesis entitled **"FACILE CHEMICAL STRATEGIES FOR THE PREPARATION OF MULTIWALLED CARBON NANOTUBE-BASED COMPOSITE ELECTRODES FOR SENSING APPLICATIONS"** is based on the original work done by me under the guidance of Dr. Manu R., Assistant Professor and HOD, Research and Post Graduate Department of Chemistry, Sri Vyasa N.S.S. College, Wadakkanchery and has not been included in any other thesis submitted previously for the award of any degree. The contents of the thesis have gone through plagiarism check using iThenticate software at C.H.M.K. Library, University of Calicut, and the similarity index found within the permissible limit. I also declare that the thesis is free from AI generated contents.

Reshma M.

Wadakkanchery

12-02-2024

12/02/24

Dr. Manu R.

Dr.R. MANU
Assistant Professor
PG & Research Department of Chemistry
Sri Vyasa NSS College
Wadakkanchery, Thrissur - 680 623

Dedicated to My Parents,

My Family & My Mentor

ACKNOWLEDGEMENT

It was exhilarating to be on the path of research during the last few years of my life and I use this opportunity to express my sincere gratitude to all who encouraged and supported me in the fruitful completion of my thesis. First and foremost I would like to express my sincere gratitude towards my Research supervisor Dr. Manu R. Assistant professor and HOD, Research and PG Department of Chemistry, Sri Vyasa N.S.S. College, who have given me an opportunity to do research under his guidance. His patience, immense knowledge, unwavering support and encouragement, focused approach together with the constructive guidance throughout the work made the way for the successful completion of my dissertation. From the bottom of my heart, I thank him for the advices and motivations provided by him on my hardships that have aided me, back on the track of research. I strongly believe that the experience and guidance provided by him will benefit my future work and life.

I express my sincere gratitude to the doctoral committee members, Prof. Dr. P. Raveendran and Prof. Dr. Rajeev. S. Menon for their valuable suggestions and the comments for improving the research work. I also acknowledge other doctoral committee members Sri. P. E. Muhammed Abdul Rasheed, Dr. Suja Haridas for their valuable suggestions provided during the annual progress meetings of the research work.

I would like to acknowledge Dr. Geetha P , Principal, SVNSS Wadakkanchery and the former principal Mrs. Kavitha. K , their support and encouragement has helped me a lot in the path of research at SVNSS College.

I acknowledge CSIR, New Delhi, India for providing JRF and SRF fellowships during the research period. I also acknowledge DST-FIST, New Delhi for the financial assistance provided for the purchase of instruments needed to conduct research.

I am thankful to all the teachers of Research and PG Department of Chemistry, SVNSS College. I am immensely thankful to Dr. Nisha Nandakumar for her constant support and motivation, Dr. Rohini K.N for her advices and encouragement and Dr. Akhil. K. Nair for his help and timely assistance during the research period. I also thank Dr. Divya. A. S, Dr. Ragi. K, Ms. Nimya Sankar for their concern and amiable nature towards me during the research life. I am thankful to the lab staffs especially Sandeep and Smitha for their support. I would also like to acknowledge the former HOD Dr. G. Devika Rani for her advices.

I express my heartiest thanks to Dr. K. M. Devadas , Assistant professor and HOD, Department of Physics, SVNSS college for the kind co-operation and help rendered during my research work. I am thankful to the faculty of other departments also for their support.

I would like to acknowledge Dr. Jyothi. G. Nair, UGC Librarian , SVNSS College for her advices and encouragement. I express my gratitude to all the non-teaching and administrative staffs of SVNSS College for the timely dispersal official the procedures.

I would like to extend my thanks to Mrs. Aiswarya. P , my colleague who supported me in moving forward. I will cherish the beautiful moments that we spent together in research lab. I would like to acknowledge all my friends who have supported me during the entire research period.

I acknowledge CSIF, University of Calicut, SAIF-STIC, Cochin, CSIR-CECRI, Karaikudi, C-MET, Thrissur, Amrita Vishwa Vidyapeetham, Coimbatore, St. Thomas College, Thrissur, PSG institute of Advanced Studies, Coimbatore for extending help in doing various sample analysis.

I would like to thank Dr. Ambili. V. K, Assistant professor and HOD, and Dr. Priya.S, Assistant professor, Department of Chemistry, NSS College Nemmara for the motivation they have given me to step into research. I also thank all my teachers who have guided me in all my academic process.

Last but not the least, I would like to express my deepest sense of gratitude to my dearest parents, my father Mr. Muthukumaran. A (late) and my beloved mom, Mrs. Suseela. N (late). My mom has always been my support system for all my achievements throughout my life and her untimely demise during my research journey was irreparable. From the bottom of my heart I thank my brother Dr. Roshith. M, has been a pillar throughout my life. His unconditional support has provided me with confidence which was the driving force throughout the entire research journey. I express my sincere thanks to my mother-in-law, sister-in-laws, nephew and niece and all relatives who constantly supported me throughout.

From the bottom of my heart, I express my sincere gratitude to my companion Mr. Sajeesh. T and my daughter Saanvi. S whose untiring support and patience given me strength during the research journey. They have been my courage and sincerely saying, the fulfillment of this venture would not be possible without them. Their adaptable nature, unconditional love and support, the motivation and encouragement that they have provided has led me in successful completion of my thesis.

I genuinely thank all the personalities who directly or indirectly helped me in the path of research.

I trust and thank Almighty, the Supreme power who has showered blessings on me throughout my life.

Reshma M.

ABSTRACT

The thesis focuses on the development of different composites, based on MWCNT which finds application in various electrochemical sensing platforms. MWCNTs possess some excellent properties and this gets enhanced when metals or metal oxides are coalesced on to the CNT matrix. MWCNT composites of distinctive nature were fabricated by employing different noble metals like silver, palladium and ruthenium. Besides these metals certain metal oxides of tungsten, cobalt and iron are also incorporated. As different materials are successfully integrated, the newly formed MWCNT hybrids could possess some unique properties of all the materials that is being incorporated. More over surface functionalisation of MWCNTs provide more binding sites for the anchoring of metals and metal oxides. Further more such mild functionalisation technique can protect CNTs from structural damage also. The thesis elaborate on the fabrication of four distinct nanocomposites based on MWCNT and their usefulness in various applications. These include Ag/fMWCNT, Cu-WO_3-MWCNT, Pd@MWCNT-Co_3O_4 and RuO_2/Fe_3O_4/MWCNT composite electrode.

Ag/fMWCNT flexible films were fabricated through facile method in which silver is being deposited on to MWCNT films by electroless deposition process. The substrate employed in this work is PET, which is flexible and the fabricated electrode can be employed for sensing dopamine. Electrochemical methods like cyclic voltammetry, differential pulse voltametry and chronoamperometry were used to study the sensing behavior of the electrode towards dopamine. The LOD values were found to be 0.7 μM. The electrode also exhibited good pseudocapacitive behavior.

Another flexible film electrode Cu-WO_3-MWCNT utilized the techniques viz. electroless and electrodeposition process for its formation. Tungsten oxide was incorporated on to MWCNT matrix which was then deposited on to electroless copper substrate. The preliminary and qualitative sensing of ageing of lubricant oils was studied using this electrode. This was revealed by electrochemical impedance studies.

One another work reports on the development of Pd@MWCNT-Co_3O_4 film. The relevance of the electrode lies in the fact that cobalt oxide employed for the fabrication was recovered from spent lithium-ion battries. The cobalt was extracted from the used lithium ion batteries and then converted into oxide form and finally palladium incorporated MWCNT is being deposited on to Co_3O_4 film by

electrophoretic deposition process. The developed Pd@MWCNT-Co_3O_4 electrode was used as glucose sensor. The sensing behavior of the electrode towards glucose was revealed from the chronoamperometric studies and the limit of detection was found to be 0.6 μM.

Another composite electrode based on MWCNT is from RuO_2 and Fe_3O_4 mixed oxide. The composite was drop casted on to glassy carbon electrode and the sensing behavior of the composite towards simultaneous detection of ascorbic acid and dopamine was studied using cyclic voltammetry and differential pulse voltammetry. The limit of detection was found to be 1.12 μM for ascorbic acid and 0.11 μM for dopamine.

In brief, all the nanocomposite electrodes of MWCNTs fabricated were developed through different facile strategies that were found to have good sensing capability towards different analyte molecules. The procedures adopted for the fabrication process were simple and economical. The composites films were characterized by different analytical and instrumental methods. The sensing characteristics were studied using different electrochemical techniques. All the electrodes were found to be stable and reproducible.

Keywords

Multiwalled carbon nanotube

Composite electrodes

Sensing applications

Electrochemical sensing

സംഗ്രഹം

മൾട്ടിവാൾഡ് കാർബൺ നാനോ ട്യൂബ് (MWCNT) സംയുക്തങ്ങളുടെ നിർമ്മാണവും ഇലക്ട്രോ കെമിക്കൽ സെൻസിങ് മേഖലകളിൽ ഇവയുടെ ഉപയോഗവുമാണ് ഈ പ്രബന്ധത്തിൽ ഉൾപ്പെടുത്തിയിരിക്കുന്നത്. വളരെയധികം സവിശേഷതകളുള്ള MWCNT മെട്രിക്കിലോട്ട് ലോഹങ്ങളോ, ലോഹ ഓക്സൈഡുകളോ സംയോജിപ്പിക്കുമ്പോൾ കിട്ടുന്ന സംയുക്തത്തിന് ഗുണങ്ങൾ ഏറെയാണ്. ഉൽകൃഷ്ട ലോഹങ്ങളായ സിൽവർ, പലേഡിയം, റുഥീനിയം, ലോഹ ഓക്സൈഡുകളായ ടങ്സ്റ്റൻ, കോബാൾട്, അയേൺ എന്നിവ MWCNT യുമായി സംയോജിപ്പിച്ചാണ് വിവിധതരം MWCNT ഹൈബ്രിഡ് കോംപോസിറ്റുകൾ നിർമ്മിച്ചിരിക്കുന്നത്. വ്യത്യസ്ഥ ലോഹങ്ങളും ലോഹസംയുക്തങ്ങളും സംയോജിപ്പിച്ചതിനാൽ പുതിയതായി രൂപപ്പെട്ട MWCNT ഹൈബ്രിഡുകൾക്ക് സംയോജിപ്പിച്ച പദാർത്ഥങ്ങളുടെ തനതായ ഗുണങ്ങൾ ഉണ്ടായിരിക്കും. ലോഹങ്ങളെയും ലോഹസംയുക്തങ്ങളേയും ഉൾക്കൊള്ളുന്നതിനുള്ള ബൈൻഡിംഗ് സൈറ്റുകൾ നിർമ്മിക്കുവാനായി MWCNT യെ ശരിയായ രീതിയിലുള്ള ഫങ്ഷണലൈസേഷൻ നടത്തേണ്ടതുണ്ട്. MWCNT യുടെ നാല് വ്യത്യസ്ഥ നാനോ കോമ്പോസിറ്റുകളായ Ag/fMWCNT, Cu-WO_3-MWCNT, Pd@MWCNT-Co_3O_4, RuO_2/Fe_3O_4/ MWCNT കോംപോസിറ്റ് ഇലക്ട്രോഡ് എന്നിവയുടെ നിർമ്മാണവും പ്രായോഗികതയുമാണ് ഈ പ്രബന്ധത്തിൽ ഉൾപ്പെടുത്തിയിരിക്കുന്നത്.

ഇലക്ട്രോലെസ് ഡിപോസിഷൻ പ്രക്രിയയിലൂടെ സിൽവർ MWCNT ഫിലിമിലേക്ക് സംയോജിപ്പിച്ചാണ് Ag/fMWCNT ഇലക്ട്രോഡ് നിർമ്മിച്ചിരിക്കുന്നത്. ഇത്തരത്തിൽ നിർമ്മിച്ച ഇലക്ട്രോഡിന് ഡോപമിൻ സാന്നിധ്യം തിരിച്ചറിയാൻ കഴിയുമെന്ന് കണ്ടെത്തി. ഇലക്ട്രോകെമിക്കൽ അനലിറ്റിക്കൽ രീതികളായ സൈക്ലിക് വോൾട്ടാമെട്രി, ഡിഫറെൻഷ്യൽ പൾസ് വോൾട്ടാമെട്രി, ക്രോണോ ആംബ്രോമെട്രി എന്നിവയിലൂടെയാണ് ഇലക്ട്രോഡിന് ഡോപമിൻ സെൻസറായി പ്രവർത്തിക്കാൻ കഴിയുമെന്ന് കണ്ടെത്തിയത്. ലിമിറ്റ് ഓഫ് ഡിറ്റക്ഷൻ മൂല്യം 0.7 µM ആണെന്ന് കണ്ടെത്തി. ഇലക്ട്രോഡ് നല്ല സ്യൂഡോ കപ്പാസിറ്റീവ് സ്വഭാവവും പ്രകടിപ്പിച്ചു.

ഈ ഗവേഷണത്തിന്റെ ഭാഗമായി നിർമ്മിക്കാൻ കഴിഞ്ഞ മറ്റൊരു ഇലക്ട്രോഡായിരുന്നു Cu-WO_3-MWCNT. ഈ ഇലക്ട്രോഡ് നിർമ്മാണത്തിനായി ഇലക്ട്രോലെസ് ഡിപ്പോസിഷൻ, ഇലക്ട്രോ

ഡിപ്പോസിഷൻ ടെക്നിക്കുകളാണ് ഉപയോഗിച്ചത്. WO_3-MWCNT ഹൈബ്രിഡ് നിർമ്മിച്ച്, ഈ സംയുക്തത്തെ ഇലക്ട്രോലെസ് കോപ്പർ സബ്സ്ട്രേറ്റിലേക്ക് നിക്ഷേപിക്കുകയും ചെയ്തു. ഇലക്ട്രോ കെമിക്കൽ ഇംപീഡൻസ് സ്പെക് ട്രോസ്കോപ്പിക്ക് ടെക്നിക്കിലൂടെ ഈ ഫ്ലക്സിബിൾ ഇലക്ട്രോഡ് ഉപയോഗിച്ച് ലൂബ്രിക്കന്റ് ഓയിലുകളുടെ പ്രവർത്തനക്ഷമത പരിശോധിക്കാമെന്ന് കണ്ടെത്തി.

വളരെയേറെ പ്രയോജനപ്രദമായ Pd@MWCNT-Co_3O_4 ഇലക്ട്രോഡും ഈ ഗവേഷണ പ്രവർത്തനത്തിലൂടെ നിർമ്മച്ചെടുക്കാൻ സാധിച്ചു. ഈ ഇലക്ട്രോഡ് നിർമ്മാണത്തിന് ഉപയോഗിച്ച കൊബാൾട്ട് ഓക്സൈഡ് ഉപയോഗശൂന്യമായ ലിഥിയം അയോൺ ബാറ്ററികളിൽ നിന്ന് വീണ്ടെടുത്തതാണ്. ഉപയോഗശൂന്യമായ ബാറ്ററികളിൽ നിന്ന് കൊബാൾട്ട് വേർതിരിച്ചെടുത്ത് പിന്നീട് ഓക്സൈഡ് രൂപത്തിലേക്ക് പരിവർത്തനം ചെയ്തു. Pd@MWCNT ഇലക്ട്രോഫോറ്റിക് ഡിപ്പോസിഷൻ പ്രക്രിയയിലൂടെ Co_3O_4 ഫിലിമിലേക്ക് നിക്ഷേപിക്കുകയും ചെയ്തു. ഗ്ലൂക്കോസിന്റെ സാന്നിധ്യം തിരിച്ചറിയാനുള്ള സവിശേഷ ശേഷി ഈ ഇലക്ട്രോഡിനുണ്ടെന്ന് ക്രോണോ ആംപെറോമെട്രിക് പഠനത്തിലൂടെ കണ്ടെത്തി. ഗ്ലൂക്കോസിന്റെ ലിമിറ്റ് ഓഫ് ഡിറ്റക്ഷൻ മൂല്യം 0.6 µM ആണെന്ന് ഈ ഇലക്ട്രോഡിലൂടെ കണ്ടെത്താൻ കഴിഞ്ഞു.

അവസാനമായി പഠനം നടത്തിയ MWCNT സംയുക്തം, RuO_2/ Fe_3O_4/ MWCNT യാണ്. ഈ സംയുക്തത്തെ ഗ്ലാസ്സി കാർബൺ ഇലക്ട്രോഡിലേക്ക് (GCE) ഡ്രോപ്പ് കാസ്റ്റ് ചെയ്തു. അതിന്റെ ഫലമായി ലഭിച്ച RuO_2/ Fe_3O_4/ MWCNT/GCE ഇലക്ട്രോഡിന് ഒരേ സമയം ഡോപമിന്റെയും അസ്കോർബിക് ആസിഡിന്റെയും സാന്നിധ്യം തിരിച്ചറിയാൻ കഴിഞ്ഞു.

ഇതിനായി ഇലക്ട്രോകെമിക്കൽ ടെക്നിക്കുകളായ സൈക്ലിക് വോൾട്ടാമെട്രി, ഡിഫറൻഷ്യൽ പൾസ് വോൾട്ടാ മെട്രി ടെക്നിക്കും ഉപയോഗപ്പെടുത്തി . അസ്കോർബിക് ആസിസിൻ്റെ ലിമിറ്റ് ഓഫ് ഡിറ്റക്ഷൻ മൂല്യം 1.12 µM ഉം ഡോപമിന്റേത് 0.11 µM ആണെന്ന് കണ്ടെത്തി.

വൈവിധ്യമാർന്ന ടെക്നിക്കുകളിലൂടെ നിർമ്മിച്ച വ്യത്യസ്ഥ MWCNT ഹൈബ്രിഡ് ഇലക്ട്രോഡുകൾ വിവിധ പദാർത്ഥങ്ങളിലെ തന്മാത്രകളുടെ സാന്നിധ്യം തിരിച്ചറിയാനുള്ള സെൻസറുകളായി ഉപയോഗപ്പെടുത്താമെന്ന് കണ്ടെത്തി. ലളിതമായി നിർമ്മിച്ച ഈ ഇലക്ട്രോഡുകൾ കാര്യക്ഷമതയുള്ളതും പുന:ർനിർമ്മിക്കാവുന്നതുമാണ്.

PREFACE

The research work carried out here focus on different facile strategies adopted for the fabrication of distinct types of MWCNT composites which finds application in different sensing platforms. Carbon nano tubes (CNTs) are considered as the allotropes of carbon which is an intermediate between graphite and cages of fullerenes. Among the conductive carbon based nanomaterials, CNTs are used for wide variety of applications. This is due to its excellent properties which include weightlessness, high specific area, small size, bio-compatibility and excellent thermal and chemical stability. Based on the number of cylindrical walls CNTs are again classified as SWCNTs and MWCNTs. Among the above two classification, MWCNTs are dominant over SWCNTs due to several reasons which include excellent stability, more ease of mass production, low cost and easy functionalization. MWCNTs finds use in various fields like additive manufacturing technology, field emitters, electromagnetic absorbing materials, catalysts for various chemical reactions, lithium battery anodes, energy conversion and energy storage devices, nano composites, super capacitors, nano probes, drug delivery platforms and also sensors. The research work dealt with fabrication of different types of MWCNT composites embedding different metals and metal oxides. These specific composites find application in sensing various analytes. The preparations of nanocomposites were found to be simple and economic. The main objectives of the thesis include fabrication of MWCNT based hybrid nano composites that can be utilised in various non enzymatic sensing platforms. The research focussed on electrochemical sensing of various types of analyte molecules using the synthesised MWCNT composite electrodes. MWCNTs were properly functionalised for the fabrication of these mentioned composites. Acid functionalisation method was adopted for the functionalisation of MWCNT and this could improve the dispersibility of MWCNT. For the development of various MWCNT composite electrode materials different metals and metal oxides are being incorporated into MWCNT matrix. The metals mainly included silver, copper, palladium and metal oxides used in fabrication of different composite electrodes are oxides of cobalt, tungsten, ruthenium and iron. The thesis deals with the sensor application of four different MWCNT composites. These include Ag/fMWCNT electrode, Cu-WO_3-fMWCNT composite film electrode, Pd@MWCNT-Co_3O_4 electrode and RuO_2/Fe_3O_4/MWCNT composite. The fabricated

MWCNT hybrid composites were characterised using different analytical and electrochemical techniques. The flexible Ag/fMWCNT electrode fabricated through benign reducing agent was capable of sensing dopamine and also exhibited excellent limit of detection. The fabricated flexible film also exhibited good pseudocapacitive behaviour. Another MWCNT Composite film electrode was fabricated by incorporating WO_3/MWCNT composite on to copper substrate and this sensor was used for studying ageing of lubricant oils. A glucose sensor fabricated using Co_3O_4 electrode in which palladium incorporated MWCNT is being deposited using electrophoretic deposition. In this work Co_3O_4 has been recovered from spent lithium-ion batteries and the developed Pd@MWCNT-Co_3O_4 electrode was used as a non-enzymatic glucose sensor. The ternary composite electrode based on RuO_2/Fe_3O_4/MWCNT could simultaneously detect both dopamine and ascorbic acid.

The entire work of the Ph.D. thesis has been structured into nine chapters.

Chapter-1 deals with the various types of carbon nano materials. A short description of various carbon nanomaterials including fullerenes, carbon nanotubes, graphene, carbon nanodiamonds, carbon nano horns, carbon dots, carbon nano fibres and carbon black are detailed in this chapter. A comprehensive description of carbon nanotubes which include different types of CNTs, synthesis methods, important properties, purification techniques together with functionalisation methods are discussed in Chapter 1.

The literature survey dealing with the importance of MWCNT hybrid composite in various domains is discussed in Chapter-2. The exclusive review of research on MWCNT focus on potential application of MWCNTs and their composites. This chapter also highlights on the properties of MWCNT composites for sensing various analyte molecules.

The common experimental methods adopted for the research work are highlighted in Chapter-3. The fabrication techniques of different MWCNT-based hybrids and the characterization techniques adopted to study the synthesized hybrid composites have been outlined in this chapter.

Chapter-4 discusses on process fabrication of flexible Ag/fMWCNT electrodes using benign reducing agent and its application as a dopamine senor. The method of

preparation is facile and cost-effective. The electrochemical techniques were adopted for the sensor characterization. The method includes chronoamperometric technique and differential pulse voltammetry. The sensor possessed good reproducibility, excellent stability and has very good limit of detection.

The application of flexible Cu-WO_3-MWCNT film electrode as a sensor for studying ageing characteristics of lubricant oils is discussed in Chapter-5. The flexible Cu-WO_3-MWCNT electrode was fabricated using electrochemical deposition process viz. electroless and electrophoretic deposition. The fabricated film exhibited good sensing behavior for determining aging characteristics of lubricant oil as revealed by the impedance studies.

Chapter-6 portrays on the development of a glucose sensor. The Pd@MWCNT-Co_3O_4 composite electrodes were employed for non-enzymatic detection of glucose molecules. The beauty of the experiment lies in the fact that the cobalt oxide used in the fabrication of the composite is recovered from spent Li-ion batteries. The electrochemical response of the modified electrode towards non-enzymatic glucose sensing was studied using the cyclic voltammetry and chronoamperometry. The nanocomposite electrode possessed superior sensing behaviour along with excellent stability, selectivity and good reproducibility. The results revealed the potential usefulness of spent materials from batteries for developing various systems for myriad applications.

One other piece of work delves into fabrication of MWCNT composite prepared as a ternary composite of RuO_2/Fe_3O_4/MWCNT/GCE which could detect both dopamine and ascorbic acid simultaneously and this is highlighted in Chapter-7. MWCNT provided numerous sites for the incorporation of metal oxides of iron and ruthenium. The electrochemically stable nano composites provided valid results in detection of both the analytes as revealed from cyclic voltammetric and differential pulse voltammetric studies.

The entire work done is concisely summarized in Chapter 8. All the developed nanocomposites were found to be ideal candidates for executing their role in the electrochemical sensing field. Future scope of the synthesised MWCNT composites is detailed in Chapter 9.

ABBREVIATIONS

0D-NMs	Zero Dimensional Nano materials
1D-NMs	One Dimensional Nano materials
2D-NMs	Two Dimensional Nano materials
3D-NMs	Three Dimensional Nano materials
AA	Ascorbic acid
AFM	Atomic Force Microscope
ATR	Attenuated total reflection
CA	Chrono-amperometry
CB	Carbon Black
CCVD	Catalytic Chemical Vapour Deposition
CDs	Carbon Dots
CNFs	Carbon Nano fibres
CNHs	Carbon Nano horns
CNMs	Carbon-Based Nano materials
CNTs	Carbon Nano tubes
CPDs	Carbonized Polymer Dots
CQDs	Carbon Quantum Dots
CTAB	Cetyl trimethyl ammonium Bromide
CV	Cyclic Voltammetry
CVD	Chemical Vapour Deposition
DA	Dopamine
DFAFC	Direct Formic Acid Fuel Cell
DLC	Diamond-like Carbon
DMFC	Direct Methanol Fuel Cells
DPV	Differential Pulse Voltammetry
DSSCs	Dye Sensitized Solar Cells
EDLCs	Electrochemical double- layer capacitors
EDX	Energy Dispersive X-ray Diffraction
EFM	Electrostatic Force Microscope

EIS	Electrochemical Impedance Spectroscopy
EM	Electromagnetic
EMA	Electromagnetic wave absorption
EPD	Electrophoretic Deposition
ESs	Electrochemical super capacitors
FESEM	Field emission scanning electro microscopy
fMWCNT	Functionalised Multi walled Carbon Nano Tubes
FTIR	Fourier - Transform Infrared
FTO	Fluorine-doped Tin Oxide
GCD	Galvanostatic Charge-Discharge
GCE	Glassy Carbon Electrode
GQDs	Graphene Quantum Dots
HER	Hydrogen Evolution Reaction
HFCVD	Hot Filament Chemical Vapour Deposition
ITO	Indium-doped Tin Oxide
LCDs	Liquid Crystal Displays
LOD	Limit of Detection
MEMS	Micro-Electro Mechanical System
MPECVD	Microwave Plasma Enhanced Chemical Vapour
MPM	Molecular Precursor Method
MWCNTs	Multiwalled Carbon Nano tubes
NCD	Nano crystalline diamond
NEMS	Nano electromechanical system
NMP	N-methyl pyrrolidone
OER	Oxygen Evolution Reaction
OLED	Organic Light emitting devices
PBS	Phosphate Buffer Solution
PDMS	Poly dimethyl Siloxane
PECVD	Plasma Enhanced Chemical Vapour Deposition
PEMFCs	Polymer Electrolyte Membrane Fuel Cells
PEN	Polyethylene Naphthalene
PET	Polyethylene Terephthalate

PNDs	Particulate Nano diamonds
PV	Photo Voltaic
PVC	Poly Vinyl Chloride
RFCVD	Radio Frequency Chemical Vapour Deposition
RSD	Relative Standard Deviation
SC	Sodium Collate
SCE	Saturated Calomel Electrode
SDBS	Sodium Dodecyl Benzene Sulfonate
SDS	Sodium Dodecyl Sulphate
SEM	Scanning Electron Microscopy
SLS	Sodium Ligno sulfonate
SPR	Surface Plasmon Resonance
STM	Scanning Tunnelling Microscope
SWCNTs	Single-Walled Carbon Nano tubes
TAN	Total Acid Number
TBN	Total Base Number
TCFs	Transparent Conductive Films
UV-Vis	Ultra violet-Visible

CONTENTS

Page No.

CHAPTER 1

INTRODUCTION

1.1. CARBON-BASED NANOMATERIALS (CNMs)

The tetravalency and catenation ability of carbon makes it unique comparing other elements. These carbon atoms can undergo different types of hybridization viz. sp, sp^2 and sp^3. Diamond and graphite are the two widely known allotropic forms of carbon. Contemporary research delves into modification of carbon based nano structures for application in various fields. The unusual properties of carbon-based nanomaterials widens the scope of research which leads to discovery of superior materials. Carbon nanomaterials (CNMs) can be classified into various categories based on the dimensions of the particles and also based on their geometrical structure. The CNMs exhibit various shapes which include horns (carbon nanohorns), tubes (carbon nanotubes), and spherical or ellipsoid shapes (fullerenes) [1,2]. Based on the dimensions, these materials are again classified into zero dimensional nanomaterials (0D-NMs), one dimensional nanomaterials (1D-NMs), two dimensional nanomaterials (2D-NMs) and three-dimensional Nanomaterials (3D-NMs). Fullerenes and carbon dots are included in the class of 0D-NMs, carbon nanofibres, carbon nanotubes, and diamond nanoplatelets come under the category of 1D-NMs, graphene, graphite sheets, and diamond nanoplatelets have been categorized into 2D-NMs and 3D-NMs include nanocrystalline diamond and nanostructured diamond-like carbon. The different forms of carbon nanoallotropes are shown in Figure-1.1 and Figure-1.2.

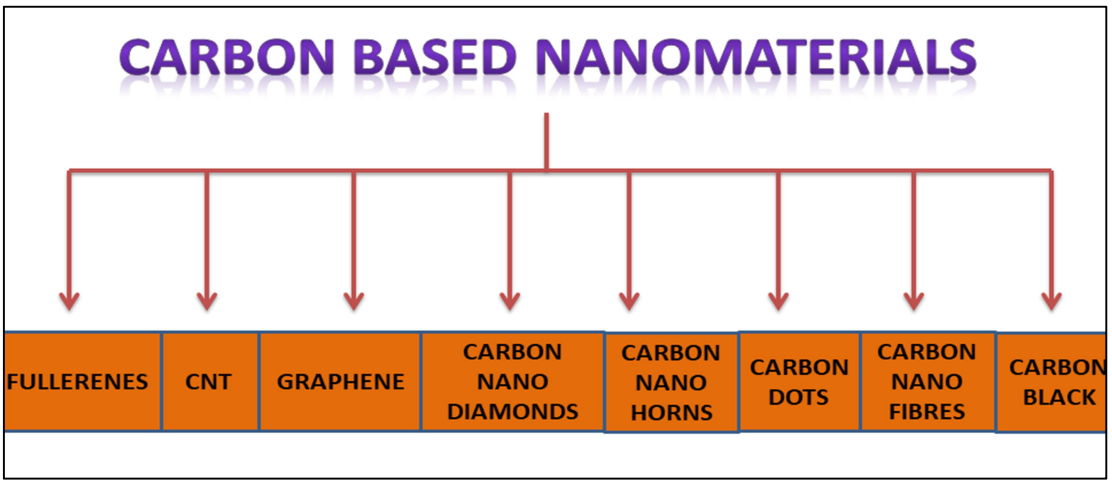

Figure-1.1. Classification of carbon based nanomaterials.

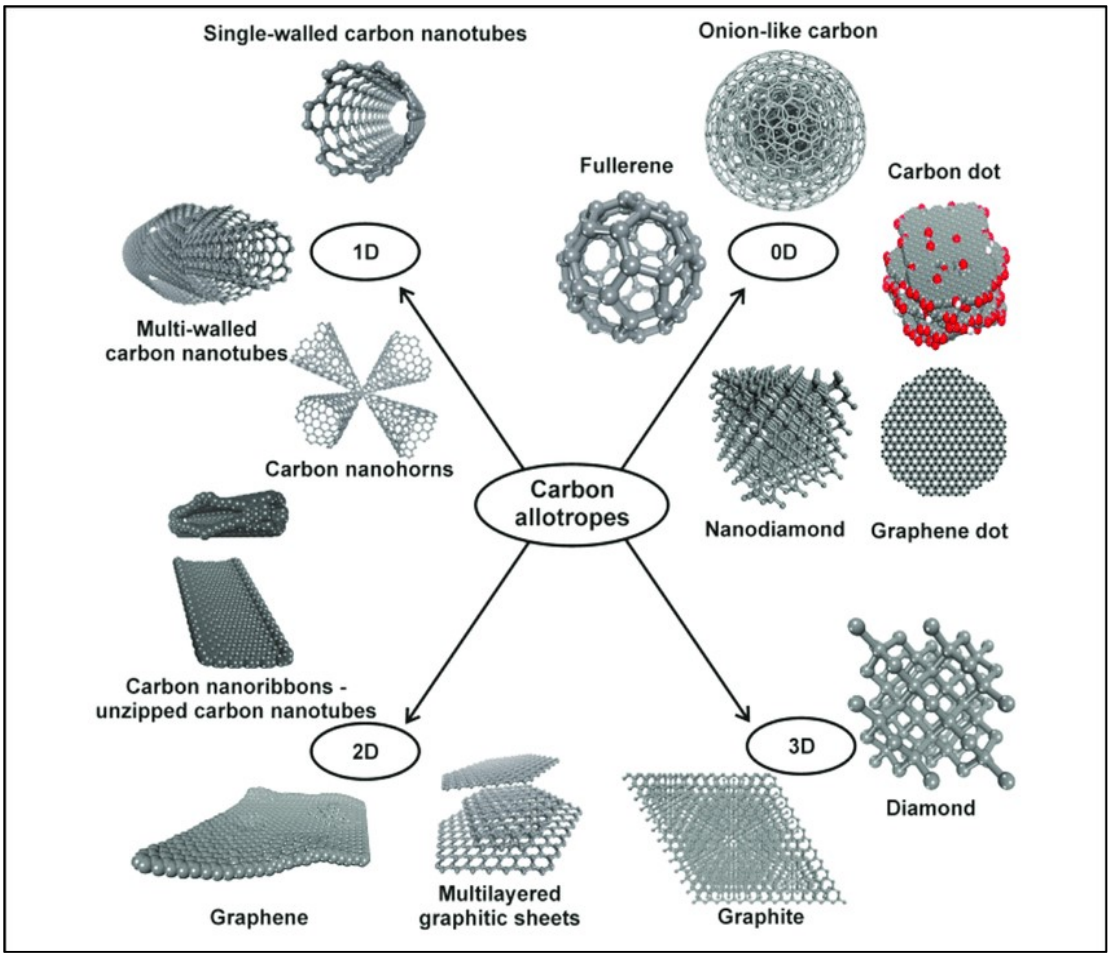

Figure-1.2. Classification of carbon nano allotropes based on different dimensions [3]. (Copyright 2015, American Chemical Society)

1.1.1. Fullerenes

Fullerenes are one of the allotropic modifications of carbon invented in 1985 by H. W. Kroto, R. F. Curl, and R. F. Smalley [4]. The carbon atoms in fullerenes are sp^2 hybridized. The Fullerene family was formed with atomic Cn clusters (n>20), comprising pentagonal and hexagonal faces. The extensively studied fullerene is C_{60} in which there are 12- five-membered rings and 20 six membered rings. Fullerene has a diameter of 0.7 nm [5]. Fullerenes are found in the soot of flames produced during combustion [6]. The synthesis of fullerenes mainly includes sputtering, electric arc discharge, and electron beam ablation methods [7]. The application of fullerenes in the medical field mainly includes cancer therapies, gynecological malignancies, and MRI [8,9].

1.1.2. Carbon Nanotubes

Carbon nanotubes (CNTs), discovered by S.Iijima in 1991 is one of the allotrophic modification of carbon with sp^2 hybridized carbon atoms. CNTs are rolled-up graphene sheets in cylindrical or tubular forms having diameter in nanometers. CNTs are further classified as single-walled carbon nanotubes (SWCNTs) and multiwalled carbon nanotubes (MWCNTs). The diameter of SWCNTs is around 1-3 nm and those of MWCNTs range from 5-25 nm with length of around 10 microns [10,11]. Chemical vapour deposition (CVD), Carbon arc discharge and laser ablation methods are commonly employed for synthesizing CNT. Due to the excellent features of these nanotubes, they find applications in sensing platforms, nano-electromechanical systems and biomedical applications [12–14].

1.1.3. Graphene

In 1947, P. R. Wallace identified graphene and later A. Geim and K. Novoselov carried out further investigation of the sample. Graphene is a 2D allotrophic form of carbon with carbon atoms in sp^2 hybridization. The interatomic distance between carbon hexagons is 0.142 nm. Graphene can be modified into other allotropic forms of carbon. If graphene is wrapped up 0D fullerenes are formed, if rolled up it forms 1D nanotubes and if stacked up 3D graphite is formed. This is shown in the Figure-1.3 [15,16]. The synthesis method employed for the fabrication of layered graphene includes solvo-thermal production, liquid phase exfoliation, CVD peeling off from graphite and also other techniques [17,18]. Graphene finds its application in electrochemical sensors, photo-catalytic materials etc. due to its unique characteristics [19,20].

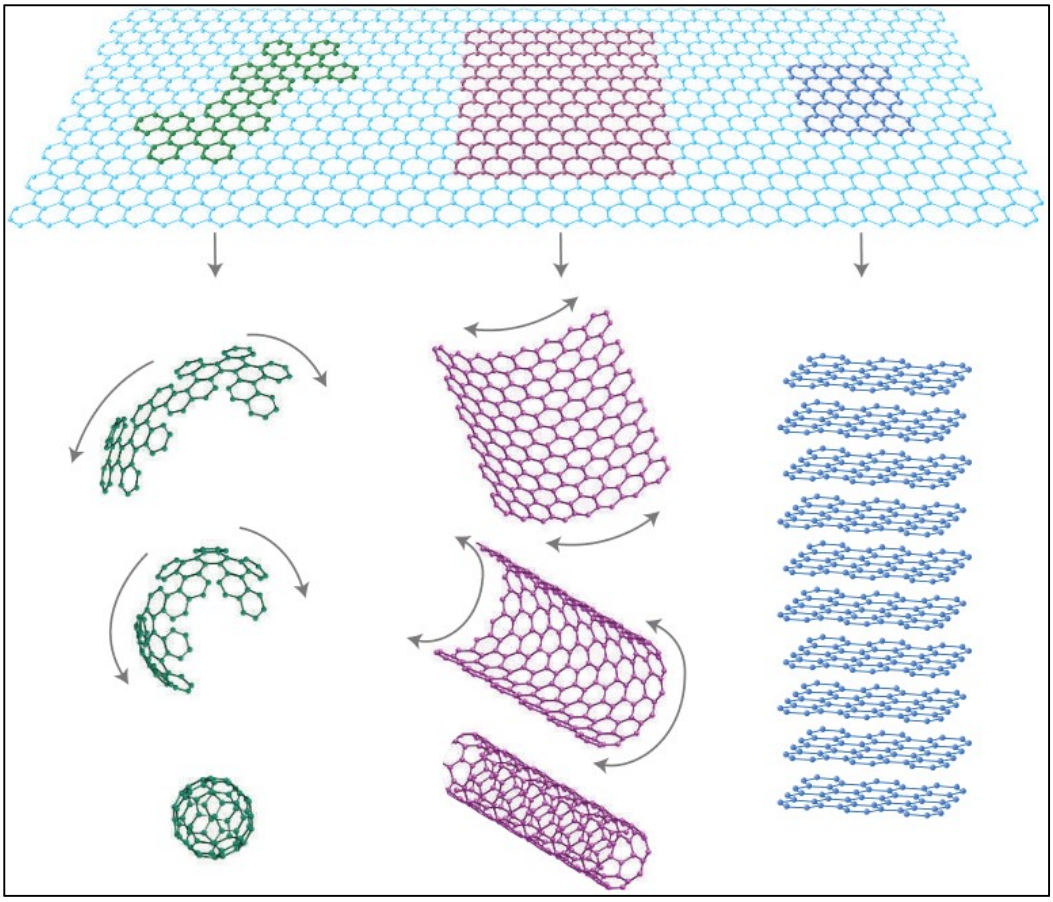

Figure-1.3. Different forms of graphene [16] (Copyright (2007)

1.1.4. Carbon Dots

Carbon dots (CDs) are the new class of materials in the carbon family with the size of carbon atoms below 10 nm. These zero-dimensional materials possess significant properties. Carbon dots possess excellent photoluminescence and their small size, low toxicity, and biocompatibility make them important in the area of biosensing [21,22]. The synthesis method mainly involves hydrothermal methods, pyrolysis, electrochemical methods etc. [23,24]. Based on the mechanism of formation and the properties, carbon dots are classified as carbon quantum dots (CQD), graphene quantum dots (GQDs), and carbonized polymer dots (CPDs) [25].

1.1.5. Carbon Nanofibres

Carbon nanofibres (CNFs) are wire-shaped nanostructures. The diameter of nano fibers varies between 10 to 500 nm. The synthesis method of CNFs mainly includes plasma enhanced chemical vapour deposition, thermal chemical vapour

deposition, and electrospinning methods [26–28]. CNFs are used for electrochemical sensing applications due to their excellent properties like large surface area, good electrical conductivity, and biocompatibility.

1.1.6. Carbon Nanodiamonds

Carbon nanodiamonds are nanoparticles exhibiting properties similar to diamonds and can exist in various forms like nanocrystalline diamond (NCD) films, nanostructured diamond-like carbon (DLC) films, and particulate nanodiamonds (PNDs) [29]. Nanodiamonds are formed by detonation. The CNDs display fluorescence properties and hence can be used as biomarkers and in bio-labeling studies [30].

1.1.7. Carbon Nanohorns

Carbon nanohorns (CNHs) consist of sp^2-bonded carbon atoms and exist as closed cages. It is also known as nanocones consisting of a diameter ranging from 2-5 nm and length ranging from 40−50 nm [31]. The synthesis method mainly includes arc discharge, laser ablation, and joule heating method [32, 33]. CNHs find their use as drug carriers, biosensors, supercapacitors, dye-sensitized solar cells etc.

1.1.8. Carbon Black

The combustion of petroleum products yields Carbon black (CB). They are spherical nanoparticles of size varying from 3.0 to 100 nm. The carbon black nanoparticles can be prepared by thermal plasma process [34]. The presence of sp^2 hybridized carbon atoms makes carbon atoms to functionalize with different biomolecules on the surface. This could find applications in the field of bio-sensing and electrochemical sensing applications [35].

1.2. CARBON NANOTUBES

Carbon nanotubes (CNTs) are quasi-one-dimensional straight tubes that resemble graphene in most of its physical properties. Carbon atoms in CNTs are sp^2 hybridized and have cylindrical structure formed from the rolled up graphene sheets. A σ- π rehybridization occurs due to strong curvature of carbon nanotubes resulting in three σ bonds to be located slightly out the plane and due to this π orbital getting

more delocalized outside the tube. This is the reason why CNTs possess excellent electrical, thermal and conducting properties than graphite.

CNTs can exist as single-walled carbon nanotubes (SWCNT) and multiwalled carbon nanotubes (MWCNT). Iijima invented MWCNT in 1991 and SWCNT in 1993 [10]. SWCNT consists of a single well and the wall of the nanotube consists of only one graphene layer thickness having a diameter varying between 0.4 and 2 nm. They may also be called as graphene nanotubes. MWCNT consists of concentric SWCNT in which multiple layers of graphene are rolled up to form a tube shape with a diameter ranging from 2 to 100 nm [36]. Besides SWCNT and MWCNT, there exist polymerised SWCNT, nanotorus, and nanobuds [37]. The hardness of polymerized SWCNT is compared to diamond. They are formed when many SWCNTs get coiled. Nanotorus CNTs is a kind of zero-dimensional CNT-based structure in which carbon nanotubes are bend into torus shaped or possess a donut shape. These are also known as carbon nanoring and possess high magnetic moment [38]. Carbon nanobuds are novel fullerene-CNT hybrid nanostructure in which fullerenes gets attached to the outer surface of CNTs by covalent bonds [39]. These five different types of CNTs classified based on structure are shown in Figure-1.4.

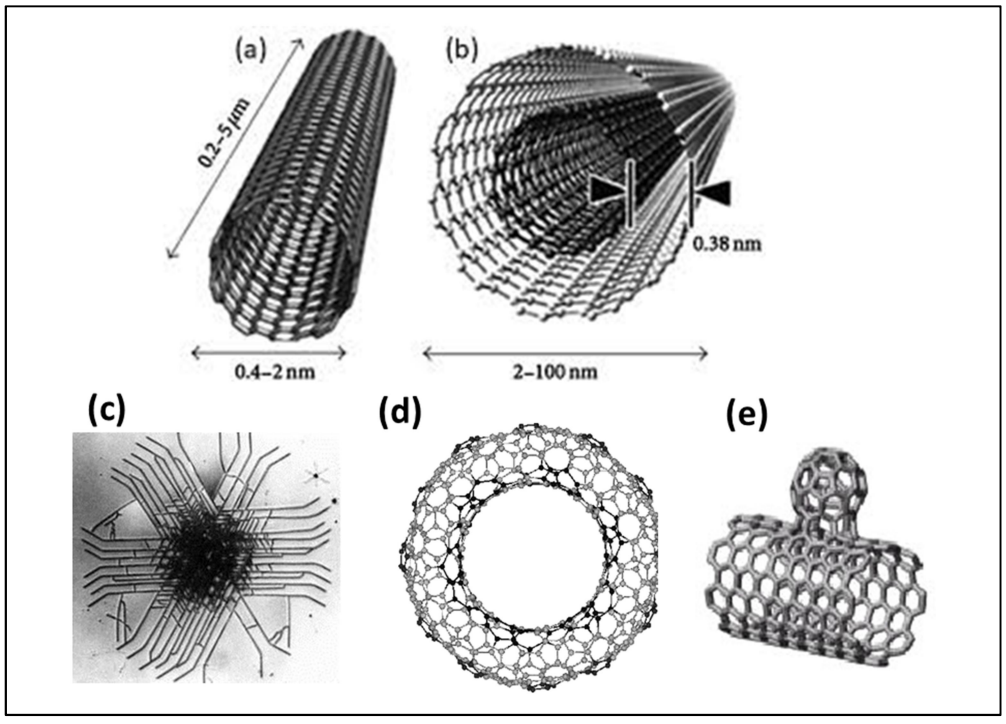

Figure-1.4. Diagrams of (a) Single-walled CNTs (SWCNTs) and (b) Multi-walled CNTs (MWCNTs) (c) Polymerised SWCNT (d) Nanotorus (e) Nanobuds (36,37).

Graphene sheets can be rolled to into form tubular structures in three distinct ways depending upon the direction, which determine the unique properties of single-walled carbon nanotubes. These include armchair, zigzag, and chiral as shown in Figure-1.5. The chiral vector $\overrightarrow{Ch}$ determines the circumference of the CNTs. It is also known roll-up vector and is defined by $C_h = na_1 + ma_2$ (where n and m are integers and a_1 and a_2 are graphite lattice vectors). A (m,n) carbon nanotube can be visualized by rolling up of graphene sheet in such a way that the tip of the chiral vector touches its tail. This criterion determines the existence of three distinct forms of nanotubes [40,41]. If m=0, CNTs form a zig-zag structure. If m=n then the armchair structure is formed whereas m≠n makes the chiral form of CNT. The above structures are also classified based on chiral angles [42]. If chiral angle Θ=0 then zig-zag structures are formed and if Θ=30 armchair structures are formed. Chiral nanotubes correspond to 0 <Θ< 30°.The properties of the nanotube change from metallic to semiconducting depending upon the change in chiral vectors. Armchair CNTs display metallic properties whereas other arrangements of CNTs exhibit semiconducting properties. The ends of MWCNT are closed by half-fullerene molecules which are dome-shaped and they appear to be straight whereas SWCNT tends to form bundles.

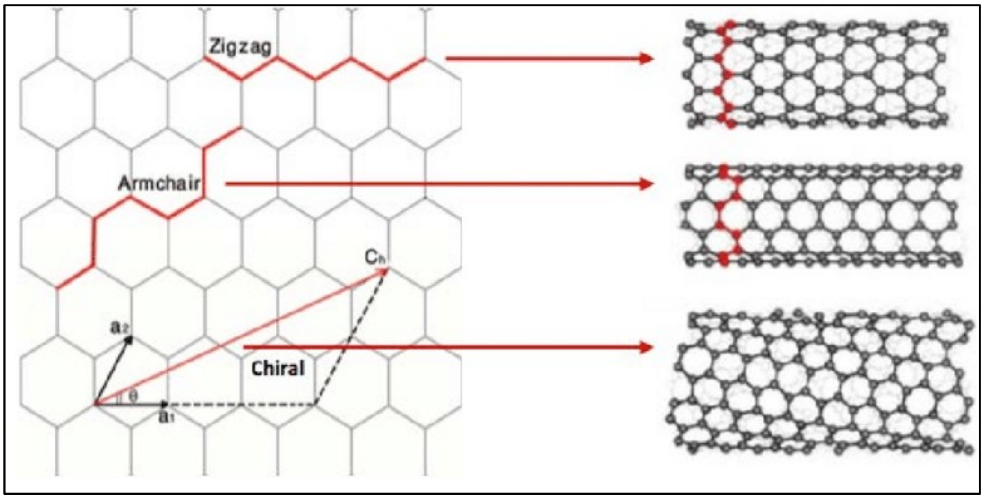

Figure-1.5. Schematic diagram showing armchair, zigzag, and chiral forms of carbon nanotubes [39].

The diameter (D) of the carbon nanotube is given by $D = |C_h|/\Pi = a\sqrt{n^2+nm+m^2}/\Pi$. Chiral angle (Θ) is given by $\Theta = \sqrt{3}m / \text{Tan}\ (m+2n)$. Thus structures of SWCNT and MWCNT can be generated by using lattice constant and inter-tube spacing.

Two structural models are commonly used to relate MWCNT. These include the Parchment model and the Russian doll model. If the graphene sheet is wrapped in such a way that it resembles a rolled newspaper then the model is termed as Parchment model and if graphite sheets are arranged in concentric layers then the model is referred to as the Russian Doll model [43]. Both models have been highlighted in Figure-1.6. A summary on the classification of CNTs [44] is given in Figure-1.7.

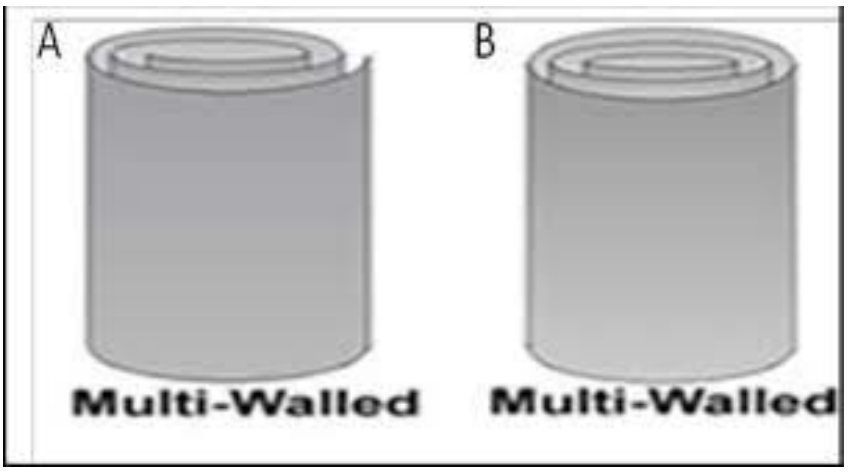

Figure-1.6. Two structural models of MWCNT (a) Parchment model and (b) Russian Doll model [40].

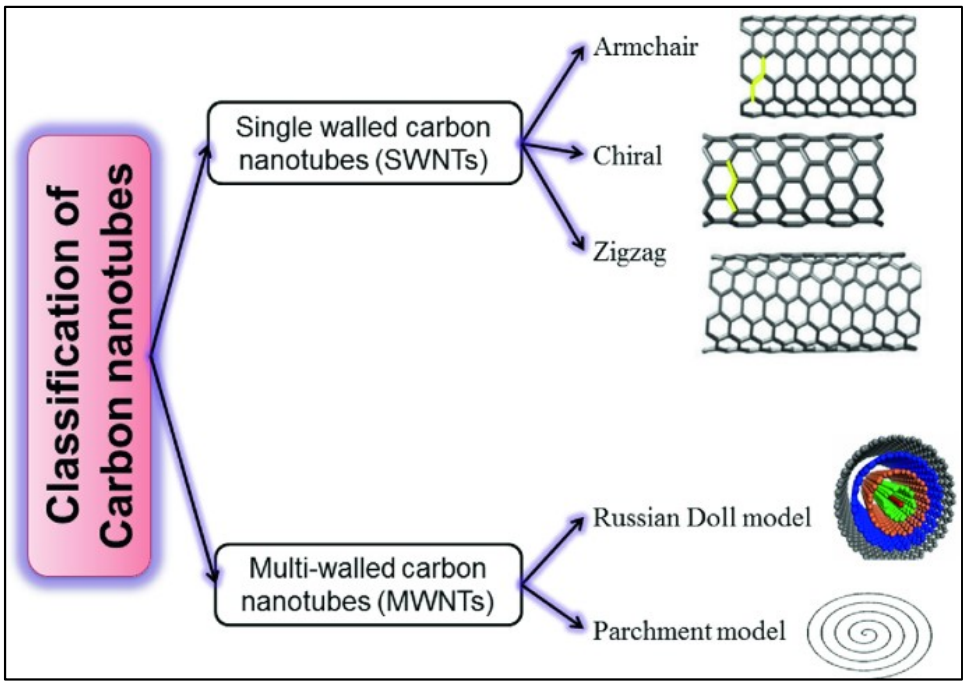

Figure-1.7. Summary of classification of CNTs [44].

1.2.1. SYNTHESIS OF CNTs

Different methods such as chemical vapour deposition, arc discharge process, hydrothermal method, pulsed laser deposition method and laser ablation method are employed for the synthesis of CNT. In these various processes, three methods are most commonly employed for the synthesis of CNT viz. arc discharge, laser ablation and chemical vapor deposition methods [45–47].

(a) Electric Arc Discharge

This is one of the most common methods used for the synthesis of SWCNTs and MWCNTs with only a few structural defects. Arc discharge setup mainly includes two graphite electrodes of high purity kept at an atmospheric pressure of 500 torr under a helium atmosphere. The electrodes are separated by a distance of 1-2 mm inside the chamber. A direct current of 50 to 100 A and a potential difference of nearly 20 V, develops a temperature greater than 3000 °C between the two electrodes which vaporizes carbon atoms. As a result, anode will get consumed and the evaporated carbon atoms get deposited on the cathode in the form of a 'cylindrical hard deposit or cigar-like morphology'. For the production of SWCNTs, the anode used is graphite doped with metal catalyst (Co, Ni, Fe etc.) and pure graphite as cathode. Pure graphite rods in the presence of hydrogen gas are used for the production of MWCNTs [48,49]. The CNTs synthesized using this method usually tend to be short and there is only little control over the alignment and this method requires purification.

(b) Laser Ablation

The laser ablation method is another promising method involved in the synthesis of carbon nanotubes. In this method graphite target kept inside a quartz tube under high temperature in an inert environment is vaporized by a high-power laser beam. The vaporized carbon species is swept along with flowing inert gas and the mixture is cooled to produce large clusters from which desired CNTs are produced. For the production of SWCNTs, a similar technique and principle are applied for laser ablation and arc discharge process. The only difference is that here a strong laser beam is made to strike the graphite target which holds a catalyst such as cobalt or nickel. The size and diameter of nano tube can be varied by tuning the laser

properties, nature of gas and its pressure, composition of the catalyst and its growth temperature [50–52]. The advantage of this method lies in the fact that low metallic impurities are being produced and the disadvantage of the laser ablation method is that the method is not so economical due to the requirement of pure graphite rods and high energy laser source.

c) Chemical Vapor Deposition

Chemical vapor deposition (CVD) is the most versatile and economical method for synthesizing CNTs. The different types of CVD techniques include- catalytic CVD (CCVD), microwave plasma enhanced CVD (MPECVD), radio frequency CVD (RFCVD), hot filament CVD (HFCVD), and water assisted CVD. CCVD is further classified as thermal CVD and plasma enhanced CVD (PECVD). The CVD process used for the synthesis of CNTs mainly includes two steps- preparation of catalyst particles on the substrate which is followed by the decomposition of carbon precursor resulting in the formation of nanotubes. Sputtering, physical vapor deposition and dip coating are mainly used for catalyst preparation. The substrate is finally heated in a carbon-rich environment (carbon sources mainly include carbon monoxide, methane, acetylene etc) at a temperature of 500-1000 ºC. By controlling the experimental parameters such as temperature, type of hydrocarbons used, catalyst type etc., we can produce CNTs in a variety of forms [53–56].

1.2.2. PURIFICATION OF CNT

Carbon nanotubes synthesized by various methods may contain a lot of impurities and this depends on the mode of synthesis. The purification process can be done through a gas phase, liquid phase and intercalation method to improve CNT purity. The impurities may include amorphous carbon, metal impurities, other carbonaceous particles etc. The unwanted large aggregates of graphite can be removed by filtration. Catalyst particles can be removed by dissolution in acidic solvents, fullerenes can be removed by organic solvents and amorphous carbon clusters are removed by chromatographic techniques. The air oxidation technique is used to remove amorphous carbon or polyhedral graphite-like particles from MWCNTs synthesized by the arc discharge technique. Surfactant-aided sonication,

size exclusion chromatography and ultrasonic assisted microfiltration are the commonly used nondestructive methods adopted for the separation of CNTs from amorphous carbon and catalytic impurities. Besides these techniques, fluorination, bromination, and density gradient ultra-centrifugation methods are also concomitantly applied for the purification process. The ultimate aim of the purification process is the production of clean CNTs which can be produced in a single step without loss of its inherent properties [57–61].

1.2.3. FUNCTIONALISATION OF CNTs

CNTs are ideal nanoscale materials that finds applications in numerous fields. However, the chemical inertness of CNT due to their sp^2 hybridized carbon atoms with the hexagonal network, makes them insoluble in almost all solvents and there limits its applications. Functionalization of CNTs is done to overcome these limitations and the most common functionalization methods include- covalent functionalization, defect group functionalization, non-covalent exohedral functionalization, and endohedral functionalization [62,63]. These are shown in Figure-1.8. Controlled functionalization of CNTs are still in dilemma and the solubility issues exist after all sort of functionalization methods .It is also noted that CNT functionalization result in fragmentation of nanotubules into smaller units and also change in hybridization occurring during functionalization techniques results in the disruption of π electron system which inturn results in change in the electrical and thermal properties of CNTs. Furthermore some of the reagents used for functionalization are not ecofriendly. So new researches focus on development of CNTs in which properties are not altered to a great extend.

(a) Covalent functionalization

Side wall halogenation is one of the covalent approaches for the functionalistaion of CNTs. These mainly include fluorination, chlorination and bromination and such coupling of halogen groups with carbon nanotubes makes it soluble in protic solvents [64,65]. Moreover, further substitution can be accomplished by replacing the fluorinated groups with alkyl groups [66]. Hydrogenated CNTs can be produced using glow discharge, proton bombardment or by carrying out birch reduction [67–69]. The attachment of various moiety through cyclo-addition reaction

has also been reported. The tubular CNTs can be functionalized by carbene [2+1] cycloaddition, nitrene [2+1] cycloaddition, 1,3 dipolar cycloaddition, Bingel [2+1] cyclopropanation reactions, Diels-Alder cycloaddition etc. [70–74]. Covalent functionalization of CNTs can be done by thermal and photochemical methods and also by nucleophilic and electrophilic addition reactions [75-78]. The chemical reactivity of nanotubes can be further enhanced by the addition of inorganic compounds which result in the formation of nanotube-metal complexes and also by ozonolysis reaction which yields CNT- ozonides [79,80]. Mechano-chemical functionalization which includes ball milling technique, glow discharge plasma activation technique and grafting of polymers onto the surface of CNTs are also some of the covalent functionalization approaches [81-83].

(b) Defect group functionalization

Defect sites created on the surface of CNTs serve as a base for further anchoring of other functional groups onto the CNT surface. The surface oxygenated functionalities can be attached to CNT surface by oxidative process. The oxidation also helps to remove the impurities like amorphous carbon which is usually produced during the synthesis process. The carboxylic functionalities can be further modified into acid chlorides, esters, amides, amines, porphyrins etc. [84–87]. The introduction of such groups makes CNTs soluble in various solvents and can be applied in various fields. The attachment of CNTs to biomolecules is another type of defect group functionalization by which different bio-electronic systems can be framed. Biomolecules can also provide an environment for further derivatization in CNT tubes. The carbon nanotubes can act as a nano connector which amplifies the electrical signals in the nanotube-enzyme system and by sensing proteins, DNA and other biomolecules [88–90]. Polymers can be grafted onto the defect sites of CNTs and hence these CNTs are found to be well-dispersed in common organic solvents [91–93].

(c) Non-covalent exohedral functionalization

CNTs form bundles that are held together strongly which makes it difficult to form a homogeneous dispersion. Noncovalent exohedral functionalization is one kind approach in which CNT bundles are exfoliated to prepare individual CNTs in which the electronic network of the tubes is retained. The widely used noncovalent wrapping

agents involved in the functionalization of CNTs include polymers, surfactants, polynuclear aromatic compounds and biomolecules [94-97]. Nanotube-polymer composites mainly include epoxy composites, hydrocarbon polymers, acrylates, conjugate polymers, polycarbonates, fluoro-polymers, polyvinyl alcohol, polyethylene glycol, silicon etc. Organic acids and their salts have been applied for CNT functionalization. Commonly used surfactants include sodium dodecyl benzene sulfonate (SDBS), sodium dodecyl sulfate (SDS), sodium collate (SC), cetyltrimethylammonium bromide (CTAB), benzethonium chloride, triton X-100, tween-80, sodium lignosulfonate (SLS). Physical methods are also adopted to prepare CNT dispersion which include ultrasonication, dielectrophoresis combined with mega sonification and plasma techniques [98].

(d) Endohedral functionalization

Endohedral filling of CNTs mainly involves trapping of different elements of appropriate sizes into the inner cavities of carbon nanotubes. These elements mainly include fullerenes and their derivatives, inorganic species, metallocenes, metals, metal-oxides, biomolecules, liquids etc. Such types of encapsulations on CNTs allow CNTs to find applications in a vast number of fields, since this type of functionalization results in combined properties of both CNTs and the encapsulated species [99–101].

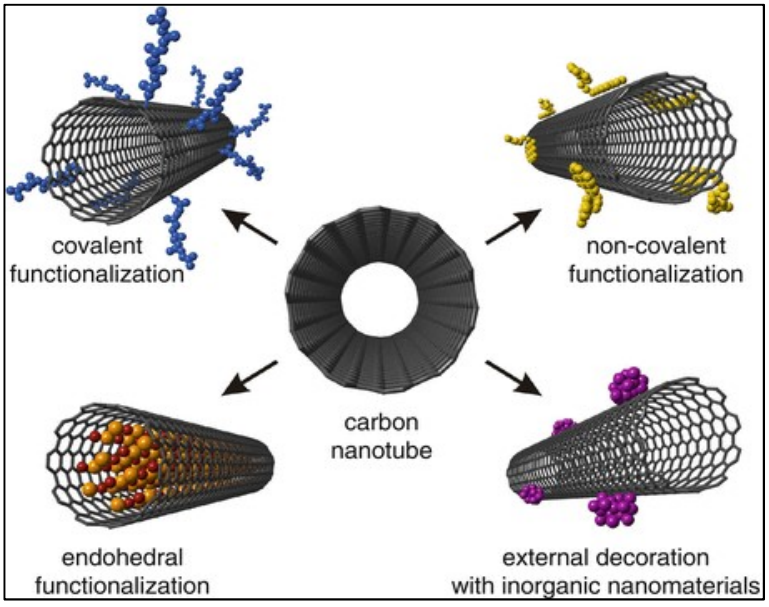

Figure-1.8. Scheme showing various functionalization techniques of Carbon nanotubes (62).

1.2.4. PROPERTIES OF CNTs

Due to excellent thermal, mechanical, electronic and optical properties, CNTs and their composites finds application in various fields. The tensile strength of CNT is very high compared to steel as well as kevlar.

(a) Mechanical properties

CNTs are highly elastic and their elasticity is examined in terms of modulus of elasticity or elastic modulus. CNTs are flexible and can retain their original shape and are prone to less deformation when strong compression force is exerted. CNTs do not undergo any damage on being kinked, bent, twisted and buckled on the application of compressive force in axial direction. The major factor influencing the mechanical properties of CNTs is diameter. The mechanical properties get enhanced when the tube diameter increases. A very high modulus and high tensile strength are observed for CNTs which is of the order of 1 TPa and 10 GPa. The remarkable strength, exceptional flexibility and resilience are the important mechanical properties of the CNTs which are reflected in the composites constituting CNTs. In the case of CNT-polymer matrix composites the reinforcement of CNT into the polymer matrix increases the mechanical strength [102–104].

(b) Electronic properties

In CNTs each carbon atom is bonded to three other carbon atoms by sp^2 hybrid orbitals and the fourth valence which remains free contributes to the conducting nature of CNTs. The electrical conductivity also depends on the chiral nature of CNT. The metallic and semiconductor nature of CNTSs depends on the chiral integers n and m. Nanotubes act as a 1D metal if |n-m| is a multiple of three otherwise they possess semiconducting nature. The electron transport in SWCNTs is considered to be ballistic where as for MWCNTs it is quasi-ballistic or diffusive. The remarkable electronic properties of CNTs facilitate these materials as well as their composites to find application in molecular electronics which include field-effect transistors, rectifiers, vacuum microelectronics, sensors etc [105–107]. CNTs also find application in quantum computing and other switching applications.

(c) Optical properties

The symmetry and structure of SWCNTs enable them to act as promising materials for opto electronic and optical applications. Optical properties in CNTs arise due to three processes which include photo absorption, relaxation and photo emission [108]. SWCNTs have been found to exhibit both the highest photoluminescence quantum yield and Raman scattering abilities [109,110]. The chirality of semiconducting SWCNTs can be analyzed by the optical signals in the near infrared region and different kinds of metallic SWCNTs can be found by studying the absorption signal in the blue UV region.

(d) Thermal properties

CNTs and their hybrid composite materials find applications in thermal management in industries since incorporation of CNTs into composites improves the thermal conductivity of the initial material. The thermal conductivity of carbon nanotube is higher than graphite. Several factors that influence thermal properties of CNT-based composites. These include diameter and length of tubes, morphology, impurities, phonon active modes etc. CNTs and their composites are employed in micro and optoelectronic devices due to their high thermal conductivity [111–113].

1.2.5. APPLICATIONS OF CNTs

Among the various carbon nanomaterials, carbon nanotube possess extraordinary physical and chemical properties and hence they are widely explored in to various fields including electrochemical sensing, piezoelectric sensing and gas sensing. CNTs also possess antibacterial and antifungal activity which attributes them in the field of biological systems.

(a) CNTs as electrochemical biosensors

Basically, an electrochemical biosensor consists of a bioreceptor and a transducer. Bioreceptor consists of a biological recognition element that is combine with a transducer in which the electrode converts the recognition event to an electrical signal thereby distinguishing the analyte in the sample. CNTs with other nanoparticles and polymers can act as electrochemical sensors for the recognition of various analytes like dopamine, albumin, glucose, amino acids, quercetin, heavy metals such

as lead and mercury, hydrogen peroxide, phenol, bilirubin [114-119] etc. The extraordinary electron transport properties and the improved electrocatalytic activity of CNTs enhances the sensing ability of the electrodes which in turn helps in lowering the limit of detection of various analytes.

(b) CNTs as gas sensor

Gas sensors find application in environmental, industrial and medical fields. CNT-based hybrid composites show good analytical performance which includes good response time, excellent stability, and recovery in sensing various gas molecules. The various CNT-based composites developed were found to sense gases like NOx, ammonia, sulphur dioxide, chlorine, volatile organic compounds, various pollutants etc [120-123]. The introduction of nanomaterials as gas sensors paves an alternative for conventional methods which require bulky instrumentation methods and skilled labor.

(c) CNTs as piezoelectric sensor

The electromechanical properties of MWCNTs have been widely applied for fabrication of stretchable sensors on various substrates. These sensors are found to be highly compatible, economic, specific and flexible. CNT-based piezo electric sensors are mainly employed in strain sensing, measuring pressure and human functions as these types of sensors are employed in gloves and bandages. Moreover these composite sensors of CNT are highly stable and they show excellent sensitivity, linearity and good detection limit [124,125].

(d) CNTs for drug targeting and cancer diagnosis

The hydrophobic nature of CNTs makes them excellent candidates for drug transfer as well as targeted drug delivery. Targeted drug delivery refers to the delivery of a therapeutic drug to a precise part over an extended period. In CNT-modified composites, the diameter of nanotube and the composition determines the efficiency of the drug release. The excellent pharmacokinetic properties of CNTs make them suitable for drug targeting and also in gene delivery. The optical properties of CNTs enable their use in the field of photo therapy [126,127]. MWCNTs are also employed in cancer diagnosis and its further treatments [128].

(e) CNTs for antibacterial and antifungal activity

The antibacterial activity of MWCNT mainly depends upon the aspect ratio. The carbon nanotubes with shorter length and smaller diameters interact with the microbes when compared to tubes of longer lengths and larger diameters. The antibacterial mechanism of CNTs mainly includes the formation of close association of CNT with the cell membrane followed by damage of the cell membrane with the release of DNA content. Functionalization of CNTs decreases the toxicity and increase the anti-microbial activity. MWCNTs together with its composites are found to enhance the antibacterial activity against various bacteria [129,130]. Chitosan derivatives along with MWCNT were found to exhibit good anti-fungal activity against a large number of fungi [131].

(f) CNTs for energy storage devices

The chemical inertness, excellent conducting behavior and good mechanical properties qualify CNTs and their composites to act as supercapacitors. The double layer formation between the CNT composites and electrolyte interface results in charge storage mechanism. A substantial increase in capacitance is noticed when CNTs are modified with metal oxides or conducting polymers [132,133].

1.3 REFERENCES

1. Acquah SFA, Penkova A V., Markelov DA, Semisalova AS, Leonhardt BE, Magi JM. Review—The Beautiful Molecule: 30 Years of C_{60} and Its Derivatives . ECS J Solid State Sci Technol. 2017;6(6):M3155–62.

2. Eun-Kyung Lim, Taekhoon Kim, Soonmyung Paik, Seungjoo Haam, Yong-Min Huh and Kwangyeol Lee. Nanomaterials for theranostics: Recent advances and future challenges. Chem Rev. 2015;115(1):327–94.

3. Georgakilas V, Perman JA, Tucek J, Zboril R. Broad Family of Carbon Nanoallotropes : Classfication , Chemistry and Applications of Fullerenes , Carbon Dots , Nanotubes , Graphene , Nanodiamonds and Combined Superstructures. Chem Rev. 2015;115:4744–4822.

4. H.W.Kroto, J.R.Heath, S.C.O'Brien, R.F.Curl and R.E.Smalley. C_{60}: Buckminsterfullerene. Nature. 1985;318.

5. Ravinder Kour, Sandeep Arya, Sheng-Joue Young, Vinay Gupta PB and Ajit Khosla. Review — Recent Advances in Carbon Nanomaterials as Electrochemical Biosensors. J Electrochem Soc. 2020;167:037555.

6. Jack B.Howard, J. Thomas McKinnon, Yakov Makarovsky ALL and Melaine J. Fullerenes C_{60} and C_{70} in flames. Nature. 1991;352.

7. Churilov GN. Plasma Synthesis of Fullerenes (Review). Instruments and Experimental Tech.2000;43(I).

8. Jinjin Shi, Lei Wang , Jun Gao, Yan Liu, Jing Zhang, Rou Ma, Ruiyuan Liu, Zhenzhong Zhang . A fullerene-based multi-functional nanoplatform for cancer theranostic applications. Biomaterials . 2014;35:5771–5784

9. Bolskar RD. Gadofullerene MRI contrast agents. Nanomedicine. 2008;3:201–13.

10. Iijima S. Helical microtubules of graphitic carbon. Nature. 1991;354:56–8.

11. Sandeep Kumar, Ruma Rani, Neeraj Dilbaghi, K. Tankeshwar and Ki-Hyun Kim. Carbon nanotubes: A novel material for multifaceted applications in human healthcare. Chem Soc Rev. 2017;46(1):158–96.

12. Yue Zhaoa, Louzhen Fan, Bo Hong, Jingling Ren, Minsheng Zhanga, Qiming Que J ji. Chemical Nonenzymatic detection of glucose using three-dimensional PtNi nanoclusters electrodeposited on the multiwalled carbon nanotubes. Sensors Actuators B Chem. 2016;231:800–10.

13. Shulan Jiang, Tielin Shi, Xiaobin Zhan, Shuang Xi, Hu Long, Bo Gong, Junjie Li, Siyi Cheng, Huang Yuanyuan and Zirong Tang. Scalable fabrication of carbon-based MEMS / NEMS and their applications : a review. J Micromechanics Microengineering. 2015;113001:113001.

14. Rana K, Kucukayan-dogu G, Bengu E. Growth of vertically aligned carbon nanotubes over self-ordered nano-porous alumina films and their surface properties. Appl Surf Sci. 2012;258(18):7112–7.

15. K.Novoselov A. K. Geim and. The rise of graphene. Nature. 2007;6.

16. Geim AK. Graphene: status and prospects. Science (80-). 2009;324(5934):1530–4.

17. Choucair M, Thordarson P, Stride JA. Gram-scale production of graphene based on solvothermal synthesis and sonication. Nat Nanotechnol. 2009;4(1):30–3.

18. Hernandez Y, Nicolosi V, Lotya M, Blighe FM, Sun Z, De S, McGovern I.T, Holland B, Byrne M, GunKo Y K, Boland J J, Niraj P, Duesberg G, Krishnamurthy S, Goodhue R, Hutchison J, Scardaci V, Ferrari A C and Coleman J N. High-yield production of graphene by liquid-phase exfoliation of graphite. Nat Nanotechnol. 2008;3(9):563–8.

19. Da Chen, Hao Zhang, Yang Liu and Jinghond Li,mGraphene and its derivatives for the development of solar cells, photoelectrochemical and photocatalytic applications. Energy Environ Sci. 2013;6:1362–87.

20. Jesse D. Fowler, Matthew J. Allen VCT, Yang Yang, Richard B. Kaner A, Weiller BH. Practical chemical sensors from chemically derived graphene. ACS Nano. 2009;3(2):301–6.

21. Liu H, Lina Zhang , Mei Yan and Jinghua Yu. Carbon nanostructures in biology and medicine. J Mater Chem B . 2017;5(32):6437–50.

22. Shuzhen Lv, Yi Li, Kangyao Zhang, Zhenzhen Linand and Dianping Tang. Carbon Dots/g-C_3N_4 Nanoheterostructures-Based Signal-Generation Tags for Photoelectrochemical Immunoassay of Cancer Biomarkers Coupling with Copper Nanoclusters. ACS Appl Mater Interfaces. 2017;9(44):38336–43.

23. Liangliang Zhu, Yongjin Yin, C-Feng Wang and Su Chen. Plant leaf-derived fluorescent carbon dots for sensing, patterning and coding. J Mater Chem C. 2013;1(32):4925–32.

24. Yongming Guo , Zhuo Wang , Huawu Shao XJ. Hydrothermal synthesis of highly fluorescent carbon nanoparticles from sodium citrate and their use for the detection of mercury ions. Carbon N Y. 2013;52:583–9.

25. Liu J, Li R, Yang B. Carbon Dots: A New Type of Carbon-Based Nanomaterial with Wide Applications. ACS Cent Sci. 2020;6(12):2179–95.

26. Zhangxing He , Manman Li , Yuehua Li , Jing Zhu , Yingqiao Jiang , Wei Meng , Huizhu Zhou , Ling Wang and Lei Dai. Flexible electrospun carbon nanofiber embedded with TiO_2 as excellent negative electrode for vanadium redox flow battery. Electrochim Acta. 2018;281:601–610.

27. MuhammadUmerZahid, , Erum Pervaiz , Arshad Hussain MS and, Niazi MBK. Synthesis of Carbon Nanomaterials from Different Pyrolysis Techniques : A Review. Mater Res ExpresS. 2018;5(April).

28. Shoukat R, Khan MI. Synthesis of vertically aligned carbon nanofibers using inductively coupled plasma-enhanced chemical vapor deposition. Electr Eng. 2018;100(2):997–1002.

29. Mochalin VN, Shenderova O, Ho D, Gogotsi Y. The properties and applications of nanodiamonds. Nat Nanotechnol .2011;7(1):11–23.

30. Perevedentseva E, Lin Y-C, Cheng MJ& Chiang-Liang Cheng. Biomedical applications of nanodiamonds in imaging and therapy Review. Nanomedicine. 2013;8:2041–60.

31. Nikolaos Karousis, Irene Suarez-Martinez, Christopher P. Ewels and Nikos Tagmatarchis. Structure , Properties , Functionalization and Applications of Carbon Nanohorns. Chem Rev. 2016;116:4850–83.

32. Yamaguchi T, Bandow S, Iijima S. Synthesis of carbon nanohorn particles by simple pulsed arc discharge ignited between pre-heated carbon rods. Chem Phys Lett. 2004;389:181–5.

33. Iijima S, Yudasaka M. Nano-aggregates of single-walled graphitic carbon nano-horns. Chem Phys Lett. 1999;309(August):165–70.

34. Frederic Fabry, Gilles Flamant LF. Carbon black processing by thermal plasma . Analysis of the particle formation mechanism. Chem Sci. 2001;56:2123–32.

35. Deroco PB, Vicentini C, Fatibello-filho O. An Electrochemical Sensor for the Simultaneous Determination of Paracetamol and Codeine Using a Glassy Carbon Electrode Modified with Nickel Oxide Nanoparticles and Carbon Black. Electroanalysis. 2015;27:2214–20.

36. HuaHe, Lien Ai Pham-Huy, Pierre Dramou, Deli Xiao, Pengli Zuo and Chuong Pham-Huy. Carbon nanotubes: Applications in pharmacy and medicine. Biomed Res Int. 2013;2013.

37. Rajesh Purohit, Kuldeep Purohit, Saraswati Rana, R.S.Rana and Vivek Patel. Carbon Nanotubes and Their Growth Methods. Procedia Mater Sci. 2014;6:716–28.

38. Liu L, Zhao J. Toroidal and Coiled Carbon Nanotubes. 2013.

39. Ji Il Choi, Hyo Seok Kim, Han Seul Kim, Ga In Lee, Jeung Ku Kang and Yong-Hoon Kim. Carbon nanobuds based on carbon nanotube caps: A first- principles study. Nanoscale. 2012;00:1–3.

40. Grobert N. Carbon nanotubes – becoming clean. Mater Today. 2007;10:28–35.

41. R. Saito, M. Fujita, G. Dresselhaus and M.S. Dresselhaus. Electronic structure of chiral graphene tubules. Appl Phys Lett. 1992;2204:67–70.

42. Rahmandoust M, Öchsner A. Buckling Behaviour and Natural Frequency of Zigzag and Armchair Single- Walled Carbon Nanotubes. J Nano Res. 2012;16:153–60.

43. Jamal M. A. Alsharefa, Mohd Raihan Taha and Tanveer Ahmed Khan. Physical dispersion of nanocarbons in composites-A review. J Technol. 2017;79:69–81.

44. Nayak MSH and AK. Carbon Nanotubes for Targeted Drug Delivery. 2019.

45. R.I. vanderwal, G.M. berger TM ticich. Carbon nanotube synthesis in a flame using laser ablation for in situ catalyst generation. Appl Phys A – Mater Sci Process. 2003;889:885–9.

46. Z. B. He, Jean-Luc Maurice, Chang Seok Lee and Costel Sorin Cojocaru and D Pribat. Nickel catalyst faceting in plasma-enhanced direct current chemical vapor deposition of carbon nanofibers. Arab J Sci Eng. 2013;35.

47. Shinde VS, Bhise MR, Rathi AM, Sapkal SB, Narkhede MB, Babhulkar MW. A review: Carbon nanotubes and its application. Asian J Pharm Inven Asian J Pharm Inven AsianJPharmInven2013,. 2013;1(August).

48. D.S.Bethune, C.H.Kiang, M.S. de Vries, G.Gorman, R.Savoy JV and RBeyers. Cobalt-catalysed growth of carbon nanotubes with single-atomic-layer walls. Nature. 1993;363:605–7.

49. Shunji Bandow, S. Asaka, Y. Saito A. M. Rao, L. Grigorian, E. Richter and PCEklund.

Effect of the growth temperature on the diameter distribution and chirality of single-wall carbon nanotubes. Phys Rev Lett. 1998;81:4780.

50. Haiyan Zhang, Yu Ding, Chunyan Wu, Yimin Chen, Yanjuan Zhu, Yanyang He and Shao Zhong, Faculty. The effect of laser power on the formation of carbon nanotubes prepared in CO_2 continuous wave laser ablation at room temperature. Phys B. 2003;325:224–9.

51. M. Yudasaka, R. Yamada, N. Sensui, T. Wilkins, T. Ichihashi and SIijima. Mechanism of the Effect of NiCo , Ni and Co Catalysts on the Yield of Single-Wall Carbon Nanotubes Formed by Pulsed Nd : YAG Laser Ablation. J Phys Chem B. 1999;10:6224–9.

52. Andreas Thess, Roland Lee, Pavel Nikolaev, Hongjie Dai, Pierre Petit, Jerome Robert, Chunhui Xu, Young Hee Lee, Seong Gon Kim, Andrew G. Rinzler, Daniel T. Colbert, Gustavo E. Scuseria, David Tomanek, John E. Fischer, Richard E. Smalley. Crystalline Ropes of Metallic Carbon Nanotubes. Science. 1996;273:483–7.

53. Enkeleda Dervishi , Zhongrui Li , Yang Xu VS, Alexandru R. Biris, Dan Lupu & Alexandru S Biris. Carbon Nanotubes : Synthesis , Properties and Applications. Part Sci Technol. 2009;27:107–25.

54. Smajda R, , J. C. Andresen , M. Duchamp , R. Meunier , S. Casimirius , K. Herna´ di , L. Forro1 and Arnaud Magrez. Synthesis and mechanical properties of CNTs produced by water assisted CVD process. Phys Status Solidi B. 2009;246:2457–60.

55. Stephen A. Steiner III, Theodore F. Baumann BCB, Raoul Blume Marcus A. Worsley, Warren J. MoberlyChan, Elisabeth L. Shaw, Robert Schlo gl, A. John Hart 0 Stephan Hofmannand Brian L. Wardle. Nanoscale Zirconia as a Nonmetallic Catalyst for Graphitization of Carbon and Growth of Single- and Multiwall Carbon Nanotubes. J Am Chem Soc. 2009;131:12144–54.

56. S.P. Patole, P.S. Alegaonkar, Hyun-Chul Lee Ji-Beom Yoo. Optimization of Water Assisted Chemical Vapor Deposition Parameters for Super Growth of Carbon Nanotubes. Carbon N Y. 2008;46:1987–93.

57. Naha S, Puri IK. A model for catalytic growth of carbon nanotubes. J Phys D Appl Phys. 2008;41:065304.

58. Fotopoulos N, Xanthakis JP. A molecular level model for the nucleation of a single-wall carbon nanotube cap over a transition metal catalytic particle. Diam Relat Mater.2010;19:557–61.

59. G. S. Duesberg, M. Burghard, J. Muster and GPhilipp . Separation of carbon nanotubes by size exclusion chromatography. Chem Commun. 1998;435–6.

60. Konstantin B. Shelimov, Rinat O. Esenaliev, Andrew G. Rinzler, Chad B. Huffman, Richard ESmalley. Purification of single-wall carbon nanotubes by ultrasonically assisted filtration. Chem Phys Lett. 1998;282:429–34.

61. Billyde Brown , Charles B. Parker , Brian R. Stoner, Jeffrey T Glass. Growth of vertically aligned bamboo-like carbon nanotubes from ammonia / methane precursors using a platinum catalyst. Carbon N Y . 2010;49:266–74.

62. Gerard Tobias, Ernest Mendoza and Belen Ballesteros. Functionalization of Carbon Nanotubes. Encyclopedia of Nanotechnology. 2016.

63. Dimitrios Tasis, Nikos Tagmatarchis, Alberto Bianco and Maurizio Prato. Chemistry

of Carbon Nanotubes. Chem Rev. 2006;106:1105–36.

64. E. T. Mickelson, I. W. Chiang, J. L. Zimmerman, P. J. Boul, J. Lozano, J. Liu, R. E. Smalley, R. H. Hauge and JLMargrave. Solvation of Fluorinated Single-Wall Carbon Nanotubes in Alcohol Solvents. J Phys Chem B. 1999;103:4318–22.

65. Eugen Unger andrew Graham, Franz Kreupl, Maik Liebau and Wolfgng Honlein. Electrochemical functionalization of multi-walled carbon nanotubes for solvation and purification. Curr Appl Phys. 2002;2:107–11.

66. Khabashesku VN, Billups WE, Margrave JL. Fluorination of Single-Wall Carbon Nanotubes and Subsequent Derivatization Reactions. Acc Chem Res. 2002;35:1087–95.

67. Bishun N. Khare, M. Meyyappan, Joel Kralj, Patrick Wilhite, Metagus Sisay, Hiroshi Imanaka, Jessica Koehne and CWB. A glow-discharge approach for functionalization of carbon nanotubes. Appl Phys Lett. 2002;81:5237.

68. S.Pekker, J-P.Salvetat, E.Jakab, J.M.Bonard, L.Forro. Hydrogenation of Carbon Nanotubes and Graphite in Liquid Ammonia. J Phys Chem. 2001;105:7938–43.

69. Bishun N. Khare, M. Meyyappan, Alan M. Cassell, Cattien V. Nguyen and Jie Han. Functionalization of Carbon Nanotubes Using Atomic Hydrogen from a Glow Discharge. Nano Lett. 2002;2:73–7.

70. Mercedes Alvaro, Pedro Atienzar, Pilar de la Cruz JLD, Vincent Troiani, Hermenegildo Garcia, Fernando Langa, Amit Palkar and LE. Synthesis, photochemistry, and electrochemistry of single-wall carbon nanotubes with pendent pyridyl groups and of their metal complexes with zinc porphyrin. Comparison with pyridyl-bearing fullerenes. J Am Chem Soc. 2006;128:6626–35.

71. Worsley KA, Moonoosawmy KR, Kruse P. Long-range periodicity in carbon nanotube sidewall functionalization. Nano Lett. 2004;4:1541–6.

72. Juan L. Delgado, Pilar de la Cruz, Fernando Langa, Antonio Urbina, Juan Casado and Juan T.Lopez Navarrete. Microwave-assisted sidewall functionalization of single-wall carbon nanotubes by Diels-Alder cycloaddition. Chem Commun. 2004;4:1734–5.

73. Michael Holzinger, Johannes Steinmetz , Damien Samaille , Marianne Glerup , Matthieu Paillet , Patrick Bernier , Lothar Ley RG. [2+1] Cycloaddition for cross-linking SWCNTs. Carbon N Y. 2004;42:941–7.

74. Hui Hu, Bin Zhao, Mark A. Hamon, Katalin Kamaras, Mikhail E. Itkis and Robert C Haddon. Sidewall Functionalization of Single-Walled Carbon Nanotubes by Addition of Dichlorocarbene. J Am Chem Soc. 2003;125:14893–900.

75. Yunming Ying, Rajesh K. Saini, Feng Liang, Anil K. Sadana and W.E.Billups. Functionalization of carbon nanotubes by free radicals. Org Lett. 2003;5:1471–3.

76. Haiqing Peng, Paul Reverdy, Valery N. Khabashesku and John L.Margrave. Sidewall functionalization of single-walled carbon nanotubes with organic peroxides. Chem Commun. 2003;3:362–3.

77. Nikos Tagmatarchis, Vasilios Georgakilas, Maurizio Prato and Hisanori Shinohara. Sidewall functionalization of carbon nanotubes through electrophilic substitution. J Nanosci Nanotechnol. 2011;11:3385–92.

78. Shimou Chen, Wenming Shen, Guozhong Wu , Daoyong Chen and Ming Jiang. A new

approach to the functionalization of single-walled carbon nanotubes with both alkyl and carboxyl groups. Chem. Phys. Lett. 2005;402:312–7.

79. Hemraj-benny T, Banerjee S, Wong SS. Interactions of Lanthanide Complexes with Oxidized Single-Walled Carbon Nanotubes. Chem. Mater. 2004;16:1855–63.

80. Mawhinney DB, Naumenko V, Kuznetsova A, Yates J and Smalley R. Infrared Spectral Evidence for the Etching of Carbon Nanotubes : Ozone Oxidation at 298 K. J Am Chem Soc. 2000;122:2383–4.

81. Hulin Li DZ. Mechanochemical Synthesis of Nanostructured Materials for Energy Conversion and Storage Devices. Handbook of Mechanical Nanostructuring. 2015. 717–733 p.

82. Qidao Chen, Liming Dai, Mei Gao, Shaoming Huang and Albert Mau. Plasma Activation of Carbon Nanotubes for Chemical Modification. J Phys Chem B. 2001;105:618–22.

83. GuoYong Xu, Ru Xia, Hu Wang, Xiang Chun Meng and Qing Ren Zhu. Grafting of thermoresponsive polymer from the surface of functionalized multiwalled carbon nanotubes via atom transfer radical polymerization. Chinese Sci Bull. 2008;53:2297–306.

84. Wang A, Zhao W. Porphyrin and Phthalocyanine Covalently Functionalized Graphene and Carbon Nanotube Nanohybrids for Optical Limiting. Chem React Inorg Chem. 2018;

85. Jason J. Stephenson, Jared L. Hudson, Ashley D. Leonard, B. Katherine Price and James MTour. Repetitive functionalization of water-soluble single-walled carbon nanotubes. Addition of acid-sensitive addends. Chem Mater. 2007;19:3491–8.

86. Narwade SS, Mali SM, Sathe BR. Amine-functionalized multi-walled carbon nanotubes (EDA-MWCNTs) for electrochemical water splitting reactions. New J Chem. 2021;45:3932–9.

87. Nurjahirah Janudin, Abdullah Luqman Chuah, Norli Abdullah, Faizah Md Yasin, Norshafiqah Mohamad Saidi and Noor Azilah Mohd Kasim. Characterization of amide and ester functionalized multiwalled Carbon Nanotubes. Asian J Chem. 2018;30:1613–6.

88. Awasthi K, Singh DP, Singh SK, Dash D, Srivastava ON. Attachment of biomolecules (protein and DNA) to amino-functionalized carbon nanotubes. New Carbon Mater. 2009;24:301–6.

89. Germarie Sánchez-Pomales, Coral Pagán-Miranda, Lenibel Santiago Rodriguez and Carlos R.Cbrera. DNA-Wrapped Carbon Nanotubes : From Synthesis to Applications. 2010.

90. Hiroyuki Maruyama, Shige H. Yoshimura, Seiji Akita, Atsuko Nagataki and Yoshikazu Nakayama. Covalent attachment of protein to the tip of a multiwalled carbon nanotube without sidewall decoration. J Appl Phys. 2012;102:094701.

91. Díez-Pascual AM. Chemical Functionalization of Carbon Nanotubes with Polymers : A Brief Overview. Macromol. 2021;1:64–83.

92. Weiwei Lin, Yonatan Rotenberg, Kevin P. Ward, Hadi Fekrmandi and Cesar Levy. Polyaniline / multi-walled carbon nanotube composites for structural vibration damping and strain sensing. J Mater Res. 2016;32:73–83.

93. Kim JW and J. Thermal Conductivity Enhancement Derived from Poly(Methyl Methacrylate)-Grafted Carbon Nanotubes in Poly(Methyl Methacrylate) / Polystyrene Blends. Polymers (Basel). 2019;11:1347.

94. Boubaker Zaidi , Nejmeddine Smida SDA, , Mohammed G. Althobaiti AGA. Polymer/Carbon Nanotube Based Nanocomposites for Photovoltaic Application: Functionalization, Structural, and Optical Properties. Polymers (Basel). 2022;14:1093.

95. D Primastari , Y Kusumastuti, M Handayani R. Functionalization of multi-walled carbon nanotube (MWCNT) with CTACe surfactant and polyethylene glycol as potential drug carrier. IOP Conf Ser Earth Environ Sci. 2022;963:012033.

96. Jijun Zhao, Jian Ping Lu, Jie Han and Chih-Kai Yang. Noncovalent functionalization of carbon nanotubes by aromatic organic molecules. Appl Phys Lett. 2003;82:3746–8.

97. Katz E, Willner I. Biomolecule-functionalized carbon nanotubes: Applications in nanobioelectronics. ChemPhysChem. 2004;5:1084–104.

98. Oxana V. Kharissova BIK and EG de CO. Dispersion of carbon nanotubes in water and non-aqueous solvents. RSC Adv. 2014;3:24812.

99. Zhang W, , Ding Q , JinRuan J, Fang J and, Ruan BH. Biomolecular Interactions and Application of Carbon Nanotubes in Nanomedicine. Austin Biomol Open Access. 2016;1:1005.

100. S. Ajori, H. Parsapour RA. Stability analysis of endohedrally functionalized carbon nanotubes with pentagonal metallic nanowires: A molecular dynamics simulation approach. Mater Res Express. 2019;6:045056.

101. Sandoval S, Tobias G. Encapsulation of Fullerenes: A versatile approach for the confinement and release of materials within open-ended multiwalled carbon nanotubes. Front Bioeng Biotechnol. 2021;9:1–12.

102. B. Arash, Q. Wang and V.K.Varadan. Mechanical properties of carbon nanotube/polymer composites. Sci Rep. 2014;4:6479.

103. J.-P. Salvetat,J.-M. Bonard, N.H.Thomson,A.J.Kulik ,L. Forr´o, W. Benoit and L. Zuppiroli. Mechanical properties of carbon nanotubes. Appl Phys A. 1999;69:255–60.

104. Yoshinobu Shimamura , Kahori Oshima , Keiichiro Tohgo , Tomoyuki Fujii , Keiichi Shirasu , Go Yamamoto , Toshiyuki Hashida , Ken Goto , Toshio Ogasawara , Kimiyoshi Naito , Takayuki Nakano YI. Tensile mechanical properties of carbon nanotube / epoxy composite fabricated by pultrusion of carbon nanotube spun yarn preform. Compos Part A . 2014;62:32–8.

105. Mindy D. Bishop GH, , Tathagata Srimani, Christian Lau DM, , Samuel Fuller Jefford Humes, Anthony Ratkovich, Mark Nelson and Max M. Shulaker. Fabrication of carbon nanotube field-effect transistors in commercial silicon manufacturing facilities. Nat Electron. 2020;3:492–501.

106. Ali Javey, Jing Guo, Qian Wang, Mark Lundstrom & HongjieDai. Ballistic carbon nanotube field-effect transistors. Nature. 2003;424:6949.

107. Ghasemi S, Moth-Poulsen K. Single molecule electronic devices with carbon-based materials: Status and opportunity. Nanoscale. 2021;13:659–71.

108. Saito R, Dresselhaus MS. Optical Properties of Carbon Nanotubes. Second Edi. Carbon Nanotubes and Graphene: Edition 2. Elsevier Ltd; 2014. 77–98 p.

109. Aravind Kumar Jagadeesan, Krithiga Thangavelu and Venkatesan Dhananjeyan. Carbon nanotubes: Synthesis, properties and applications. 21st Century Surface Science - a Handbook. 2020.

110. Scott M. Tabakman, Kevin Welsher, Guosong Hong and Hongjie Dai. Optical Properties of Single-Walled Carbon Nanotubes Separated in a Density Gradient; Length, Bundling, and Aromatic Stacking Effects. J Phys Chem C Nanomater Interfaces. 2010;114:19569–75.

111. Yuan Xu, Yi Zhang and Ephraim Suhir. Thermal properties of carbon nanotube array used for integrated circuit cooling. J Appl Phys. 2006;100:074302.

112. J. Hone,M.C.Llaguno, M.J. Biercuk, A.T.Johnson, B. Batlogg, Z.Benes J E Fischer. Thermal properties of carbon nanotubes and nanotube-based materials. Appl Phys A Mater Sci Process.2002;74:339–43.

113. Ibrahim KS.Carbon nanotubes-properties and applications: a review. Carbon Lett. 2013;14:131–44.

114. Beden N, Hassan, Hamidi E, Palecek MT, And, Gorton L. Subnanomolar Determination of Dopamine by Electrochemical Sensor based on AuNPs- MWCNTs and Mannan-Os (VI) Adducts. Insights Anal Electrochem. 2016;2:1–8.

115. Xianwen Kan, Tingting Zhang, Min Zhong XL. CD/AuNPs/MWCNTs based electrochemical sensor for quercetin dual-signal detection. Biosens Bioelectron. 2016;77:638–43.

116. Mourya A, Mazumdar B, Sinha SK. Application of CeO_2-MWCNTs nanocomposite for heavy metal ion detection in aqueous solutions by electrochemical technique. Clean Mater. 2021;2:100021.

117. Tai-Cheng Chou, Kai-Yu Wu, Fu-Xiang Hsu and Cheng-Kang Lee. Pt-MWCNT modified carbon electrode strip for rapid and quantitative detection of H_2O_2 in food. J Food Drug Anal. 2018;26:662–9.

118. Yajing Wang, Jiankang Wang, Zhongping Yao CL, Taiping Xie, Qihuang Deng and Zhaohua Jiang. Ni Nanoparticle Anchored on MWCNT as a Novel Electrochemical Sensor for Detection of Phenol. Nano. 2018;13:1–10.

119. Thangamuthu M, , Willimann Eric Gabriel, Christian Santschi and Oliver J.F. Martin. Electrochemical sensor for bilirubin detection using screen printed electrodes functionalized with carbon nanotubes and graphene. Sensors. 2018;18:800.

120. Defu Ma, Yanjie Su, Tian Tian, Huan Yin, Tingting Huo, Feng Shao, Zhi Yang, Nantao Hu and Yafei Zhang. Highly Sensitive Room-Temperature NO_2 Gas Sensors Based on Three-Dimensional Multiwalled Carbon Nanotube Networks on SiO_2 Nanospheres. ACS Sustain Chem Eng. 2020;8:13915−13923.

121. Vu Truong Duong, Cong Tu Nguyen, Huu Bac Luong Assoc. Prof. Dr. , Duc Chien Nguyen, Prof. Dr., Huu Lam Nguyen Assoc. Prof. D. Ultralow-detection limit ammonia gas sensors at room temperature based on MWCNT/WO_3 nanocomposite and effect of humidity. Solid State Sci. 2021;113:106534.

122. Nikesh Ingle, , Savita Mane, Pasha Sayyad, Bodkhe G, AL-Gahouari T, Manasi Mahadik, Sumesh Shirsat and Mahendra D. Shirsat . Sulfur Dioxide (SO_2) Detection Using Composite of Nickel Benzene Carboxylic (Ni_3BTC_2) and OH-Functionalized Single Walled Carbon Nanotubes (OH-SWNTs). Front Mater. 2020;7:1–7.

123. Arti Dinkarrao Rushi, Kunal Prasanta Datta, Prasanta Sudarshan Ghosh Ashok Mulchandani and Mahendra D. Shirsat. Functionalized Carbon Nanotubes for Detection of Volatile Organic Pollutant. Perspective of Carbon Nanotubes. 2019.

124. Park K, Tran P, Deaton N, Desai JP. Multi-walled Carbon Nanotube (MWCNT)/PDMS-based Flexible Sensor for Medical Applications. Int Symp Med Robot ISMR 2019. 2019;1–8.

125. Zuoli He, Gengheng Zhou, Joon-Hyung Byun, Sang-Kwan Lee, Moon-Kwang Um, Byeongjin Park, Taehoon Kim, Sang Bok Lee and Tsu-Wei Chou. Highly stretchable multi-walled carbon nanotube/thermoplastic polyurethane composite fibers for ultrasensitive, wearable strain sensors. Nanoscale. 2019;11:5884–90.

126. Jha R, Singh A, Sharma PK, Fuloria NK. Smart carbon nanotubes for drug delivery system: A comprehensive study. J Drug Deliv Sci Technol. 2020;58:101811.

127. Hossein Zare,Sepideh Ahmadi, Amir Ghasemi, Mohammad Ghanbari, Rabiee N, Bagherzadeh M, Karimi M, Webster TJ, Michael R Hamblin and EMostafavi. Carbon nanotubes: Smart drug/gene delivery carriers. Int J Nanomedicine. 2021;16:1681–706.

128. Shihui Wen , Hui Liu , Hongdong Cai , Mingwu Shen and Xiangyang Shi. Targeted and pH-Responsive Delivery of Doxorubicin to Cancer Cells Using Multifunctional Dendrimer-Modified Multi-Walled Carbon Nanotubes. Adv Heal Mater. 2013;2:1267–76.

129. Saima Rafique ,Shazia Bashir, Rizwan Akram , Farrukh Bashir Kiyani , Shagufta Raza, Mozaffar Hussain and Sayyeda Kaneez Fatima. Variation in the Performance of MWCNT / ZnO Hybrid Material with pH for Efficient Antibacterial Agent. Biomed Res Int. 2022;2022:1–11.

130. Shika Lohan, Kaiser Raza, Saloni Singla, Sanjay Chhibber , Sheetu Wadhwa, O.P. Katare,Pramod Kumar and Bhupinder Singh . Studies on Enhancement of Anti-microbial Activity of Pristine MWCNTs Against Pathogens. AAPS PharmSciTech. 2016;17:1042–8.

131. Wang X, Zhou Z, Chen F. Surface Modification of Carbon Nanotubes with an Enhanced Antifungal Activity for the Control of Plant Fungal Pathogen. Materials (Basel). 2017;10:1375.

132. Danhua Zhu, Qianjie Zhou, Aiqin Liang, Weiqiang Zhou , Yanan Chang, Danqin Li, Jing Wu, Guo Ye, Jingkun Xu and Yong Ren. Two-step preparation of carbon nanotubes / RuO_2 / polyindole ternary nanocomposites and their application as high-performance supercapacitors. Front Mater Sci. 2020;14:109–119.

133. Boyang Che, Hui Li, Dan Zhou, Youfang Zhang, Zhihui Zeng, Chenyang Zhao, Chaobin He, Erjia Liu and Xuehong Lu. Porous polyaniline / carbon nanotube composite electrode for supercapacitors with outstanding rate capability and cyclic stability. Compos Part B. 2019;165:671–8.

CHAPTER 2

REVIEW OF LITERATURE

2.1. MWCNT Hybrid Composites-"Limelight in Research"

Carbon nano tubes (CNTs) are considered as the allotrope of carbon which is an intermediate between graphite and fullerenes. Among the conductive carbon based nanomaterials, CNTs are used for wide variety of applications. This is due to its excellent properties which include weightlessness, high specific area, small size, bio-compatibility and excellent thermal, chemical stability. Based on the number of cylindrical walls CNTs are again classified as SWCNTs and MWCNTs. Among the above two classification, MWCNTs are dominant over SWCNTs due to several reasons which include (1) Excellent stability (2) More ease of mass production (3) Low cost and (4) Easy functionalization [1].

MWCNTs are good thermal and electrical conductors and the high aspect ratio of MWCNTs enables them to perform as electron field emitters. MWCNTs are involved in the synthesis of electrically conductive polymers and also in the preparation of some composites with improved structures. In the medicinal field MWCNTs play an indispensable role since they have the capability to act as biosensors and also they are found to be effective in targeting certain type of tumor cells [2]. MWCNTs plays an inevitable role in the development of solar cells, as these gets incorporated with in iron coated silicon wafer, the need for orienting the cells to face the sun by mechanical means gets reduced since MWCNTs has already been aligned vertically. MWCNTs also play an important role in battery research. Recent work delves to substitute graphite in lithium ion battery with MWCNTs, as they are thousand times more conductive than amorphous carbon containing electrodes. It has been observed that, the evolution of flexible sensors using certain materials could alter the electrical and mechanical properties and hence these can replace the micro-electro mechanical (MEMS) based silicon sensors in the microelectronic world [3]. Flexible sensors can be fabricated using different types of polymers and nanomaterials. The polymers mainly employed include polydimethyl siloxane (PDMS), polyethylene terephthalate (PET), polyethylene naphthalene (PEN), poly vinyl chloride (PVC) etc [4-7] etc. Among the second category of nanomaterials involved in the fabrication of sensors, MWCNTs plays an important role when compared to graphite, graphene etc. Thus in short, MWCNTs can function as efficient transistors and can be used in the construction of flat panel displays, energy storage

materials and solar cells. The enhanced electrical, thermal and mechanical properties of MWCNTs also pave the way for these materials to become a part of composite materials in the fabrication of sensors and also for the above mentioned applications. In short MWCNTs finds its applications as catalysts, electron field emitters of cathode ray lighting elements, flat panel displays, gas discharge tubes in telecom networks, lithium battery anodes, nanolithography, nano-electrodes, nano-probes for scanning tunneling microscope (STM), atomic force microscope (AFM) and electrostatic force microscope (EFM) tips. Furthermore these MWCNTs are excellent materials which can be employed in the field of sensors, energy storage materials especially supercapacitors, drug delivery systems, additive manufacturing technology, hydrogen storage stuffs and also reinforcements in composites.

2.2. Additive Manufacturing Technology

The carbon nano allotropes together with the polymers plays a revolutionary role in the 3D printing additive manufacturing (AM) processes. MWCNTs when introduced in a polymer matrix, results in improvement in the properties of polymers to a great extent. It is possible to tune the properties of polymers by changing the composition of MWCNTs inorder to produce flexible and light weight conductors. The only essential criteria for the synthesis of MWCNT-polymer composite is the requirement of homogeneous dispersion of CNT in polymer matrix which is achieved by proper functionalization techniques and sonication methods. Studies based on the synthesis of multifunctional polylactic acid (PLA)-multiwalled carbon nanotubes (MWCNTs) nanocomposite, nitrogen-doped bamboo-shaped carbon nanotube-poly vinyl chloride (N-BCNT/PVC) composite, MWCNT- acrylonitrile butadiene styrene (ABS) polymer, composite materials of sodium cholate modified MWCNT with thermoplastic like polyamides and polyurethanes (s-CNT/PA12 ands-CNT/PU), poly-ether-ether-ketone- carbon nanotube (PEEK–CNT) composite, Polypropylene/ carbonnanotube (PP-CNT) nanocomposites (PPCNT), multi-walled carbon nanotubes - poly (methyl methacrylate) (MWCNT/PMMA) [8-16] has been carried out. Polymer MWCNT composites were found to be applicable in serving various functions.

2.3. Photocatalysts

MWCNT composites can act as efficient photocatalyst and electrocatalyst serving various purpose. Semiconductors like TiO_2, ZnO, BiO, CdS are commonly used photocatalyst engaged in the photocatalytic degradation of pollutants. When MWCNT is combined with these semiconducting materials, the photocatalytic efficiency is being boosted and such hybrid composites can be used to minimize the pollutants entering the environment via, waste water treatment [17]. MWCNT mediated TiO2 composites, ZnO/MWCNT composites, MWCNT mediated bismuth, CdS, Ag are also explored as efficient photocatalyst utilized for the removal of pollutants by photocatalytic process. In short, combination of appropriate amount of MWCNTs and semiconductor materials results in creation of an efficient degradation mechanism.

2.4. Electrocatalysts

One of the advanced and cleaner energy technology involved in hydrogen production is electrochemical water splitting. The reactions proceeding in an electro-catalytic cell during the splitting of water is hydrogen evolution at cathode and oxygen evolution at anode. Various hybrid composites of MWCNTs are very well capable of performing its role as a stable and durable electrocatalysts. Composites of MWCNT together with nickel, ruthenium, molybdenum etc. shows superior activity towards hydrogen evolution reactions (HER) [29–31]. Besides HER reactions, MWCNT and its hybrids with various metals and metal oxides are capable of performing oxygen evolution reaction (OER) reactions also. In one of the study it is found that surface oxidized MWCNTs shows an excellent OER activity even in the absence of metal oxide catalyst [32]. The metal oxides of cobalt, copper, iridium etc. can form hybrid composites with MWCNT which can support OER reactions [33–35]. Some of the MWCNT hybrids can function as bifunctional electro-catalysts for overall water splitting [36]. The hetero-doping of nitrogen and sulphur to MWCNTs can enhance its ORR activity [37]. Some bi-functional catalysts can even play a dual role in oxygen evolution and oxygen reduction reactions [38]. It is very well established that electrocatalyst act as a support system for the transportation of charges in direct methanol fuel cells (DMFC). Metallic nanoparticles like Au, Ag, Pd, Rh, Pt and its alloys are commonly used anode materials involved in the methanol

oxidation reactions. MWCNT hybrid materials can act as substitute for these materials. MWCNTs act as strong support for the deposition of metallic nanoparticles and thereby enhancing the electrocatalytic activity in direct methanol fuel cells [39] and direct formic acid fuel cell (DFAFC) [40]. Metals co-doped with MWCNT can also perform its role as cathodic catalyst for alkaline membrane fuel cells [41] and in some cases MWCNTs act as electrocatalyst in polymer electrolyte membrane fuel cells (PEMFCs) [42]. Thus MWCNT is one of the promising support material for synthesizing electro catalysts due to its large surface area and high conductivity.

2.5. Field Emitters

Some of the diverse fields in which CNTs are established as promising material include flat displays, high resolution electron beam instruments, microwave amplifiers, X-ray sources and lighting tubes. MWCNTs can be utilized as field emitters since these have a potential to act as cold cathodes, they possess long term stability, minimal fluctuations and emits high current. MWCNTs can be decorated with various metals, metal oxides inorder to improve the field enhancement properties so that these can find applications in smart conductors, 3D displays and field emission displays [43–46].

2.6. Electromagnetic Absorbing Materials

Nowadays, the electromagnetic (EM) waves are used in electronic devices, healthcare devices, military, radar detection equipment's, pollution control and in stealth technology. Inorder for the absorption of electromagnetic waves, electromagnetic wave absorption (EMA) materials are required. The excellent properties of MWCNTs such as high electrical conductivity, light weight, greater surface area and high dielectric polarization ability enables MWCNTs to act as EMA materials and hence replaces the traditionally used electromagnetic materials that includes carbon black, graphite, ferrite composites etc. MWCNTs are activated with metals, metal oxides, magnetic materials, semiconductor dielectrics, polymers etc. in order to reinforce the attenuation properties of electromagnetic waves and these absorbed EM waves can be converted into thermal or any other forms [47–51].

2.7. Drug Delivery Platforms

There are numerous report on application of MWCNTs in targeted drug delivery systems. The unique properties of MWCNTs has attracted the pharmaceutical researchers and envisaged them to replace traditional drug carrier systems. It has been established that carbon nanotubes can be functionalized with biomolecules which include proteins, drugs, antibodies, DNA etc. The tubular structure of MWCNTs with numerous internal cavities has provided strong adsorption and a route for the attachment of desired functional groups. This has benefitted in high drug loading capacity which can improve the drug delivery mechanism there by improving the productiveness of the various drugs. The tubular structure of CNTs acts just like a needle and penetrates easily into the nucleus or cytoplasm of the cells enabling the drugs to reach the desired target site [52–54]. MWCNTs has created a breakthrough by actively involving in drug delivery systems, bioimaging, vaccine delivery, gene delivery, gene therapy etc. Drug delivery of various drugs like doxorubicin, dipyridamole, carbamazepine, silibinin etc has been carried out using MWCNTs [55–57].

2.8. Hydrogen Storage

Hydrogen is one of the ecofriendly fuel for clean and sustainable energy resources. But the storage and transportation of it is cumbersome that limits its application as green fuel. Hydrogen can be stored in three forms- either as compressive gas or liquid hydrogen in cryogenic form or in solid state. MWCNTs plays an important role in assisting hydrogen storage by acting as sorbent materials due to its enhanced adsorption properties. The hydrogen storage capacity is further enhanced by blending the MWCNTs with different metals or suitable hybrids. It is also noted that desorption of adsorbed hydrogen is also possible through adopting suitable experimental conditions [58–62].

2.9. Energy Conversion

With the advancement of material science, novel materials have been fabricated with advanced properties. MWCNTs are one among those materials which seek attention of global energy analysts and plays a key role in renewable energy conversion. MWCNTs due to its high abundance and low cost, together with its

special properties such as optical transparency, high conductivity and electrocatalytic activity find applications in transparent conductive films (TCFs) and solar cells [63]. MWCNTs and its modified forms are used to fabricate TCFs which are used as electrode materials in photovoltaic (PV) devices , liquid crystal displays (LCDs), transparent displays, touch panels and touch sensors and organic light emitting devices (OLED). MWCNTs are found to be flexible and can transmit light in UV and mid-IR spectral region and hence are found to be efficient candidates for replacing traditional TCFs like indium-doped tin oxide (ITO) and fluorine-doped tin oxide (FTO). The TCFs of MWCNTs were fabricated using various techniques which include spin coating, spray coating, molecular precursor method (MPM), hot press method [64-67] etc.

MWCNTs provide an excellent path for the movement of photo-generated electrons in dye sensitized solar cells (DSSCs). MWCNTs can serve as scaffold materials by establishing their significant role in the areas of working electrode, counter electrode and electrolyte of dye sensitized solar cells. In dye sensitized solar cells, dyes are usually absorbed by the working electrode and the effective functional materials consists of composites of different types of semiconducting metal oxide in which CNTs are incorporated within the composite matrix. Such hybrid materials helps in improving the charge transport processes, reducing the multiple grain boundaries thereby preventing the recombination of charges. Thus power conversion efficiency and short circuit current density are improved to a great extend [68,69]. The electrolytes which are used in dye sensitized solar cells include quasi solid state electrolytes in addition to various types of ionic liquids. Acid functionalized MWCNTs when compounded with these ionic liquid electrolytes has enhanced power conversion efficiency which increases the conductivity. The conventional counter electrodes used in DSSCs include ITO glass with thin layer of platinum deposited on it. The higher sheet resistance of MWCNTs have qualified them to perform their role as counter electrodes in DSSCs. The metallic and polymeric nanocomposites of MWCNTs are widely explored as the substitute for traditional counter electrodes [70–72].

2.10. Energy Storage

The hybrid materials of MWCNTS play an indispensable role in energy storage purposes which found application in various portable electronic devices. The open structure of CNTs and the enriched chirality makes the electron transport in CNT based hybrid materials. MWCNTs finds application in lithium ion batteries as it is used to develop both cathodic and anodic materials. Pristine CNTs and doped CNTs serves as very good anode material. Moreover CNTs can also act as conductive additives in anode fabrication with various types of nanostructured materials like transition metal oxides, silicon etc [73,74]. MWCNTs are found to be capable of acting as very good conductive materials in cathode along with the lithium metal oxides by establishing a good chemical bonding between them [75,76]. Further work is going on for developing electrode materials with free standing CNT in which active materials have been coated from its slurry form. Such robust materials with amazing features like high energy density and power density are the future materials for energy storage purposes. Besides these, research is progressing to incorporate CNTs in the areas of other rechargeable batteries which include lithium-sulphur batteries and lithium–air batteries [77-80]. Novel attempts has begun to commercialize such rechargeable batteries incorporating MWCNTs as cathode active materials.

In addition to LIBs, lithium-sulphur batteries and lithium-air batteries, the other modes of energy storage mechanism mainly includes electrochemical supercapacitors (ESs). These electrochemical supercapacitors can bridge the gap between ordinary capacitors and batteries and hence finds use in mobile phones, toys, electrical utilities, camera, medical appliances etc. The electrochemical supercapacitors are classified into two categories based on the charge-discharge mechanism. These mainly include electrochemical double- layer capacitors (EDLCs) and pseudocapacitors [81]. The charge storage mechanism in EDLCs involve non faradaic reactions on electrode surface where as in pseudocapacitor is due to reversible faradaic charge transfer on or near the electrode surface. MWCNTs can perform its role as electrochemical supercapacitor by establishing its role as conductive additives due to its large surface area and high conductivity. The low percolation threshold of MWCNTs enables diffusion of various ions towards its surface. CNT based electrodes especially MWCNT-polymer composites and

MWCNT-metal oxide composites fabricated by various methods are discovered to be excellent charge storing devices which can perform well as supercapacitors [82]. Conductive polymer electrodes as well as stretchable supercapacitors are developed by incorporation of polymers into MWCNTs. Such composites are found to exhibit good stability along with high specific capacitance [83,84]. Apart from these, MWCNT- metal oxides composites owns excellent pseudocapacitive properties [85,86]. Nowadays researchers are on the way to develop active materials based thick electrodes, which can very well perform as solid state super capacitors [87,88]. Studies suggests that, advanced MWCNTs composites are capable of accomplishing its role as supercapacitors by offering high charge-storage capacity.

2.11. Sensors

Sensors are devices used along with an electronic device capable of producing an output signal on behalf of any chemical or biological changes occurring in a system. Advances in technology have replaced the macrosensors by micro and nanosensors that finds applications in micro-electromechanical system (MEMS) and nanoelectromechanical system (NEMS) technology. The basic mechanism involved in sensing are; recognition of the receptor by the analyte and transduction to generate an output signal. MWCNT based sensors are found to be isotropic, possess high magnitude of sensing and also give fast response with high sensitivity. The large surface area of CNTs together with its high conductivity are the factors which make CNTs advantageous in the field of sensors. The sensors which are economic, easy to use and which are able to provide single-shot measurements are generally preferred in sensing platforms as chemical and biological sensors. Chemical sensors are devices which produce signals in response of chemical changes occurring in an analyte solution. If the recognition material involved in sensing is biological in nature, then it is called as a biosensor. MWCNTs and its hybrids has entrenched its role as sensors for a very long period. MWCNT-composite sensors are ultra-low energy consuming sensors and can perform its role as pressure sensors, strain sensors, piezo electric sensors, temperature gradient sensors, gas sensors, biosensors etc [89–91].

2.11.1. Pressure, Strain, Temperature and Humidity Sensors

MWCNT composites are promising candidates for the fabrication of compact and low cost flexible pressure sensors which can produce signals under external pressure. This enabled the replacement of silicon based sensors. Pressure sensors can be classified as resistive, capacitive and piezo electric sensors. MWCNT composites plays a crucial role in fabrication of all the three types of above mentioned pressure sensors [92–94]. MWCNTs along with suitable filler materials are excellent piezoelectric materials that finds application in various fields like medicine, automotive and energy harvesting systems [95–97]. Various composites of MWCNTs have been prepared by blending polymers and conductive nanomaterials for strain sensing applications. The sensors are found to be stable and exhibits high sensitivity [98–100]. Besides these, a large number of MWCNT-polymer composites find application in cryogenic temperature appliances. MWCNTs are very well capable of detecting changes in temperature and hence these are implemented to manufacture temperature sensors, thus making a substantial contribution to the microelectronic world [101–103]. The porous nature of MWCNTs and the large surface to volume ratio facilitates them to absorb large amount of molecules. The humidity responsiveness of MWCNT nanohybrids are excellent and hence such sensors can be employed for touchless positioning interface devices, biomedical applications, wearable electronic systems, soft robotics, skin-like electronics etc [104–107].

2.11.2. Gas Sensors

MWCNTs are prospective materials for gas sensing applications due to its hollow nature and large surface to volume ratio. These two features together with the excellent electrical conductivity are accountable for the adsorption and storage of gas molecules [108,109]. Polymers which are vapor sensitive, metal oxides which are semiconducting in nature and also porous materials are often incorporated along with MWCNTs for gas sensing mechanism. Gas sensing mechanism mainly involves adsorption and desorption of gas molecules in the interface between the analyte and sensing material. Gas sensors finds applications in pharmaceutics, for detecting leakage of gases in industries, environment monitoring, space exploration etc. MWCNT hybrids are found to be efficient as chemical sensor for detecting gases like nitrogen dioxide (NO_2), ammonia (NH_3), methane (CH_4), carbon dioxide (CO_2) and

hydrogen sulphide (H_2S) [110-122]. MWCNT based sensors are found to be well efficient in detecting volatile organic compounds (VOCs) like acetone, ethanol, benzene, toluene [123-131] etc. Thus MWCNTs when modified with certain noble metals or polymers or metal oxides or even when undergone activation to the walls of the tubules, can be applied for gas sensing applications at room temperatures. Thus a wide range of compact and commercially affordable sensors employing MWCNTs are manufactured for various applications.

2.11.3. Electrochemical Sensor for the Detection of Drugs and Heavy metals

Electrochemical sensors are devices capable of converting the reactions occurring on the surface of the electrode into measurable electrical signals. In such sensors the electrodes act as a transducer. Analyte will be either oxidized or reduced on the electrode surface. Thus a quantifiable information is obtained by measuring the current occurring due to the reaction between the analyte and electrode. The working principle of an electrochemical sensor is shown in Figure-2.1. Basically electrochemical sensors are classified into three types depending on the type of output signal. These include potentiometric, amperometric and impedimetric sensors where the output signals are voltage, current and impedance. In potentiometric sensors, potential is measured between working electrode and reference electrode of an electrochemical cell and is based on the formation of nernestian equilibrium. This gives information about the concentration of analyte. Alternatively, in the case of amperometric electrochemical sensing, current produced by the electroactive species are measured on application of constant potential. The impedimetric sensors work on the principle of EIS technique. The surface impedance of the electrochemical system under investigation is measured on application of small sinusoidal AC potential [132–134].

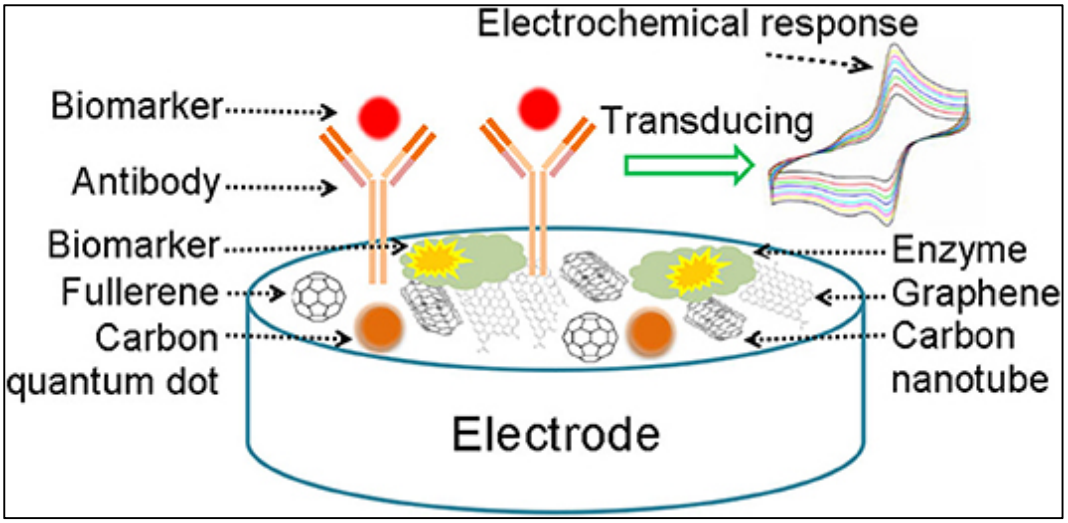

Figure-2.1. Schematic diagram showing the electrochemical sensing mechanism [134].

The results of the sensor performance of an electrochemical sensor are interpreted using various electrochemical sensing variables. The parameters governing the performance of an electrochemical sensor for its applicability in sensing platforms includes linear range, limit of detection, selectivity, sensitivity, recovery etc. In sensor studies, response signals of the electrode are measured on addition of analyte at various concentrations. The particular range of concentration of the analyte selected for sensor studies is considered as the linear range. Calibration curves are drawn by considering the linear range of concentration with respect to the response signals produced by the electrode. From the linear calibration curves the limit of detection (LOD) is calculated. LOD refers to the lowest concentration of the analyte that can be reliably detected with acceptable statistical certainty. Other important variables by which the analytical performance of an electrochemical sensor can be obtained are selectivity and recovery. Selectivity refers to the capability of the electrode to recognize the analyte of interest in presence of various interfering molecules. Acceptable recoveries should be obtained inorder for the electrochemical sensor to be authentic. The percentage recoveries of the analyte are calculated by comparing the results of spiked and unspiked portions of the sample under consideration. It has also been noted that pH plays a very significant role in the sensing performance of the sensor towards various analytes of interest. A slight change in pH of the medium can dramatically produce variations in the response

signals. So it is very important to choose appropriate medium with definite pH for the sensor studies [135,136].

Numerous biologically active materials including pharmaceutical compounds can be detected by using electro-analytical techniques especially voltammetry. Suitable electrodes are to be fabricated for the detection of drug molecules. MWCNT composite can act as sensors for the detection of different class of substances in commercial tablets. Researchers have discovered that MWCNT composite electrodes are very much efficient in detection of several classes of drugs including antipyretics, antidepressents, analgesics, opiate analgesics, ophthalmic drugs etc. [137-142]. Apart from drug detection, specialized MWCNT composites are very much capable of sensing synthetic dyes in food products and also fungicides in certain medicines [143,144].

One other major environmental issue is the pollution caused by heavy metals. These non-biodegradable pollutants arises from various natural as well as antropogenic factors. The high level of such pollutants can cause detrimental effects for environment as well as for human health. Low cost electrochemical sensors fabricated using MWCNTs and suitable composites can monitor the elevated levels of heavy metal ions in the environment [145–148].

2.11.4. Non-enzymatic Electrochemical Detection of Various Analytes

Various analytes like hydrogen peroxide, urea, glucose, ascorbic acid, dopamine etc can be detected by various methods which includes colorimetry, fluorimetry, chemiluminescene, electrochemical methods and so on. Among these methods, electrochemical technique is mostly preferred due to its low cost and high sensitivity. Electrochemical detection of these analytes can further be classified as enzymatic electrochemical sensors and non-enzymatic electrochemical sensors. Despite the fact that enzymatic sensors of MWCNTs in which biomolecules have been immobilised are highly sensitive for analyte molecules, certain drawbacks are related with such sensors. In the case of enzymatic sensors, the enzymes tend to denature to small changes in temperature, pH and humidity. The expensive nature of enzymes together with the monotonous immobilization procedures and sluggish purification techniques limits its use as sensors. Non-enzymatic sensors can eradicate

such limitations since various MWCNT based nanostructures are found to be economical, stable and possess long life. The synergistic effect of MWCNTs and the desired metal or metal oxide or polymers makes the non-enzymatic sensing mechanism trouble-free for the detection of various molecules. In spite of all these advantages, non enzymatic sensors requires high working potential, undergoes redox reactions which are unfeasible to predict and undergoes slow electrokinetic mechanisms leading to feeble response signals [149].

Advanced MWCNT based nanocomposites have been fabricated for the non-enzymatic electrochemical detection of H_2O_2. H_2O_2 represents the group of reactive oxygen species and is one of the common by-products of several enzymatic reactions. MWCNTs incorporated with metal, metal oxides, polymers, quantum dots etc are found to be sensitive for the detection of H_2O_2 molecules in accordance with various literatures [150–154]. Similar to hydrogen peroxide detection, detection of urea is also a very important since this is most commonly used in fertilizer industry, dairy, food and pharmaceutical fields. The presence of urea beyond a permissible level can cause severe health problems. MWCNT urea sensors are found to be highly stable and sensitive and hence these can replace enzymatic sensors commonly available for urea detection. Various MWCNT hybrid electrode materials have been explored by various researchers for the non-enzymatic sensing of urea [155–158].

Nowadays, continuous monitoring of blood glucose levels are crucial, since the conditions of diabetes mellitus are rising globally among mankind. A rich profusion of highly efficient and selective non-enzymatic glucose sensors have been fabricated in the past decades for glucose sensing. This has led to the way to replace the ideal enzyme, ‘glucose-l-oxidase’ for glucose oxidation reaction which played a dominant role in the first, second and third generation of glucose sensors. Finally fourth generation glucose sensors included a novel idea for the development of non-enzymatic glucose sensors which can directly oxidise glucose on the surface of electrodes constituting the desired nanomaterials [159,160]. The schematic diagram of glucose oxidation mechanism on electrode surface is shown in the Figure-2.2. MWCNT composites in conjunction with various metals, metal oxides, metal complexes, alloys, polymers, quantum dots and other carbon materials provides an ideal platform for the oxidation of glucose molecules. These surface modified MWCNTs enhance the electrocatalytic oxidation mechanism due to the increased

surface area along with the intrinsic electronic properties. Metals like platinum, gold, cobalt, nickel, ruthenium, copper etc, their bimetallic forms or their oxide forms or other polymers etc are often distributed on MWCNTs to achieve the desired glucose sensing mechanism. Voltammetric techniques and amperometric techniques are mostly employed in the electrochemical detection of glucose molecules [161–164]. The non-enzymatic sensors developed for glucose sensing can also be applied in the fuel cell industry. Researchers are on their way to replace batteries in the portable devices by glucose or other saccharide fuel cells in the near future [165,166].The non-enzymatic glucose sensors are capable of detecting sugar in food stuffs and hence such type of sensors finds application in food industry also.

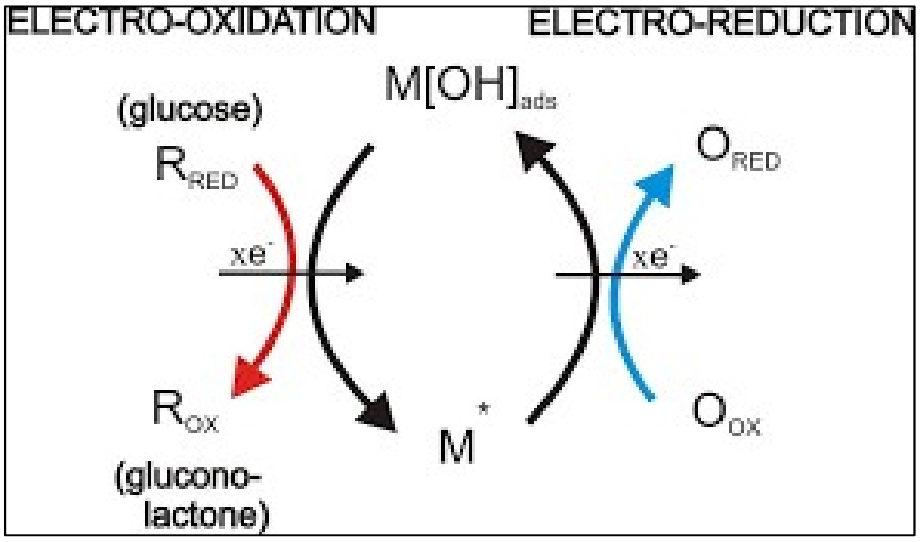

Figure-2.2. Schematic diagram representing oxidation of glucose [160].

MWCNT hybrids play a vital role in sensing of an important catecholamine neurotransmitter dopamine which helps in controlling behavioural and physiological conditions. Dopamine can act both as an excitory neurotransmitter and also an inhibitory neurotransmitter. Higher dopamine level can lead to heart failure, drug addiction and hypertension where as low dopamine level can result in alzheimer's disease, parkinson's disease, depression, stress etc. The principle behind detection of dopamine by amperometry, differential pulse voltammetry and cyclic voltammetry is the conversion of dopamine to dopamine-o-quinone by the sensing material on the working electrode surface [167,168]. The superior electron transfer ability between the electrode surface and the biomolecules and excellent electrical conductivity of metals, increased surface area and biocompactible nature of metal oxide nanostructure

drives them to be embedded as functional materials in the MWCNTs. MWCNTs modified with other carbon materials and also with conducting polymers are also explored in biosensing of the neurotransmitter [169–172]. In recent studies, it is noted that biosensor performances of many electrode materials increased when MWCNTs were functionalized with highly efficient materials and such modified electrodes can detect dopamine at very low levels even in presence of common interferants. Ascorbic acid is one of the common interferent molecule whose oxidation potential lies close to the potential of dopamine. Certain hybrid sensors of MWCNTs can detect ascorbic acid alone [173–175] and detection of ascorbic acid is also very important similar to dopamine since abnormal levels can lead to parkinson's diseases, alzheimer's disease and cardiovascular disorders. These type of hybrid electrochemical sensors are found to be stable, can operate at low temperatures and can detect the analytes in real samples. In summary, MWCNT-hybrid materials with excellent electrocatalytic activity are found to be efficient sensors for sensing dopamine along with the common interferents like ascorbic acid and uric acid [176]. Table-2.1 summarizes the different types of MWCNT-hybrid systems employed in the electrochemical sensing of various analytes.

Table 2.1: MWCNT-hybrid Systems for Electrochemical Sensing

Sl no	Electrode Material	Analyte detected	Linear range	LOD	Reference
1	MWCNT-CuBTC	Glucose	0.2-1 mM	10 µM	[161]
2	MWCNT/Ni-Co	Glucose	5-10 mM	1.2 µM	[162]
3	CHI-GOx/APTES/MWCNT-dPIn	Glucose	0.01-100 mM	10 µM	[163]
4	MWCNT/ZnO QDs	Glucose	0.1-2.5 µM	0.2 µM	[164]
5	Co_3O_4@MWNT	Glucose	Upto 11 mM	2 µM	[165]
6	MWCNT-RuO_2/CPE	Glucose	0.5-50 mM	33 µM	[177]
7	Ni $(OH)_2$-CNT-PVDF	Glucose	0.25-39.26 mM	0.023 mM	[178]
8	Pt Ag/MWCNT	Glucose	1-25 mM	600 µM	[179]
9	Pd- Ni@f-MWCNT	Glucose	0.01-1.4 mM	0.026 µM	[180]

10	Au-Pd/MWCNTs	Dopamine	0.98-200 µM	0.058 µM	[169]
11	ErGO/MWCNTs/PPy	Dopamine	25-1000 mM	2.3 nM	[170]
12	GQDS-MWCNT	Dopamine	0.005-100 µM	0.87 nM	[171]
13	f-MWCNT/AgNP	Dopamine	0-8 µM	0.2778 µM	[172]
14	Cu-NPs/c-MWCNT/PANI	Ascorbic acid	5-600 µM	1 µM	[173]
15	MWCNT-AONP	Ascorbic acid	0.16-0.640 µM	0.3663 µM	[174]
16	AF-MWCNT/EPI-CPE	Ascorbic acid	0-8 µM	4.1 µM	[175]
17	Zn-Ni NPs@f-MWCNT	Uric acid, Ascorbic acid and Dopamine	0.25-1.7 mM (dopamine) 0.2-1.2 mM (ascorbic acid)	0.0655 µM 0.5 µM	[176]
18	SnO_2/MWCNT/CPE	Dopamine, Uric acid and Ascorbic acid	0.3-50 µM (dopamine) 3-200 µM (Uric acid) 0.1-5 Mm (Ascorbic acid)	0.03 µM 1 µM 50 µM	[181]
19	Pt –MWCNT-Graphene	Dopamine and Ascorbic acid	2-50µM (dopamine) 100-120 µM (Ascorbic acid)	0.5 µM 10 µM	[182]
20	Acridine Orange - MWCNT	Dopamine and Ascorbic acid	0.1-90 µM (dopamine) 0.1-90 µM (Ascorbic acid)	0.03 µM 0.03 µM	[183]

CuBTC: Copper-1,3,5-benzene tricarboxylic acid

MWCNT: Multi walled carbon nanotubes

CHI-GOx: Glucose oxidase mixed with chitosan

APTES: 3-aminopropyl triethoxy silane

dPIn: doped polyindolle

QDs: Quantum dots

CPE: Carbon paste electrode

Ppy: Polypyrrole

ErGO: Electrochemically reduced graphene oxide

PANI: Poly aniline

AO: Antimony oxide

AF: Amino functionalized

EPI: Electro active polyimide

2.12. Scope of the Present Work

MWCNT- hybrids play a very dominant role in electrocatalysis of various analyte molecules. This is due to the outstanding properties of MWCNTs which include high surface area, small size, highly stable nature and excellent electrical and thermal properties. Thus MWCNT hybrid composites can perform its role in sensing and energy storage applications. The main problem regarding MWCNTs is their poor dispersability, which can be overcome by acid functionalization. When various metals and metal oxides are incorporated on these functionalized MWCNTs, a dramatic shift in properties is being noted which further leads to an enhanced sensing mechanism.

The focus theme of the present investigation is on development of facile, low cost and ecofriendly preparation of MWCNT hybrid films decorated with various metals and metal oxides which include Ag, Pd, WO_3, RuO_2, Fe_3O_4, Co_3O_4. These composites are prepared by various techniques including dip coating, drop casting, electroless and electrophoretic deposition techniques on various substrates inorder to find application in sensing of different analytes like dopamine, ascorbic acid, glucose etc. The fabricated Ag/fMWCNT and Cu-WO_3-MWCNT electrodes are flexible films

applied for sensing dopamine and analyzing the quality of lubricant oils which is subjected to various heat treatments. The Pd@MWCNT-Co_3O_4 electrode was used as an efficient sensor towards glucose oxidation. The cobalt oxide required for the development of the electrode is extracted from the spent Li-ion batteries, thus exploring a new step towards battery waste management. The hybrid composite RuO_2-Fe_3O_4-MWCNT synthesised using hydrothermal synthesis is an ideal sensor capable of simultaneous detection of dopamine and ascorbic acid. Some of the modified electrodes are also capable of performing its role as pseudocapacitors. In short, all the different hybrid electrode materials prepared can perform its role in sensing various analytes with high efficiency.

2.13. Objectives of the Present Investigation

The present work carried out deals with the fabrication of MWCNT based hybrid composites that can be utilized in various non-enzymatic sensing platforms. The hybrid composites included incorporation of metals like Ag, Pd etc and also some oxides of tungsten, ruthenium and iron on to MWCNT resulting in the formation of Ag/fMWCNT, Cu-WO_3-MWCNT, Pd@MWCNT-Co_3O_4electrode and RuO_2-Fe_3O_4-MWCNT composite electrodes. These individual composite electrodes can serve as sensors in the electrochemical detection of various analytes.

The motivation behind the present research work is briefed.

- A facile and economic method to develop flexible Ag/fMWCNT electrode film for sensing dopamine. The pseudocapacitive nature of fabricated film is also evaluated.
- The fabrication of flexible Cu-WO_3-fMWCNT electrode used to analyse the quality of engine oils subjected to various heat treatments. The electrodes were fabricated employing electroless and electrophoretic deposition techniques.
- For glucose sensing mechanism, an efficient Pd@MWCNT-Co_3O_4 electrode was developed by electrodeposition process. The cobalt required for the preparation of Co_3O_4 electrode was extracted from the spent lithium-ion batteries.
- Synthesis of RuO_2-Fe_3O_4-MWCNT composites by simple hydrothermal method, and the modified RuO_2-Fe_3O_4-MWCNT /GCE was used for the simultaneous electrochemical detection of both dopamine and ascorbic acid.

2.14. REFERENCES

1. Md Eshrat E Alahi. Multi-Walled Carbon Nanotubes-Based Sensors. In: Scholarly Community Encyclopedia. 2021.

2. V.R. Raphey, T.K. Henna, K.P. Nivitha, P. Mufeedha, Chinnu Sabu KP. Advanced biomedical applications of carbon nanotube. Mater Sci Eng. 2019;100:616–30.

3. Wen N, Zhang L, Jiang D, Wu Z, Li B, Sun C and Guo Z. Emerging flexible sensors based on nanomaterials: recent status and applications. J Mater Chem A. 2020;8:25499–527.

4. Chen J, Zheng J, Gao Q, Zhang J, Zhang J, Omisore OM, Wang L and Li H . Polydimethylsiloxane (PDMS)-based flexible resistive strain sensors for wearable applications. Appl Sci. 2018;8:345.

5. Siqi Li, Pengfei Lin, Liupeng Zhao, Chong Wang, Deye Liu, Fangmeng Liu, Peng Sun, Xishuang Liang, Fengmin Liu, Xu Yan, Yuan Gao GL. The room temperature gas sensor based on Polyaniline@flower-like WO_3 nanocomposites and flexible PET substrate for NH3 detection. Sensors Actuators, B Chem . 2018;259:505–13.

6. Ismael G. Serrano, J. Panda, Tomas Edvinsson and M.Venkata Kamalakar. Flexible transparent graphene laminates via direct lamination of graphene onto polyethylene naphthalate substrates. Nanoscale Adv. 2020;2:3156–63.

7. Mahmoud A Hussein, MM Alam, Abdullah MAsiri, Zahra M Al-Amshany, Khdejah SHajeeassa and Mohammed MRahman. Ultrasonic-assisted fabrication of polyvinyl chloride/mixed graphene-carbon nanotube nanocomposites as a selective Ag^+ ionic sensor. J Compos Mater. 2019;53:2271–84.

8. Parnian P. A Short Review on: Recent Advances in the Use of Carbon Nanotubes in Additive Manufacturing of Polymer Matrix Composites. Macromol Symp. 2022;405:1-4.

9. Nectarios Vidakis, Markos Petousis, Mirto Kourinou, Emmanuel Velidakis, Nikolaos Mountakis, Peder Erik Fischer-Griffiths, Sotirios Grammatikos & Lazaros Tzounis. Additive manufacturing of multifunctional polylactic acid (PLA)-multiwalled carbon nanotubes (MWCNTs) nanocomposites. Nanocomposites . 2021;7:184–99.

10. Laszlo Vanyorek , Emoke Sikora , Tamas Balogh , Krisztina Roman , Kalman Marossy, Peter Pekker , Tamas J. Szabo, Bela Viskolcz, Bela Fiser. Nanotubes as polymer composite reinforcing additive materials – A comparative study. Arab J Chem. 2020;13:3775–82.

11. Bartłomiej Podsiadły , Piotr Matuszewski andrzej Skalski and Marcin Sloma. Carbon Nanotube-Based Composite Filaments for 3D Printing of Structural and Conductive Elements. Appl Sci. 2021;11:1272.

12. Shangqin Yuan, Yun Zheng, Chee Kai Chua, Qingyu Yan KZ. Electrical and Thermal Conductivities of MWCNT/Polymer Composites Fabricated by Selective Laser Sintering. Compos Part A . 2017;105:203–13.

13. Lorenzo Paleari, , Mario Bragaglia, Francesco Fabbrocino, Raimondo Luciano and Francesca Nanni. Self-Monitoring Performance of 3D-Printed Poly-Ether-Ether-Ketone Carbon Nanotube Composites. Polymers (Basel). 2023;15:1–14.

14. Bikiaris D. Microstructure and Properties of Polypropylene/Carbon Nanotube

Nanocomposites. Materials (Basel). 2010;3:2884–946.

15. Deep N, Mishra P. Evaluation of mechanical properties of functionalized carbon nanotube reinforced PMMA polymer nanocomposite. Sci Direct . 2018;4:207–15.

16. Vijay Patel , Unnati Joshi AJ, Raul Duarte Salgueiral Gomes Campilho , Ankit D. Oza , Chander Prakash , Emanoil Linul, Sandeep Kumar and Kuldeep Kumar Saxena. Strength Evaluation of Functionalized MWCNT-Reinforced Polymer Nanocomposites Synthesized Using a 3D Mixing Approach. Materials (Basel). 2022;15:7263.

17. Kranthi Kumar Gangu, Suresh Maddila, Sreekantha B. Jonnalagadda. A review on novel composites of MWCNTs mediated semiconducting materials as photocatalysts in water treatment. Sci Total Environ . 2019;646:1398–412.

18. Zhijun Li, Lumei He, Liqiang Jing, Jingsheng Lin and Yunbo Luan. Facile synthesis of phosphate-functionalized MWCNT-TiO_2 nanocomposites as efficient photocatalysts and insights into the roles of nanostructured carbon. Chempluschem. 2013;78:670–6.

19. Lei Zhu, Ze-DaMeng andWon-COD. MWCNT-based Ag_2S-TiO_2 nanocomposites photocatalyst: Ultrasound-assisted synthesis, characterization and enhanced catalytic efficiency. J Nanomater. 2012;2012.

20. Thillai Sivakumar Natarajan, Joon Yeob Lee, Hari C. Bajaj, Wan-Kuen Jo RJ, Tayade. Synthesis of multiwall carbon nanotubes/TiO_2 nanotube composites with enhanced photocatalytic decomposition efficiency. Catal Today . 2017;282:13–23.

21. Wan Y, Cong T, Liang Q, Li Z, Xu S, Peng Y and Lu D. Facile in-situ solvothermal method to synthesize ZnPc-MWCNTs composites with enhanced visible light photocatalytic activity. Ceram Int . 2016;42:2425–30.

22. Malekkiani M, Heshmati Jannat Magham A, Ravari F, Dadmehr M. Facile fabrication of ternary MWCNTs/ZnO/Chitosan nanocomposite for enhanced photocatalytic degradation of methylene blue and antibacterial activity. Sci Rep . 2022;12:1–22.

23. M.F. Sanakousar, Vidyasagar. C.C , Victor M. Jiménez-Pérez , B.K. Jayanna , Mounesh , A.H. Shridhar KP. Efficient photocatalytic degradation of crystal violet dye and electrochemical performance of modified MWCNTs/Cd-ZnO nanoparticles with quantum chemical calculations. J Hazard Mater Adv . 2021;2:100004.

24. Jagadish Krishnegowda , Abhilash Mavinakere Ramesh , Akshatha Gangadhar S. Hydrothermal processing of interfacial $BiCeO_3$/MWCNTs photocatalyst for rapid dye degradation and its biological interest. J Environ Chem Eng . 2021;9:105774.

25. S. Vadivel, J. Theerthagiri, J. Madhavan, T. Santhoshini Priya NB. Enhanced photocatalytic activity of degradation of azo, phenolic and triphenyl methane dyes using novel octagon shaped BiOCl discs/MWCNT composite. J Water Process Eng . 2016;10:165–71.

26. Banizi ZT, Seifi M, Askari MB, Dehaghi SB, Zadeh MHR zadeh. Photoluminescence and photocatalytic studies of cadmium sulfide/multiwall carbon nanotube (CdS/MWCNT) nanocomposites. Optik (Stuttg) . 2018;158:882–92.

27. Nagajyothi PC, Veeranjaneya Reddy L, Devarayapalli KC, Prabhakar Vattikuti S V., Wee YJ. Environmentally Friendly Synthesis: Photocatalytic Dye Degradation and Bacteria Inactivation Using Ag/f-MWCNTs Composite. J Clust Sci . 2021;32:711–8.

28. Md. Asjad Hossain, Md. Elias, Dali Rani Sarker, Zidnia Rahman Diba, Jannatul

Morshed Mithun, Md Abul Kalam Azad, Iqbal Ahmed Siddiquey, Mohammed M. Rahman, Jamal Uddin MNU. Synthesis of Fe- or Ag-doped TiO_2–MWCNT nanocomposite thin films and their visible-light-induced catalysis of dye degradation and antibacterial activity. Res Chem Intermed . 2018;44:2667–83.

29. Liju Elias and A.ChitharanjanHegde. Electrolytic Synthesis of Ni-W-MWCNT Composite Coating for alkaline hydrogen evolution reaction. J Mater Eng Perform J. 2018;27:1033–9.

30. Do Hyung Kweon , Mahmut Sait Okyay , Seok-Jin Kim , Jong-Pil Jeon, Hyuk-Jun Noh, Noejung Park, Javeed Mahmood & Jong-Beom Baek. Ruthenium anchored on carbon nanotube electrocatalyst for hydrogen production with enhanced Faradaic efficiency. Nat Commun . 2020;11:1278.

31. Theophile Niyitanga, Prescott E. Evans, Thilini Ekanayake, Peter A. Dowben and Hae Kyung Jeong. Carbon Nanotubes-Molybdenum Disulfide Composite for Enhanced Hydrogen Evolution Reaction Department of Physics , Institute of Basic Science , Daegu University , Gyeongsan 712- 714 , Republic of Korea Department of Physics and Astronomy , University of Neb. Journel Electroanal Chem. 2019;845:39–47.

32. Xunyu Lu, Wai-Leung Yim, Bryan H.R. Suryanto and Chuan Zhao. Electrocatalytic oxygen evolution at surface- oxidized multiwall carbon nanotubes. J Am Chem Soc. 2015;137:2901–7.

33. Amutha Chinnappan, Dongxiao Ji, Chinnappan Baskar, Xiaohong Qin SR. 3-Dimensional MWCNT/CuO nanostructures use as an electrochemical catalyst for oxygen evolution reaction. J Alloys Compd . 2018;735:2311–7.

34. Cheng Y, Fan Yang, Jiafang Gong, Bohua Wu, Zhao Zhang and Jia Chu. Platinum Nanoparticles Decorated IrO_2 @ MWCNT as an Improved Catalyst for Oxygen Evolution Reaction. ChemistrySelect. 2021;6:7542–50.

35. Yu-Xia Zhang, Xin Guo, Xue Zhai Yi-Ming Yan and Ke-Ning Sun. Diethylenetriamine (DETA)-assisted anchoring of Co_3O_4 nanorods on carbon nanotubes as efficient electrocatalysts for the oxygen evolution reaction†. J Mater Chem A . 2015;3:1761–8.

36. Syedah Afsheen Zahra and Syed Rizwan. MWCNT-modified MXene as cost-effective efficient bifunctional catalyst for overall water splitting. RSC Adv. 2022;12:8405–13.

37. Gutru Rambabu, Zarina Turtayeva, Feina Xu, Gael Maranzana,Me´lanie Emo, Se´bastien Hupont, Mohamed Mamlouk, Alexandre Desforges and BV. Insights into the electrocatalytic behavior of nitrogen and sulfur co-doped carbon nanotubes toward oxygen reduction reaction in alkaline media. J Mater Sci. 2022;57:16739–54.

38. Yulong Liu, Drew C. Higgins, Jason Wu, Michael Fowler, Zhonhwei Chen. Cubic spinel cobalt oxide / multi-walled carbon nanotube composites as an efficient bifunctionalelectrocatalyst for oxygen reaction. Electrochem commun . 2013;34:125–9.

39. Asma Bensghaïer, Viplove Bhullar, Navdeep Kaur, Momath Lo, Myriam Bdiri, Aman Mahajan MC. " Painted CNT "@ Au nanoparticles : a nanohybrid electrocatalyst of direct methanol oxidation. Emergent Mater. 2021;4:515–24.

40. Pingping Yang , Li Zhang , Xuejiao Wei, Shiming Dong and Yuejun Ouyang. Pd_3Co1 Alloy Nanocluster on the MWCNT Catalyst for Efficient Formic Acid Electro-Oxidation. Nanomaterials. 2022;12:4182.

41. Ivar Kruusenberg, Dilip Ramani, Sander Ratso, Urmas Joost, Rando Saar, Protima Rauwel, Arunachala M. Kannan and Kaido Tammeveski. Cobalt–Nitrogen Co-doped Carbon Nanotube Cathode Catalyst for Alkaline Membrane Fuel Cells. ChemElectroChem. 2016;3 (9):1455–65.

42. Chanchal Gupta, Priyanka H. Maheshwari and Rama Kant. Effect of heat treatment and functionalization of MWCNT nanocomposite on the performance PEMFC electrocatalyst. AIP Conf Proc. 2020;030678:5–9.

43. Shabeena Saifi, Shama Parveen, Sunny Khan, Javid Ali, M. Husain and MZulfequar. Iron oxide-coated MWCNTs nanohybrid field emitters : a potential cold cathode for next-generation electron sources. J Mater Sci Mater Electron . 2020;31:17482–90.

44. Chen G, Song Y. Field emission from lateral Multiwalled carbon nanotube Yarn emitters. Front Mater |. 2016;3:1–6.

45. Richard J Parmee, Clare M Collins, William IMilne and Matthew TCole. X-ray generation using carbon nanotubes. Nano Converg. 2015;2:1–27.

46. Alexander A. Kuznetzov, Sergey B. Lee, Mei Zhang, Ray H. Baughman, Anvar A.Zakhidov. Electron field emission from transparent multiwalled carbon nanotube sheets for inverted field emission displays. Carbon N Y . 2009;48:41–6.

47. Cheng Bi, Meifang Zhu, Qinghong Zhang, Yaogang Li, Honqzhi Wang. Electromagnetic wave absorption properties of multi-walled carbon nanotubes decorated with La-doped $BaTiO_3$ nanocrystals synthesized by a solvothermal method. Mater Chem Phys . 2011;126:596–601.

48. Fakharpour M, Karimi R. Electromagnetic wave absorption properties of MWCNTs-COOH / cement composites with different shapes of chiral , armchair and zigzag. Fullerenes, Nanotub Carbon Nanostructures . 2021;29:386–93.

49. Xuegong Huang, Danpig Yu and Simin Wang. Microwave Absorption Properties of Multi-Walled Carbon Nanotubes/Carbonyl Iron Particles/Polyurethane Foams. Materials (Basel). 2022;15:5690.

50. Zhou Wang and Guang-Lin Zhao. Electromagnetic wave absorption of multi-walled carbon nanotube – epoxy composites in the R band. J Mater Chem C . 2014;2:9406–11.

51. Honglong Xing, Qingping Liu, Ligang Zhang, Ye Liu and Mingqiang Hu. One-Pot Hydrothermal Synthesis of MWCNT / ZrO_2 Composites for Enhancing Electromagnetic Wave Absorption Performance. Nano. 2020;15:1–10.

52. Julia Meihua Tan, Saifullah Bullo, Sharidha Fakurazi & Mohd Zobir Hussein. Preparation , characterisation and biological evaluation of biopolymer - coated multi - walled carbon nanotubes for sustained - delivery of silibinin. Sci Rep . 2020;10:16942. 73963-8

53. GP. Bhagath Singh, Chandu Baburao, Vedayas Pispati, Harshvardhan Pathipati, Narashimha Muthy SP and BGR. Carbon nanotubes-A novel drug delivery system. IJRPC. 2012;2:523–32.

54. Ghodsi Mohammadi Ziarani , Shadi Tahmasebi Ashtiani, Fathemeh Mohajer and Alizera Bandiei. The role of carbon nanotubes in antibiotics drug delivery. Front Drug Chem Clin Res. 2021;4:1–12.

55. Zhu W, Huang H, Dong Y, Han C, Sui X, Jian B. Multi-walled carbon nanotube-based

systems for improving the controlled release of insoluble drug dipyridamole. Exp Ther Med. 2019;17:4610–6.

56. Hossein Zare, Sepideh Ahmadi, Amir Ghasemi MG, Navid Rabiee M, Bagherzadeh M, Karimi TJ, Webster, Michael R Hamblin, Ebrahim Mostafavi. Carbon nanotubes: Smart drug/gene delivery carriers. Int J Nanomedicine. 2021;16:1681–706.

57. Giulia Risi, Nora Bloise, Daniele Merli, Antonia Icaro-Cornaglia, Antonella Profumo, Maurizio Fagnoni, Eliana Quartarone, Marcello Imbriani and Livia Visai. Invitro study of multiwall carbon nanotubes (MWCNTs) with adsorbed mitoxantrone (MTO) as a drug delivery system to treat breast cancer. RSC Adv. 2014;4:18683–93.

58. Muthu RN, Rajashabala S, Kannan R. Hexagonal boron nitride (h-BN) nanoparticles decorated multi-walled carbon nanotubes (MWCNT) for hydrogen storage. Renew Energy . 2016;85:387–94.

59. Ranveer A. Carbon Nanotubes and Its Environmental Applications. JECET. 2015;4:304–11.

60. Edgar Mosquera-Vargas , Rocío Tamayo , Mauricio Morel , Martín Roble, Donovan E.Diaz-Droguett. Hydrogen storage in purified multi-walled carbon nanotubes : gas hydrogenation cycles effect on the adsorption kinetics and their performance. Heliyon . 2021;7:e08494.

61. M. Mehrabi , P. Parvin, A. Reyhani, S. Z. Mortazavi. Hydrogen storage in multi-walled carbon nanotubes decorated with palladium nanoparticles using laser ablation/chemical reduction methods. Mater Res ExpresS. 2017;4.

62. Mosquera E, , Donovan E. Diaz-Droguett , Nicolás Carvajal , Martin Roble, Mauricio Morel, Rodrigo A. Espinoza . Characterization and hydrogen storage in multi-walled carbon nanotubes grown by aerosol-assisted CVD method. Diam Relat Mater . 2014;43:66–71.

63. Sandeep Kumar, Monika Nehra, Deepak Kediab, Neeraj Dilbaghi, K Tankeshwara Ki-Hyun Kim. Carbon nanotubes : A potential material for energy conversion and storage. Prog Energy Combust Sci. 2017;000:1–35.

64. Xiaogang Sun, Jie Wang, Wei Chen, Xu Li, Manyuan Cai, Long Chen, Zhiwen Qiu, Yapan Huang, Chengcheng Wei, Hao Hu and Guodong Liang. Transparent Conducting Thin Film Preparation of Carbon Nanotube. 2018.

65. S. Muhl, R. Aquilar Osorio and U.A.Martinez Huitle. Transparent conductive carbon nanotube films. Rev Mex F´ısica. 2017;63:439–47.

66. Hiroki Nagai, Naoki Ogawa and Mitsunobu Sato. Deep-ultraviolet transparent conductive MWCNT/SiO_2 composite thin film fabricated by uv irradiation at ambient temperature onto spin-coated molecular precursor film. Nanomaterials. 2021;11:1358.

67. L.N. Saw , M. Mariatti, A.R. Azura , A. Azizan, J.K.Kim. Transparent, electrically conductive and flexible films made from multiwalled carbon nanotube/epoxy composites. Compos Part B . 2012;43:2973–9.

68. Fahmid Kabir , Syed Nazmus Sakib and Sheikh Shehab Uddin. Effect of MWCNT 's concentration in TiO_2 based DSSC and degradation study of the cell. J Renew Sustain Energy. 2019;11:025906.

69. Bayram Kilic, Sunay Turkdogan, Aykut Astam, Oguz Can Ozer, Mansur Asgin, Hulya Cebeci Deniz Urk and Selin Pravadili Mucur. Preparation of Carbon Nanotube /

TiO_2Mesoporous Hybrid Photoanode with Iron Pyrite (FeS_2) Thin Films Counter Electrodes for Dye-Sensitized Solar Cell. Nat Publ Gr. 2016;6:27052.

70. Yonrapach Areerob, Chaowalit Hamontree, Phitchan Sricharoen, Nunticha Limchoowong, Supinya Nijpanich, Theeranuch Nachaithong Won-Chu Oh and Kongsak Pattarith. Synthesis of novel $MoWO_4$ with ZnO nanoflowers on multi-walled carbon nanotubes for counter electrode application in dye-sensitized solar cells. Sci Rep . 2022;12:12490.

71. Jia-Wun Li , Yu-Sheng Chen , Yan-Feng Chen , Jian-Xun Chen , Chung-Feng Jeffrey Kuo, Liang-Yih Chen and Chih-Wei Chiu. Enhanced Efficiency of Dye-Sensitized Solar Cells Based on Polymer-Assisted Dispersion of Platinum Nanoparticles/ Carbon Nanotubes Nanohybrid Films as FTO-Free Counter Electrodes. Polymers (Basel). 2021;13:3103.

72. Mehmood U, Ishfaq A, Sufyan M. Nanocomposites of Multi-walled Carbon Nanotubes and Titanium dioxide (MWCNTs / TiO_2) as affective counter electrode materials for Platinum-free Dye-Sensitized Solar Cells (DSSCs). Sol Energy . 2021;220:949–52.

73. Chaturvedi P, Kanagaraj AB, Choi D. $LiCrTiO_4$ -MWCNT self-standing electrodes as high performance anode for flexible Li-ion batteries. Mater Lett . 2021;304:130665.

74. Thauer E, , Alexander Ottmann , Philip Schneider, Lucas Möller, Lukas Deeg, Rouven Zeus , Florian Wilhelmi , Lucas Schlestein CN, Ghunaim R, Markus Gellesch , Christian Nowka , Maik Scholz , Marcel Haft , Sabine Wurmehl, Karolina Wenelska EM, , Aakanksha Kapoor , Ashna Bajpai, Silke Hampel and Rudiger Klingeler. Filled Carbon Nanotubes as Anode Materials for Lithium-Ion Batteries. Molecules. 2020;25:1064.

75. Guohui Qin, Quanping Wu, Jun Zhao, Qianqian Ma, Chengyang Wang. C/$LiFePO_4$/MWCNTs cathode material with enhanced electrochemical performance for lithium-ion batteries. J Power Sources . 2014;248:588–95.

76. Yindan Liu & Guohua Gao & Xing Liang & Guangming Wu. Nanofibers of V_2O_5 /C@ MWCNTs as the cathode material for lithium-ion batteries. J Solid State Electrochem. 2018;22:2385–93.

77. Mingbo Zheng, Yao Chi, Qin Hu, Hao Tang, Xinliang Jiang, Li Zhang, Songtao Zhang, Huang Pang and Qiang Xu. Carbon nanotube-based materials for lithium-sulfur batteries. J Mater Chem A. 2019;7:17204–41.

78. Wei H, , Yong Liu XZ, , Fei Wang, , Xinyuan Ren , Feng Tao , Tengfei Li, Guangxin Wang and Fengzhang Ren. Application of Carbon Nanotube-Based Materials as Interlayers in High-Performance Lithium-Sulfur Batteries: A Review. Front Energy Res. 2020;8:1–12.

79. Nomura A, Ito K, Kubo Y. CNT Sheet Air Electrode for the Development of Ultra-High Cell Capacity in Lithium-Air Batteries. Sci Rep. 2017;7:1–8.

80. Jingbo Yang , Dingtao Ma , Yongliang Li , Peixin Zhang, Hongwei Mi , Libo Deng , Lingna Sun, Xiangzhong Ren. Atomic layer deposition of amorphous oxygen-deficient TiO_2-x on carbon nanotubes as cathode materials for lithium-air batteries. J Power Sources . 2017;360:215–20.

81. Parnia Forouzandeh, Vignesh Kumaravel and Suresh.C.Pillai. Electrode materials for supercapacitors: A review of recent advances. Catalysts. 2020;10:1–73.

82. Jiang K, Gerhardt RA. Fabrication and Supercapacitor Applications of Multiwall Carbon Nanotube Thin Films. J Carbon Res Rev. 2021;7:70.

83. Ates M, Serin MA, Calisskan S. Electrochemical supercapacitors of PANI/MWCNT, PEDOT/MWCNT and PANI-CO-EDOT/MWCNT nanocomposites. Polym Bull . 2019;76:3207–31.

84. Xi Wang, Chongyang Yang, Jie Jin, Xingwei Li, Qilin Cheng and Gengchao Wang. High-performance stretchable supercapacitors based on intrinsically stretchable acrylate rubber/MWCNTs@conductive polymer composite electrodes. J Mater Chem A. 2018;6:4432–42.

85. Christopher Nolly, Chinwe O. Ikpo, Miranda M. Ndipingwi, Precious Ekwere and Emmanuel IIwuoha. Pseudocapacitive Effects of Multi-Walled Carbon Nanotubes-Functionalised Spinel Copper Manganese Oxide. Nanomaterials. 2022;12:3514.

86. Adekunle AS, Ozoemena KI, Agboola BO. MWCNTs/metal (Ni, Co, Fe) oxide nanocomposite as potential material for supercapacitors application in acidic and neutral media. J Solid State Electrochem. 2013;17:1311–20.

87. Vikas Sharma, Kim SJ, Kim NH, Lee JH. All-solid-state asymmetric supercapacitor with MWCNT-based hollow $NiCo_2O_4$ positive electrode and porous Cu_2WS_4 negative electrode. Chem Eng J . 2021;415:128188.

88. Pal R, Goyal SL, Rawal I. High-performance solid state supercapacitors based on intrinsically conducting polyaniline/MWCNTs composite electrodes. J Polym Res. 2020;27:179.

89. Rajalakshmi Maheswaran, Balasivanandha Prabhu Shanmugavel. A Critical Review of the Role of Carbon Nanotubes in the Progress of Next - Generation Electronic Applications. J Electron Mater . 2022;51:2786–800.

90. https://www.utmel.com. Sensor Basics: Classification, Working Principle and application.

91. http://www.tescagobal.com. What Is A Sensor? Different Types Of Sensors With Applications.

92. A.Z. Hajjaja, K.N. Chappandaa, N.M. Batra, M.A.A. Hafiz, P.M.F.J. Costa, MIYounis. Miniature pressure sensor based on suspended MWCNT. Sensors Actuators A Phys . 2019;292:11–6.

93. Tim Mike de Rijk and Walter Lang. Low-Cost and Highly Sensitive Pressure Sensor with Mold-Printed Multi-Walled Carbon Nanotubes Dispersed in Polydimethylsiloxane. Sensors. 2021;21:5069.

94. YiCheng Yang, ShiYu Liu, Jin Pan and JianGang Lu. A Highly Sensitive Resistive Pressure Sensor with MWCNT Nanoparticles- Liquid Crystal-PDMS Composite. SID Symp Dig Tech Pap. 2018;49:1913–6.

95. S. Banerjee, W. Du, U. Sundar and K.A.Cook-Chennault. Piezoelectric and Dielectric Characterization of MWCNT-Based Nanocomposite Flexible Films. J Nanomater. 2018;2018.

96. Hosseini SM, Yousefi AAY. Piezoelectric sensor based on electrospun PVDF-MWCNT-Cloisite 30B hybrid nanocomposites. Org Electron . 2017;50:121–9.

97. Shuaichao chen, Jianlin Luo, Xiaoli Wang, Qiuyi Li, Liucong Zhou CL& chao feng.

Fabrication and Piezoresistive / Piezoelectric Sensing Characteristics of Carbon Nanotube / PVA / Nano-ZnO Flexible Composite. Sci Rep . 2020;10:8895.

98. Tarun Singla, Amrinder Pal Singh, Suresh Kumar, Gagandeep Singh and Navin Kumar. Characterization of MWCNTs-polystyrene nanocomposite based strain sensor. In: J Process MeProc IMechE Part E: J Process Mechanical Engineeringhanical Engineering. 2020. p. 1–7.

99. Kaiyan Huang , Huiming Ning , Ning Hu , Feng Liu , Xiaopeng Wu, Shu Wang , Yaolu Liu , Rui Zou , Weifeng Yuan , Alamusi LW. Ultrasensitive MWCNT / PDMS composite strain sensor fabricated by laser ablation process. Compos Sci Technol . 2020;192:108105.

100. Anindya Nag, Md. Eshrat EAlahi, Subhas Chandra Mukhopadhyay and Zhi Liu. Multi-Walled Carbon Nanotubes-Based Sensors for Strain Sensing Applications. sensors. 2021;21:1261.

101. G. Matzeu,A. Pucci,S. Savi,M. Romanelli, F. D. Francesco. A temperature sensor based on a MWCNT / SEBS nanocomposite. Sensors Actuators A Phys . 2012;178:94–9.

102. Rajarajan Ramalingame, Jose Roberto Bautista-Quijano OK and, Danrlei de Farias Alves. Temperature Self-Compensated Strain Sensors based on MWCNT-Graphene Hybrid Nanocomposite. J Compos Sci. 2019;3:96.

103. Bogdan Florian Monea, , Eusebiu Ilarian Ionete, Stefan Ionut Spiridon, Daniela Ion-Ebrasu and Emil Petre. Carbon Nanotubes and Carbon Nanotube Structures Used for Temperature Measurement. sensors. 2019;19:2464.

104. C. L. Cao, C. G. Hu, L. Fang, S. X.Wang, Y. S. Tian and C.Y. Pan. Humidity Sensor Based on Multi-Walled Carbon Nanotube Thin Films. J ofNanomaterials. 2011;2011.

105. Vikram S. Turkani DM, Binu B. Narakathu, Tahseen S. Saeed, Sherine O. Obare, Bradley J. Bazuin and Massood Z. Atashbar. A highly sensitive printed humidity sensor based on a functionalized MWCNT/HEC composite for fl exible electronics application. Nanoscale Adv. 2019;1:2311–22.

106. Kim HS, Kang JH, Hwang JY. Wearable CNTs - based humidity sensors with high sensitivity and flexibility for real - time multiple respiratory monitoring. Nano Converg . 2022;9:35.

107. Mohit Tannarana, Pratik M. Pataniya, Sanjay A. Bhakhar, G. K. Solanki, Jignesh Valand, Som Narayan, Kirit D. Patel, Prafulla K. Jha and V. M. Pathak. Humidity Sensor Based on Two-Dimensional $SnSe_2$ /MWCNT Nanohybrids for the Online Monitoring of Human Respiration and a Touchless Positioning Interface. ACS Sustain Chem Eng. 2020;8:12595–602.

108. Wang Y, Yeow JTW. A Review of Carbon Nanotubes-Based Gas Sensors. J Sensors. 2009;2009.

109. Md.Masud Rana, Dauda Sh. Ibrahim, M.R. Mohd Asyraf, S. Jarin, Amanullah Tomal A. A review on recent advances of CNTs as gas sensors. Sens Rev. 2017;37:127–36.

110. Jin-Chern Chiou and Chin-Cheng Wu . A Wearable and Wireless Gas-Sensing System Using Flexible Polymer/Multi-Walled Carbon Nanotube Composite Films. Polymers (Basel). 2017;9:457.

111. Nisreen M. Al-Makram and Wasan R. Saleh. Functionalized multi-walled carbon

nanotubes network sensor for NO_2 gas detection at room temperature. AIP Conf Proc. 2020;2290:050031.

112. Nguyen Manh Hung, Nguyen Duc Chinh, Tien Dai Nguyen, Eui Tae Kim, GyuSeok Choi, Chunjoong Kim DK. Carbon nanotube-metal oxide nanocomposite gas sensing mechanism assessed via NO_2 adsorption on n-WO_3/p -MWCNT nanocomposites. Ceram Int . 2020;46:29233–43.

113. Alexander G. Bannov, Maxim V. Popov andrei E. Brester and Pavel B. Kurmashov. Recent Advances in Ammonia Gas Sensors Based on Carbon Nanomaterials. Micromachines. 2021;12:186.

114. Debasis Maity, Mathankumar Manoharan and Ramasamy Thangavelu Rajendra Kumar. Development of the PANI / MWCNT Nanocomposite-Based Fluorescent Sensor for Selective Detection of Aqueous Ammonia. ACS Omega. 2020;15:8414–22.

115. Prashant Shukla , Pooja Saxena , Devinder Madhwal , Nitin Bhardwaj, Vinod Jain. Electrostatically functionalized CVD grown multiwalled carbon nanotube / palladium nanocomposite (MWCNT / Pd) for CH_4 detection at room temperature. Res Sq. 2022;0–20.

116. George Chimowa, Zamaswazi P. Tshabalala, Amos A. Akande, George Bepete, Bonex Mwakikunga, Suprakas S. Ray, Evans M. Benecha. Improving methane gas sensing properties of multi-walled carbon nanotubes by vanadium oxide filling. Sensors Actuators B. 2017;247:11–8.

117. Michela Sainato, Md Tanim Humayun, Lara Gundel, Paul Solomon, Liliana Stan, Ralu Divan IP. Parts Per Million CH_4 Chemoresistor Sensors Based on multi wall Carbon Nanotubes / Metal-oxide Nanoparticles. IEEE sensors. 2016; (1):4–6.

118. R.George, L.A.Kumar MA. Synthesis of nanotubular NiO-CNT composite and its application in temperature independent CO_2 gas sensors fabricated using interdigitated silver electrode. Dig J Nanomater Biostructures. 2019;14:213–24.

119. Zohauddin Ahmad, Naseema, Samrah Manzoora, Mohammad Talib, S.S. Islam PM. Self-standing MWCNTs based gas sensor for detection of environmental limit of CO_2. Mater Sci Eng B . 2020;255:114528.

120. Ami Hannon and Jing Li. Solid State Electronic Sensors for Detection of Carbon Dioxide. sensors. 2019;19:3848.

121. Jae Hoon Bang, Ali Mirzaei, Myung Sik Choi , Seungmin Han , Ha Young Lee , Sang Sub Kim Hyoun Woo Kim. Decoration of multi-walled carbon nanotubes with CuO / Cu_2O nanoparticles for selective sensing of H_2S gas. Sensors Actuators B Chem . 2021;344:130176.

122. Parsafar, Nahid; Ghafouri, Vahid; Banaei A. Electrochemical Sensing of H2S Gas in Air by Carboxylated Multi-walled Carbon Nanotubes. Iran J Chem Chem Eng. 2019;38:53–62.

123. Jin-Chern Chiou, Chin-Cheng Wu and Tse-Mei Lin. Sensitivity Enhancement of Acetone Gas Sensor using Polyethylene Glycol / Multi-Walled Carbon Nanotubes Composite Sensing Film with Thermal Treatment. Polymers (Basel). 2019;11:423.

124. Sheng-Joue Young, Yi-Hsing Liu, Zheng-Dong Lin, Kumkum Ahmed, MD Nahin Islam Shiblee,Sean Romanuik, Praveen Kumar Sekhar, Thomas Thundat, Larry Nagahara, Sandeep Arya, Rafiq Ahmed, Hidemitsu Furukawa and Ajit Khosla. Multi-

Walled Carbon Nanotubes Decorated with Silver Nanoparticles for Acetone Gas Sensing at Room Temperature. J Electrochem Soc. 2020;167.

125. Debasis Maity, Krishnamoorthy Rajavel, Ramasamy Thangavelu Rajendra Kumar. Polyvinyl alcohol wrapped multiwall carbon nanotube (MWCNTs) network on fabrics for wearable room temperature ethanol sensor. Sensors Actuators B Chem . 2018;261:297–306.

126. Shaalan NM, Ahmed F, , Mohamed Rashad, Osama Saber SK, Aljaafari A, Ashoaibi A, Ezzeldien Mahmoud A Z and Ezzeldien M. Low-Temperature Ethanol Sensor via Defective Multiwalled Carbon Nanotubes. Materials (Basel). 2022;15:4439.

127. Abolanle Adekunle, Oluwatobi S. Oluwafemi, Ncapayi Vuyelwa, Rotimi Sadiku , John Agee, Sunday Ojo and Sandila Songca. Ethanol Sensor Based On Platinum-MWCNT-NiO Nanoparticles Platform Electrode. Int J Electrochem Sci. 2012;7:2695–709.

128. Thanattha Chobsilp, Worawut Muangrat, Chaisak Issro, Weerawut Chaiwat, Apiluck Eiad-ua, Komkrit Suttiponparnit, Winadda Wongwiriyapan and Tawatchai Charinpanitkul. Sensitivity Enhancement of Benzene Sensor Using Ethyl Cellulose-Coated Surface-Functionalized Carbon Nanotubes. J sensors. 2018;2018:9.

129. Thanattha Chobsilp, Winadda Wongwiriyapan, Chaisak Issro, Worawut Muangrat, Weerawut Chaiwat, Apiluck Eiad-ua, Tawatchai Charinpanitkul and Komkrit Suttiponpanit. Study on Effect of Acid and Heat Treatments of Multi-Walled Carbon Nanotubes on Benzene Detection. Adv Mater Res. 2015;1103:105–11.

130. Nadra Bohli, Meryem Belkilani, Juan Casanova-Chafer, Eduard Llobet and Adnane Abdelghani. Multiwalled carbon nanotube based aromatic volatile organic compound sensor : sensitivity enhancement through 1-hexadecanethiol functionalisation. Beilstein J Nanotechnol 2019,. 2019;10:2364–73.

131. Ni Luh Wulan Septiani, Brian Yuliarto, Nugraha, Hermawan Kresno Dipojono. Multiwalled carbon nanotubes – zinc oxide nanocomposites as low temperature toluene gas sensor. Appl Phys A. 2017;123:166.

132. Zhang C, Du X. Electrochemical Sensors Based on Carbon Nanomaterial Used in Diagnosing Metabolic Disease. Front Chem. 2020;8:1–8.

133. Faria RAD de, Luiz Guilherme Dias Heneine, Tulio Matencio, Younès Messaddeq. Recent trends in the electroanalytical detection of food fraud. Int J Biosens Bioelectron. 2019;5:63–7.

134. Nitin Kumar Sharma, Abhimanyu Nain, Kuldeep Singh, Nisha Rani, Anuj Singal. Impedimetric Sensors : Principles , Applications and Recent Trends. IJITEE. 2019;8:4015–25.

135. Elio Desimoni, Barbara Brunetti. Presenting Analytical Performances of Electrochemical Sensors . Some Suggestions. Electroanalysis. 2013;25:1645–51.

136. Loock H, Wentzell PD. Detection limits of chemical sensors : Applications and misapplications. Sensors Actuators B Chem . 2012;173:157–63.

137. Arthur T. Chipeture, Daniel Apath, Mambo Moyo and Munyaradzi Shumba. Multiwalled carbon nanotubes decorated with bismuth (III) oxide for electrochemical detection of an antipyretic and analgesic drug paracetamol in biological samples. J Anal Sci Technol. 2019;5.

138. Aftab Aslam Parwaz Khan. Electrocatalytic Behavior and Determination of Amitriptyline Drug with MWCNT@Celllulose Composite Modified Glassy Carbon Electrode. Materials (Basel). 2020;13:1708.

139. Mahadeva Singh Jat, Varsha Jakhar and D. K. Sharma. Electrochemical determination of anti-depressant drug mirtazapine employing nafion/f-MWCNTs composite at glassy carbon electrode. Int J Pharm Sci Res. 2021;12:6442–52.

140. Jayant I. Gowda, Arunkumar T. Buddanavar, Sharanappa T. Nandibewoor. Fabrication of multiwalled carbon nanotube- surfactant modified sensor for the direct determination of toxic drug 4-aminoantipyrine. J Pharm Anal . 2015;5:231–8.

141. Qian Yu, Xianhui Yang, Yan Chen. Electrochemical Detection of Codeine in Pharmaceutical Tablets Using a Tungsten Oxide Nanoparticles and Carbon Nanotubes Modified Electrode. Int J Electrochem Sci. 2016;11:6862–72.

142. Ersin Demir, Onur Inam, Recai Inam and HassanY.Aboul-Enein. Voltammetric Determination of Ophthalmic Drug Dexamethasone Using Poly-glycine Multi Walled Carbon Nanotubes Modified Paste Electrode. Curr Anal Chem. 2018;14:83–9.

143. Kobun Rovina, Shafiquzzaman Siddiquee and Sharifudin Md Shaarani. An electrochemical sensor for the determination of tartrazine based on CHIT / GO / MWCNTs / AuNPs composite film modified glassy carbon electrode. Drug Chem Toxicol . 2019;44:447–57.

144. Xue Zhang, Juan Du, Dongping Wu, Xiaoyi Long, Dan Wang, Jianhua Xiong, Wanming Xiong and Xiaoning Liao. Anchoring Metallic MoS_2 Quantum Dots over MWCNTs for Highly Sensitive Detection of Postharvest Fungicide in Traditional Chinese Medicines. ACS Omega. 2021;6:1488–96.

145. Endale Tesfaye, Bhagwan Singh Chandravanshi NN and Merid Tessema. Development of a new electrochemical method for the determination of copper (II) at trace levels in environmental and food samples. RSC Adv. 2022;12:35367–82.

146. S.P. Sreekanth, Abdullah Alodhay, Abdulaziz K. Assaifan, Khalid Eidah Alzahrani, Muthumareeswaran Muthuramamoorthy, Hend I. Alkhammash , Saravanan Pandiaraj, Abdullah M. Alswieleh , Quyet Van Le, R. Mangaiyarkarasi andrews Nirmala Grace, Vimala Raghavan. Multi-walled carbon nanotube-based nanobiosensor for the detection of cadmium in water. Environ Res . 2021;197:111148.

147. Hasan Bagheri, Abbas Afkhami HK, Mosayeb Rezaei, Ali Shirzadmehr. Chemical Simultaneous electrochemical determination of heavy metals using a triphenylphosphine / MWCNTs composite carbon ionic liquid electrode. Sensors Actuators B Chem . 2013;186:451–60.

148. Gilbert Ringgit, Shafiquzzaman Siddiquee, Suryani Saallah and Mohammad Tamrin Mohamad Lal. A sensitive and rapid determination of zinc ion (Zn^{2+}) using electrochemical sensor based on f - MWCNTs / CS / PB / AuE in drinking water. Sci Rep . 2022;12:18582.

149. Dayakar Thatikayala, Deepalekshmi Ponnamma, Kishor Kumar Sadasivuni, John-John Cabibihan, Abdulaziz Khalid Al-Ali, Rayaz A. Malik, Booki Min. Non-Enzymatic Electrochemical Sensing. In: Scholarly Community Encyclopedia. 2019.

150. C. Revathi, Rajavel Krishnamoorthy,MSaranya and Rajendrakumar Rt. MWCNT Based Non-Enzymatic H_2O_2 Sensor : Influence of Amine Functionalization on the Electrochemical H_2O_2 Sensing. J Electrochem Soc. 2016;163:627–32.

151. Dongqing Xu, Bingbing Hou , Lisheng Qian, Xueji Zhang and Guodong Liu. Non-Enzymatic Electrochemical Sensor Based on Sliver Nanoparticle-Decorated Carbon Nanotubes. Molecules. 2019;24:3411.

152. Muthu Dinesh, Chinnasamy Revathi, Yuvaraj Haldorai, Ramasamy Thangavelu Rajendra Kumar. Birnessite MnO_2 decorated MWCNTs composite as a nonenzymatic hydrogen peroxide sensor. Chem Phys Lett . 2019;731:136612.

153. Zhiying Miao, Di Zhang and Qiang Cheng. Non-enzymatic Hydrogen Peroxide Sensors Based on Multi-wall Carbon Nanotube/Pt Nanoparticle Nanohybrids. Materials (Basel). 2014;7:2945–55.

154. Huaan Zhong & Ruo Yuan & Yaqin Chai & Yu Zhang & Chengyan Wang & Feng Jia. Non-enzymatic hydrogen peroxide amperometric sensor based on a glassy carbon electrode modified with an MWCNT / polyaniline composite film and platinum nanoparticles. Microchim Acta. 2012;176:389–95.

155. Hend S. Magar, Rabaey Y.A. Hassan and Mohammed Nooredeen Abbas. Non - enzymatic disposable electrochemical sensors based on CuO/Co_3O_4 @ MWCNTs nanocomposite modified screen - printed electrode for the direct determination of urea. Sci Rep . 2023;13:2034.

156. Thao Quynh Ngan Tran, Gautam Das, HHYoon. Nickel-metal organic framework / MWCNT composite electrode for non-enzymatic urea detection. Sensors Actuators B Chem . 2017;243:78–83.

157. Thao Quynh Ngan Tran, Suk Won Yoon, Bang Ju Park, Hyon Hee Yoon. CeO_2-modified $LaNiO_6.FeO_4.O_3$ perovskite and MWCNT nanocomposite for electrocatalytic oxidation and detection of urea. J Electroanal Chem . 2018;818:76–83.

158. Subodh Barthwal and Nakshatra B. Singh. Urea detection by ZnO-MWCNT nanocomposite sensor. Mater Today Proc . 2020;29:749–52.

159. N. S. Oliver, C. Toumazou, A.E.G.Cass and D. G. Johnston. Glucose Sensors : A Review of Current and Emerging Technology. Diabet Med. 2009;26:197–210.

160. Kathryn E. Toghill and Richard G. Compton. Electrochemical Non-enzymatic Glucose Sensors : A Perspective and an Evaluation. Int J Electrochem Sci. 2010;5:1246–301.

161. Victor Vinoth, Gowrishankar Subramaniyam, Sambandam Anandan , Hector Valdes, Paulraj Manidurai. Non-enzymatic glucose sensor and photocurrent performance of zinc oxide quantum dots supported multi-walled carbon nanotubes. Mater Sci Eng B. 2021;265:115036.

162. K.Ramachandran, T. Raj kumar, K. Justice Babu and G. Gnana kumar. Ni-Co bimetal nanowires filled multiwalled carbon nanotubes for the highly sensitive and selective non-enzymatic glucose sensor applications. Sci Rep. 2016;6:36583.

163. Adriana Remes, Florica Manea , Sorina Motoc (m. Ilies) , Anamaria Baciu, Elisabeta I. Szerb, Jorge Gascon and Georgiana Gug. Highly Sensitive Non-Enzymatic Detection of Glucose at MWCNT-CuBTC Composite Electrode. Appl Sci. 2020;10:8419.

164. Katesara Phasuksom and Anuvat Sirivat. Chronoampermetric detection of enzymatic glucose sensor based on doped polyindole / MWCNT composites modified onto screen-printed carbon electrode as portable sensing device for diabetes. RSC Adv Open. 2022;12:28505–18.

165. Jiao K, Jiang Y, Kang Z, Peng R, Jiao S and Hu Z. Three-dimensional Co_3O_4 @ MWNTs nanocomposite with enhanced electrochemical performance for nonenzymatic glucose biosensors and biofuel cells. R SocOpen sci. 2017;4:170991.

166. Yue Zhao, Louzhen Fan , Dongmei Gao, Jingling Ren, Bo Hong. High-power non-enzymatic glucose biofuel cells based on three- dimensional platinum nanoclusters immobilized on multiwalled carbon nanotubes. Electrochim Acta . 2014;145:159–69.

167. Sophie Lakard, Ileana –Alexandra Pavel and Boris Lakard. Electrochemical Biosensing of Dopamine Neurotransmitter : A Review. Biosensors. 2021;11:179.

168. Liu X, Liu J. Biosensors and sensors for dopamine detection. View. 2021;2:1–16.

169. Zhen Zhu , Hsiang-Ning Luk , Yu-Shih Liu , Ren-Jang Wu, Ming-Hung Chung and Xu-Jia Chang. Preparation of Bimetallic Au-Pd / MWCNTs Electrode for Detection of Dopamine. Minerals. 2022;12:1145.

170. Vijayaraj Kathiresan, Dinakaran Thirumalai, Thenmozhi Rajarathinam, Miri Yeom, Jaewon Lee, Suhkmann Kim J-HY and S-CC. A simple one-step electrochemical deposition of bioinspired nanocomposite for the non-enzymatic detection of dopamine. J Anal Sci Technol. 2021;12.

171. Qitong Huang, Xiaofeng Lin, Lili Tong and Qing-Xiao Tong. Graphene Quantum Dots/Multiwalled Carbon Nanotubes Composite-Based Electrochemical Sensor for Detecting Dopamine Release from Living Cells. ACS Sustain Chem Eng. 2020;8:1644–50.

172. Isa Anshori, Lavita Nuraviana Rizalputri, Raih Rona Althof, Steven Sean Surjadi, Suksmandhira Harimurti, Gilang Gumilar, Brian Yuliarto and M urni Handayani. Functionalized multi-walled carbon AgNP) nanocomposites as non-enzymatic electrochemical biosensors for dopamine detection. Nanocomposites . 2021;7:97–108.

173. T. Huang, L. Yeh, H. Huang, Z. Nian, Y. Yeh, Y. Chou, J. Yeh and Mei-Hui Tsai. The use of carbon paste electrode mixed with multiwall carbon nanotube/electroactive polyimide composites as electrode for sensing ascorbic acid. Polym Chem. 2014;5:630–7.

174. Pholoso Calvin Motsaathebe and Omolola Ester Fayemi. Electrochemical Detection of Ascorbic Acid in Oranges at MWCNT-AONP Nanocomposite Fabricated Electrode. Nanomaterials. 2022;12:645.

175. Nidhi Chauhan, Jagriti Narang, Rachna Rawal, Chandra Sekhar Pundir. A highly sensitive non-enzymatic ascorbate sensor based on copper nanoparticles bound to multi walled carbon nanotubes and polyaniline composite. Synth Met . 2011;161:2427–33.

176. Aysun Savk, Buse Özdil, Buse Demirkan, Mehmet Salih Nasa, Mehmet Harbi Calimli, Mehmet Hakkı Alma, Inamuddin, Abdullah M. Asiri FŞ. Multiwalled carbon nanotube-based nanosensor for ultrasensitive detection of uric acid , dopamine and ascorbic acid. Mater Sci Eng C. 2019;99:248–54.

177. Tehrani RMA, Ghani SA. MWCNT-ruthenium oxide composite paste electrode as non-enzymatic glucose sensor. Biosens Bioelectron . 2012;38:278–83.

178. Yan Xing, Guangwei Gao, Guangming Zhu, Jihua Gao, Zaochuan Ge and Haipeng Yang. A Nonenzymatic Electrochemical Glucose Sensor Based on $Ni(OH)_2$ -CNT-PVDF Composite and Its Application in Measuring Serum Glucose. J ofThe

Electrochem Soc. 2014;161:106–10.

179. Lin K, Yang C, Chen S. Fabrication of a Nonenzymatic Glucose Sensor Based on Multi- Walled Carbon Nanotubes Decorated with Platinum and Silver Hybrid Composite. Int J Electrochem Sci. 2015;10:3726–37.

180. Hassan Karimi-Maleh , Kemal Cellat , Kubilay Arıkan , Aysun Savk , Fatemeh Karimi F, Sen. Palladium – Nickel nanoparticles decorated on Functionalized-MWCNT for high precision non-enzymatic glucose sensing. Mater Chem Phys. 2020;250:123042.

181. Daming Sun, Qian Zhao, Feng Tan, Xiaochun Wang and Jinsuo Gao. Simultaneous detection of dopamine, uric acid and ascorbic acid using SnO_2 nanoparticles/multi-walled carbon nanotubes/carbon paste electrode. Anal Methods. 2012;4:3283–9.

182. Zhao-Ning Huang, Jiao Zou, Jie Teng, Qi Liu, Meng-Meng Yuan, Fei-Peng Jiao, Xin-Yu Jiang, Jin-Gang Yu. A novel electrochemical sensor based on self-assembled platinum nanochains - Multi-walled carbon nanotubes-graphene nanoparticles composite for simultaneous determination of dopamine and ascorbic acid. Ecotoxicol Environ Saf . 2019;172:167–75.

183. Reza H, Mehrjardi Z. Preparation of Acridine Orange-MWCNT Modified Electrode for Voltammetric Detection of Dopamine in the Presence of Ascorbic Acid. Iran J Anal Chem. 2021;8:102–9.

CHAPTER 3

COMMON EXPERIMENTAL METHODS

3.1. INTRODUCTION

Various experimental methods were employed for the fabrication of CNT based hybrid nano composites on different substrates for sensor and capacitor applications. The composite material involved in the fabrication of working electrodes and also sensor studies of the various working electrode towards particular analytes are characterized by various techniques. The present chapter discusses on common methods adopted for the fabrication of electrodes and their different characterization techniques. These methods include electrochemical as well as other analytical techniques viz. spectroscopic, physico-chemical and microscopic methods. Electrochemical studies include cyclic voltammetry (CV), differential pulse voltammetry (DPV), chronoamperometry (CA) etc. Electrochemical impedance spectroscopy (EIS) and galvanostatic charge-discharge techniques were also explored to predict the behavior of working electrode under different experimental conditions. Scanning electron microscopy (SEM) and Field emission scanning electro microscopy (FESEM) as well as AFM are the techniques employed for analyzing morphology and topography of the films formed on the substrates. Surface Chemical analysis of the films are analysed by energy dispersive X-ray diffraction (EDX) and mapping studies. Other characterization techniques viz. Ultra violet-visible (UV-Vis) spectroscopy, fourier – transform infrared (FTIR) and raman spectroscopy are also used for characterization of the synthesized composites.

3.2. Electrochemical Methods & Techniques

3.2.1. Process methods for Electrode Fabrication

As per the literature report the substrates commonly employed for fabrication of sensors include copper in the form of foils, pins, sheets, nickel foams, steel, titania, silicon wafers, ITO, FTO etc. The substrates used in the present study include polyethylene terephthalate film and copper film. Poly ethylene terephthalate (PET) films which are transparent and flexible was made conducting through metallization process and was used as substrate with improved properties such as reflectivity, electrical conductivity, abrasion resistance etc. Metallization can be done on such substrates by various techniques like brush plating with a metal paint, plasma spray deposition technique, sputtering, electroforming, and dipping the substrate in metal

paint, electroplating, electroless plating and vapour deposition techniques [1]. In the present work electroless plating on polyethylene terephthalate sheets was employed which is further deposited with desired nanocomposite material of interest for specific application. The modified poly ethylene substrates were deposited with MWCNT anchored with different metal composites for various sensing applications.

The substrates to be studied should be subjected to various pretreatment process. The pretreatment step varies according to the nature of substrates and it is one of the indispensable preliminary steps employed in the fabrication of electrodes. The flexible PET substrates are roughened using various grades of silicon carbide paper and then cleaned using mild acid followed by alkali and deionized water. The film substrate was thoroughly washed in running water and then dried. Further the substrates are sensitized with stannous chloride and activated with palladium chloride so as to facilitate electroless deposition process.

Electroless deposition is an auto catalytic process where metal ions are chemically reduced and deposition takes place on to the substrate from the bath solution without the passage of current. The substrates which has undergone sensitization and activation process develops a built-in-potential due to which deposition occurs on the substrate surface from the metal ion bath [2,3]. The metallic coatings formed are found to be adherent in nature. A schematic cell set up for electrolytic and electroless deposition (R denotes reducing agent) are shown in the Figure-3.1.

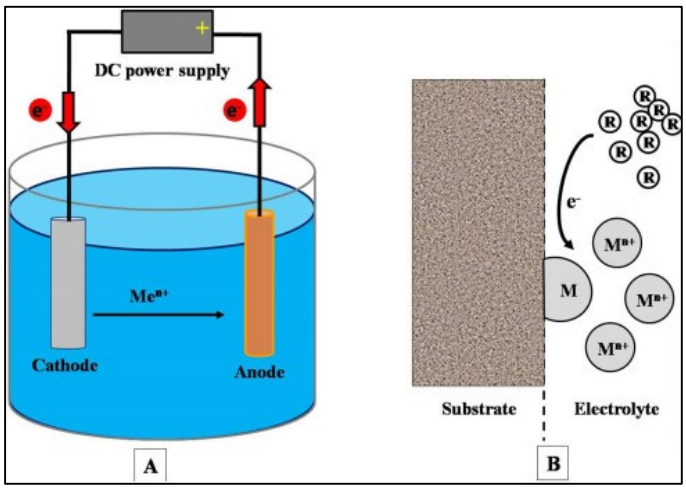

Figure-3.1. Schematic diagram representing (A) Electrolytic deposition process (B) Electroless deposition process [3].

Another method of forming thin films on substrates is through electrophoretic deposition (EPD). EPD is one of the simplest and easiest ways to obtain thin films of carbon nano tubes from its corresponding homogeneous solutions. When compared with other processing methods, electroless and electrophoretic deposition are simple and cost-effective. Moreover thickness of the deposit, its uniformity etc can be controlled so that properties of the electrodes can be controlled [4]. The schematic diagram for electrophoretic deposition of CNT is shown in Figure-3.2.

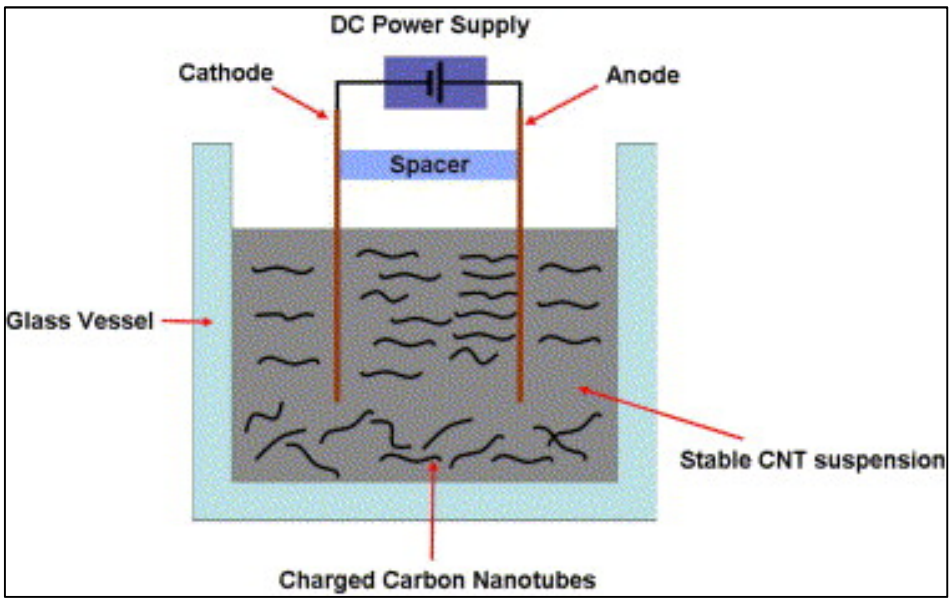

Figure-3.2. EPD of carbon nanotubes [4].

Dipcoating and dropcasting are very similar deposition techniques applied to deposit CNTs from solutions. In dip coating process, the substrate or the sensing probe is dipped into the desired solution or suspension and removed at a controlled rate. The deposition process is repeated until a desired thickness is obtained on the substrate. On the other hand if the dispersion is spread on to a substrate, then the process is called dropcasting. After both process the liquid medium in substrate is evaporated by either leaving the substrate to stand for long period of time or by placing in an oven [5]. The dipcoating and dropcasting process is shown in Figure-3.3.

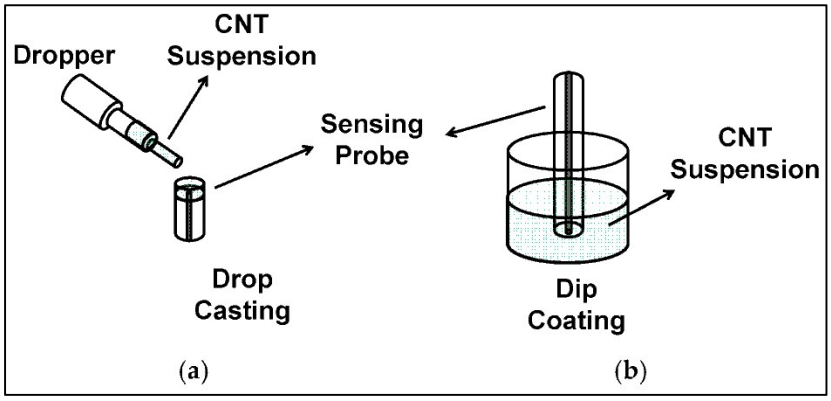

Figure-3.3. Deposition techniques (a) Drop casting (b) Dip coating [5].

3.2.2 Electrochemical techniques

a) Cyclic Voltammetry (CV)

Cyclic voltammetry is one of the most popular electroanalytical technique. It provides information about the electrochemical reactions including electrochemical kinetics, reversibility of reactions, reaction mechanisms, electrocatalytic process and so on. One of the important parameter which plays an important role in voltammetric behavior of the sample is scan rate. If the peak current increase with increasing scan rate, then it signifies a better pseudocapacitive nature of the electrode and the peak current is calculated using Randles-Sevick equation.

$i_p = 2.69 \times 10^5 n^{3/2} AC V^{1/2} D^{1/2}$

i_p is the peak current, n is the number of electrons, A is the area of the working electrode, C is the concentration of the electroactive species at the electrode, v is the scan rate, D is the diffusion coefficient. The current i_p increases with increase in scan rate and this is also directly proportional to the concentration of electroactive species.

A reaction is termed as reversible reaction if ratio of cathodic and anodic current is equal to one. If ratio is not equal to one, then reaction is quasi reversible and finally if the oxidized or reduced product is not reversible, then the system is considered to be irreversible. The difference in anodic and cathodic peak potentials give the number of electrons involved in a reversible reaction.

$\Delta E_p = |E_p^A - E_p^C| = 59/n \text{ m V}$

$\Delta E_p$is the difference in anodic and cathodic peak potential, E_p^A is the oxidation peak potential, E_p^C is the reduction peak potential, n is the number of electrons involved.

CV can also give a detailed idea regarding capacitance behavior and hence specific capacitance (Cs) can be calculated using the formula

$Cs = \int Idv/m \text{ v } \Delta V$

ΔV is the potential window, m is the mass of electroactive species in grams, v is the scan rate in m V/s, $\int Idv$ is the area under the curve of plot I vs V.

The electrochemical set up for doing all the electrochemical characterization consists of three electrode arrangement comprising of working electrode, reference electrode and counter (auxillary) electrode. Saturated calomel electrode and Ag/AgCl electrode are used as reference electrode and platinum is used as the counter electrode. The instrument used for doing all the electrochemical characterization is biologic SP-200 is shown in the Figure-3.4. A cyclic voltammogram is obtained as we sweep potential from initial to final range. A current flows through the electrode which can either oxidise or reduce the analyte and the current I between working and counter electrode is measured and plotted against potential and is shown in the Figure-3.5 [6–8].

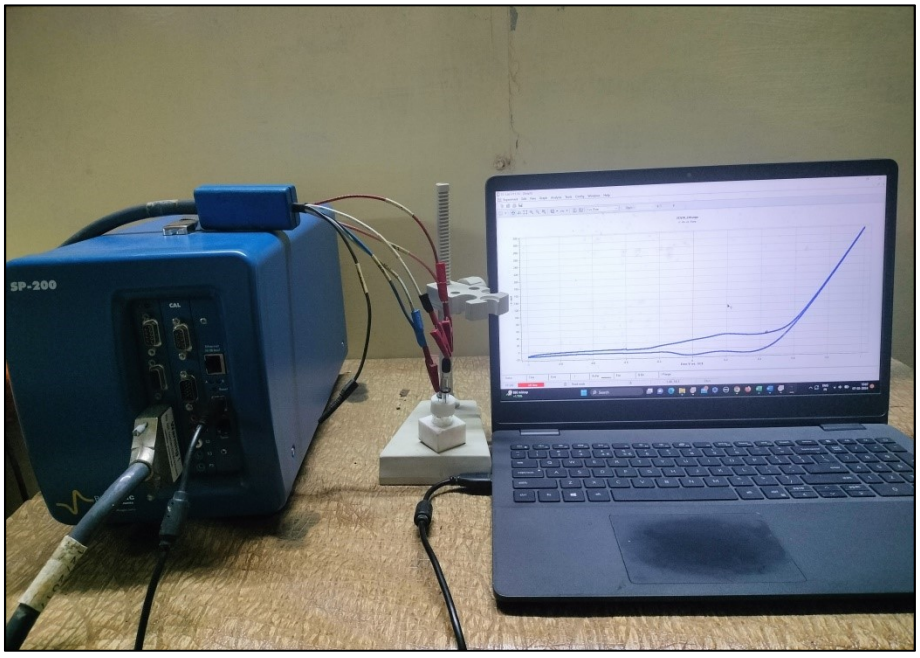

Figure-3.4. Electrochemical Workstation Biologic SP-200

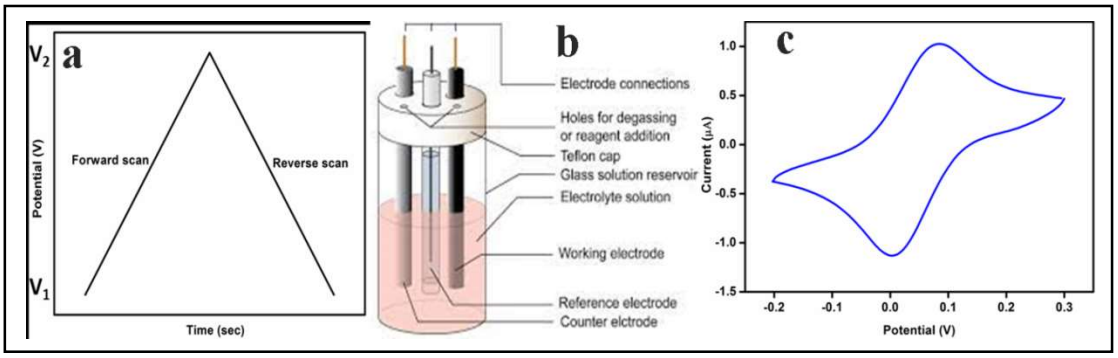

Figure-3.5. (a) Variation of working electrode potential as a function of time (b) Electrochemical cell set up (c) CV of the simplest redox couple (adapted from reference 8).

b) Differential Pulse Voltammetry (DPV)

DPV is a widely used electrochemical technique which finds application in sensing of metal ions, biomolecules etc. In this technique small amplitude short pulses are superimposed on slowly changing the base potential. The current is measured before the application of pulse and after the end of the pulse. The difference between the two currents are recorded and is plotted against the base potential to yield differential pulse voltammmogams. These are shown in Figure-3.6. DPV technique effectively reduces back ground current and as a result faradaic current becomes free of capacitive current. The low capacitive current leads to high sensitivity in case of DPV technique. Besides this, small step sizes in DPV leads to narrow voltammetric peaks [9,10].

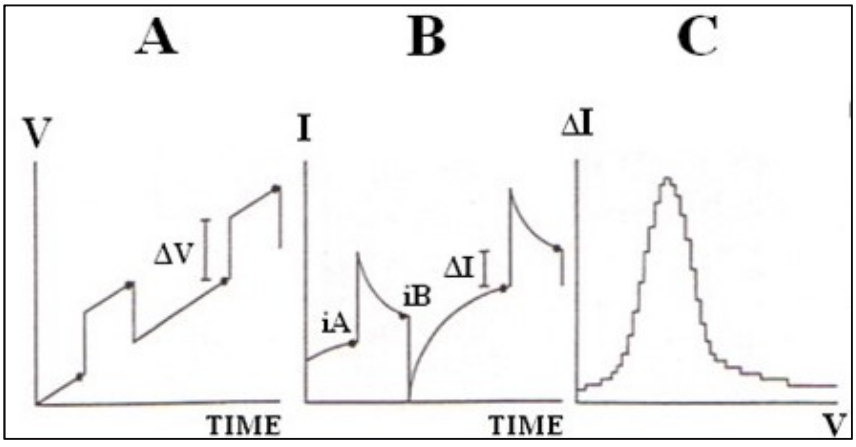

Figure-3.6. (A) Application of small amplitude pulses (B) Measurement of differential pulses (C) DPV voltammogram showing ΔI against applied potential [9].

c) Chronoamperometry (CA)

Chronoamperometry as the name implies is a time-dependent technique where the applied potential of working electrode is changed and the resulting current flow from the faradaic process is measured as a function of time as shown in the Figure-3.7. In short, working electrode is stepped from a potential in which there occurs no electrode reactions to a point where mass transport limited current occurs and accordingly current-time transient is being recorded. Changes in current response is due to increase or decrease in diffusion layer of analyte at the surface of working electrode. This electrochemical technique is very useful in the studies related to electro-catalysis and electrochemical sensing [11–13].

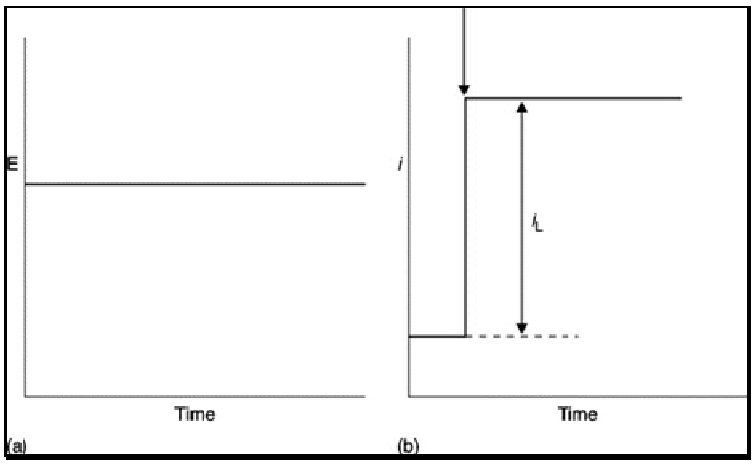

Figure-3.7. (a) Input and (b) Output signal for chronoamperometry [13].

d) Electrochemical Impedance Spectroscopy (EIS)

The various processes occurring in solutions, solid-liquid and solid-solid interfaces are studied using EIS technique. The conductivity of the electrode material, resistance, capacitance, inductance etc can be measured using this sophisticated technique. In this technique current is measured on application of sinusoidal potential. Thus impedance is obtained over a wide range of frequencies. Nyquist plot and bode plot are the graphical forms obtained from the data obtained in the EIS studies. A semicircle is obtained in the nyquist plot indicating the charge transfer limitations and warburg impedance is obtained in a diffusion-controlled process. When impedance is plotted against frequency, bode plot are obtained and is shown in the Figure-3.8. EIS is applied in the study of sensors, biosensors, corrosion, supercapacitors etc [14,15].

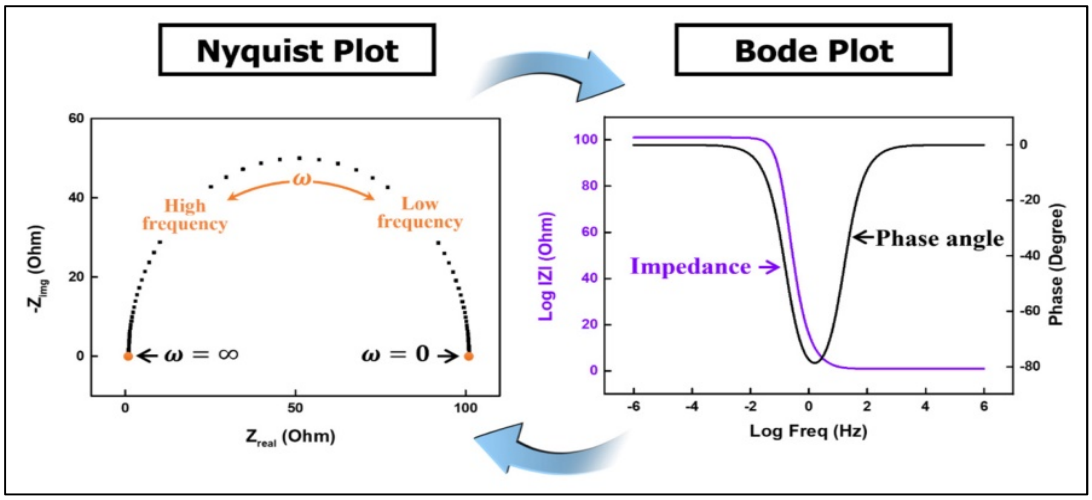

Figure-3.8. Nyquist plot (left) and Bode plot (right) [15].

e) Galvanostatic Charge-Discharge Studies (GCD)

Charge discharge technique was used to evaluate the performance of the electrode material including IR drop, electrochemical double layer mechanism etc. as a function of time. A precise determination of specific capacitance can be done using this technique. In this technique current at the working electrode is kept constant and resulting potential is measured as a function of time.

Specific capacitance can be calculated using the formula

Specific Capacitance = $I\Delta t/ A\Delta V$

I is the current in mA, t is the discharge time in seconds, A is the area of electrode in cm^2, ΔV is the potential window.

A cycle in GCD means a single loop including both charging and discharging. However the GCD plots of EDLC material and pseudocapacitive materials are different. The non-linearity in the plots of pseudo capacitive materials is due to the redox reactions and these are all shown in the Figure-3.9. The specific capacitance, cyclic stability etc of a composite electrode can be obtained from the GCD studies [16,17].

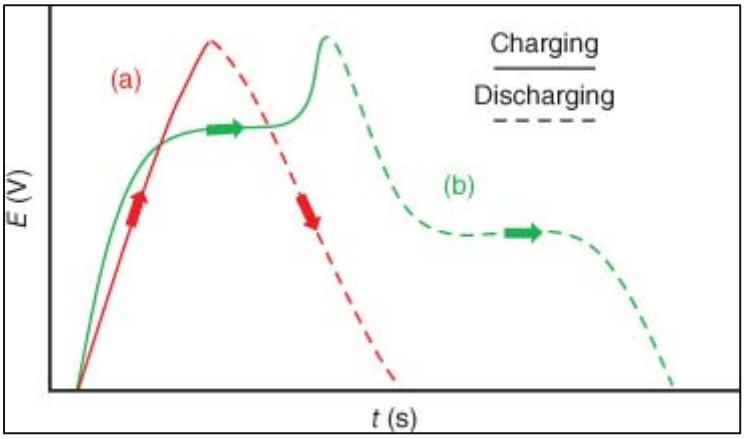

Figure-3.9. Charge-discharge curves for (a) EDLC and (b) Pseudocapacitive material [16].

3.2.3. Analytical Techniques

a) X-ray Diffraction (XRD)

XRD is a highly versatile non-destructive technique used to investigate crystal structure and chemical composition of various crystalline materials. X-ray beams are projected on to a sample and the way in which X-ray beam undergo change in intensity after striking the atoms is being scrutinized. X-rays are scattered in different directions and hence they interfere with each other. Bragg's law helps to study these interferences and to determine different characteristics of polycrystalline materials. The diffraction pattern produced on diffraction of X-rays by interacting with various planes of atoms provide information about atomic arrangement with in the crystal. On interaction of X-rays with the sample, a constructive interference is produced when Bragg's law is satisfied.

Bragg's law is given by

$n\Lambda = 2d\sin\Theta$

n is an integer, Λ is the wavelength of X-ray beam, d is the interplanar spacing between rows of atoms and Θ is the angle between X-ray and the plane.

Diffraction pattern can be regarded as a chemical fingerprint since these gives information regarding the constituents present in the sample. By analysing the peak position, the structural determination of unknown samples can be found on comparing

the obtained diffraction pattern to the database of known parameters. When X-ray strikes a nanocomposite, the obtained spectrum consists of a summative nature of the scattering characteristics of all particles present in the composite material [18–20]. The instrument and principle behind XRD technique is shown in Figure-3.10.

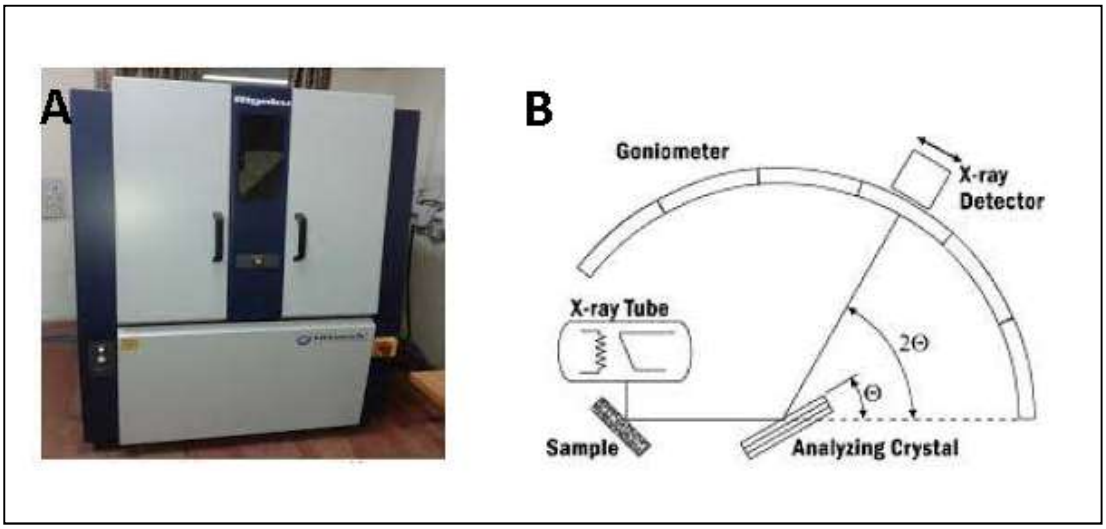

Figure-3.10. (A) Rigaku Ultima IV (B) Schematic diagram representing the instrumentation of XRD instrument (19).

b) Energy Dispersive X-ray Spectroscopy (EDS/EDX)

EDX analysis is an analytical technique which is used to characterize elemental composition or chemical characterization of materials. EDX is usually used in conjuction with field emission scanning electron microscope. During the process the specimen is bombarded with a beam of high energy electrons, which excites the atoms of the specimen resulting in the release of X-rays. The energy of X-rays corresponds to the characteristic atom responsible for its generation. It is possible to study EDX spectrum for a specific point of the sample or an entire region [21,22]. EDX analysis of electrolessly deposited flexible copper films, Ag/MWCNT films electrophoretic deposited Cu-WO_3-MWCNT, Pd@MWCNT-Co_3O4 and RuO_2-Fe_3O_4-MWCNT are carried out.

c) Field Emission Scanning Electron Microscope (FESEM)

FESEM is a sophisticated technique used to investigate the topographical details which includes size, shape and imperfections in the nanocomposites with a very high resolution. FESEM is one of the microscope which works with electrons

instead of light. The electrons liberated from the source, scan the specimen in a zig-zag pattern and gives the useful information regarding the morphology of nanostructure. The field emission source is usually a tungsten wire with a pointed tip so as to focus the entire electric field to a very good level. The primary electrons liberated are accelerated under a high electric field and are focused on to the electronic lenses so that narrow beams can be generated. These primary electrons when strikes the specimen produces secondary electrons which are emitted from atoms and these electrons are capable of producing signals which are identified by the detector and finally signals are amplified and converted to a scan image which is processed further. On collision of primary electrons with sample, besides secondary electrons; back scattered electrons and X-rays are also generated. Surface morphology of specimen is determined by considering the angle and velocity of secondary electrons and backscattered electrons [23–27]. These all are shown in the Figure-3.11.

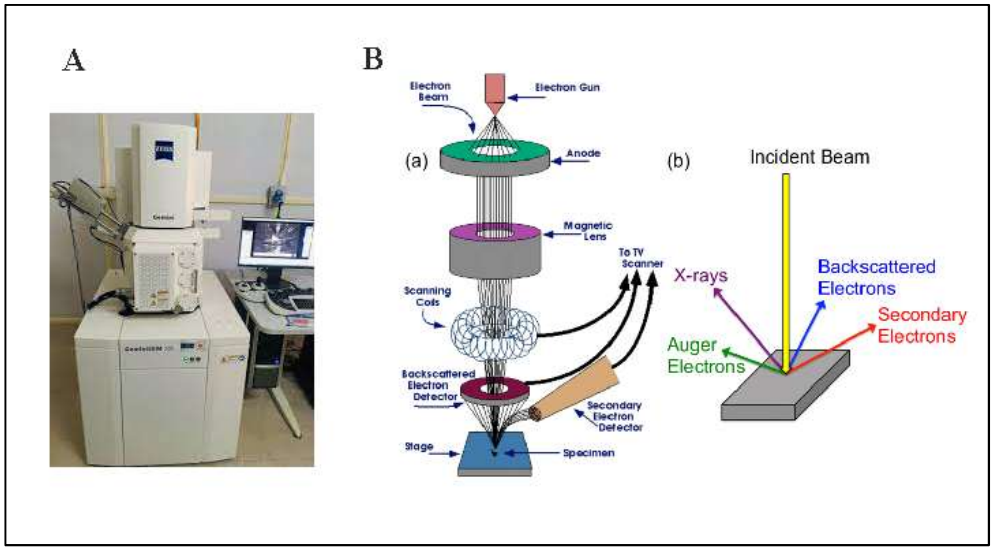

Figure-3.11. **(**A) Zeiss Gemini SEM 300 (B) Schematic diagram of scanning electron microscopy set up [25]**.**

d) Atomic Force Microscopy (AFM)

Atomic force microscopy is a topographical technique used to measure the surface roughness and mechanical properties at atomic resolution in a three dimensional mode. This is one of the scanning probe microscope (SPM) which uses the fine probe to scan the surfaces in many ways. So this can also be regarded as the

modified version of scanning tunneling microscope (STM). AFM does not use electrons or beam of light to investigate the surface properties.

The principle behind AFM is the interaction between the tip and the sample. AFM tip is attatched to a flexible cantilever and when the probe is moved along the surface, generated forces deflects the cantilever. This deflection is called 'stiffness of cantilever', which is measured. Most of the AFMs use laser beam detection in which photodiodes are used. These photodiodes are position sensitive detectors. The basic instrumental set up is shown in Figure-3.12. Widely used mode for analyzing the surface properties of different samples is the contact mode where the AFM tip is in contact with the surface of the sample. Thus this robust technique helps in analyzing polymers, films, fibers, powders, adsorbed molecules etc [28,29].

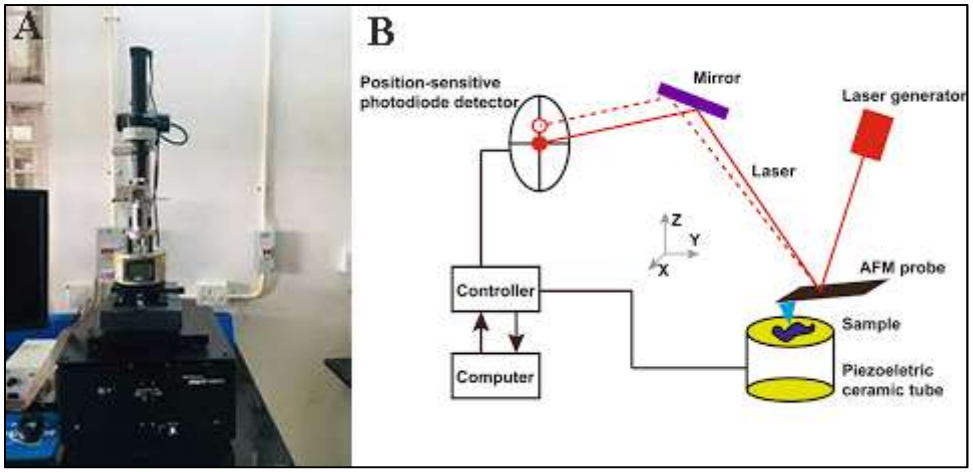

Figure-3.12. (A) Bruker multimode 8 AFM (B) Schematic diagram for AFM working principle [29].

e) Fourier-Transform Infrared (FTIR) Spectroscopy

The absorption or emission infrared spectrum of solids, liquids and gases are obtained using FTIR technique. This characterization technique is used to identify various functional groups in the compounds. FTIR technique takes advantage over dispersive spectrometer, since this can give information over a wide spectral range from 4000 to 400 cm^{-1}. The most common FTIR method for nanocomposite characterization includes attenuated total reflection (ATR), transmission, diffuse reflectance and specular reflection spectroscopy. FTIR technique uses IR source which emits radiations and this radiations are made to pass through Michelson

interferometer. Interferometer consists of beam splitter, fixed mirror and moving mirror. The beam splitter splits up the light beam which is again reflected by the mirrors and finally spectra is generated depending upon the absorbed or transmitted radiations. This is shown in the Figure-3.13. Each molecule will be having unique infrared fingerprint making it easier for identification. FTIR spectrum is represented by wave number on x-axis and absorbance or transmittance on y-axis [30–33].

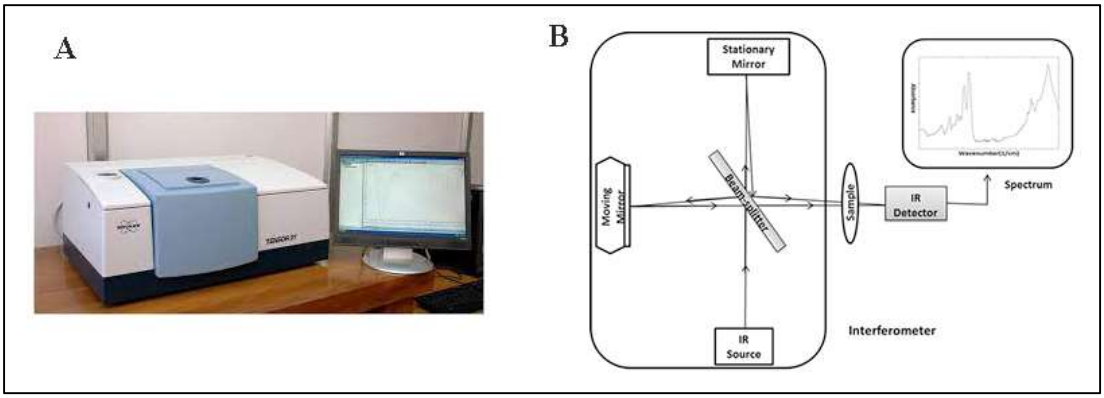

Figure-3.13. (A) Bruker Tensor 27 FTIR (B) Working principle of FTIR [30].

f) Raman Spectroscopy

Raman spectroscopy is a non-destructive technique which involves elastic scattering of photons. Depending on the frequencies of incident light and scattered light different types of scattering lines occurs. These includes rayleigh scattering, stokes line and anti-stokes lines. Instrumentation technique mainly includes scattering of light by the sample when sample absorbs monochromatic rays from the laser source. The interferometer detects these raman scattered light which involves fourier transform methods. Raman spectroscopy can provide information regarding organic molecules, inorganic molecules, metal complexes, functional groups and also fingerprints of organic species [34,35]. Raman microscope and schematic diagram regarding the working principle of raman microscope is shown in Figure-3.14.

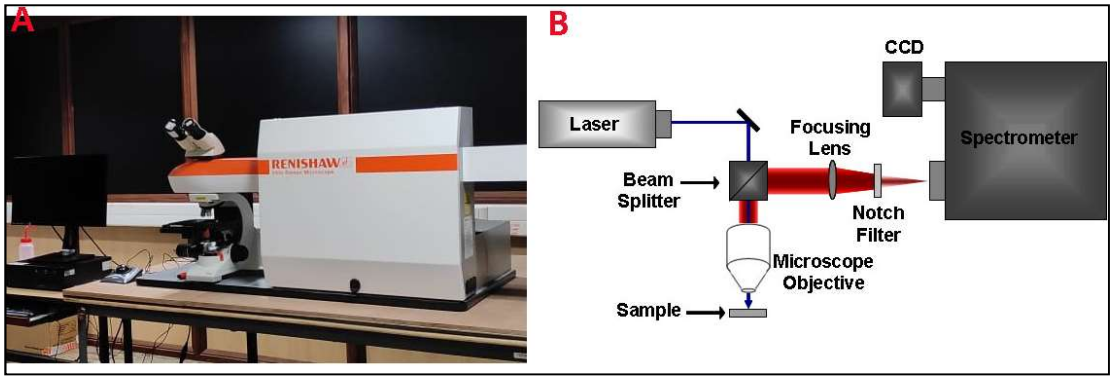

Figure-3.14. (A) Renishaw confocal raman microscope (B) Schematic diagram representing working principle of raman microscope [34].

g) Ultraviolet- Visible (UV-Vis) Spectroscopy

UV-Visible spectrophotometry is widely used for fundamental and applied research applications due to its low cost and easy implementation techniques. Inorder to characterize the sample by UV-Visible spectroscopy, sample must be a chromophore (absorb in the UV-Vis region). UV-Visible spectrometer calculates the amount of light transmitted through a sample. The homogeneous absorbing materials obeys Beer's law as

$A=\epsilon bc= -\log T=\log(1/T)$

A is the Absorbance, ϵ is the molar absorptivity, b is the thickness of sample, c is the concentration and T is the transmittance.

The visible and ultraviolet light is used to analyse the chemical structure of the substance. This charcterisation technique is used to analyse DNA and RNA, bacterial culture, pharmaceutical analysis, analyzing quality of food in food industry etc. Optical properties of nanocomposites comprising of metals, oxides, semiconducting nanocrystals etc can be studied using this technique.

In UV-Vis Spectrophotometer, deuterium lamp or xenon lamp serves as the light source. The light from the source enters the monochromator which comprises of mirrors, slits and grating. The two available configurations of the instrument are single beam and double beam configuration. The transmitted or reflected light from the sample are converted into a signal by the detector and hence measurement is also

made. Thus transmittance is measured with respect to wavelength in UV-visible spectrum. These all are highlighted in Figure-3.15.

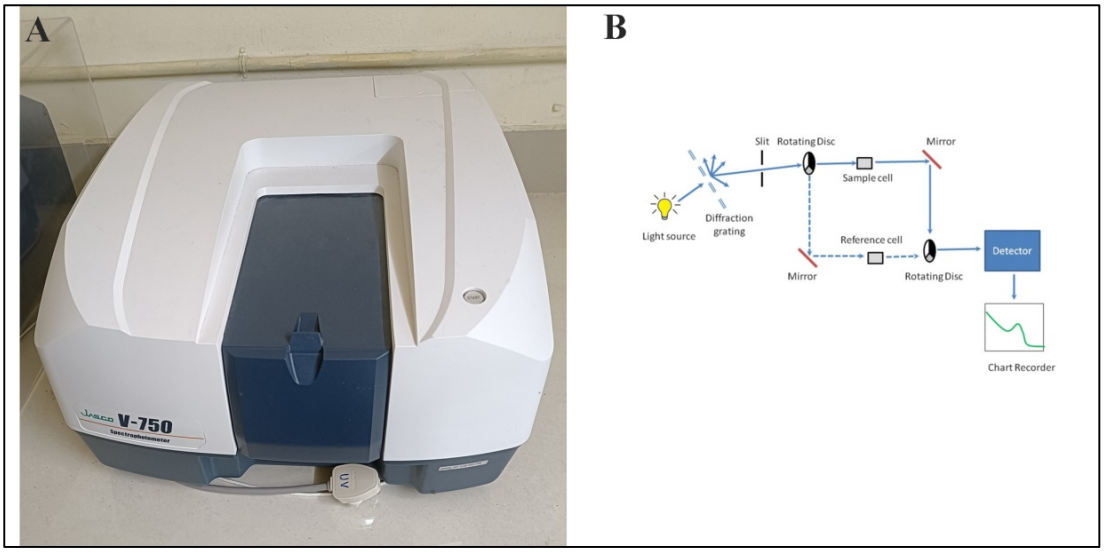

Figure-3.15. (A) Jasco V-750 (B) Working principle of UV-visible spectrophotometer [34].

The above illustrated characterization techniques were used for analyzing the efficacy of the synthesized materials and its behavior under specific condition. These methods help to scrutinize the different samples prepared by various techniques which further find its applications in sensing platform. The behavior of modified electrodes were studied using both analytical and electrochemical techniques, however electrochemical methods plays an indispensable part in the sensor studies of various species using the developed electrodes.

3.3. REFERENCES

1. Equbal A, Dixit NK, Sood AK. Electroless Plating on Plastic. Int J Sci Eng Res. 2013;4(8).

3. Carraro C, Maboudian R, Magagnin L. Metallization and nanostructuring of semiconductor surfaces by galvanic displacement processes. Surf Sci Rep. 2007;62:499–525.

3. Ghosh S. Electroless copper deposition: A critical review. Thin Solid Films. 2018;669:641–58.

4. Aldo R. Boccaccini, Johann Cho , Judith A. Roether , Boris J.C. Thomas , E. Jane Minay MSPS. Electrophoretic deposition of carbon nanotubes. Carbon N Y. 2006;44:3149–60.

5. Tan YC. Chemical Sensing Applications of Carbon Nanotube-Deposited Optical Fibre

Sensors. chemosensors. 2018;6:55.

6. P.S. J, Sutrave DS. A Brief Study of Cyclic Voltammetry and Electrochemical Analysis. Int J ChemTech Res. 2018;11:77–88.

7. Noémie Elgrishi, Kelley J. Rountree, Brian D. McCarthy, Eric S. Rountree, Thomas T. Eisenhart and JLD. A Practical Beginner's Guide to Cyclic Voltammetry. J Chem Educ. 2018;95:197–206.

8. Hsiang-Wei Wang , Cameron Bringans , Anthony J. R. Hickey , John A. Windsor PAK and ARJP. Cyclic Voltammetry in Biological Samples: A Systematic Review of Methods and Techniques Applicable to Clinical Settings. Signals. 2021;2:138–58.

9. Crespi F. Differential Pulse Voltammetry: Evolution of an In Vivo Methodology and New Chemical Entries, A Short Review. J new Dev Chem. 2020;2:30–3.

10. Janet G. Osteryoung & Mary M. Schreiner. Recent Advances in Pulse Voltammetry. C R C Crit Rev Anal Chem. 1988;19:S1–27.

11. Guy OJ, Walker KAD. Graphene Functionalization for Biosensor Applications. Second Edi. Silicon Carbide Biotechnology. Elsevier Inc.; 2016. 85–141.

13. Rezaei B, Irannejad N. Electrochemical detection techniques in biosensor applications. Electrochemical Biosensors. Elsevier Inc.; 2019. 11–43.

13. Honeychurch KC. Printed thick-film biosensors. Print Film. 2012;13:366–409.

14. Basics of Electrochemical Impedance Spectroscopy Introduction. Electrochemical Research-Impedance https://www.gamry.com/ application-notes/EIS/basics-of-electrochemical-impedance-spectroscopy/ (accessed 2021 -09 -07).

15. Woosung Choi, Heon-Cheol Shin, Ji Man Kim J-YC and W-SY. Modeling and applications of electrochemical impedance spectroscopy (EIS) for lithium-ion batteries. J Electrochem Sci Technol. 2020;11:1–13.

16. Brian Kihun Kim, Serubbable Sy, Aiping Yu and JZ. Electrochemical Supercapacitors for Energy Storage and Conversion. Handb Clean Energy Syst. 2015;

17. Sanjeev K. Ujjain, Rohit Bhatia, Preety Ahuja PA. Highly Conductive Aromatic Functionalized Multi-Walled Carbon Nanotube for Inkjet Printable High Performance Supercapacitor Electrodes. PLoS One. 2015;10:1–13.

18. Ameh ES. A review of basic crystallography and X-ray diffraction applications. Int J Adv Manuf Technol. 2019;105:3289–303.

19. Bunaciu AA, Udriştioiu E gabriela, Aboul-Enein HY. X-ray Diffraction: Instrumentation and Applications. Crit Rev Anal Chem. 2015;45:289–99.

20. Holder CF, Schaak RE. Tutorial on Powder X-ray Diffraction for Characterizing Nanoscale Materials. ACS Nano. 2019;13:7359–65.

21. Cardell C, Guerra I. An overview of emerging hyphenated SEM-EDX and Raman spectroscopy systems: Applications in life, environmental and materials sciences. Trends Anal Chem. 2016;77:156–66.

23. Shindo, D., Oikawa T. Energy Dispersive X-ray Spectroscopy. Anal Electron Microsc Mater Sci. 2002;81–103.

23. Walock M. Nanocomposite coatings based on quaternary metal nitrogen and nanocarbon systems. University of Alabama at Birmingham. 2013. 189 p.

24. Inkson BJ. Scanning electron microscopy (SEM) and transmission electron microscopy (TEM) for materials characterization. Materials Characterization Using Nondestructive Evaluation (NDE) Methods. Elsevier Ltd; 2016. 17–43.

25. Schematic for scanning electron microscopy column. 2003;2003. Available from: http://www-archive.mse.iastate.edu/microscopy/path3.html

26. Shubham Sharma, , Swarna Jaiswal BD and AKJ. Nanostructured Materials for Food Applications : Spectroscopy , Microscopy and Physical Properties. Bioengineering. 2019;26:1–17.

27. Joshi M, Bhattacharyya A, Ali SW. Characterization techniques for nanotechnology applications in textiles. Indian J Fibre Text Res. 2008;33:304–17.

28. Vahabi S. Atomic Force Microscopy Application in Biological Research : A Review Study. Iran J Med Sci. 2013;38.

29. Xiangying Deng, Fang Xiong, Xiayu Li, Bo Xiang, Zheng Li, Xu Wu, Can Guo, Xiaoling Li, Yong Li, Guiyuan Li WX and ZZ. Application of atomic force microscopy in cancer research. J Nanobiotechnology. 2018;16:1–15.

30. Faghihzadeh F, Nelson M. Anaya, Laura A. Schifman V, Oyanedel-Craver. Fourier transform infrared spectroscopy to assess molecular-level changes in microorganisms exposed to nanoparticles. Nanotechnol Environ Eng. 2016;1:1–16.

31. Abdul Rohman , Mohd Al'Ikhsan . Ghazali , Anjar Windarsih , Irnawati , Sugeng Riyanto FMY and SM. Comprehensive Review on Application of FTIR Spectroscopy Coupled with Chemometrics for Authentication Analysis of Fats and Oils in the Food Products. Molecules. 2020;25:5485.

33. Catherine Berthomieu and Rainer Hienerwadel. Fourier transform infrared (FTIR) spectroscopy. Photosynth Res. 2009;101:157–70.

33. Ahmed Fadlelmoula, Diana Pinho, Vitor Hugo Carvalho SOC and GM. Fourier Transform Infrared (FTIR) Spectroscopy to Analyse Human Blood over the Last 20 Years : A Review towards Lab-on-a-Chip Devices. Micromachines. 2022;13:187.

34. Pavan M. V. Raja & Andrew R. Barron. Physical Methods in Chemistry and Nano Science. 2013.

35. McCreery RL. Raman Spectroscopy for Chemical Analysis. 2000.

CHAPTER 4

FLEXIBLE Ag/fMWCNT ELECTRODE FABRICATED THROUGH BENIGN REDUCING AGENT FOR DOPAMINE SENSING AND PSUEDOCAPACITIVE APPLICATION

4.1. INTRODUCTION

Dopamine is chemically 3,4-Dihydroxyphenylethylamine and is catecholamine neurotransmitter which plays an important role in controlling the human behavior and various physiological processes. Variation in the level of neurotransmitter dopamine leads to various neurological disorder which include various disorders like Parkinson disease, Alzheimer, HIV infection, senile dementia and schizophrenia [1–3]. Dopamine concentration in the human body should be monitored inorder to trace and diagonise such diseases. The analytical methods like high performance liquid chromatography, spectrophotometry, gas chromatography, colorimetry, fluorescence spectroscopy etc has been employed for dopamine detection. An electrochemical method for detection of dopamine is found to be simple, specific and sensitive. Since dopamine is an electroactive compound, electrochemical methods which give fast response and requires low cost equipment are constantly employed for the detection of dopamine using various modified nanocomposites including metal nanoparticles, metal oxides, polymers, 2D materials etc [4–7].

Several methods are employed for the synthesis of metal nanoparticles and their functionalized products. Among these chemical reductions, electrochemical technique, photochemical reductions are commonly employed. Chemical methods have various limitations since it includes use of toxic reducing agents, lack of reusability of reagents and its impacts on environment. In order to overcome these limitations, synergistic application of nanotechnology and biotechnology is to be focused during synthesize and fabrication of these type of materials/coating. Green chemistry route is a nonconventional method adopted to synthesis metal and metal oxide nanoparticles. Among the biological methods, use of plant extracts serves as an efficient path for the synthesis of nanoparticles due its dual role of behaving as a reducing as well as capping agents. These can reduce metal ions to nanoparticles through single step green synthesis process [8–10]. The preparation methods and efficiency of these type of process may not be on par when compared with other conventional methods, yet the process opens its route due to the feasible and environment friendly nature on account of less toxicity, easy availability and generation of non-toxic by-products. The emerging developments in nanotechnology

has extended its contribution in the field of electronics, optoelectronics, medicines, solar cells etc [11,12]. The promising properties of metallic nanoparticles are due to their large surface area to volume ratio [13,14].

The biomedical application of gold and silver nanoparticles makes them important in the field of nano-biotechnology. Silver nanoparticles finds applications in various areas such as integrated circuits, fillers, sensors, cell electrodes, antimicrobials and these applications grab the scientists to focus their research in the field of silver nanoparticles or incorporation of silver nanoparticles in various matrixes [15]. Physical and chemical methods are employed for the preparation and stabilization of metal nanoparticles [16,17]. In order to overcome the toxicity and other environmental issues, researchers now focus their work on green synthesis of nanoparticles. Various biological methods such as microbial as well as plant mediated synthesis have been developed for the synthesis of nanoparticles. Various plant extracts has been used as green reductant for silver nanoparticle synthesis. Plant extract can serve both as reducing and capping agent for the synthesis of silver nanoparticles. Moreover these green reagents enables stable and shape controlled synthesis of silver nanoparticles [18–21]. Nano silver particles have great adaptability when it is incorporated with other materials and such distinctive properties of silver nanoparticles makes it efficient candidate for wide range of applications. Carbon nanotubes (CNTs) possess high tensile strength, excellent mechanical characteristics, good electrical conductivity, high thermal conductivity and large specific surface area. Various works has been reported in which MWCNT is used to modify the electrode surface. Moreover a small amount of metal catalyst can always enhance the sensitivity towards the electrochemical detection of various drugs. Multi-walled CNTs (MWCNT) can serve as good supports for silver nanoparticles which enables the fabrication of Ag-MWCNT composites at minimized cost [22–24]. Fabrication of such composites results in the integration of properties of both materials and these enhanced properties can lead to wide range of potential applications. New methods have been developed for electroplating non-conductive plastic moldings so that they can serve as efficient substrates for the electroless deposition process. Flexible PET substrates are also employed as substrates after proper pretreatment processes [25–27].

The present work describes on the development of Ag/fMWCNT flexible conducting films by electroless deposition technique using plant extract as reducing agents. The plant extract chosen for the present work is of Melissa Officinalis [28]. The extract acts as both reducing as well as stabilizing agent for the preparation of silver nanoparticles. In the present work Polyethylene films were subjected to various pretreatment procedure and dip coated with fMWCNT before electroless deposition. Ag/fMWCNT flexible conducting films exhibited pseudo capacitive behavior and exhibit good sensing behavior toward the detection of dopamine as revealed from various analysis.

4.2. EXPERIMENTAL METHODS

4.2.1. Preparation of plant extract based reducing agent

Fresh leaves of Melissa Officinalis was washed with plenty of water, shade dried for a week and ground into a fine powder. The leaves powder (10 g) were extracted using hot percolation method taking 50 ml of double distilled water and were boiled for 15 minutes. Extract was cooled down, centrifuged and filtered with whatman filter paper No:1 to remove residues if any present. The clear extracts were stored at 4 °C for further use. The extract prepared serves as both reducing and capping agent during the synthesis of silver nanoparticles.

4.2.2. Functionalisation of MWCNT

Multi walled carbon nanotubes (OD:30-50 nm, length:10-30 μm) were functionalized by acid treatment. About 1 g of MWCNTs were refluxed with H_2SO_4 and HNO_3 in the ratio 3:1 and stirred for about 5 hrs at 70 °C. Functionalised multi walled carbon nano tubes (fMWCNT) are filtered through poly carbonate membrane and washed with double distilled water until pH was neutral. Now this is kept in oven at 50 °C for overnight. A dispersion of fMWCNT was prepared by sonication of the dried product in aqueous Triton-X-100.

4.2.3. Process of electroless deposition

Electroless bath consists of 5 mM 20 ml $AgNO_3$ solution which is maintained at a pH not less than 8. pH is adjusted using sodium carbonate and ammonia. In the case of silver nitrate bath, the bath pH is a prime factor that desires the basic

characteristic of the deposit. Substrate taken for the experiment was polyethylene terephthalate film which is flexible and non-conductive. The sheets were cut into small pieces of size 2 cm x 5 cm and was slightly roughened using various grade silicon carbide paper mainly with P 2000, P 200, P 280 to make the surface more adherent for adsorbing metal ions. The surface was pre-cleaned with acetone to remove any impurities. It was then soaked in dilute HCl and dilute NaOH to make surface clean. After this, substrate was sensitized using 0.1 M $SnCl_2$ and activated using 0.0014 M $PdCl_2$ solution for a period of 5 minutes. After each step of pretreatment, substrate was rinsed thoroughly with demineralized water. The pretreated substrate is used for further experimental purpose.

4.2.4. Fabrication of flexible conductive films of Ag/fMWCNT

The pretreated substrate was dip-coated with fMWCNT containing precursor solution prepared using Triton X-100 acting as surfactant for uniform dispersion of fMWCNT, followed by drying under IR lamp. The process is repeated until thin film of fMWCNT was formed on the polyethylene sheet. The polyethylene flexible substrate was dipped in the prepared electroless bath of colloidal silver. About 10 ml of the leaf extract which serves as reducing agent was slowly added and stirred. Reduction of $AgNO_3$ takes place which results in deposition of Ag nanoparticles on substrate. The deposited polyethylene substrate was taken after some time which was optimized based on the film characteristics and deposit properties. Thus an adherent coating of Ag/fMWCNT was formed in the flexible film.

4.2.5. Preparation of dopamine samples

Dopamine samples of varying concentrations were prepared for analyzing sensor characteristics of the fabricated Ag/fMWCNT electrode. Various concentration of dopamine ranging from 1 μM- 40 μM was prepared from dopamine hydrochloride using doubly distilled water. The prepared solution of neurotransmitter was analyzed through different electrochemical techniques. An interference study was carried by adding 0.1 mM ascorbic acid and real sample analysis was carried out in bovine serum.

4.2.6. Characterization techniques of Ag/fMWCNT flexible Electrode

UV-Visible spectrophotometer (Jasco UV, V-750) was used to study the absorbance spectrum of colloidal nanoparticles of silver in the range of 200–800 nm. FTIR (Bruker-Tensor 27) studies revealed the presence of various functional groups in the plant extract responsible for reduction of silver nitrate to silver and also in the films containing Ag/fMWCNT. Elemental analysis of the fabricated electrode was confirmed using Energy dispersive X-ray analysis (EDAX) and morphology of the electrodes were characterized using Field emission scanning electron microscopy (FESEM-Gemini 300) which is attached with an EDAX equipment. Atomic force microscopy (AFM-Bruker multimode) studies were also employed to study the surface topography and roughness. Electrochemical characterization were carried out using Biologic SP-200 Model. The three electrode set up employed which included platinum electrode as counter electrode, saturated calomel electrode (SCE) as reference electrode and fabricated Ag/fMWCNT electrode as working electrode in Phosphate Buffer Solution (PBS). Sensor characteristics of the electrode were studied using cyclic voltammetry, differential pulse voltammetry and chronoamperometric techniques.

4.3. RESULTS AND DISCUSSION

4.3.1. Fabrication of Ag/fMWCNT flexible films using electroless Deposition

Deposition was performed on the pretreated substrate as detailed in the experimental part. Plant extracts contains alkaloids, phenolic acid, polyphenols, sugars, terpenoids, flavonoids etc. as bioactive agents. These compounds which contain active chemical agents can have a profound effect during nano particle synthesis and its deposition at optimum reaction condition. The extract whose photograph is being shown in Figure-4.1 (A) was added to the solution of silver nitrate which is adjusted to an appropriate pH. This treatment can convert metal ions from its monovalent or divalent state to zero valence state. Silver nanoparticle formation was observed as the silver nitrate changed the color on addition of leaf extract. Biosynthesis of Ag nanoparticles was confirmed by the color change of the solution which intensified during the course of reaction

which can be visually observed as in Figure-4.1(B). The color change is mainly attributed to the excitation of Ag nanoparticles by surface plasmon vibrations [29]. The change of color from yellow to dark brown indicated the change in concentration of silver nanoparticles. The size of particles and concentration increased during time. UV- Visible absorption spectrum showed the presence of characteristics surface plasmon resonance (SPR) band of silver in the range of 421 nm [30,31]as shown in Figure-4.1 (C). These reduced Ag nanoparticles were made to replace palladium ions by the means of electroless deposition process in the pretreated flexible substrate which is dip coated with fMWCNT dispersion. fMWCNT formed by dip coating also provided enough nucleation sites for the deposition of silver. The fabricated flexible Ag/fMWCNT films is shown in Figure-4.1 (D)

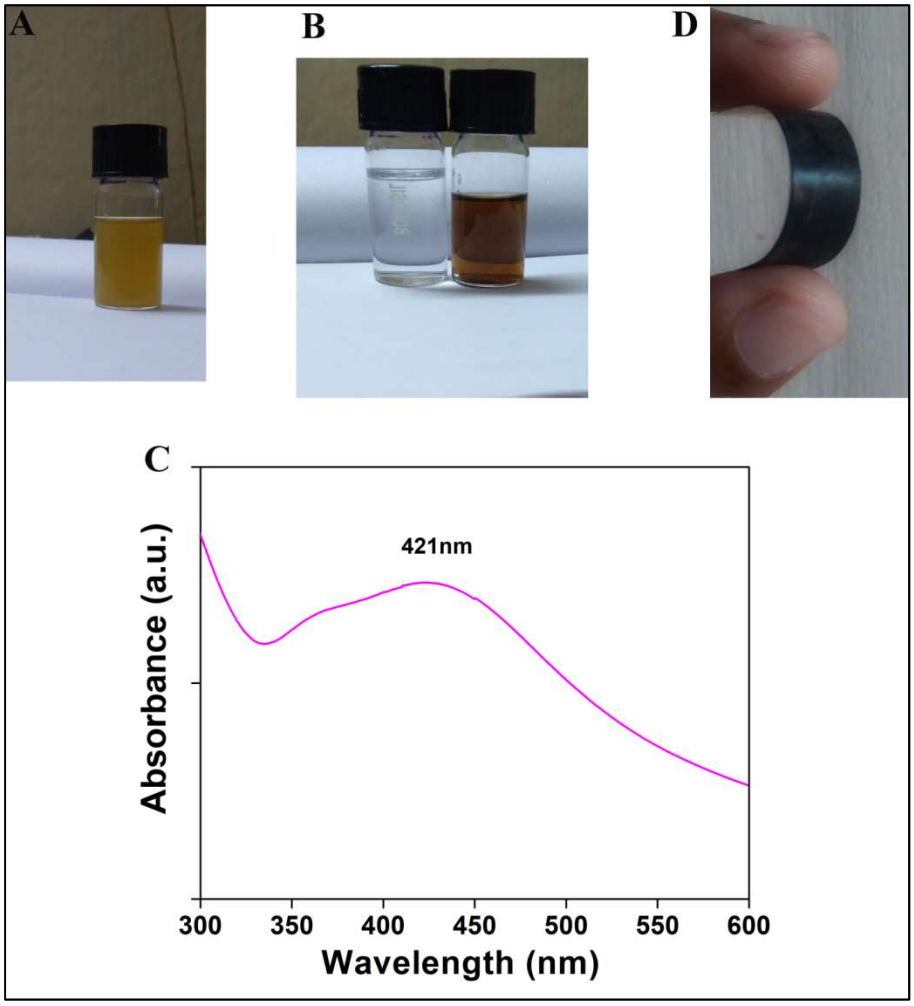

Figure-4.1. (A) The leaf extract. (B) The color change of Silver nitrate before and after addition of leaf extract. (C) UV-Vis spectra of synthesised silver nanoparticles. (D) Fabricated flexible Ag/fMWCNT film.

4.3.2. Elemental analysis and morphology of the Ag/fMWCNT flexible film

Energy dispersive X-ray analysis (EDAX) revealed the presence of silver and carbon in the functionalized MWCNT by the distinct peaks. A strong peak at 0.2 keV and 3 keV in the EDAX spectrum observed in Figure-4.2 shows the presence of elemental carbon and metallic silver [32,33]. FESEM images of the Ag/fMWCNT deposit is shown in Figure-4.3. The results strongly confirms the reducing and capping nature of leaf extract employed for the preparation of silver nanoparticles. The carbon nanotubes within the metal matrix were uniformly distributed and there was no agglomeration and the tubular structure was intact as revealed from SEM analysis. AFM images of Ag/fMWCNT nano composite film shows that surface was more or less uniform and there was no voids in the deposit as revealed from Figure-4.4. The average surface roughness of the deposit was found to be 18.9 nm.

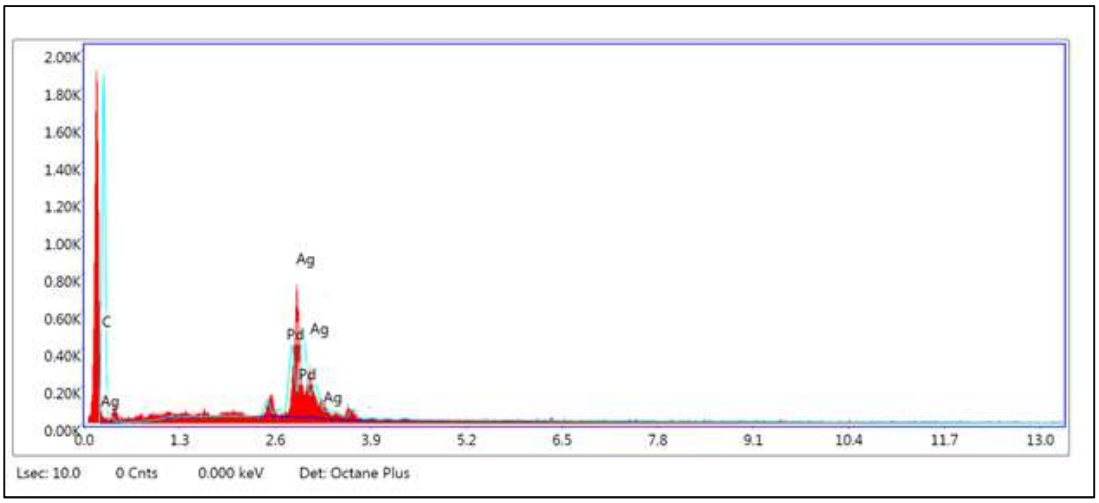

Figure-4.2. EDAX Spectrum of synthesised Ag/fMWCNT electrode.

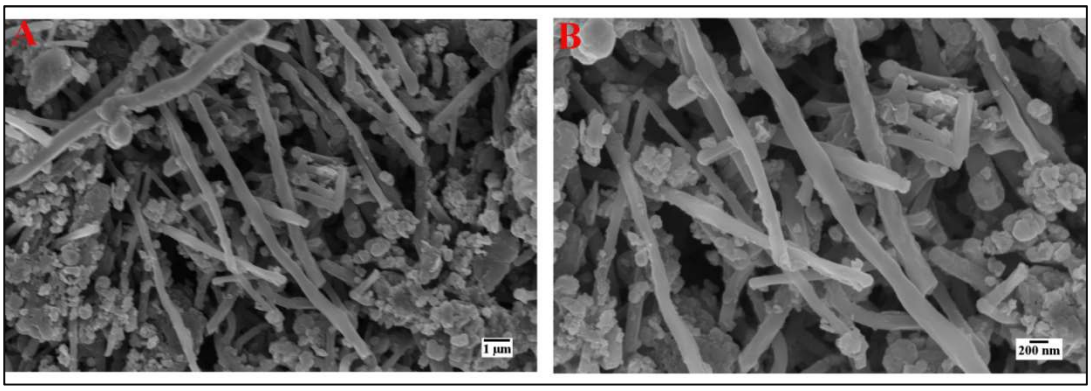

Figure-4.3. FESEM images of flexible Ag/fMWCNT film at different resolutions prepared by electroless deposition.

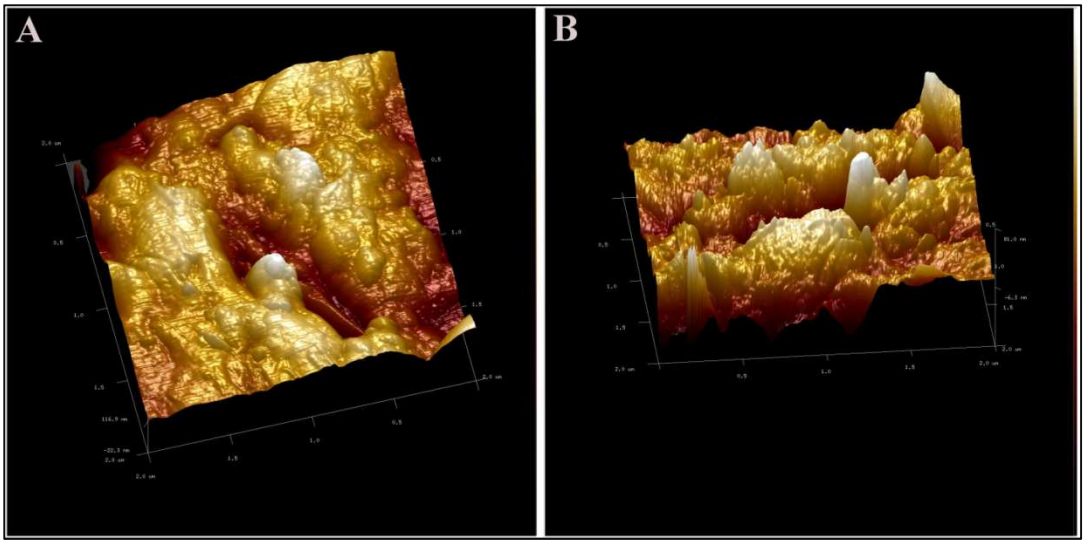

Figure-4.4. (A) Three dimensional AFM image Ag/fMWCNT film. (B) 3D flattened image.

4.3.3. FTIR analysis of the Ag/fMWCNT composite films

FTIR spectra of Ag/fMWCNT composite films in Figure-4.5 revealed the presence of organic compounds in the plant extract of Melissa officinalis. The phytochemical components mainly present in the plant extract include rosamarinic acid as major component as reported elsewhere [34]. The band associated with 3253 cm^{-1} and 3367 cm^{-1} is due to stretching vibrations of O-H group in phenols as well as CNT-OH stretching. The C-H bond of alkanes was revealed by the peak at 2990 cm^{-1}. The band at 2875 cm^{-1} corresponds to the stretching bands of methylene group of oxidised MWCNT. The interaction of hydroxyl group of gallic acid contained in plant extract with the partial positive charge of Ag nanoparticles results in the band at 2383 cm^{-1}. The peaks at 1677 cm^{-1} and 2105 cm^{-1} is due to the C=C and C≡C bands of aromatic or aliphatic compounds. The carbonyl group of oxidised MWCNT and C=C stretching band of the same is indicated by the bands at 1749 cm^{-1} and 1599 cm^{-1}. The presence of $COCH_3$ in aromatic compounds is indicated by the band at 1406 cm^{-1}. The intense peak at 1128 cm^{-1} and 1292 cm^{-1} is attributed to the C-O bonds present in various organic compounds of the plant extract [35,36]. All the above analysis data proved that the flexible films of Ag/fMWCNT formed by electroless deposition using the present process contains various functional groups that are originated from the compounds generally found in the plant extract.

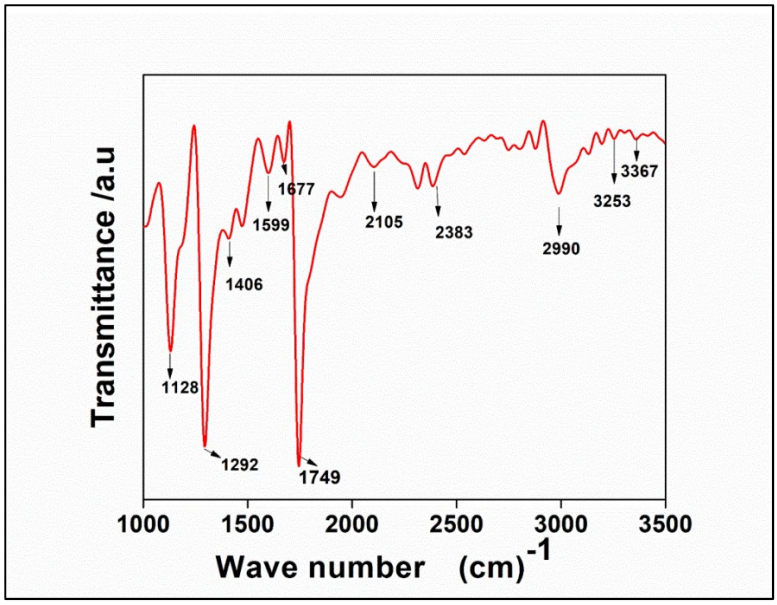

Figure-4.5. FTIR Spectra of Ag/fMWCNT films prepared using Melissa officinalis as reducing agent.

4.3.4. CV Analysis of Ag/fMWCNT composite films

The CV curves of Ag/fMWCNT electrodes in PBS solution was studied in the potential range between −0.2 and 0.9 V at various scan rates from 2 mV to 100 mV/s. The redox peaks obtained are mainly due to faradaic reaction. Although there was no drastic shift in anodic as well as cathodic peak potential values with increasing scan rate, yet the slight shift noted can be due to internal resistance of the electrode. This reflects that, the deposit was more adherent and stable even at very high current load as shown in the Figure-4.6 (A). A linear increase in anodic and cathodic peak current was observed when peak current was plotted against square root of scan rate which is shown in the inset of Figure-4.6 (B). The anodic and cathodic peak intensities are related to the scan rate by Randles-Sevcik equation [37].

$$ip = 2.69 \times 10^5 \cdot n^{3/2} \cdot A \cdot D^{1/2} \cdot C \cdot V^{1/2} \quad (1)$$

where, ip = peak current in ampere, n = electron stoichiometry, A = area of the electrode in cm^2, D = diffusion coefficient in cm^2/s, C = concentration of the species in mol/cm^3 and V = scan rate in volts/s.

The R square values for anodic peak current and cathodic peak current was found to be 0.9798 and 0.9661 which is in good agreement with the linear regression equation.

Specific capacitance of 305 F/g was observed for a scan rate of 2 mV/s. The higher specific capacitance is ascribed to the stability of Ag/fMWCNT composite electrode prepared by nontoxic reagents and that influenced the fast electron movement within the electrode-electrolyte interface. This could be attributed to the even distribution of functionalised MWCNT within Ag matrix, forming a uniform deposit morphology, which renders facile electrolyte penetration in the matrix and better conducting nature of the deposit. It was also observed that values of specific capacitance decreased as scan rate increased and this decrease was marginal at higher scan rate as shown in Figure-4.6 (C). Figure-4.6 (D) shows the CV curves for 10 th and 1000 th cycles at a scan rate of 50 mV/s in PBS solution. The retention values of specific capacitance were found to be 86%. This retention value ascribes to the excellent stable nature of the fabricated flexible electrode [38].

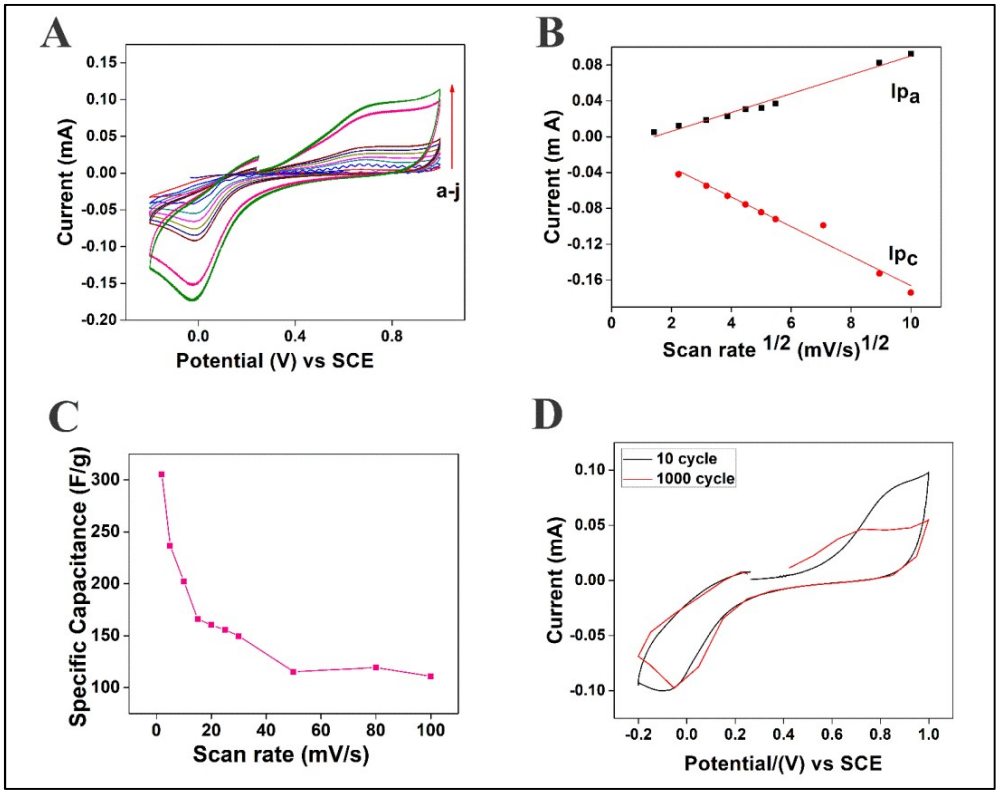

Figure-4.6. (A) CV curves at different scan rates (a-j) (2, 5, 10, 15, 20, 25, 30, 50, 80 and 100 mV/s.).(B) Plot of variation of anodic and cathodic peak current against square root of can rate. (C) Plot of Specific capacitance as a function of scan rate. (D) CV curves for 10^{th} and 1000^{th} cycles were studied at a scan rate of 50 mV/s in PBS solution.

4.3.5. Analysis on charge storage properties of the electrode

Nyquist plots were drawn within the frequencies range of 100 mHz to 100 kHz at zero volt bias. According to equivalent circuit theory, the vertical trend in the nyquist plot at low frequencies indicates the capacitive behavior [39–42].The presence of a semicircle in high frequency region and a straight line in low frequency region is the characteristic of pseudo capacitor material. Figure-4.7 (A) shows the nyquist plots for the fabricated electrode. Pseudo capacitor materials show nyquist plots as a semicircle in high frequency region and nearly a straight line along the imaginary axis at low frequency region which purely indicated the dominant nature of capacitive behavior as reported in literature [43–45]. In the present study the double semicircles, although one small compared to another reveals the porous nature of the electrodes which is shown in inset of Figure-4.7 (B). The experimental data is to be fitted in order to represent an equivalent circuit. The equivalent circuit framed gave a good fit in the nyquist plot which was obtained experimentally. In the nyquist plot where semicircle in the impedance plot corresponds to the kinetics controlled (charge transfer) and uncompensated solution resistance between the WE and RE (RΏ) controlled regime. The raising arm of the curve corresponds to the mass transfer (diffusion) controlled regime [46–48]. In order to further asses the behavior of electrode material, bode plots are plotted in which phase angle is a function of frequency. For an ideal capacitor phase angle is −90º. In the Figure-4.7 (C), the phase shift is measured to be −82º in the low frequency region which indicates the capacitive behavior of the electrode material. Bode plot of log |Z| vs log frequency shown in Figure-4.7 (D) revealed the presence of Warburg component of impedance which supported the above explanations [49,50].

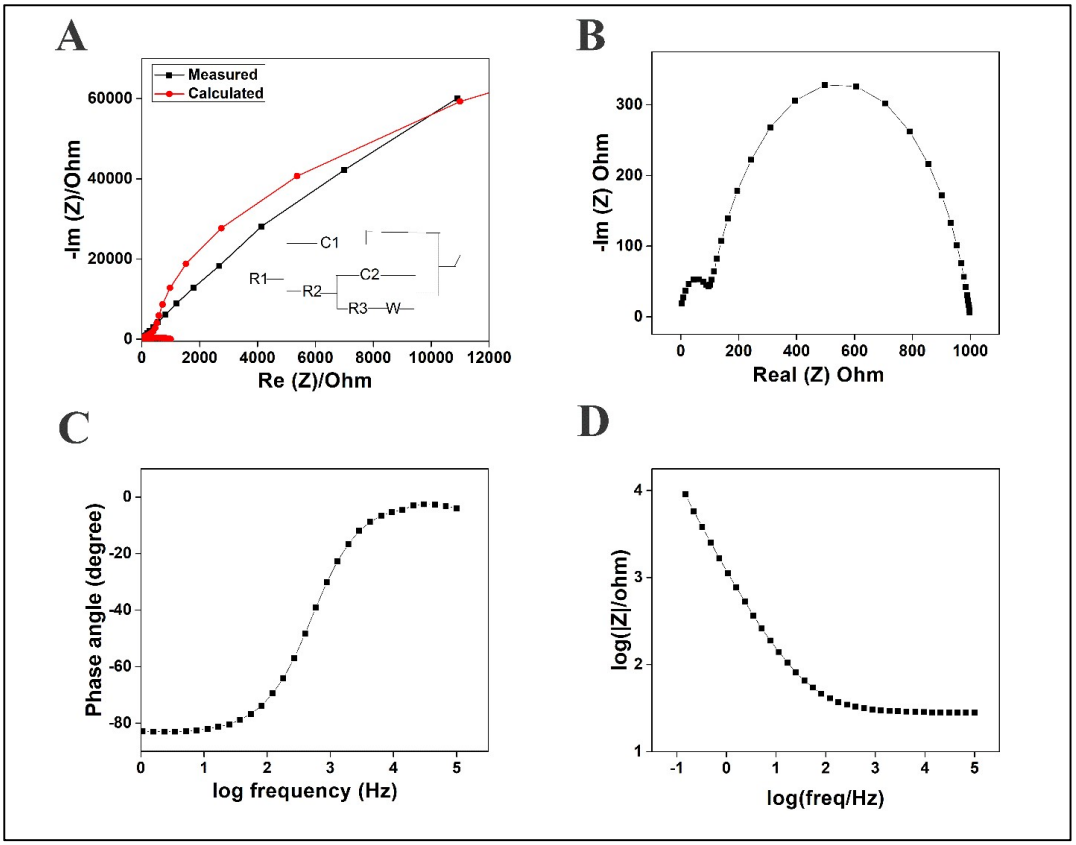

Figure-4.7. (A) Measured nyquist plot and calculated nyquist plot for the matched equivalent circuit given below. (B) Enlarged view of nyquist plot at high frequency region and the corresponding equivalent circuit. (C) Bode plot showing phase shift against log frequency. (D) Bode plot of log Z against log frequency.

4.3.6. Electrochemical studies for detection of neurotransmitter dopamine in presence of ascorbic acid.

Studies were conducted to analyze the sensing behavior of the film for detection of dopamine in presence of ascorbic acid. A well-defined cyclic voltammogram with an oxidation peak potential of 0.2 V was observed. Figure-4.8 (A) shows the cyclic voltammograms of DA obtained on addition of 10 µM DA in 0.1 M PBS (pH= 7) at a scan rate of 50 mV/s. Differential pulse voltammograms obtained for electrochemical oxidation of DA (10 µM) supplements the results of CV studies by showing good response curves for detection of dopamine as shown in Figure-4.8 (B). Dopamine usually co-exists with ascorbic acid and the oxidation potential of both species are close to each other. DPV studies conducted by varying the concentration of dopamine in presence of 0.1mM ascorbic acid clearly illustrated that the flexible Ag/fMWCNT film is very much selective toward the

neurotransmitter dopamine. The presence of single peak in the DPV results showed the electro-oxidation of dopamine only, in presence of ascorbic acid. DPV studies were conducted for dopamine concentration ranging from 1 µM to 40 µM as shown in Figure-4.8 (C). The linear variation of current with increase in concentration (shown in the inset of Figure-4.8 (C) was obtained in DPV studies with an R square value of 0.9978. The detection limit was estimated to be 0.7 µM. The chrono amperometric response of various concentration of dopamine was also studied for concentration ranging from 1 µM-10 µM. The current response was noted for a period of 30 s for various concentrations as shown in Fig. 4.8 (D). When current at ten seconds was plotted against concentration, a linear relationship was noted with an R square value of 0.9802 which shows good agreement with linear regression equation. This is shown in the inset of Fig. 4.8 (D). The detection limit (LOD) was calculated by using the criterion 3σ/s andwas found to be 0.88 µM (S/N = 3). Electron transfer occurs between the phenyl ring and CNT surface when dopamine molecule comes close to Ag/fMWCNT electrode surface. A two electron oxidation process occurs resulting in formation of dopamine-o-quinone as shown in Scheme 4.1. The results of both studies signifies the good electrocatalytic activity of Ag/fMWCNT electrode towards dopamine oxidation due to interaction between various functional groups of dopamine and the electrode material [51,52].

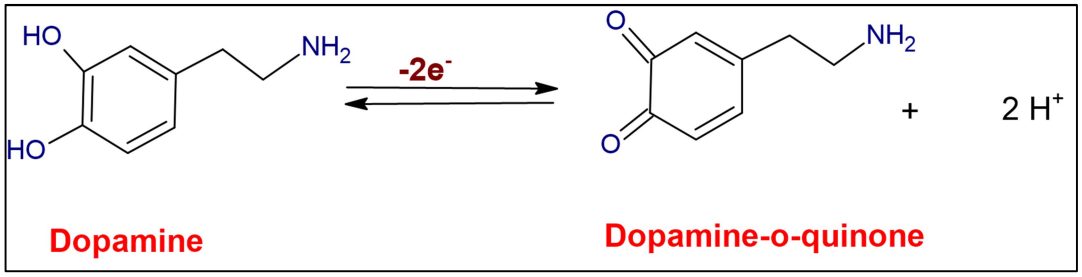

Scheme 4.1 Conversion of dopamine to dopamine-o-quinone.

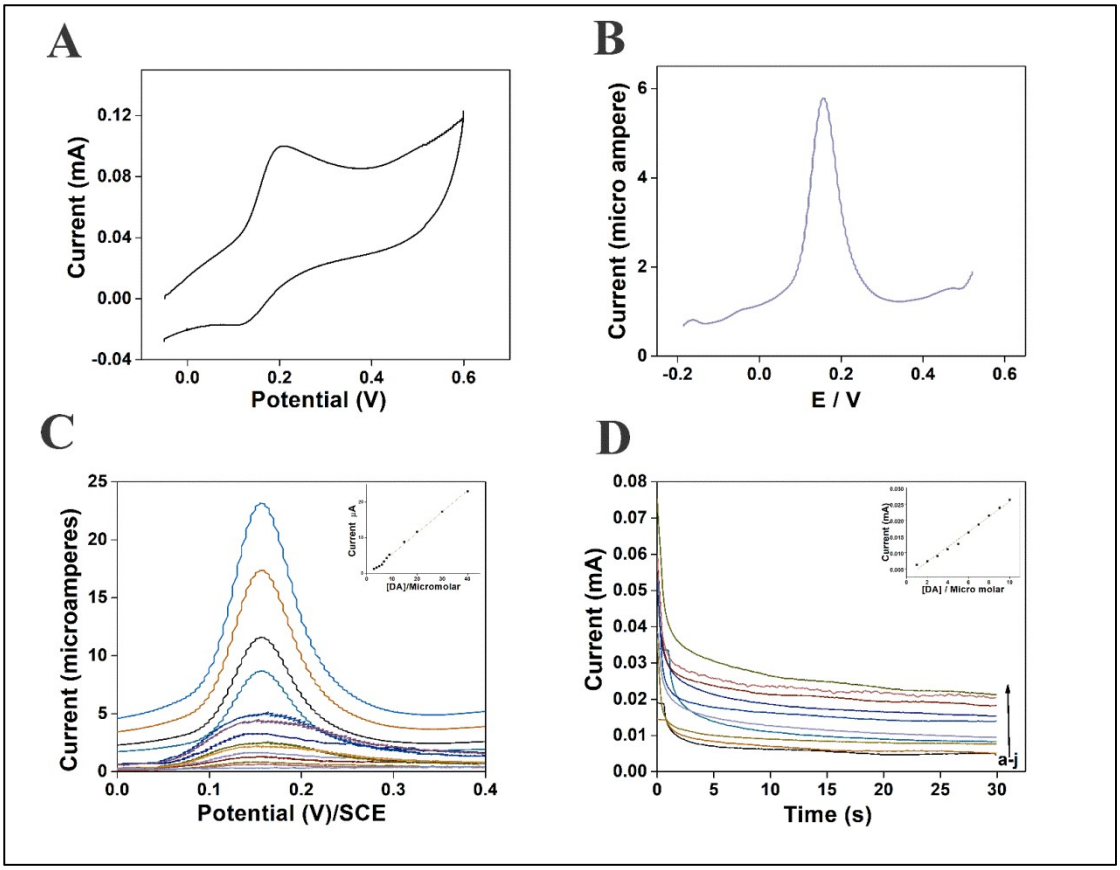

Figure-4.8. (A) Cyclic voltammograms at flexible Ag/fMWCNT in PBS containing DA (10 µM) at scan rate of 50 mV/s. (B) Differential pulse voltammogram for DA at Ag/fMWCNT flexible electrode. (C) DPV responses for different dopamine concentrations (0, 0.5, 1.0, 2.0, 3.0, 4.0, 5.0, 6.0, 7.0, 8.0, 9.0, 15.0, 20.0, 30.0 and 40.0 µmol L^{-1}) in presence of 0.1 mM ascorbic acid on flexible Ag/fMWCNT film electrode in PBS buffer solution. Inset shows the variation of current with concentration. (D) The chronoamperometric curves of dopamine with increase in concentration from 1–10 µM. Inset shows the variation of current with concentration of dopamine.

4.3.7. Reproducibility and stability

Five flexible electrodes of Ag/fMWCNT were fabricated through electroless deposition process using ecofriendly reducing agent for the detection of 10 µM dopamine. All sensors exhibited almost similar response currents to the dopamine samples and the RSD was found to be 2.84 %. This indicates the excellent reproducibility of the sensor. The sensor was stored in air tight containers in dry location and was kept at room temperature. After 30 days also sensor retained 90 % of

its initial responses. This indicates the long term stability of the flexible Ag/fMWCNT electrode [53].

4.3.8. Real sample analysis

In order to validate the versatility of the fabricated flexible Ag/fMWCNT film, dopamine concentration in physiological environment for two samples were studied using bovine serum. After diluting the samples with PBS, DPV studies were conducted by spiking the samples with dopamine. The percentage recovery was found to be 102.5 and 101 %. The results are listed in Table- 4.1. This indicates the potential usefulness of the sensor in detecting dopamine in real samples [54].

Table- 4.1. Determination of dopamine in bovine serum

Sample	Spiked (μM)	Found (μM)	Recovery (%)
Serum 1	4	4.1	102.5
Serum 2	8.5	8.6	101

4.4. CONCLUSIONS

In the present study, flexible Ag/fMWCNT film fabricated through simple eco-friendly process exhibited pseudo capacitive behavior and also possessed high sensing characteristics. The spectroscopic analysis could confirm different groups present in the deposit. EDAX analysis and morphology of the fabricated electrode revealed pore free and uniform deposit character with the presence of elements such as carbon and silver in major proportion. The results of electrochemical analysis such as differential pulse voltammetry and chronoamperometry confirmed the usefulness and selectivity of flexible Ag/fMWCNT electrode as sensors for dopamine. Sensor characteristics of the electrode for the analytical detection of dopamine showed a linear current concentration calibration plot with a detection limit of 0.7 μM. The electrode exhibited excellent reproducibility and stability. The flexible Ag/fMWCNT electrodes showed conducting behavior and also possessed good cyclic performance. The present process could deliver flexible Ag/fMWCNT composite film electrode using environmentally benign reducing agents that possessed good sensor characteristics and energy storage properties.

4.5. REFERENCES

1. Xu Guangyuan, Jarjes ZA, Desprez V, Kilmartin PA. Selective, sensitive Point-of-care determination of dopamine With a novel disposable PEDOT/Laser scribed graphene sensor. Biosens Bioelectron . 2018;107:184–91.

2. Raj CR, Okajima T, Ohsaka T. Gold nanoparticle arrays for the voltammetric sensing of dopamine. J Electroanal Chem. 2003;543:127–33.

3. B.Jill Venton and R. Mark Wightman. Psychoanalytical electrochemistry: dopamine and behaviour. In: Analytical Chemistry. 2003. p. 414–21.

4. Li-qing Q, Zhang Y, Gao F, Wu Q, Xu P. A highly sensitive dopamine sensor based on a polyaniline/reduced graphene oxide/Nafion nanocomposite. Chinese Chem Lett . 2016;3704:1–8.

5. Khan AF, Brownson DAC, Randviir EP, Smith GC, Banks CE. 2D Hexagonal Boron Nitride (2D-hBN) explored for the electrochemical sensing of dopamine. Anal Chem. 2016;88:9729–37.

6. Roychoudhury A, Basu S, Kumar S. Dopamine biosensor based on surface functionalized nanostructured nickel oxide platform. Biosens Bioelectron . 2015;84:72–81.

7. S. Ramakrishnan, K. R.Pradeep, A. Raghul, R. Senthilkumar, Murali Rangarajan and Nikhil K. Kothurkar. One-step synthesis of Pt-decorated graphene- carbon nanotube for electrochemical sensing of dopamine, uric acid and ascorbic acid. Anal Methods. 2015;7:779–86.

8. Gardea-Torresdey JL, Gomez E, Peralta-Videa JR, Parsons JG, Troiani H, Jose-Yacaman M. Alfalfa sprouts: A natural source for the synthesis of silver nanoparticles. Langmuir. 2003;19(4):1357–61.

9. Shankar SS, Rai A, Ahmad A, Sastry M. Controlling the optical properties of lemongrass extract synthesized gold nanotriangles and potential application in infrared-absorbing optical coatings. Chem Mater. 2005;17(3):566–72.

10. Shankar SS, Ahmad A, Sastry M. Geranium leaf assisted biosynthesis of silver nanoparticles. Biotechnol Prog. 2003;19(6):1627–31.

11. Shah AH, Manikandan E, Basheer Ahamed M, Ahmad Mir D, Ahmad Mir S. Antibacterial and Blue shift investigations in sol-gel synthesized $Cr_xZn_{1-x}O$ Nanostructures. J Lumin . 2014;145:944–50.

12. Song JY, Kim BS. Rapid biological synthesis of silver nanoparticles using plant leaf extracts. Bioprocess Biosyst Eng. 2009;32(1):79–84.

13. Tan M, Wang G, Ye Z, Yuan J. Synthesis and characterization of titania-based monodisperse fluorescent europium nanoparticles for biolabeling. J Lumin. 2006;117(1):20–8.

14. Khalil KA, Fouad H, Elsarnagawy T, Almajhdi FN. Preparation and characterization of electrospun PLGA/silver composite nanofibers for biomedical applications. Int J Electrochem Sci. 2013;8(3):3483–93.

15. Kotthaus S, Günther BH, Haug R, Schäfer H. Study of isotropically conductive bondings filled with aggregates of nano-sized Ag-particles. IEEE Trans Components

Packag Manuf Technol Part A. 1997;20(1):15–20.

16. Chen W, Cai W, Zhang L, Wang G, Zhang L. Sonochemical processes and formation of gold nanoparticles within pores of mesoporous silica. J Colloid Interface Sci. 2001;238(2):291–5.

17. Frattini A, Pellegri N, Nicastro D, De Sanctis O. Effect of amine groups in the synthesis of Ag nanoparticles using aminosilanes. Mater Chem Phys. 2005;94(1):148–52.

18. Si W, Lei W, Han Z, Zhang Y, Hao Q, Xia M. Electrochemical sensing of acetaminophen based on poly(3,4-ethylenedioxythiophene)/graphene oxide composites. Sensors Actuators, B Chem. 2014;193:823–9.

19. Hasanpour F, Taei M, Tahmasebi S. Ultra-sensitive electrochemical sensing of acetaminophen and codeine in biological fluids using $CuO/CuFe_2O_4$ nanoparticles as a novel electrocatalyst. J Food Drug Anal. 2018;26(2):879–86.

20. Bui MPN, Li CA, Han KN, Pham XH, Seong GH. Determination of acetaminophen by electrochemical co-deposition of glutamic acid and gold nanoparticles. Sensors Actuators, B Chem. 2012;174:318–24.

21. Sharma VK, Yngard RA, Lin Y. Silver nanoparticles: Green synthesis and their antimicrobial activities. Adv Colloid Interface Sci. 2009;145(1–2):83–96. 22. Ajayan PM. Nanotubes from Carbon. Chem Rev. 1999;99(7):1787–99.

23. Erik T. Thostenson, Zhifeng Ren and Tsu-Wei Chou. Advances in the science and technology of carbon nanotubes and their composites: a review. Compos Sci Technol. 2001;61(6):1899–912.

24. Iijima S. Helical microtubules of graphitic carbon. Nature. 1991;354:56–8.

25. Zheng Q, Ip WH, Lin X, Yousefi N, Yeung K K, Li Z and Kim J K. Transparent conductive films consisting of ultralarge graphene sheets produced by Langmuir-Blodgett assembly. ACS Nano. 2011;5(7):6039–6051.

26. Ryu K, Zhang D, Liu X, Polikarpov E, Tompson M, Zhou C. Transparent, conductive and flexible carbon nanotube films and their application in organic light emitting diodes. Mater Res Soc Symp Proc. 2006;936:19–24.

27. Ha YH, Nikolov N, Pollack SK, Mastrangelo J, Martin BD, Shashidhar R. Towards a transparent, highly conductive poly (3,4-ethylenedioxythiophene). Adv Funct Mater. 2004;14(6):615–622.

28. Lemon Balm. University of Maryland Medical System.

29. Pirtarighat S, Ghannadnia M, Baghshahi S. Antimicrobial effects of green synthesized silver nanoparticles using Melissa officinalis grown under in vitro condition. Nanomed J. 2017;4(3):184–190.

30. Sedaghat S. Green Biosynthesis of silver functionalized multi-walled carbon nanotubes, using Satureja Hortensis L water extract and its bactericidal activity. J Nanoanalysis. 2017;4(1):59–64.

31. Anandalakshmi K, Venugobal J . Green Synthesis and characterization of silver nanoparticles using Vitex negundo (Karu Nochchi) leaf extract and its antibacterial activity. Med Chem (Los Angeles). 2017;07(07):218–25.

32. Anandalakshmi K, Venugobal J, Ramasamy V. Characterization of silver nanoparticles by green synthesis method using Pedalium murex leaf extract and their antibacterial activity. Appl Nanosci. 2016;6(3):399–408.

33. Feng YI, Yuan H. Electroless plating of carbon nanotubes with silver. 2004;9:3241–3.

34. Irina Fierascu, Milen I. Georgiev, Alina Ortan, Radu Claudiu Fierascu, Sorin Avramescu, Daniela lonescu, Anca Nicoleta Sutan, Alexandru Brinzan and Lia-Mara Ditu. Phyto-mediated metallic nano-architectures via Melissa officinalis L.: synthesis, characterization and biological properties. Sci Rep . 2017;7:1–3.

35. de Jesús Ruíz-Baltazar Á, Reyes-López SY, Larrañaga D, Estévez M, Pérez R. Green synthesis of silver nanoparticles using a Melissa officinalis leaf extract with antibacterial properties. Results Phys. 2017;7:2639–43.

36. Gandomi-Ravandi S and Javed Safari. Silver decorated multi-walled carbon nanotubes as a heterogeneous catalyst in the sonication of 2-aryl-2, 3-dihydroquinazolin-4 (1H)-ones. RSC Adv. 2014;4:11654–60.

37. Rana S, Rahman MA, Alam AM S. A CV Study of copper complexation with guanine Using glassy carbon electrode in aqueous medium. ISRN Electrochem. 2014;2014.

38. Li HB, Yu MH, Wang F X, Liu P, Liang Y, Xiao J, Wang C X, Tong Y X and Yang G W. Amorphous nickel hydroxide nanospheres with ultrahigh capacitance and energy density as electrochemical pseudocapacitor materials. Nat Commun. 2013;4:1–7.

39. Jogade SM and Sutrave DS. Electrochemical performance of Mn doped Co_3O_4 supercapacitor : Effect of aqueous electrolytes. J Mater Sci Eng. 2017;6(3):4–8.

40. Prasanna BP, Avadhani DN, Muralidhara HB, Chaitra K, Thomas VR, Revanasiddappa M and Kathyayini N. Synthesis of polyaniline/ZrO_2 nanocomposites and their performance in AC conductivity and electrochemical supercapacitance. Bull Mater Sci. 2016;39(3):667–75.

41. Bidhan Pandit and Babasaheb R.Sankapal. Highly conductive energy efficient electroless anchored silver nanoparticles on MWCNTs as supercapacitive electrode. New J Chem. 2017;41:10808–14.

42. Dar FI, Moonooswamy KR, Es-souni M. Morphology and property control of NiO nanostructures for supercapacitor applications. Nanoscale Res Lett. 2013;8:1–7.

43. C. van der Horst, B. Silwana, EIwuoha and V Somerset. Synthesis and characterization of bismuth-silver nanoparticles for electrochemical sensor applications. Anal Lett. 2015;48:1311–32.

44. Raicopol M, Pruna A, Pilan L. Supercapacitance of Single-Walled Carbon Nanotubes-Polypyrrole Composites. J Chem. 2013;2013.

45. Zhang W, Tan Y, Gao Y, Wu J, Tang B. Ultra fine nano zirconia as electrochemical pseudocapacitor material. Ceram Int. 2014;41:1–5.

46. González S, Cáceres F, Fox V, Souto RM. Resistance of metallic substrates protected by an organic coating containing aluminum powder. Prog Org Coatings 46. 2003;46:317–23.

47. Grossi M, Riccò B. Electrical impedance spectroscopy (EIS) for biological analysis and food characterization : A review. J Sens Sens Syst. 2017;6.

48. Palraj S, Selvaraj M, Muthukrishnan S. Effect of pretreatments on electrodeposited epoxy coatings for electronic industries. Mater Sci. 2016;3:214–30.

49. Ping H, Lin L, Chon C, Wei E, Diau G. Anodic TiO_2 nanotube arrays for dye-sensitized solar cells characterized by electrochemical impedance spectroscopy. Ceram Int . 2012;38(8):6253–66.

50. Enrique J. Parra, FXavier Rius and Pascal Blondeau. A potassium sensor based on non-covalent functionalization of multi-walled carbon nanotubes. Analyst. 2013;138.

51. F. Gao, X. Cai, X. Wang, C. Gao, S. Liu, F. Gao and Q. Wang. Highly sensitive and selective detection of dopamine in the presence of ascorbic acid at graphene oxide modified electrode. Sensors Actuators B Chem. 2013;186:380–387.

52. Nasirizadeh N, Shekari Z, Zare HR, Ahmar H. Developing a sensor for the simultaneous determination of dopamine, acetaminophen and tryptophan in pharmaceutical samples using a multi-walled carbon nanotube and oxadiazole modified glassy carbon electrode. J Braz Chem Soc. 2014;24:1846-1856.

53. Raveendran J, Resmi PE, Ramachandran T, Nair BG, Babu TGS. Fabrication of a disposable non-enzymatic electrochemical creatinine sensor. Sensors Actuators B Chem. 2017;243:589–595.

54. Cheng M, Zhang X, Wang M, Huang H, Ma J. A facile electrochemical sensor based on well-dispersed graphene-molybdenum disulfide modified electrode for highly sensitive detection of dopamine. J Electroanal Chem. 2017;786:1–7.

CHAPTER 5

Cu-WO_3-fMWCNT COMPOSITE FILM ELECTRODE AS SENSOR FOR STUDYING AGEING OF LUBRICANT OILS

5.1. INTRODUCTION

Metal oxide based composite electrodes were widely explored for their use as sensors, pseudo capacitors, negative electrodes etc. owing to their characteristic properties such as spatial confinement, high surface energy, strong surface adsorption and increased surface to volume ratio. Transition metal oxides and refractory metal oxides viz. IrO_2, RuO_2 etc. were widely researched for their specific application in myriad fields due to their inherent properties [1–7]. Among the various oxides, WO_3 has attracted significant research owing to its distinctive properties such as multiple oxidation state, wide potential window in different electrolytes and good physico-chemical properties [8–11]. WO_3 is an n-type semiconductor having photo-catalytic and electro-catalytic property. The band gap of WO_3 is 2.5–2.8 eV. The properties of WO_3 make it an efficient candidate in the field of electrochromic devices, gas sensors, secondary battery materials, catalytic materials and in optical devices. Studies have been conducted on the capacitive behavior of oxides of tungsten, vanadium, manganese etc. These metal oxide serve as an alternative material for energy storage application and hence can replace highly expensive materials. There are numerous reports on preparation and application of tungsten oxide based metal composites. Various techniques such as thermal decomposition, pyrolysis, ion exchange reaction, sol-gel, electrochemical processes and chemical vapor deposition methods were employed for the synthesis of WO_3 nanoparticles [12–18]. Electrochemical methods has the distinction of easy of application, very less time and also inexpensive compared to other techniques for fabrication of metal oxide based nano composite electrodes.

The use of metal oxide based electrodes as sensors has been widely explored in various fields. By using these type of electrodes it is possible to know the aging of various grades of lubricant oils that are commonly employed in machineries. As we know, the complex nature of various lubricants used in different equipment makes it difficult to foresee the failure caused to machines by the use of degraded lubricant oils. A substantial change in lubricants can happen due to various reasons. These include oxidation due to high temperature, contamination by water, ethylene glycol, soot, fuel etc. Lubricant oils ends its life by building up of acids, contamination by soot, oxidation and base depletion. During this time a change in properties of oils like

total acid number [TAN], total base number [TBN], viscosity etc changes. The building up of polar components especially carboxylic acids, ionic species, aldehyde and ketones leads to increase in conductivity. Generally lubricants are changed after particular service time or based on engine mileage without proper testing to see the efficacy of the oil after its long term usage. Here electrochemical method offer an easy way to determine the efficacy of the oil using simple procedures and in very less time [19–24]. Studies has been carried out to determine the viscosity changes, moisture content, oxidative changes and total acid number during its long term usage by using various methods [25–27]. Frequent monitoring of engine oil has to be carried out to protect the engine as well as to reduce the maintenance cost of the machines. In this context the present work considers the application of metal oxide based electrode towards sensing the characteristic components of aging oils.

Metal oxide functionalized with carbon nanotube could improve electron transport properties, surface area and sensing characteristics of the composite material [28,29]. The photo-catalytic property of WO_3 towards degradation of compounds such as azo dyes and polycyclic aromatic hydrocarbons have been reported in several articles [30,31]. Different structure of WO_3 viz. nano rods, nanotubes, nano whiskers, nano plates have been explored for specific applications [32,33]. Hybrid composite films of metal oxide-multi walled carbon nanotubes provide an easy way of detection of various biochemical compounds. Electrochemical detection of various chemicals have been reported by using these type of hybrid composite electrodes. Among the various methods adopted for the fabrication of metal oxide-CNT based composite electrodes, electrochemical methods have the advantage of controlling the size distribution through optimizing the deposition parameters and easy of deposition. Formation of composite materials of nano metal oxide anchored carbon nano-materials can be carried out from dispersions of these type of oxides, anodic oxidation of metal layers, and also by electrodeposition from a precursor solution under optimized conditions [34–36].

The present work relies on the deposition of WO_3-functionalized MWCNT (fMWCNT) composite on to flexible copper substrate and the use of the electrode as sensor for evaluating the aging process of lubricants. The fabrication of Cu-WO_3-fMWCNT composite film involves the initial formation of conducting layer of copper over flexible polyethylene films through electroless deposition, followed by

electrodeposition of WO_3 functionalized MWCNT on to the preformed copper films. The morphology and chemical composition of the composite films were analyzed by Scanning Electron Microscopy and Energy Dispersive X-ray Spectroscopy. The Cu-WO_3-fMWCNT composite films showed increased energy storage characteristics as revealed from the electrochemical studies. The fabricated film electrode has good sensing behavior towards the compounds that develops following the aging of lubricant oils as revealed from cyclic voltammetry and electrochemical impedance spectroscopy measurements.

5.2 EXPERIMENTAL METHODS

5.2.1. Fabrication of flexible copper film

PET films were cut into desired size of 2 × 5 cm and slightly roughened with smooth silicon carbide paper. The slightly roughened surface improves the adhesion of the deposit to the substrate as noted from peeling tests. After surface roughening and washing with distilled water the substrate was subjected to various pretreatment process viz. cleaning with acetone, followed by agitating the substrate in dilute HCl and with dilute NaOH for two minutes in each solution. Further the substrate was thoroughly rinsed with distilled water and its surface sensitized by soaking in 0.1 M stannous chloride for 10 min and was subsequently activated by dipping into 0.0014 M palladium chloride solution for about 10 min. After each of these pretreatment steps the substrate was rinsed with distilled water. Copper was electroless deposited on to the pretreated polyethylene film from a bath containing copper sulfate (5 g/L), sodium potassium tartarate (2 g/L) and formaldehyde (8 ml/L) as reducing agent under alkaline condition at pH 11. The deposition time was chosen to reach the required film thickness, which was estimated by gravimetric method. In the present work the deposition time was fixed to 5 min and the apparent thickness of the film was 1 μm. The obtained copper deposited film was used as substrate for further deposition process. The entire process starting from the pretreatment of the substrate to the final electrodeposition was optimized and was found reproducible as revealed from the sample characterization.

5.2.2. Preparation of tungstite ($WO_3.H_2O$)

Hydrothermal method was employed for the synthesis of WO_3 nanoparticles through acid precipitation. About 1 g of tungstate salt ($Na_2WO_4.2H_2O$) was well dissolved in 100 ml of deionised water and then 30 ml 6 N HCl was added drop wise to get an amorphous precipitate. The beaker was kept in ice under constant stirring to maintain the temperature below 5 °C during addition of acid to the tungstate salt. The precipitate of tungstic acid (H_2WO_4) was washed several times with deionized water to bring the pH to 6. The precipitate which was taken in a crucible with a lid was dried at 60 °C in an oven for 24 h. After that the powder was calcined at 500 °C for about 2 h.

5.2.3. Functionalisation of MWCNT

MWCNT (OD-30–50 nm, length 10–30 μm) purchased from Sigma- Aldrich was functionalized by acid treatment method. 1 g MWCNT was accurately weighed and refluxed with acid in the ratio 3:1 (H_2SO_4: HNO_3) for one hour. It was agitated overnight at a constant temperature of 70 °C, filtered through polycarbonate membrane and washed with distilled water to make the pH neutral followed by drying in oven at 60 °C. The synthesized fMWCNT powder was used without further treatment.

5.2.4. Electrodeposition of WO_3-fMWCNT on to flexible copper substrate

The obtained powder of tungsten oxide was dispersed in deionized water under sonication and the pH was adjusted to 10 by addition of ammonia solution resulting in the formation of ammonium tungstate. The solution is added drop wise to already prepared fMWCNT powder and kept for 2 h at 75 °C under sonicated conditions. The solution containing a mixture of WO_3 and fMWCNT was centrifuged and calcined at 400 °C for 2 h. The obtained WO_3-fMWCNT powder was made into a dispersion and was used as precursor for electrodeposition process. WO_3-fMWCNT suspension was then deposited on to flexible copper substrate by electrodeposition at a fixed current of 0.5 mA for a period of 15 min. The thickness of the electrodeposited film was 2.5 μm. The entire fabrication process has been represented by Scheme 5.1. The fabricated WO_3-fMWCNT electrodes were used for determining the aging characteristics of the oil. Fresh oils were subjected to heat treatments for various time

(15, 24, 48 h) to effect oxidation of the oil in order to study the change in characteristic property of the oil.

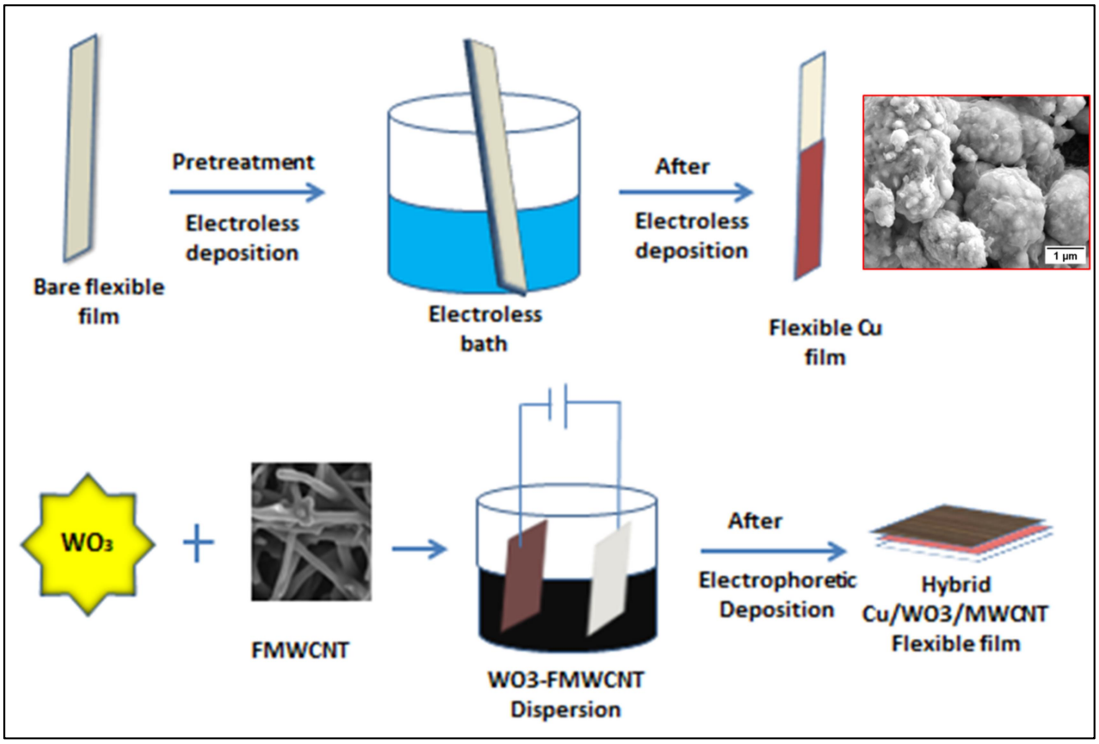

Scheme 5.1 represents the fabrication of Cu-WO_3-fMWCNT composite film.

5.2.5. Characterization techniques

X-ray diffractometry (Rigaku Ultima IV)was employed to determine the prominent planes of the composite. The source was Cu-Kα ray having wavelength of 1.5418 Å, and operated at, 40 kV with a current of 30 mA in the Bragg–Brentano geometry. EDX analysis [Carl Zeiss] with an operating voltage of 10 kV and having resolution of 136 eV was employed for the elemental analysis. The surface morphology was studied using SEM (Vega 3, Tescan) with an operating voltage of 15 kV. Fourier Transform Infrared Spectroscopy in attenuated total reflection mode confirmed the presence of various functional groups in the film. The band gap of the semiconductor material was determined from absorbance measurements using UV-Visible spectrometer (JascoV-750). Electrochemical characterization was carried out using the Biologic SP-200 electrochemical workstation with a three-electrode set-up. The aging characteristics of the lubricant oil was analyzed by comparing the electrochemical impedance spectroscopy measurements of various base oil samples with the oxidized oils under standard conditions. Impedance analysis is a useful

technique as it can be applied for complex non-aqueous systems as well as industrial lubricants to study the aging characteristics.

5.3. RESULTS AND DISCUSSION

5.3.1. XRD analysis of tungsten oxide

XRD patterns of bare OHP film and copper film formed by electroless deposition process are shown in Figure-5.1 (A) and (B). A strong peak at 25.7º is noticed for the bare substrate and the peak intensity got reduced when copper was deposited on to the film. XRD pattern observed in Figure-5.1(B) for flexible copper substrate formed by electroless deposition process gave three significant peaks at 2Ɵ values 44.4º , 51.8º and 76.5º corresponding to (111), (200) and (220) planes [37–40]. XRD analysis of WO_3 powder revealed crystalline structure of WO_3. As the moisture content and volatile components of the sample were removed during synthesis, WO_3 were converted from one phase to another making the structure more crystalline as revealed from the sharp peaks in XRD pattern. XRD patterns have three prominent peaks attributed to monoclinic WO_3 (JCPDS 43–1035) as shown in Figure-5.1 (C). The three peaks corresponding to 2θ values of 23.12, 23.68, 24.25 attributed to (002), (020), (200) crystal planes for WO_3 and the one at 34.6 is related to (202) plane. Other peaks were also observed which corresponds to other standard patterns reported in JCPDS for WO_3 [41–48]. XRD analysis of fMWCNT revealed a prominent peak for (002) plane corresponding to graphitic face at 26.2 $^{\circ}$ [49,50]. In the case of XRD pattern of WO_3-fMWCNT composite film the individual peaks for WO_3 and fMWCNT are clear but showed a merged appearance as shown in Figure-5.1 (C).

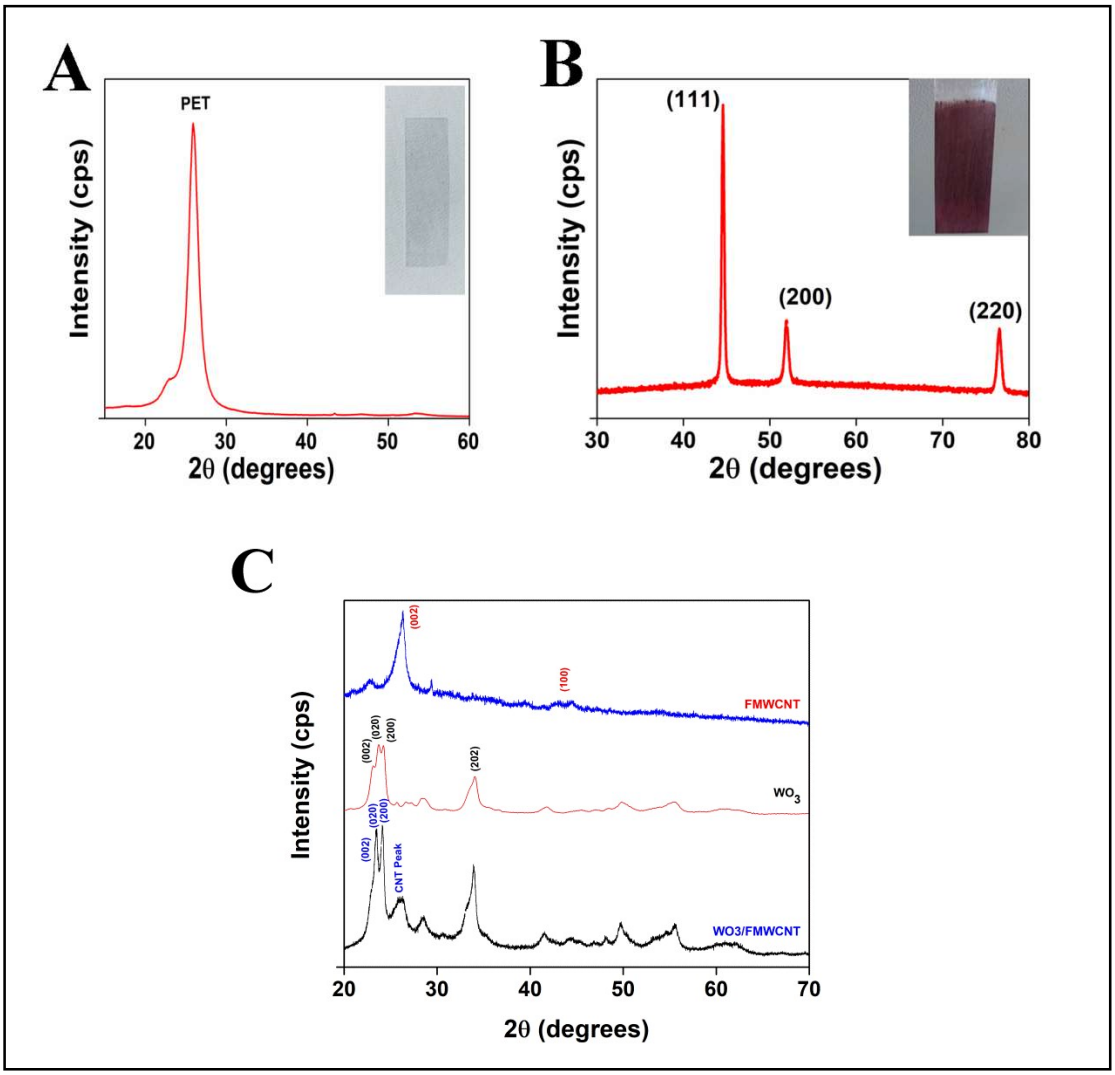

Figure-5.1. (A) XRD of the bare substrate (inset shows the photograph of bare substrate) (B) Cu film formed after electroless deposition process (inset shows the photograph of electroless copper substrate) (C) XRD pattern for powder fMWCNT, WO_3 and WO_3-fMWCNT Composite.

5.3.2. Optical Properties of WO_3-fMWCNT

UV-Visible spectroscopic analysis of the WO_3-fMWCNT composite showed an absorption peak at wavelength of 472 nm as in Figure-5.2 (A). Assuming that WO_3-fMWCNT has an indirectly allowed transition, the band gap energy was calculated using the following Eq. (1).

$$[\alpha h\nu]^{1/n} = A\,[h\nu - Eg] \quad (1)$$

Here α represents the absorption coefficient, Eg is the absorption band gap, n corresponds to the nature of transition. In the present case $n = 2$ as the transition is

assumed to be indirectly allowed. Tauc plot (inset) as shown in Figure-5.2 (B) gave a band gap of 2.58 eV for WO_3-fMWCNT solution [51,52].

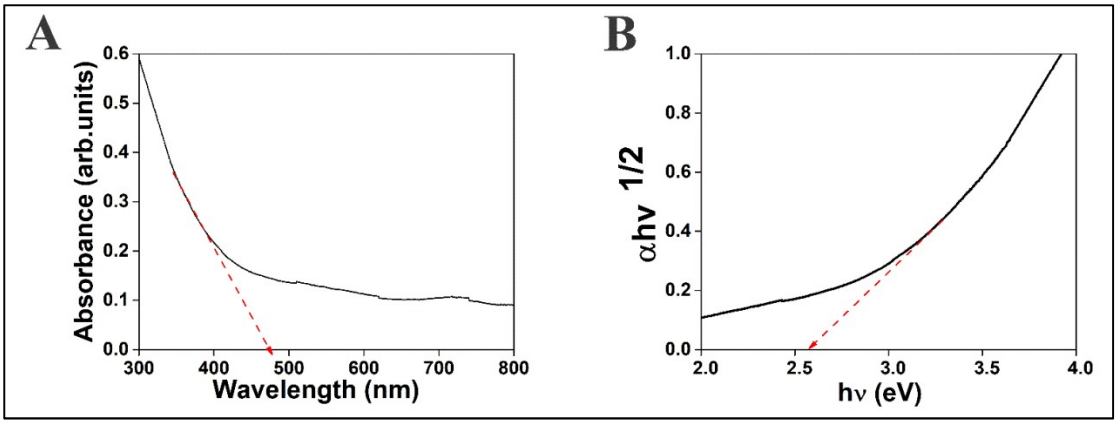

Figure-5.2. (A) Absorption spectra (B) Tauc plot for WO_3-fMWCNT

5.3.3. Elemental characterization and surface morphology of the Cu-WO_3- fMWCNT film

The surface morphology and elemental analysis of the Cu-WO_3- fMWCNT composite film was taken as such without any pretreatment of the film sample. EDX analysis confirmed the presence of copper, tungsten and carbon in the fabricated Cu-WO_3-fMWCNT film as shown in Figure-5.3. Although the percentage abundance of copper and carbon was high compared to tungsten, yet the presence of tungsten in the deposited film was detectable as revealed from the EDX analysis. Figure-5.4 shows the mapping pattern of the elements that shows the percentage abundance of the various elements in the deposited film within the scanned area. The EDX result confirmed that, concentration of different element present in the deposit supplement the observation of XRD analysis. The surface morphology of the nano composite film is presented in Figure-5.5 for two different areas of the fabricated hybrid Cu-WO_3-fMWCNT deposit. From the SEM images shown in Figure-5.5 (A) and (B) it is evident that for one region of the film a network morphology can be observed with thick stems linked by numerous short branches. This may be attributed to the dendritic nature of the WO_3 deposit formed onto fMWCNT forming a hybrid morphology. In the regions next to it, the surface resembles an agglomerated morphology consist of loosely attached WO_3-fMWCNT distributed over the copper film as shown in Figure-. 5.5 (C) and (D). As WO_3-fMWCNT composite was

distributed throughout the copper film the surface was moderately porous in nature [53]. From the SEM analysis it can be concluded that the Cu-WO_3-fMWCNT deposit showed more or less uniform morphology over the entire surface attributed to the deposition conditions employed.

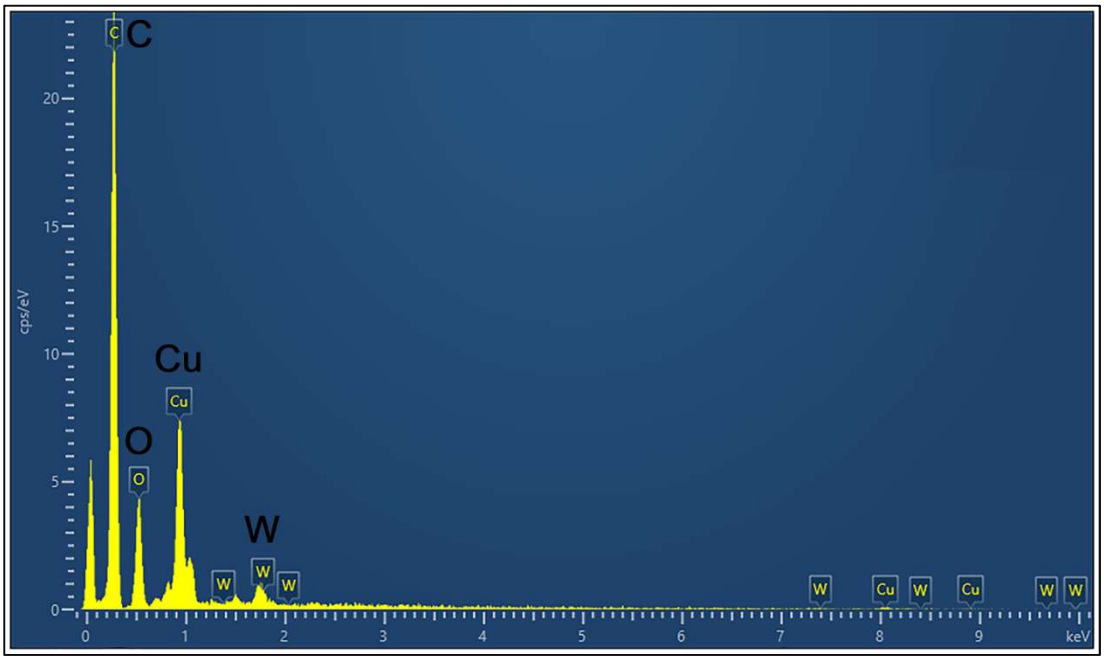

Figure-5.3. EDX spectrum of the flexible Cu/WO_3/MWCNT electrode.

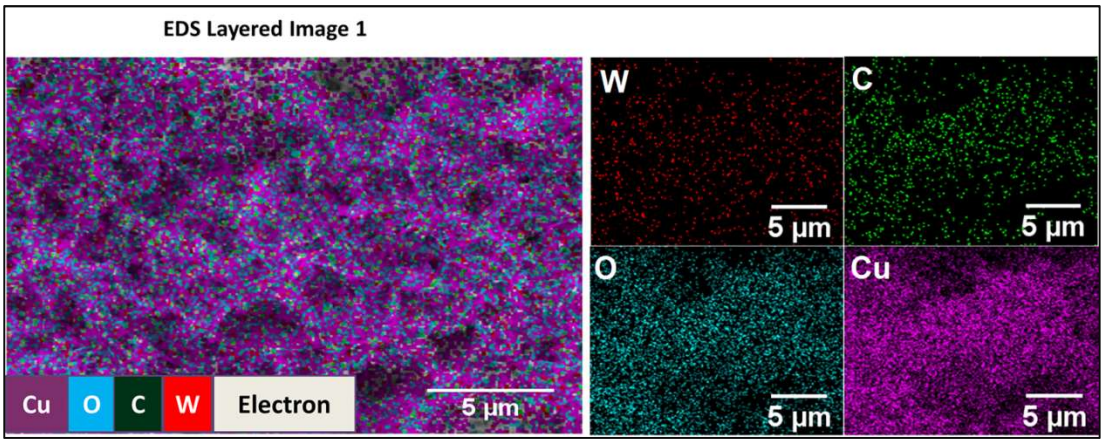

Figure-5.4. EDX mapping studies of various elements shown in EDX analysis.

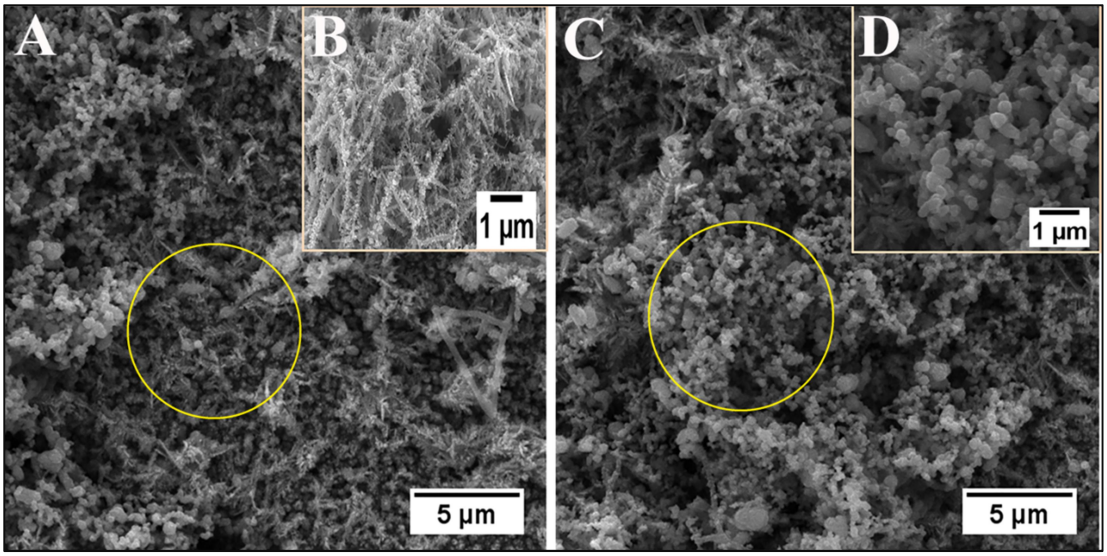

Figure-5.5. SEM images of Cu-WO_3-fMWCNT electrode for two different areas at two magnifications are shown in (A) and (C). The inset (B and D) is the enlarged view of the circled area.

5.3.4. FTIR spectrum of the composite film

The synthesized WO_3 powder was characterized by FTIR technique and is shown in Figure-5.6 (A). The FTIR peaks found in the region of 650-800 cm^{-1} corresponds to O-W-O stretching vibrations. The peak at 970 cm^{-1} is due to the stretching of W=O bonds in $WO_3.H_2O$. The bending mode of –OH group is indicated by the peak at 1630 cm^{-1}. The broad peaks at 3500-3700 cm^{-1} corresponds to the stretching mode of –OH group in water or hydroxyls [54,55].

The presence of WO_3-fMWCNT in the film was again confirmed by FTIR studies. This is shown in Figure-5.6 (B). The functional group present in fMWCNT and the oxygen attached to tungsten were identified by this analysis. The asymmetric CH_2 stretching vibration of WO_3-fMWCNT is shown by the characteristic band at 2921 cm^{-1}. The adsorption band at 1715 cm^{-1} and 1596 cm^{-1} corresponds to the stretching vibration of carbonyl group and conjugated $C = C$ bonds. The band at 1245 cm^{-1} and 1428 cm^{-1} corresponds to C–OH group formed after acid treatment of MWCNT. The stretching mode of O-W-O is found in the range of 600–840 cm^{-1} and bending mode of $W = O$ shows peak in the range of 900–1100 cm^{-1}. The FTIR result confirms the presence of WO_3- fMWCNT in the copper film [56,57].

The photographs of the synthesized WO_3 powder and the fabricated flexible Cu-WO_3-fMWCNT electrode are shown in the inset of Figure-5.6 (A) and (B).

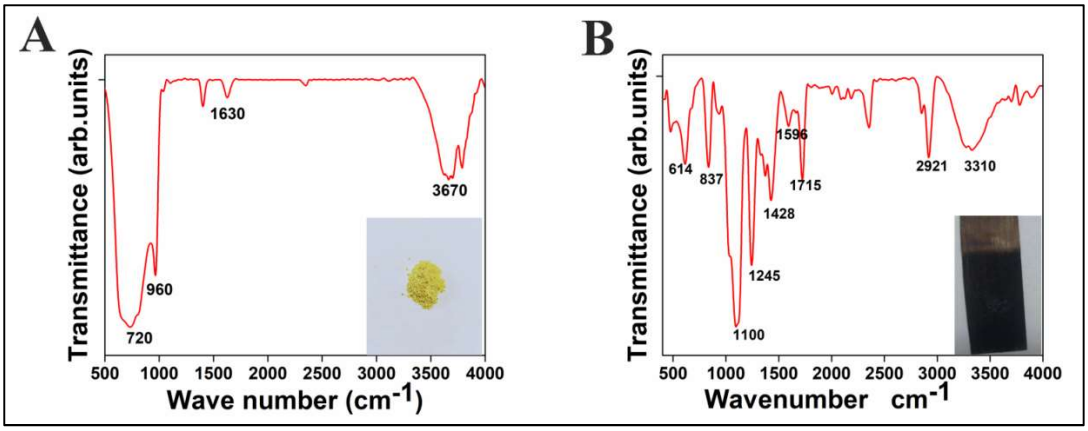

Figure-5.6. FTIR spectrum (A) $WO_3.H_2O$ powder and (B) Cu-WO_3-fMWCNT electrode.

5.3.5. Cyclic voltammetry analysis of Cu-WO_3-fMWCNT film

Cyclic voltammteric analysis of the composite film during different stages of fabrication process were condcuted to explore the electrochemical performance. A three electrode setup consist of Ag/AgCl electrode as the reference electrode, large area Pt as the counter electrode and Cu-WO_3-fMWCNT composite film electrode as the working electrode was taken for CV analysis. Figure-5.7 shows comparison of CV curves obtained for copper deposited film and Cu-WO_3-fMWCNT composite film at a scan rate of 100 mV/s within the potential range from - 1 V to +1 V in phosphate buffer solution. The cyclic voltammograms of copper film formed by electroless deposition process on to the polyethylene film exhibited two anodic and two cathodic peaks, characteristic for copper deposit. The anodic peaks Ipa^1 and Ipa^2 corresponds to oxidation of Cu (0) to Cu (I) and Cu (I) to Cu (II). The two cathodic peaks Ipc^1 and Ipc^2 corresponds to reduction of Cu (II) to Cu (I) and reduction of Cu (I) to Cu [58]. A distinct peak behavior was noted after electrodeposition of WO_3-fMWCNT on to copper film. The redox peaks characteristic for copper were replaced by another set of redox peaks signifying the presence of WO_3-fMWCNT deposit in the fabricated film. It is also noted that conversion of W^{6+} –W^{5+} occurs and H^+ ion might have a tendency to incorporate into WO_3 deposit resulting in the formation of tungsten bronze. The deposition of WO_3-fMWCNT on to the copper film substrate increased the specific capacitance when compared with the specific capacitance of pure copper film. This

makes the fabricated Cu-WO_3-fMWCNT composite film to act as good pseudo capacitive material having good energy storage characteristics. This can be attributed to the surface faradaic reaction attributed through improved electron transfer and the larger surface area due to incorporation of CNT. Inorder to verify the electrode stability, CV analysis of the Cu-WO_3- fMWCNT electrode were carried out under specific conditions. The CV response were analysed for different scan rates starting from 2 mV/s to 100 mV/s in the potential range of 1 V to -1 V. The behavior of the composite film is shown in Figure-5.8. The specific capacitance observed for electrode at 2 mV/s was found to be 500 F/g and specific capacitance slightly decreased with increasing scan rates. The variation of specific capacitance with scan rate is shown in Figure-5.9. This can be ascribed to the synergistic effect of more faradaic reaction and double layer capacitance. The calcination conditions employed during WO_3 synthesis may create oxygen vacancies and that could improve the energy storage capacity of Cu-WO_3-fMWCNT film. The CV behavoiur of the fabricated electrode with respect to various cycle is shown in Figure-5.10. The stability and retention behavior of the electrode was also studied. After 2000 cycles the electrode exhibited 85% of the original behavior and after 3000 cycles the film electrode retained 80% of the retetion behavior. These result shows that the charge transfer process occured between electrode-electrolyte system was good and the electrode was found to be stable [59]. The result clearly tells that Cu-WO_3-fMWCNT composite film has superior adherence and the deposit was intact after specific cycle of operations.

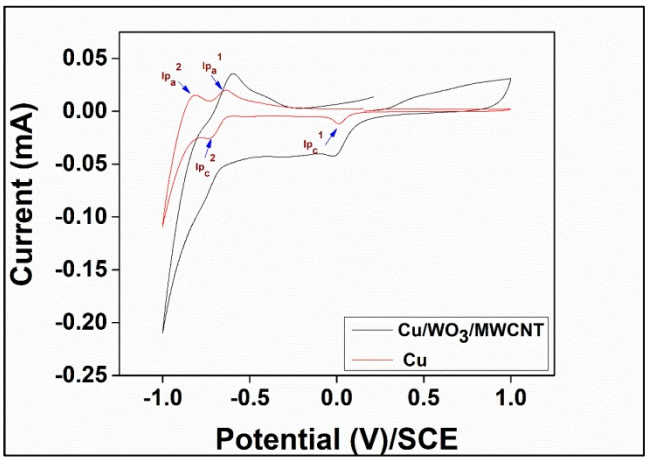

Figure-5.7. Comparison of CV curves of flexible copper substrate and Cu-WO_3- fMWCNT electrode at a scan rate of 100 mV/s in PBS solution.

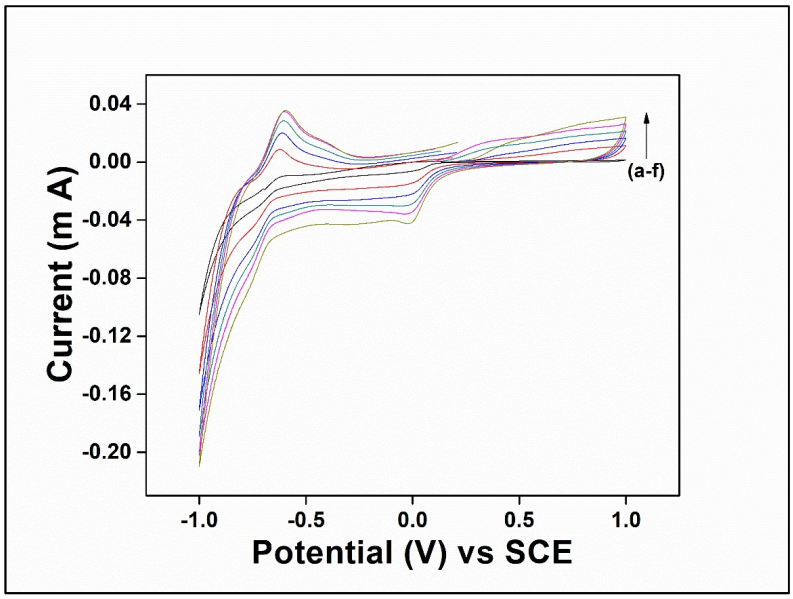

Figure-5.8. CV curves obtained for Cu-WO_3-fMWCNT composite electrode for scan rates (a) 2 mV/s (b) 20 mV/s (c) 40 mV/s (d) 60 m V/s (e) 80 mV/s and (f) 100 mV/s at potential ranging from - 1 V to +1 V in PBS buffer.

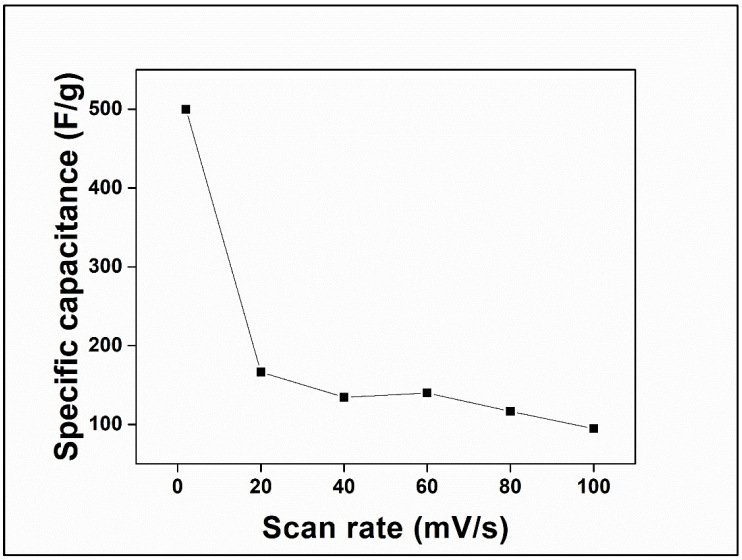

Figure-5.9. Variation of specific capacitance with scan rate of the fabricated Cu- WO_3-fMWCNT electrode.

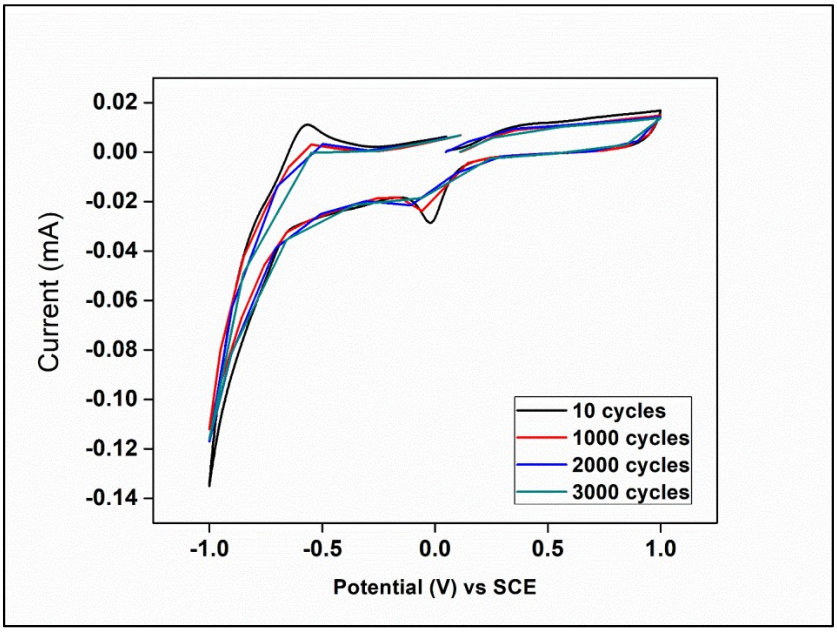

Figure-5.10. CV curves of the Cu-WO_3-fMWCNT electrode for 10^{th}, 1000^{th}, 2000^{th} and 3000^{th} cycles at a scan rate of 50 mV/s in PBS solution.

5.3.6. Impedance analysis of fresh and aged lubricant oils

The developed Cu-WO_3-fMWCNT film electrode was used as sensor for studying aging characteristics of lubricants by electrochemical impedance spectroscopy (EIS) technique. Fresh oil sample was subjected to heat treatment at a temperature of 80 $^{\circ}$C for varying time duration so as to effect oxidation of the oil sample. The fresh as well oxidized samples were withdrawn at fixed time intervals to study the impedance response with respect to Cu-WO_3-fMWCNT composite electrode. The impedance behavior of fresh industrial lubricant and aged sample shows distinct peak appearance as observed from the nyquist plot. The equivalent circuit for the impedance plot is shown in Figure-5.11. The equivalent circuit consist of double layer capacitance in parallel with R2 and R3 for the adsorption process and the charge transfer resistance that occur at the electrode. In addition, warburg impedance for diffusion controlled reaction was also included in the equivalent circuit. Impedance behavior of fresh and aged lubricant oils was studied in the frequency range from 1 MHz to 1 Hz. Oxidation of lubricants result in changes in electrical and thermal conductivity of oils due to modification of chemical additives already incorporated into the oil. Impedance analysis using the fabricated electrode supported the theoretical study that fresh lubricants possessed poor electrical

conductivity. This was clear from the graph where the initial appearance of semicircle modifies to more or less diffusion controlled process. Nyquist plots clearly shows the difference in behavior of fresh oils and aged oils. High impedance values with larger semicircular area shows the capacitive behavior and smaller semicircle represents the impedance characteristics of aged oils as shown in Figure-5.12 (A). A decrease in impedance is noticed for aged oil samples as in Figure-5.12 (B), which implies resistive behavior of the system and is shown by a semicircular plot. During aging of oils there shows increase in conductivity due to increase in oxidation by-products, wear particles as well as water. The developed electrode exhibited superior sensing characteristics for various oxidized oil samples heat treated to varying time duration extending up to 48 hrs as shown in Figure-5.13. The formation of oxidized components in the lubricant oil during its use and the degraded products produced during the cracking of hydrocarbon chains, that includes carboxylic acid, alcohols, water, carbonyl compounds etc. shifts the Rct (charge transfer resistance) values. As the oil ages the dipolar compounds become oxidized to more polar compounds leading to an increase in capacitance value. There can be an increase in the viscosity of the oil that decreases the mobility of the oil due to aging as reflected in the Rct values. A charge transfer process occur between oxidized products and the composite electrode. This may be due to adsorptive species present in the oil that leads to distorted semi-circle as observed with various oil samples heat treated at different temperature [60–64]. The results from impedance data clearly tells that the developed composite electrode can be used as sensor for studying the aging characteristics of lubricant oil.

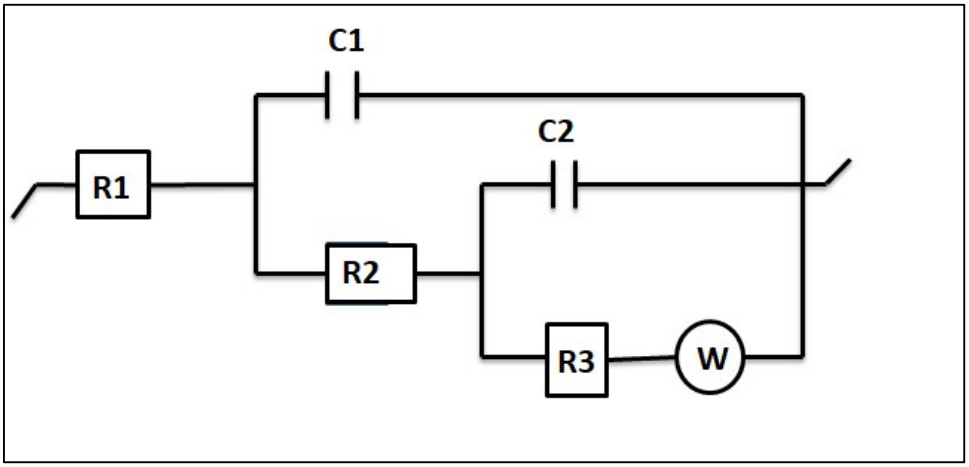

Figure-5.11. Equivalent circuit model for the impedance analysis.

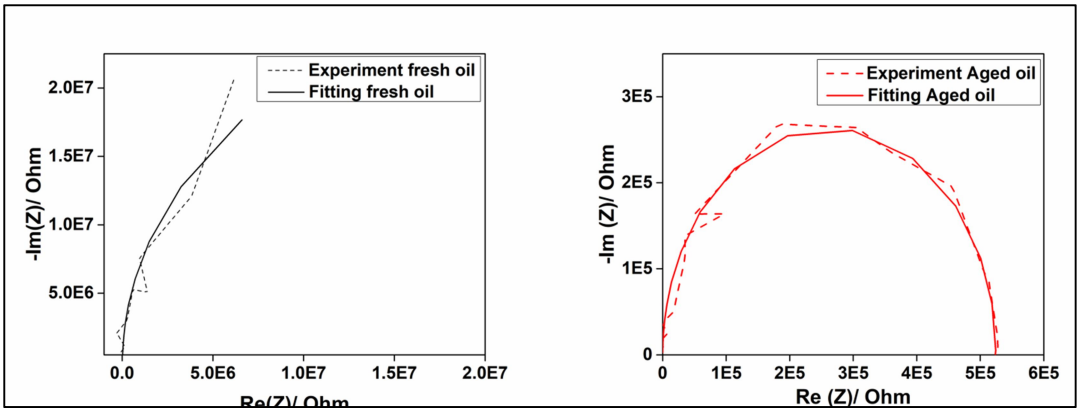

Figure-5.12. Nyquist plots of (A) fresh oil (B) aged oil.

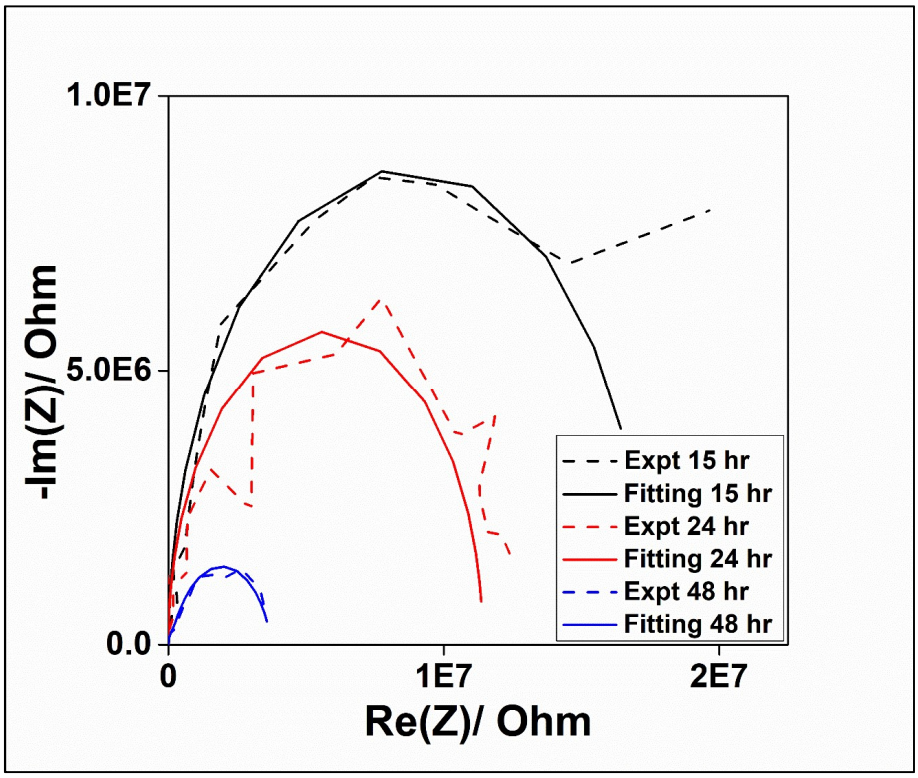

Figure-5.13. Nyquist plots for oxidized samples subjected to heat treatment at 80 ˚C for various time durations.

5.4. CONCLUSIONS

The present study describes a facile method for fabrication of composite hybrid film electrode which can be used as sensor for studying the aging characteristics of oils. Cu-WO_3-fMWCNT film electrode was developed by direct deposition technique from an optimized bath. Electrochemical deposition process viz. electroless and electrophoretic deposition method were adopted for the fabrication of flexible

Cu-WO_3-MWCNT electrode. The hybrid film electrode was characterized by various techniques. XRD analysis revealed monoclinic crystal structure for WO_3 and the UV-Vis analysis proved the optical properties of WO_3-fMWCNT composite. The presence of various elements in the electrode was revealed by EDX and FTIR analysis. SEM analysis showed a uniform and regular morphology for the deposit. Electrochemical studies revealed superior specific capacitance value and good retention factor for the developed electrode. The electrode showed good sensing behavior for determining aging characteristics of lubricant oil as revealed by the impedance studies. Studies should be extended further to make this type of hybrid electrodes as sensor for online monitoring of aging of lubricant oils during its usage itself.

5.5. REFERENCES

1. Susanti, Diah; Tsai, Dah-Shyang; Huang Y-S. Hybrid electrochemical capacitor of IrO_2 nanocrystal and hydrous RuO_2. Sci Adv Mater. 2:552-559(8).

2. Sugimoto W, Kizaki T, Yokoshima K, Murakami Y, Takasu Y. Evaluation of the pseudocapacitance in RuO_2 with a RuO_2/GC thin film electrode. Electrochim Acta. 2004;49(2):313–20.

3. Zeng YX, Han Y, Zhao Y T, Zeng Y, Yu M H, Liu Y J, Tang H, Tong Y and Lu X. Advanced Ti-Doped Fe_2O_3@PEDOT core/shell anode for high-energy asymmetric supercapacitors. Adv Energy Mater. 2015;5(12):1–7.

4. Susanti D, Tsai DS, Huang YS, Korotcov A, Chung WH. Structures and electrochemical capacitive properties of RuO_2 vertical nanorods encased in hydrous RuO_2. J Phys Chem C. 2007;111(26):9530–7.

5. Hu C-C, Chen W-C, Chang K-H. How to achieve maximum utilization of hydrous ruthenium oxide for supercapacitors. J Electrochem Soc. 2004;151(2):A281.

6. Ke YF, Tsai DS, Huang YS. Electrochemical capacitors of RuO_2 nanophase grown on $LiNbO_3$(100) and sapphire(0001) substrates. J Mater Chem. 2005;15(21):2122–7.

7. Chen LF, Yu ZY, Ma X, Li ZY, Yu SH. In situ hydrothermal growth of ferric oxides on carbon cloth for low-cost and scalable high-energy-density supercapacitors. Nano Energy. 2014;9:345–54.

8. He G, Ling M, Han X, Abou El Amaiem D I, Shao Y, Li Y, Li W, Ji S, Li B, Lu Y, Zou R, Wang F R, Brett D J L, Guo Z X, Blackman C and Parkin I P. Self-standing electrodes with core-shell structures for high-performance supercapacitors. Energy Storage Mater. 2017;9:119–25.

9. Shinde PA, Jun S C. Review on recent progress in the development of tungsten oxide based electrodes for electrochemical energy storage. ChemSusChem. 2020;13(1):11–38.

10. Zhou H, Zou X, Zhang K, Sun P, Islam M S, Gong J, Zhang Y and Yang J. Molybdenum-tungsten mixed oxide deposited into titanium dioxide nanotube arrays for ultrahigh rate supercapacitors. ACS Appl Mater Interfaces. 2017;9(22):18699–709.

11. Shen L, Du L, Tan S, Zang Z, Zhao C, Mai W. Flexible electrochromic supercapacitor hybrid electrodes based on tungsten oxide films and silver nanowires. Chem Commun. 2016;52(37):6296–9.

12. Choi YG, Sakai G, Shimanoe K, Miura N, Yamazoe N. Preparation of aqueous sols of tungsten oxide dihydrate from sodium tungstate by an ion-exchange method. Sensors Actuators, B Chem. 2002;87(1):63–72.

13. Chang KH, Hu CC, Huang CM, Liu YL, Chang CI. Microwave-assisted hydrothermal synthesis of crystalline WO_3-$WO_3 \cdot 0.5H_2O$ mixtures for pseudocapacitors of the asymmetric type. J Power Sources. 2011;196(4):2387–92.

14. Shieh J, Feng HM, Hon MH, Juang HY. WO_3 and W-Ti-O thin-film gas sensors prepared by sol-gel dip-coating. Sensors Actuators, B Chem. 2002;86(1):75–80.

15. Gu G, Zheng B, Han WQ, Roth S, Liu J. Tungsten Oxide Nanowires on Tungsten Substrates. Nano Lett. 2002;2(8):849–51.

16. Klinke C, Hannon JB, Gignac L, Reuter K, Avouris P. Tungsten oxide nanowire growth by chemically induced strain. J Phys Chem B. 2005;109(38):17787–90.

17. Su X, Xiao F, Li Y, Jian J, Sun Q, Wang J. Synthesis of uniform WO_3 square nanoplates via an organic acid-assisted hydrothermal process. Mater Lett. 2010;64(10):1232–4.

18. Hahn R, Macak JM, Schmuki P. Rapid anodic growth of TiO_2 and WO_3 nanotubes in fluoride free electrolytes. Electrochem commun. 2007;9(5):947–52.

19. Xiaoliang Zhu, Chong Zhong and Jiang Zhe. Lubricating oil conditioning sensors for online machine health monitoring – A Review. In 2017. p. 1–26.

20. Wang SS, Lee HS. The development of in situ electrochemical oil-condition sensors. Sensors Actuators B Chem. 1994;17(3):179–85.

21. Liu CC, Dudik L. Electrochemical sensors for monitoring conditions of lubricants. Encycl Appl Electrochem. 2014;(July 2019).

22. Jacob SR, Compton RG. Electrochemical studies of the automotive lubricant additive zinc n-Dibutyldithiophosphate. J Electrochem Soc. 1999;146(7):2598–605.

23. Farrington AM, Slater JM. Monitoring of engine oil degradation by voltammetric methods utilizing disposable solid wire microelectrodes. Analyst. 1997;122(6):593–6.

24. Wang SS, Lee HS. The application of a.c. impedance technique for detecting glycol contamination in engine oil. Sensors Actuators, B Chem. 1997;40(2–3):193–7.

25. Agoston A, Ötsch C, Jakoby B. Viscosity sensors for engine oil condition monitoring - Application and interpretation of results. Sensors Actuators, A Phys. 2005;121(2):327–32.

26. Soleimani M, Sophocleous M, Wang L, Atkinson J, Hosier IL, Vaughan AS, Base oil oxidation detection using novel chemical sensors and impedance spectroscopy measurements. Sensors Actuators, B Chem. 2014;199:247–58.

27. Qiang L, Jiang W, Lili C, Xiaowei L. A study of moisture content of lubricating oil based on impedance analysis. 2012;(Mems):406–9.

28. Jitianu A, Cacciaguerra T, Benoit R, Delpeux S, Béguin F, Bonnamy S. Synthesis and characterization of carbon nanotubes-TiO_2 nanocomposites. Carbon N Y. 2004;42(5–6):1147–51.

29. Akbulut H, Nalci D, Guler A, Duman S, Guler MO. Carbon-silicon composite anode electrodes modified with MWCNT for high energy battery applications. Appl Surf Sci . 2018;446:222–9.

30. Salmaoui S, Sediri F, Gharbi N. Characterization of h-WO_3 nanorods synthesized by hydrothermal process. Polyhedron . 2010;29(7):1771–5.

31. Farhadian M, Sangpour P, Hosseinzadeh G. Preparation and photocatalytic activity of WO_3-MWCNT nanocomposite for degradation of naphthalene under visible light irradiation. RSC Adv. 2016;6(45):39063–73.

32. Ngai KS, Tan WT, Zainal Z, Zawawi RBM, Zidan M. Electrochemical oxidation of ascorbic acid mediated by single-walled carbon nanotube/tungsten oxide nanoparticles modified glassy carbon electrode. Int J Electrochem Sci. 2012;7(5):4210–22.

33. Yu J, Choo KH, Niu L, Chua DHC. Synthesis of three-dimensional tungsten oxide cactus-shaped nanostructures supported on carbon nanotubes template. Electrochem Solid-State Lett. 2011;14(10):58–61.

34. Choi YW, Kim S, Seong M, Yoo H, Choi J. NH_4-doped anodic WO_3 prepared through anodization and subsequent NH_4OH treatment for water splitting. Appl Surf Sci . 2015;324:414–8.

35. Rodríguez-Pérez M, Chacón C, Palacios-González E, Rodríguez-Gattorno G, Oskam G. Photoelectrochemical water oxidation at electrophoretically deposited WO_3 films as a function of crystal structure and morphology. Electrochim Acta. 2014;140:320–31.

36. Zhu T, Chong MN, Chan ES. Nanostructured tungsten trioxide thin films synthesized for photoelectrocatalytic water oxidation: A review. ChemSusChem. 2014;7(11):2974–97.

37. Gupta S, Patidar D, Baboo M, Sharma K, Saxena NS. Investigation of Al Schottky junction on n-type CdS film deposited on polymer substrate. Front Optoelectron China. 2010;3(September):321–7.

38. Morgan KA, Tang T, Ioannis Z, Ravagli A, Craig C, Yao J, et al. High-throughput physical vapour deposition flexible thermoelectric generators. Scient. 2019;9:1–9.

39. A.Atta, E.Abdeltwab AB. Structural, mechanical and electrical properties of sputter coated copper thin films on poly ethylene terephthalate. Int J Mod Phys. 2022;36:1–22.

40. Wasly HS, El-sadek MSA, Elnobi S, Abuelwafa AA. Morphological , structural , and optical properties of flexible Tin Oxide (II) thin film via thermal evaporation technique. Eur Phys J Plus . 2022;123.

41. Joint committee on powder diffraction standards (JCPDS) FN 75-2072. No Title. In.

42. Joint committee on powder diffraction standards (JCPDS) FN 83-0950. No Title. In.

43. Joint committee on powder diffraction standards (JCPDS) FN 83-0947. No Title. In.

44. Joint committee on powder diffraction standards (JCPDS) FN 71-0131. No Title. In.

45. Abdullah SF, Radiman S, Hamid MAA, Ibrahim NB. Studies on the phase transitions and properties of tungsten (VI) oxide particles by X-Ray diffraction (XRD) and thermal analysis. J Fiz Mal. 2007;28(1):7–12.

46. Sivakumar R, Raj AME, Subramanian B, Jayachandran M, Trivedi DC, Sanjeeviraja C. Preparation and characterization of spray deposited n-type WO_3 thin films for electrochromic devices. Mater Res Bull. 2004;39(10):1479–89.

47. Fenglin Liu, Xianjie Chen, Qinghua Xia, Lihong Tian and Xiaobo Chen. Ultrathin tungsten oxide nanowires: oleylamine assisted nonhydrolytic growth, oxygen vacancy and high photocatalytic properties. R Soc Chem. 2015;5:77423–8.

48. Li S, Shelar DP, Hou CC, Chen QQ, Deng P, Chen Y. WO_3 nanospheres with improved catalytic activity for visible light induced cross dehydrogenative coupling reactions. J Photochem Photobiol A Chem . 2018;363:44–50.

49. Yu Q, Yang X, Chen Y. Electrochemical detection of codeine in pharmaceutical tablets using a tungsten oxide nanoparticles and carbon nanotubes modified electrode. Int J Electrochem Sci. 2016;11(8):6862–72.

50. Dinari M, Momeni MM, Ahangarpour M. Efficient degradation of methylene blue dye over tungsten trioxide/multi-walled carbon nanotube system as a novel photocatalyst. Appl Phys A Mater Sci Process. 2016;122(10).

51. K. Sandeep, B. Manoj and K. G. Thomas. Gold nanoparticle on semiconductor quantum dot : Do surface ligands influence Fermi level equilibration. J Chem Phys . 2020;044710.

52. Mukherjee I, Electric G, Dinda G, Moulik SP. Synthesis, characterization, and applications of microheterogeneous-templated CdS nanodispersions. J Nanopart Res. 2012;14.

53. Di J, Xu H, Gai X, Yang R, Zheng H. One-step solvothermal synthesis of feather duster-like CNT@WO3 as high-performance electrode for supercapacitor. Mater Lett . 2019;246:129–32.

54. Shouli Bai, Kewei Zhang, Liangshi Wang, Jianhua Sun, Ruixian Luo, Dianqing Li and Aifan Chen. Synthesis mechanism and gas-sensing application of nanosheet-assembled tungsten oxide microspheres. J Mater Chem A. 2014;0.

55. Mariusz Szkoda, Zuzanna Zarach , Konrad Trzcinski, Grzegorz Trykowski and Andrzej PNowak. An easy and ecological method of obtaining hydrated and non-Crystalline WO_{3-x} for application. Materials (Basel). 2020;13.

56. Susanti D, Narendra R, Wibawa D, Tananta L, Purwaningsih H. The effect of calcination temperature on the capacitive properties of WO_3-based electrochemical capacitors synthesized via a sol-gel method. Front. Mater. Sci.2013;7(4):370–8.

57. Shakeela K, Dithya ASRI, Rao CHJ, Rao GR. Electrochemical behaviour of Cu(II)/ Cu(I) redox couple in 1-hexyl-3-methylimidazolium chloride ionic liquid. J Chem Sci. 2015;127(1):133–40.

58. Thota R, Ganesh V. Chemically modified flexible strips as electrochemical biosensors. Analyst. 2014;139:4661–72.

59. Mujahid A, Dickert FL. Monitoring automotive oil degradation : analytical tools and onboard sensing technologies. Anal Bioanal Chem. 2012;404:1197–209.

60. Latif U, Dickert FL. Conductometric sensors for monitoring degradation of automotive engine oil. sensors. 2011;11:8611–25.

61. Moon S, Paek K, Lee Y, Kim J. Multiwall carbon nanotube sensor for monitoring engine oil. Electrochem Solid-State Lett. 2006;9:78–80.

62. Lvovich VF, Smiechowski MF. Impedance characterization of industrial lubricants. Electrochim Acta. 2006;51:1487–96.

63. Vorotyntsev MA, Badiali J, Inzelt G. Electrochemical impedance spectroscopy of thin films with two mobile charge carriers : effects of the interfacial charging. J Electroanal Chem. 1999;472:7–19.

64. Du Y, Wu T, Cheng J. Age detection of lubricating oil with on-line sensors. IEEE. 2015;5–8.

CHAPTER 6

DEVELOPMENT OF Pd@MWCNT-Co_3O_4 ELECTRODE USING COBALT RECOVERED FROM SPENT LITHIUM-ION BATTERIES FOR GLUCOSE SENSING

6.1. INTRODUCTION

Different types of battery/energy storage systems are concomitantly used for various types of applications that require a continuous and steady power supply. The battery materials which are dumped to earth without any recycling after their life cycle pose a great threat to the environment and human life. As the use of electric vehicles and electronic gadgets starts to grow exponentially, the pile-up of various battery waste materials that once powered various systems posed environmental concerns. Industry analysts predict that by 2020, China alone will generate some 500,000 metric tons of used Lithium-ion batteries (LIB) and that by 2030, the worldwide number will hit 2 million metric tons per year. If current trends for handling these spent batteries are not properly addressed, most of these systems may end up in landfills without any proper recycling process. These popular power packs contain valuable metals and other materials that can be recovered, processed and reused that ensures sustainable growth, protecting the mother earth. One thing we have to keep in mind is that the source of the main components that embody energy-storing materials in different batteries including metals viz. lithium, cobalt, nickel, and manganese are limited and no sooner than later this get exhausted as the source for the same is fast dwindling. So more economical and facile recycling methods are to be adopted to recover the valuable metals from these spent materials and thereby prevent their accumulation in the environment. Appropriate recycling protocol can prevent the conundrum of resource exhaustion as well as the inflation of hazardous waste in the environment [1–3].

The unique characteristics of LIB viz. small size, light weight, high power density and cell voltage, long life and low self-discharge rate make these batteries applicable in portable electronic devices, mobile phones, electronic cameras, laptops and electric vehicles [4]. The cathode materials used in LIB include $LiCoO_2$, $LiMn_2O_4$, $LiFePO_4$, $LiNi_xCo_yMn_{1-x-y}O_2$ [5,6]. Mostly all solid-state batteries use $LiCoO_2$ as cathode materials due to their high specific capacity and electronic conductivity. These LIBs also possess excellent cycle life [7]. The increasing demand for the production of LIB has subsequently resulted in the building up of battery waste and hence these are included in the category of waste electrical and electronic equipment (WEEE). The spent LIB contains heavy metals as well as toxic

electrolytes. These waste materials can result in serious environmental pollution. The toxic organic electrolytes, binder and heavy metal spills result in environmental pollution. When heated, these organic materials can produce hazardous gases like HF, Cl_2, CO_2 and CO, leading to global warming. Due to these concerns, it is highly desirable to recycle LIB. More over the economic value of spent LIB rises on the extraction of valuable metals from these batteries by various techniques [8]. Cobalt is included in the category of 'Critical Raw Materials' (CRM) due to its high economic value and lack of its supply from the corresponding sources. Natural graphite and phosphorous which are used in batteries are also included in the CRM category. So recovery of cobalt is one of the salient processes in the recycling of battery materials [9].The recovered cobalt can be converted into various forms by suitable methods. Cobalt oxide is one such material that can be synthesized by various experimental methods. The different nanostructured forms of cobalt oxide are used for sensing various analytes [10–13]. Researchers have adopted different methods for the recovery of valuable metals from spent batteries. The recycling of lithium and cobalt metals is done by various techniques including electro-dialysis coupled with chelation [14], leaching with inorganic acids [15–21]and hydrometallurgical methods involving natural organic acids [22–26]. The recycling of LIBs can be abridged into four categories which include the pyrometallurgical process, hydrometallurgical process, biometallurgical process or a combination of all the above-mentioned processes [27]. Lots of research groups focus their work on the recovery of the expensive metal cobalt since lithium is found in very low quantities and recovery of lithium from the raffinate during the hydrometallurgical extraction process results in the recovery of contaminated products with less recovery efficiency [28,29]. Cobalt metal extracted from these batteries as such and its hybrid composites find applications in various fields including sensors and supercapacitors.

Enzymatic sensors are widely researched and commonly used for real-time monitoring of glucose and other biomolecules that are found in our bodies. These sensors possess various limitations including their stability and variation in enzyme activity with respect to temperature, pH etc [30]. Research on the development of non-enzymatic glucose sensors using nanomaterials has been reported elsewhere. Metal, metal oxides and hybrid composites have been employed in the non-enzymatic detection of glucose. Metals like Au, Pd, Pt, Ni, Zn, Co, Cu, NiO, CuO, $NiCo_2O_4$ etc.

have been employed in glucose detection [31–35]. A combination of these metals has also been used for glucose sensing. Glucose sensors fabricated using noble metals are found to be highly efficient in the oxidation of glucose molecules, but their high cost limits their performance in glucose sensing.

The present work envisages on development of cobalt-based glucose sensor, cobalt being recovered from $LiCoO_2$ obtained from spent lithium batteries by leaching and further deposition of cobalt on to copper substrate using chronoamperometric technique followed by modification of the electrode with hybrid Pd@MWCNT nanocomposite using electrodeposition method. A comparative study of both Co_3O_4 and Pd@MWCNT-Co_3O_4electrodestoward glucose electrooxidation reactions has been carried out. The non-enzymatic Pd@MWCNT-Co_3O_4 showed excellent sensor response in the detection of glucose and was selective towards glucose detection in the presence of various interfering components.

6.2. EXPERIMENTAL METHODS

6.2.1. Extraction of $LiCoO_2$ powder from the spent lithium-ion batteries

Cylindrical lithium-ion cells of 3.7 V- 4.2 V were recovered from worn-out electronic gadgets. These spent LIB were manually dismantled. The plastic and steel cases were separated by making a longitudinal cut inorder to recover the packed material from the battery compartment and were dismantled extracting the various materials separately. The cathode and anode materials recovered were treated with various reagents as described. The cathodic material embedded in aluminum foil was separated and treated with 100 ml of N-methyl pyrrolidone (NMP, purity-99.9 %) at 100 ºC for 2 hours. The cathodic materials were completely removed from the aluminum substrate and these were dried at 60 ºC for 24 hours. After drying, the calcination process was done in a muffle furnace at 700 ºC for 5 hours and cooled at room temperature. The obtained powdered sample was characterized by X-ray diffractometer analysis to find the various compounds present.

6.2.2. Electrodeposition of cobalt oxide film onto the substrate from leach liquor

$LiCoO_2$ extracted by the above process was dissolved in 100 ml of leaching solution having the composition of 70 ml 3 M hydrochloric acid (HCI) and 30 ml of

hydrogen peroxide (H_2O_2). The mixture was stirred at 80 ºC for 2 hours. p^H of the solution was adjusted to 5 using 1 M NaOH solution. A thin film of cobalt oxide was deposited on the copper substrate by chronoamperometric technique using three electrode system under a constant voltage of -1V for 100s.

6.2.3. Fabrication of Pd@MWCNT-Co_3O_4 film

Functionalized multi-walled carbon nanotube was prepared as reported elsewhere[36]. 0.05g of FMWCNT was added to 20 ml of 0.05M palladium chloride solution ($PdCl_2$, purity ≥ 99.9%) and vigorously stirred for 24 hours. Pd^{2+} ions were reduced using hydrazine. Solid residue formed was centrifuged and washed with deionized water for several times and then dried at 120 ºC forming Pd@MWCNT powder. Pd@MWCNT was deposited onto Co_3O_4 film from dispersion through electrophoretic deposition process. The process was carried out at a constant potential of 10 V for 15 minutes. The fabricated Pd@MWCNT-Co_3O_4 film electrode was used for the electrochemical detection of glucose. Figure-6.1 shows the flowsheet of the entire recycling procedures of spent LIB and the fabrication ofPd@MWCNT-Co_3O_4 film for glucose sensing mechanism.

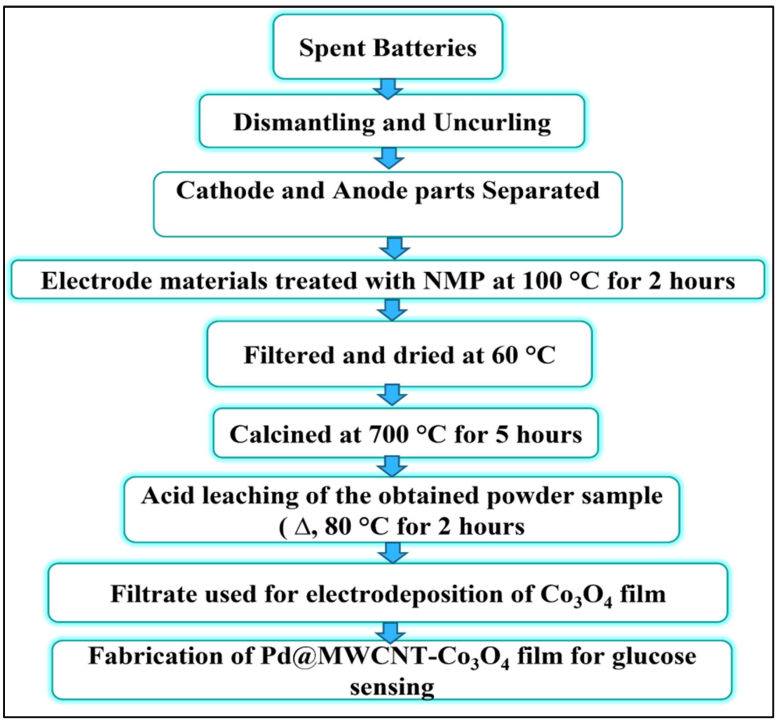

Figure-6.1. Flowsheet showing the recycling steps involved in extraction of cobalt from spent LIB for fabrication of Pd@MWCNT-Co_3O_4 film for sensing the analyte glucose.

6.2.4. Characterization Methods

The prominent planes of the synthesized Pd@MWCNT powder were analyzed using XRD (Rigaku Ultima IV). UV-Visible Spectrophotometer (Jasco UV, V-750) was used to study the absorbance spectrum of reduced and unreduced palladium in the range of 200-800 nm range. Fourier Transform Infrared Spectroscopy (FTIR) was used to analyze the powdered and the deposited samples. Energy dispersive X-ray analysis (EDX) was employed to detect the presence of various elements present in the fabricated film and the surface morphology of the electrodes was characterized using scanning electron microscopy (SEM-Gemini 300) which is attached with the EDX equipment. Electrochemical characterization of the fabricated electrodes were carried out using Biologic SP-200 Model using a three-electrode set up. The three-electrode set up consists of platinum electrode as the counter electrode, saturated calomel electrode (SCE) as the reference electrode and fabricated Pd@MWCNT-Co_3O_4 electrode as the working electrode and 0.1 M KOH solution served as the electrolyte. Sensor characteristics of the electrode were studied using cyclic voltammetry (CV) and chronoamperometric (CA) techniques.

6.3. RESULTS AND DISCUSSION

6.3.1. XRD analysis

The photograph of the spent lithium battery, uncurled cathode and anode parts are shown in Figure-6.2 (A) and Figure-6.2 (B). Figure-6.2 (D) and 6.2 (E) shows the photograph of the Co_3O_4 and Pd@MWCNT-Co_3O_4 electrodes. XRD of the calcined powder obtained from the cathode of spent LIB revealed the presence of $LiCoO_2$and the photograph of calcined $LiCoO_2$ is shown in Figure-6.2 (C). The calcination process was carried out in order to remove the organic compounds in the cathode material, especially acetylene black and poly vinylidene fluoride (PVDF) which are used as binder material. The sharp diffraction peaks at (003), (101), (104) and (107) correspond to $LiCoO_2$ and the peaks at (220) and (311) correspond to Co_3O_4 as shown in Figure-6.3(A). The mixed phases of both $LiCoO_2$ and Co_3O_4 was obtained. The cobalt oxide formed is the transformation by-product of $LiCoO_2$ [37–39]. Figure-6.3 (B) shows the XRD pattern of MWCNT which exhibits a prominent peak corresponding to (002) plane. and Figure-6.3 (C) shows the diffraction peaks of the

synthesized Pd@MWCNT powder. The diffraction peaks at (111), (200), (220), (311) and (222) correspond to the planes of palladium and the (002) plane confirms the presence of MWCNT [40,41].

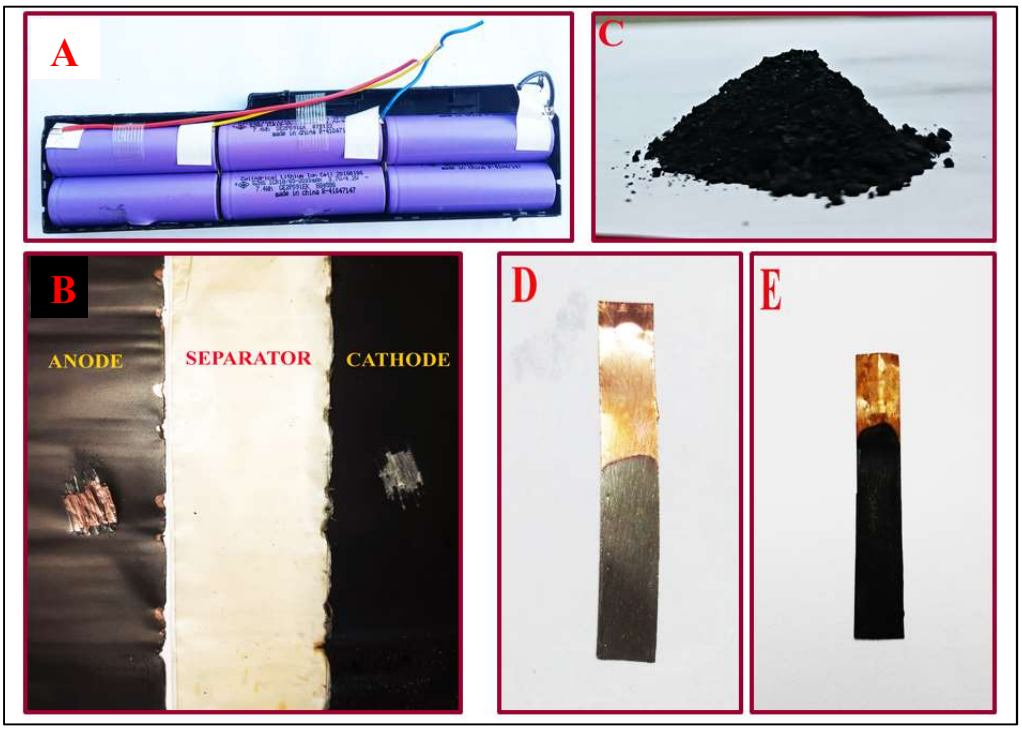

Figure-6.2. (A) Spent Lithium-ion battery (B) The separated parts of the battery including cathode,anode and separator (C) The $LiCoO_2$ powder obtained after calcination (D) Photograph of Co_3O_4 film (E) Photograph of Pd@MWCNT-Co_3O_4 film.

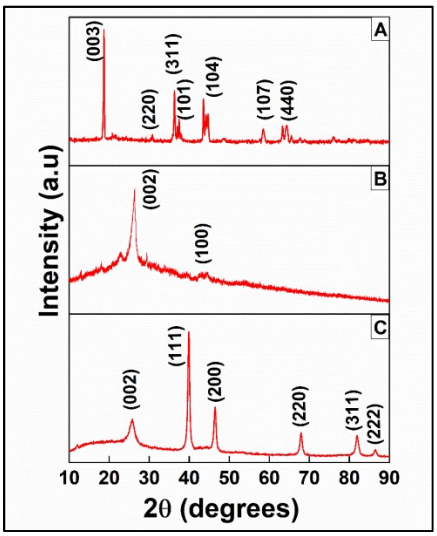

Figure-6.3. XRD analysis of (A) Calcined $LiCoO_2$ (B) MWCNT Powder and (C) Pd @MWCNT Powder.

6.3.2. Ultraviolet-Visible spectroscopic analysis

The UV-Visible Spectrum of the palladium solution was analyzed before and after reduction with hydrazine using a UV-Visible spectrophotometer. The yellow colour of palladium chloride turned colourless on the addition of hydrazine to the MWCNT-$PdCl_2$ mixture. This is the physical evidence showing the reduction of palladium (II) to palladium (0). Unreduced palladium (Pd^{2+}) shows an absorption peak at 284 nm which completely disappeared after the reduction process and this is attributed to the formation of Pd(0) nanoparticles as shown in Figure-6.4 [42].

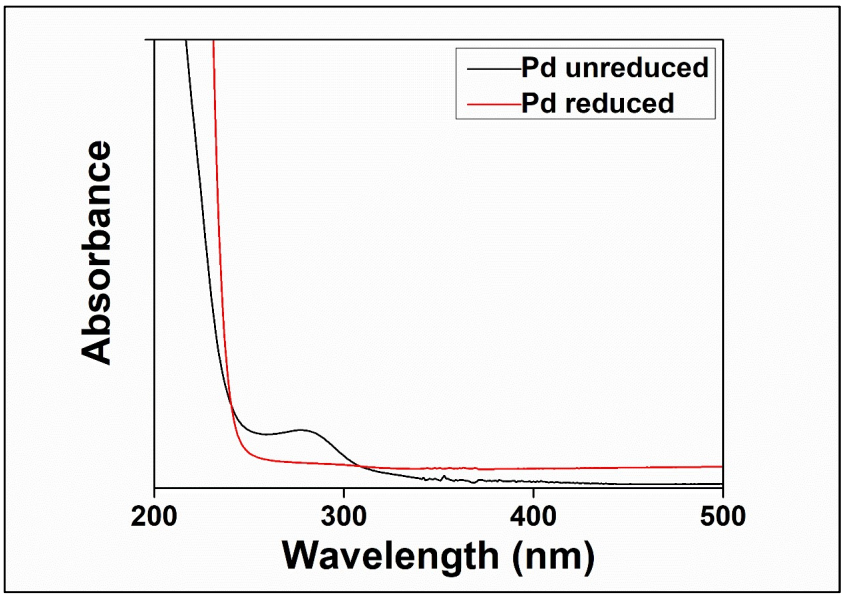

Figure-6.4. The UV-Vis spectrum of unreduced and reduced Palladium.

6.3.3. FTIR Studies

The deposited Co_3O_4 film was further characterized using FTIR spectroscopy in the range of 400 to 4000 cm^{-1}. Two well-defined peaks at 662 cm^{-1} and 552 cm^{-1}were obtained in the spectrum as shown in Figure-6.5. This corresponds to the Co-O stretching vibrations. The results confirm the formation of Co_3O_4 film on the substrate [43,44]. The inset of Figure-6.5 shows the FTIR spectrum of calcined $LiCoO_2$ and the leached residue. Both calcined and leached residue exhibited bands at 526 cm^{-1} and 628 cm^{-1} which is attributed to the bending mode of O-Co-O bonds and asymmetric stretching of Co-O bonds in CoO_6 octahedron [45,46].

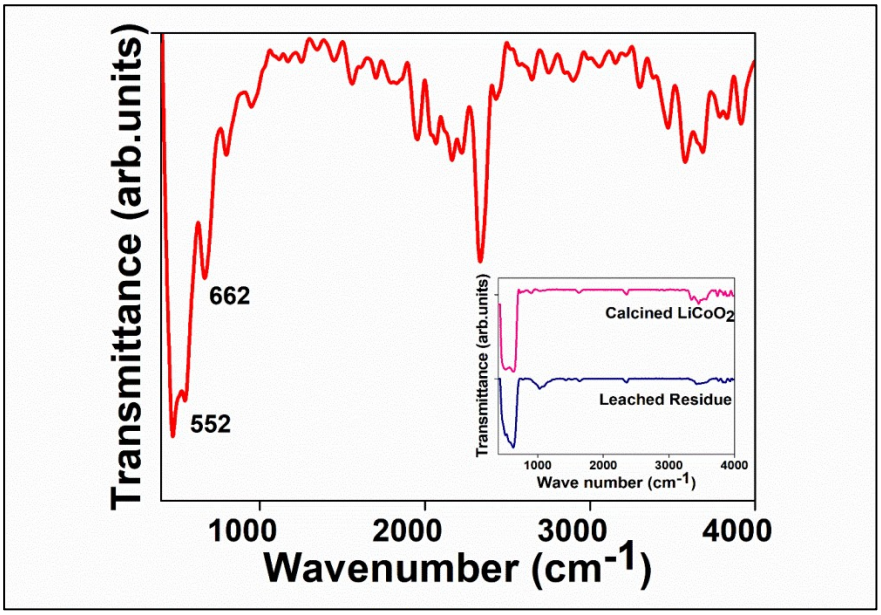

Figure-6.5. FTIR Spectrum of Co_3O_4 film. Inset showing the FTIR of calcined and leached $LiCoO_2$ powder.

6.3.4. Elemental Analysis and Surface Morphology of Pd@MWCNT-Co_3O_4 composite film

Elemental analysis and surface morphology of the composite film was done using EDX-SEM analysis. Elemental analysis of the Pd@MWCNT-Co_3O_4 electrodeposit shows the presence of various elements viz. copper, carbon, oxygen, cobalt and palladium. This is shown in Figure-6.6. SEM analysis of the deposited Co_3O_4 showed granular-like morphology over the entire matrix shown as in Figure-6.7 (A) and (B) [47]. The surface morphology was completely modified after the electro-deposition of Pd@MWCNT onto the Co_3O_4 electrode. Each spherical Co_3O_4 structure was covered by palladium-incorporated MWCNT structure. This is shown in Figure-6.7 (C) and (D). The coral reef-like superficial pattern shows the morphology of the Pd@MWCNT-Co_3O_4electrode.

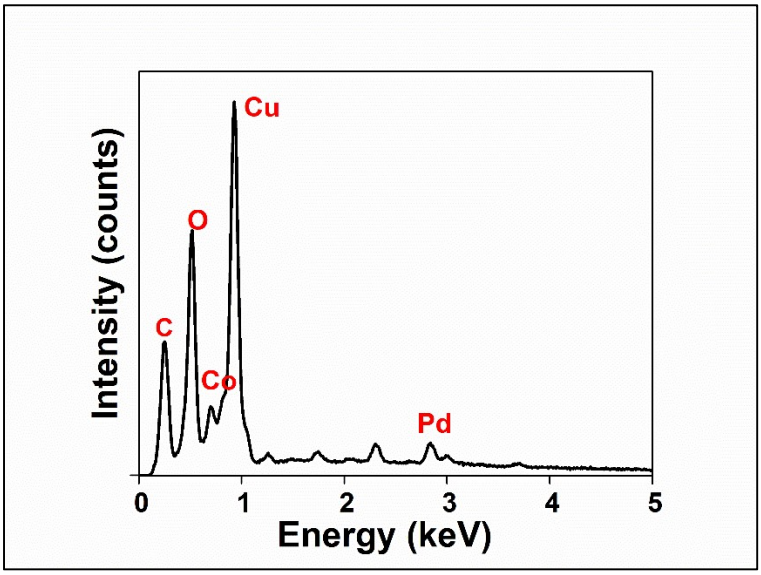

Figure-6.6. EDX Analysis of Pd@MWCNT-Co_3O_4 electrode

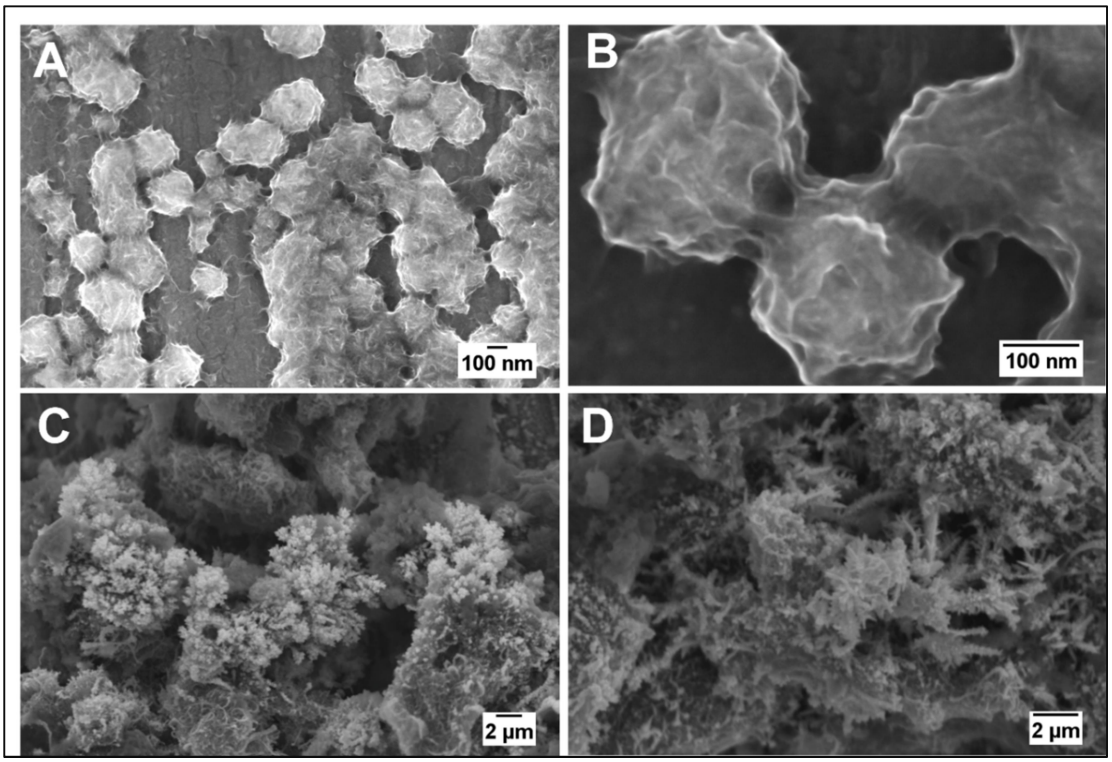

Figure-6.7. SEM images of Co_3O_4 film at different areas are shown in (A) and (B) and that of Pd@MWCNT-Co_3O_4 film is shown in (C) and (D).

6.3.5. Galvanostatic charge-discharge measurements

Galvanostatic charge-discharge measurements were carried out to evaluate the electrochemical performance of the fabricated electrode. GCD curves for Pd@MWCNT-Co_3O_4 electrode at various current densities ranging from 12 A/g to 20 A/g with a voltage window of 0-0.6 V were studied and is shown in Figure-6.8 (A). Specific capacitance was calculated using the following equation [48].

$C = I * t_d / m * \Delta V$ ---------- (1)

C is the specific capacitance, I is the charge-discharge current, m is the mass of electrochemically active material, ΔV is the potential window and t_d is the discharge time. Pd@MWCNT-Co_3O_4 electrode showed a specific capacitance of 536 F/g at 12 A/g displaying the pseudo-capacitive nature of the electrode material. The intercalation reaction involving the composite and the electrolyte may facilitate the pseudo-capacitance behavior for the composite electrode. Due to delocalized electron distribution in MWCNT, that facilitates electronic conduction which promotes the redox reaction that increases the pseudo capacitance behavior of the Co_3O_4 film. Figure-6.8 (B) shows the variation of specific capacitance with current density. The electrode exhibited excellent cyclic stability for more than 1000 cycles without any decrease in capacitance values and with 95% of the retention characteristics as shown in Figure-6.8 (C). This describes the stable nature of the deposit and the better adherence of the composite with the substrate.

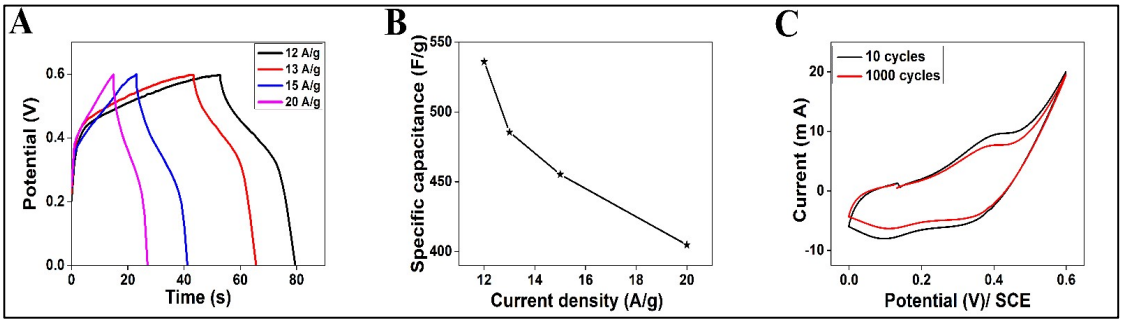

Figure-6.8. (A) GCD curves of Pd@MWCNT-Co_3O_4 electrode at various current density (B) Variation of specific capacitance with current density (C) CV curves for 10^{th} and 1000^{th} cycles at 50 mV/s in 0.1 M KOH solution

6.3.6 Cyclic voltammetric Studies of the fabricated electrodes

Cyclic voltammetric studies of the developed Pd@MWCNT-Co_3O_4 electrode were compared with Co_3O_4 electrode using three electrode set up using platinum as counter electrode and SCE as reference electrode in 0.1 M KOH solution. The cyclic voltammograms of Co_3O_4 and Pd@MWCNT-Co_3O_4electrode deposited on the copper substrate were compared in the potential range of 0 to 0.6 V and is shown in Figure-6.9 (A).The current response for Pd@MWCNT-Co_3O_4 electrode was superior when compared to Co_3O_4 electrode. Figure-8 (B) shows the redox peaks of Co_3O_4 at different scan rates. In KOH medium the fast-moving OH^- ions interacts with Co_3O_4 and gets converted into different products like $Co(OH)_2$, CoOOH and CoO_2. The inset of Figure-6.9 (B) shows the cyclic voltammogram at 5 mV/s. The two redox peaks (I, IV) and (II,III) is related to the oxidation reaction of $Co^{2+} \rightarrow Co^{3+}$ and $Co^{3+} \rightarrow Co^{4+}$ [49–51]. The reaction occurring at Co_3O_4 electrode in alkaline medium is shown below

$$Co_3O_4 + OH^- + H_2O \leftrightarrow 3CoOOH + e^-$$

$$CoOOH + OH^- \leftrightarrow CoO_2 + H_2O + e^-$$

The cyclic voltammograms of Pd@MWCNT-Co_3O_4 electrode at various scan rate is shown in Figure-6.9 (C).The shift in the current observed with respect to Pd@MWCNT-Co_3O_4 can be ascribed to the increased electron transfer rate in the presence of Pd. A linear relationship between anodic and cathodic peak current with respect to the square root of scan rate was observed for both Co_3O_4 and Pd@MWCNT-Co_3O_4electrodes. This can be ascribed to the reversible nature of the electrode reaction and also the surface-confined diffusion-controlled reaction of the electrode. The electrode behaves almost like a reversible electrode and the current response was comparable for anodic and cathodic peaks.

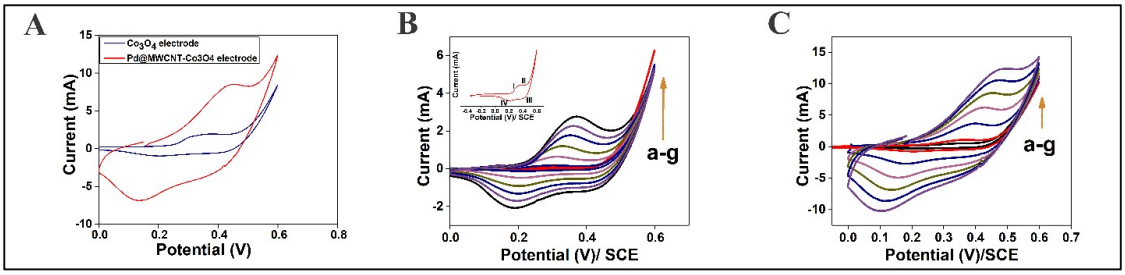

Figure-6.9. [A) Comparison of CV curves of $Co_3O_4$and Pd@MWCNT-Co_3O_4electrode in 0.1M KOH solution (B) CV curves of Co_3O_4 electrodeat various scan rates, Inset of Figure-8 (B) shows the CV curve of Co_3O_4 electrode at 5 mV/s and (C) CV curves of Pd@MWCNT-Co_3O_4 for various scan rates at 2 mV/s, 5mV/s, 20 mV/s, 40 mV/s, 60 mV/s, 80 mV/s and 100 mV/s (a-g).

The cyclic voltammetric response of the developed electrode towards glucose addition was evaluated under different experimental conditions. The potential shift observed in the CV curve for both the Co_3O_4 electrode and Pd@MWCNT-Co_3O_4 electrode with the addition of glucose can be ascribed to the better electron transfer owing to the presence of electro-active species in the electrode matrix. The marginal potential shift observed with respect to glucose addition reveals that the sensing capacity was better with respect to the modified electrode. A comparison of the cyclic voltammetric behavior of the Co_3O_4 electrode and Pd@MWCNT-Co_3O_4 electrode in the absence and in the presence of the analyte glucose is shown in Figure-6.10 (A) and 6.10 (B).The Figure-s 6.10 (C) and 6.10 (D) shows the CV curves recorded for successive addition of glucose ranging from 0.2 mM to 1.2 mM for the Co_3O_4 electrode and Pd@MWCNT-Co_3O_4 electrode. The Pd@MWCNT-Co_3O_4 modified electrode possessed a high current when compared with the Co_3O_4 electrode. This may be due to the reason that in the case of the Co_3O_4 electrode, the glucose oxidation mechanism is due to the consumption of CoO_2 by glucose molecule [52–54]. But the excellent electron transfer ability of Pd-MWCNT and the electrocatalytic nature of cobalt oxide improved the sensing behavior towards glucose with respect to the Pd@MWCNT-Co_3O_4 electrode. Due to the excellent electrical property of the Pd@MWCNT-Co_3O_4 electrode, the electron transfer process was superior that accelerate the reaction sequence which improved the sensitivity of the modified electrode for glucose detection. Pd@MWCNT-Co_3O_4 electrode possessed a synergistic effect of glucose oxidation by Co_3O_4 and palladium. The combined effect resulted in an increase in fast response towards glucose sensing. The individual components along

with MWCNT in the hybrid sensor electrode resulted in the highly selective detection of glucose molecules in the wide linear range of concentration [55–57]. A linear variation of current with respect to varying concentrations was noted for both electrodes and is shown in the inset of Figure-6.10 (C) and Figure-6.10 (D). CV Curves of Co_3O_4 film at different scan rates on addition of 0.5 mM of glucose are shown in Figure-6.11 (A). Inset of Fig 6.11 (A) shows the linear response of current for increasing scan rates on addition of 0.5 mM glucose solution to 0.1 M KOH solution. The anodic peak current increased linearly with increase in scan rates. CV curves of Pd@MWCNT/ Co_3O_4 film at different scan rates on addition of 0.5 mM of glucose are shown in Figure-6.11 (B). A linear response of current was noticed for increasing scan rates on addition of 0.5 mM glucose solution to 0.1 M KOH solution and is shown in the inset of Fig 6.11 (B). In the case of increasing amounts of glucose addition, the anodic peak current showed an increase that can be ascribed to the irreversible nature of glucose oxidation and the fast response of the reaction during specific addition. It can also be concluded that with a higher concentration of glucose, the electron transfer process at the electrode can be faster as revealed by CV analysis.

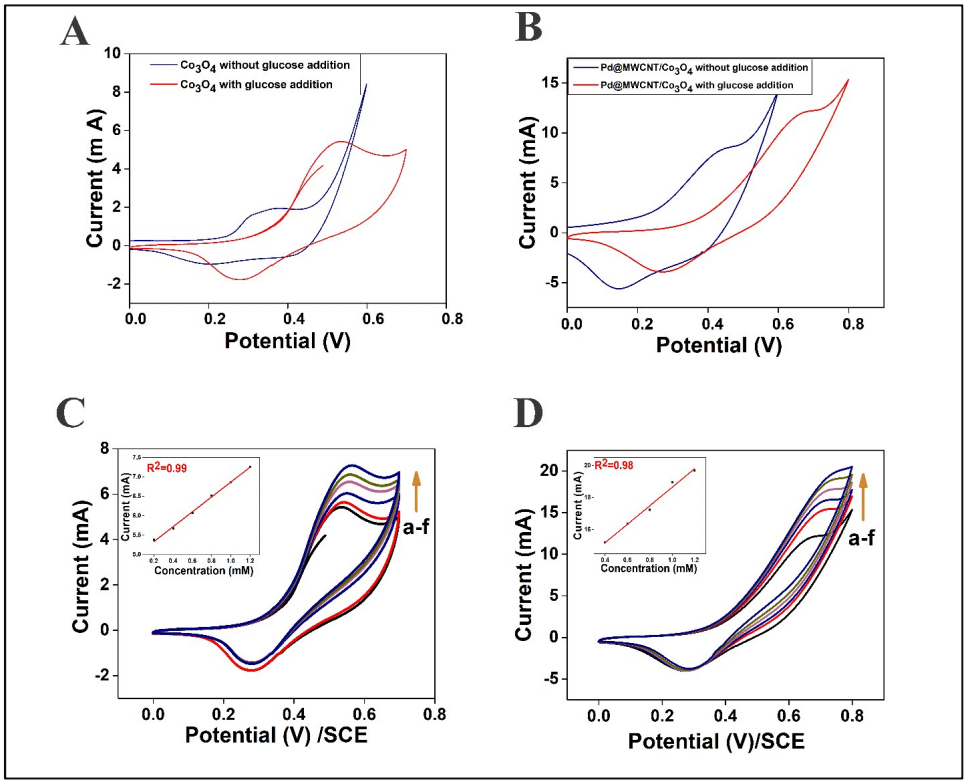

Figure-6.10. (A) CV curves of Co_3O_4 electrode with and without glucose addition (B) CV curves of Pd@MWCNT-Co_3O_4 electrode with and without glucose

addition. (C) CV curves of Co_3O_4 electrode and (D) CV curves of Pd@MWCNT-Co_3O_4 electrode for successive addition of glucose ranging from 0.2 mM to 1.2 mM. The Inset of Figures 6.10 (C) and 6.10 (D) shows a linear variation of current with varying glucose concentrations.

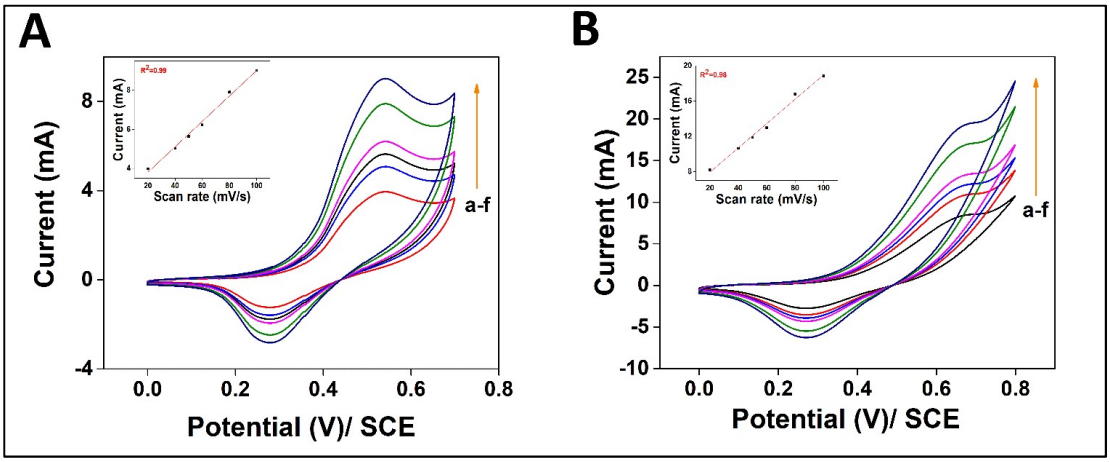

Figure-6.11. (A) CV Curves of Co_3O_4 film at different scan rates for glucose addition (a) 20 m V/s (b) 40 mV/s (c) 50 mV/s (d) 60 mV/s (e) 80 mV/s (f) 100 mV/s in 0.1 M KOH. Inset shows the variation of anodic peak current at different scan rates. (B) CV Curves of Pd@MWCNT-Co_3O_4 film at different scan rates for glucose addition (a) 20 mV/s (b) 40 mV/s (c) 50 mV/s (d) 60 mV/s (e) 80 mV/s (f) 100 mV/s in 0.1 M KOH. Inset shows the variation of anodic peak current at different scan rates.

6.3.7. Chrono-Amperometric Studies for Glucose Sensing

Chrono-amperometric studies were conducted for knowing glucose oxidation with respect to the Co_3O_4 electrode in 0.1 M KOH solution at an applied potential of 0.54 V Vs SCE. The electrode shows a linear increase in current response with the addition of glucose as shown in Figure-6.12 (A). Figure-6.12 (B) shows the current response during the addition of the lower concentration of glucose. The calibration curve shown in Figure-6.12 (E) shows the response of current on the addition of various amounts of glucose to the analyte. The linear increase of current indicates the superior electron transfer at a planar electrode satisfying the Cottrell equation. This promotes glucose oxidation at the anode causing a shift in current. The fitting plot for concentration Vs current response can be divided into two regions 0.01 mM to 0.1 mM and 0.1 mM to 1.4 mM. The linear correlation coefficients for the lower

concentration range were found to be 0.96 [58,59]. Pd@MWCNT-Co_3O_4 electrode showed superior current response to successive addition of glucose at 0.65 V in 0.1 M KOH in comparison with the Co_3O_4 electrode. The current enhanced incrementally as noted in the chronoamperogram due to low resistance offered at the electrode surface and the presence of electroactive groups by the glucose addition as in Figure-6.12 (C). The glucose addition was carried out in a linear range from 0.01 mM to 7.2 mM. The chronoamperogram of the modified electrode towards glucose sensing on addition of lower concentration of glucose are shown in the Figure-6.12 (D). Figure-6.12 (F) shows the linear calibration curve showing the current response to glucose concentration. This is divided into three linear portions-0.01 to 0.10 mM, 0.1 to 2 mM and 2 mM to 7.2 mM. The R^2 value was found to be 0.98 for lower concentrations of glucose and limit of LOD is found to be 0.6 µM. A comparison of chrono-amperometric curves at lower concentrations for both glucose sensors is shown in Figure-6.12 (G). It is noticed that with the increase in glucose concentration for both electrodes, response currents attained a constant value. This could be due to the presence of more oxygen-containing functional groups masking the active sites at higher glucose concentrations. This may interfere with reduced electrochemical activity on the electrode surface [60,61]. A comparison of the performance of various electrodes towards glucose sensing are listed in Table-6.1.

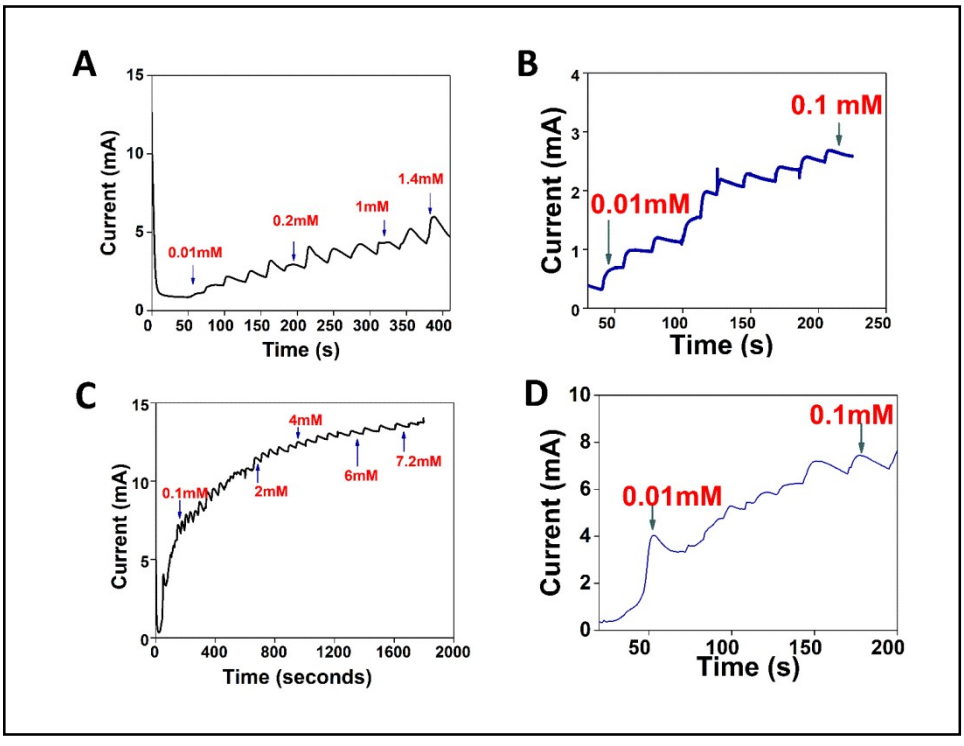

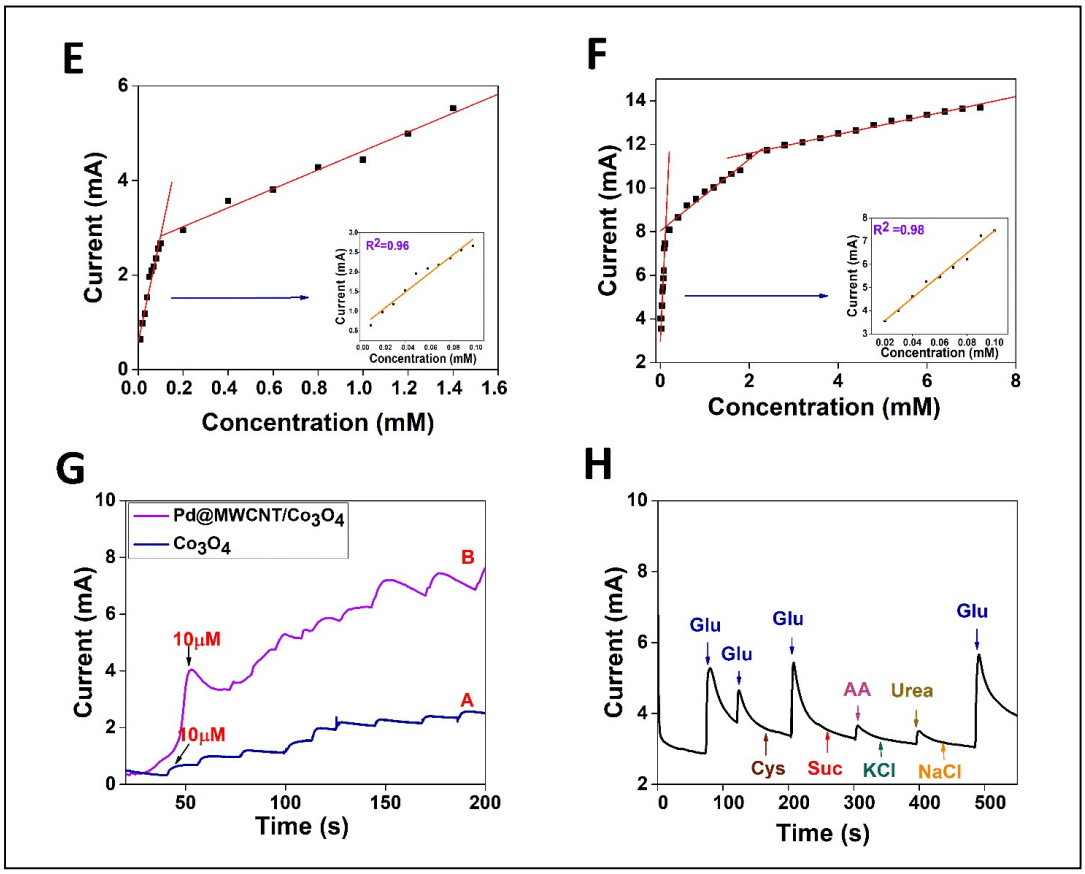

Figure-6.12. (A) Amperometric response curves of Co_3O_4 electrode at 0.54 V towards various concentrations of glucose (0.01-1.4 mM), (B) the amplified response curves at lower concentration range (0.01-0.1 mM). (C) Amperometric response curves of Pd@MWCNT-Co_3O_4 electrode at 0.65 V towards various concentrations of glucose (0.01-7.2mM). (D) the amplified response curves at lower concentration range (0.01-0.1 mM). (E) Calibration plots for electrode response with successive addition of glucose, inset shows the calibration plots in the lower concentration of glucose (0.01-0.1 mM). (F) Calibration plots of electrode response with successive addition of glucose, inset shows the calibration plots in the lower concentration of glucose (0.01-0.1 mM). (G) Comparison of amperometric responses of Co_3O_4 electrode and Pd@MWCNT-Co_3O_4 electrode for successive addition of glucose from 0.01-0.1 mM. (H) Effect of other molecules on the amperometric response of Pd@MWCNT-Co_3O_4 electrode.

6.3.8. Interference Studies

The selectivity of the developed electrode towards glucose detection was conducted by the addition of 0.1 mM Glucose (Glu) in the presence of 0.02 mM of interfering substances such as ascorbic acid (AA), urea, cysteine (Cys), sucrose (Suc),

NaCl and KCl [62–64]. The amperometric response of the developed Pd@MWCNT-Co_3O_4 electrode towards glucose in the presence of various interfering species were recorded at 0.64 V. The addition of glucose produced a significant increase in current response signals compared to the interfering species and hence the effect of interferences are neglected. Figure-6.12 (H) shows the effect of the current response curve of glucose on the addition of different interfering substances.

6.3.9. Reproducibility and Stability of fabricated Pd@MWCNT-Co_3O_4 electrode

Reproducibility and stability are the important parameters of any type of electrode material for sensing applications. The reproducibility of the electrode material was determined by measuring the response current of the fabricated Pd@MWCNT-Co_3O_4 electrode towards glucose detection consisting of a test series of five electrodes following the same experimental procedure. A similar response current was noticed and the relative standard deviation (RSD) was found to be 2.82 %. Pd@MWCNT-Co_3O_4 electrode was stored in an airtight container for a period of 30 days. The response current was monitored and the sensor retained 95 % of the original behavior. This shows the long-term stability of the fabricated electrode for its myriad applications.

6.3.10. Real Sample Analysis

In order to evaluate the performance of the developed Pd@MWCNT-Co_3O_4 electrode towards real sample analysis, glucose sensing was performed with human blood serum samples which is non-diabetic. The samples were spiked with the known concentration of glucose in 50 ml of KOH solution and amperometric measurements were conducted at 0.65 V. From the analysis it is confirmed that the Pd@MWCNT-Co_3O_4 electrode showed an acceptable recovery value of 106 % and 104 % for real sample analysis. The experimental results are listed in Table-6.2.

Table- 6.1 Comparison of performance of Pd@MWCNT-Co_3O_4 electrode towards glucose detection with previous reported works

Electrode	Linear range upto (m M)	Detection limit (μ M)	Reference
Co_3O_4 @MWCNT	11	2	[52]
Cu-Co/RGO-CHIT/GCE	6.95	10	[63]
Pd Ni@RGO/GCE	1.1	0.15	[64]
Hollow cubic Cu_2O@ Pd	0.8	0.16	[57]
Co_3O_4	5.0	0.8	[53]
Pd@MWCNT-Co_3O_4	7.2	0.6	This work

Table- 6.2 Recovery of Pd@MWCNT-Co_3O_4 composite electrode for detecting glucose in a real serum sample.

Sample	Spiked (m M)	Found (m M)	Recovery (%)
Serum 1	1.5	1.60	106
Serum 2	3.5	3.65	104

6.4. CONCLUSIONS

A facile method has been developed for the fabrication of Pd@MWCNT-Co_3O_4 composite electrodes for the non-enzymatic detection of glucose. The cobalt oxide which is recycled from the spent lithium-ion batteries was used for fabricating the electrode. Further, the Co_3O_4 film is being modified with Pd@MWCNT by electrophoretic deposition method to form Pd@MWCNT-Co_3O_4. The recovered powder from spent Li-ion batteries and the fabricated electrodes were analyzed by XRD, UV-Visible Spectrophotometer, FTIR, EDX-SEM, CV and GCD analysis. The Pd@MWCNT-Co_3O_4 possessed good electrochemical characteristics. The electrochemical response of the modified electrode towards non-enzymatic

glucose sensing was studied using the CV and CA techniques. The response of Co_3O_4 and Pd@MWCNT-Co_3O_4 electrodes towards glucose sensing were compared. Pd@MWCNT-Co_3O_4 nanocomposite electrode exhibited superior sensing behavior towards glucose oxidation within a wide range of concentration from 0.01 mM to 7.2 mM glucose with LOD of 0.6 μM. The nanocomposite electrode also possessed excellent stability, selectivity and good reproducibility. These results revealed the potential usefulness of spent materials from batteries for developing various systems for myriad applications. Furthermore, the hybrid composites of MWCNTs with valuable metals recovered from spent LIBs and conducting polymers are worth investigating comprehensively in the future for sensing various analytes.

6.5. REFERENCES

1. Min Fan, Xin Chang, Qinghai Meng, Li-Jun Wan, Yu-Guo Guo. Progress in the sustainable recycling of spent lithium-ion batteries. SusMat. 2021;1:241–254.

2. Yaqun He, Xue Yuan, Guangwen Zhang, Haifeng Wang, Tao Zhang, Weining Xie and Liping Li. A critical review of current technologies for the liberation of electrode materials from foils in the recycling process of spent lithium-ion batteries. Sci Total Environ . 2020;766:142382.

3. V. Chandran, Aritra Ghosh, Chandrashekhar K. Patil, V. Mohanavel, A.K. Priya, Robbi Rahim, R. Madavan, U. Muthuraman and Alagar Karthick. Comprehensive review on recycling of spent lithium-ion batteries. Mater Today Proc . 2021;47:167–80.

4. Li Lia, Jing Ge, Feng Wua, Renjie Chen, Shi Chen and Borong Wu. Recovery of cobalt and lithium from spent lithium ion batteries using organic citric acid as leachant. J Hazard Mater. 2010;176:288–93.

5. Cetinkaya T, Akbulut A. A different method for producing a flexible $LiMn_2O_4$ / MWCNT composite electrode for lithium ion batteries. J Appl Electrochem. 2014;44:209–14.

6. Meng Q, Zhang Y, Dong P. A combined process for cobalt recovering and cathode material regeneration from spent $LiCoO_2$ batteries : Process optimization and kinetics aspects. Waste Manag J. 2017;71:372–80.

7. Azib T, Cras F Le, Porthault H. Direct fabrication of $LiCoO_2$ thin- films in water – ethanol solutions by electrochemical – hydrothermal method. Electrochim Acta . 2015;160:145–51.

8. X. Zheng, Z. Zhu, X. Lin, Y. Zhang, Y. He, H. Cao and Z Sun. A Mini-Review on Metal Recycling from Spent Lithium Ion Batteries. Engineering. 2018;4:361–70.

9. Fabrice Mathieux, Fulvio Ardente, Silvia Bobba, Philip Nuss, Gian Andrea Blengini, Patricia Alves Dias, Darina Blagoeva, Cristina Torres de Matos, Dominic Wittmer, Claudiu Pavel, Tamas Hamor, Hans Saveyn, Bernd Gawlik, Glenn Orveillon, Dries Huygens, Elen SS. Critical raw materials and the circular economy. . Report EUR 28832 EN. 2017. Available from: https://ec.europa.eu/jrc

10. Sakeena Masrat VN, Marya Khan, Rafiq Ahmad, Vandana Ngal, Iqra Moid, Shamshad Alam, Kiesar Sideeq Bhat and Ajit Khosla. Electrochemical ultrasensitive sensing of uric Acid on non-enzymatic porous cobalt oxide nanosheets-based sensor. Biosensors. 2022;12:1140.

11. Vandana Nagal, Sakeena Masrat, Marya Khan , Shamshad Alam , Akil Ahmad, Mohammed B. Alshammari, Kiesar Sideeq Bhat, Sergey M. Novikov , Prabhash Mishra, Ajith Khosla andRafiq Ahmad. Highly sensitive electrochemical non-Enzymatic uric acid sensor based on cobalt oxide puffy balls-like nanostructure. Biosensors. 2023;13:375.

12. Nagal V, Tuba T, Kumar V, Alam S, Ahmad A. A non-enzymatic electrochemical sensor composed of nano-berry shaped cobalt oxide nanostructures on a glassy carbon electrode for uric acid detection. New J Chem. 2022;46:12333–41.

13. Nagal V, Khan M, Masrat S, Alam S, Ahmad R. Hexagonal cobalt oxide nanosheet-

based enzymeless electrochemical uric acid sensor with improved sensitivity. New J Chem. 2023;47:4206–12.

14. Iizuka A, Yamashita Y, Nagasawa H, Yamasaki A, Yanagisawa Y. Separation of lithium and cobalt from waste lithium-ion batteries via bipolar membrane electrodialysis coupled with chelation. Sep Purif Technol . 2013;113:33–41.

15. Rong-Chi Wang, Yu-Chuan Lin and She-Huang Wu. A novel recovery process of metal values from the cathode active materials of the lithium-ion secondary batteries. Hydrometallurgy . 2009;99:194–201.

16. Kyoung C, Rhee K. Reductive leaching of cathodic active materials from lithium ion battery wastes. Hydrometallurgy. 2003;68:5–10.

17. Myung S, Hyoung N, Soo J. Development of a metal recovery process from Li-ion battery wastes. Hydrometallurgy. 2005;79:172–81.

18. Dorella G, Mansur MB. A study of the separation of cobalt from spent Li-ion battery residues. J Power Sources. 2007;170:210–5.

19. Castillo S, Ansart F, Portal J. Advances in the recovering of spent lithium battery compounds. J Power Sources. 2002;112:247–54.

20. Manis Kumar Jha, Anjan Kumari, Amrita Kumari Jha, Vinay Kumar, Jhumki Hait, Banshi Dhar Pandey. Recovery of lithium and cobalt from waste lithium ion batteries of mobile phone. Waste Manag . 2013;33:1890–7.

21. Swain B, Jeong J, Lee J, Lee G, Sohn J. Hydrometallurgical process for recovery of cobalt from waste cathodic active material generated during manufacturing of lithium ion batteries. J Power Sources 167. 2007;167:536–44.

22. Jinqiu Xu, H.R. Thomas, Rob W. Francis , Ken R. Lumb, Jingwei Wang and Bo Liang. A review of processes and technologies for the recycling of lithium-ion secondary batteries. J Power Sources. 2008;177:512–27.

23. Li Li , Wenjie Qu , Xiaoxiao Zhang , Jun Lu , Renjie Chen , Feng Wu and Khalil Amine. Succinic acid-based leaching system : A sustainable process for recovery of valuable metals from spent Li-ion batteries. J Power Sources. 2015;282:544–51.

24. Li Li , Jing Ge , Renjie Chen, Feng Wua, Shi Chen and Xiaoxiao Zhang. Environmental friendly leaching reagent for cobalt and lithium recovery from spent lithium-ion batteries. Waste Manag. 2010;30:2615–21.

25. Li Li , Jun Lu , Yang Ren , Xiao Xiao Zhang , Ren Jie Chen, Feng Wu and Khalil Amine. Ascorbic-acid-assisted recovery of cobalt and lithium from spent Li-ion batteries. J Power Sources . 2012;218:21–7.

26. Sun L, Qiu K. Organic oxalate as leachant and precipitant for the recovery of valuable metals from spent lithium-ion batteries. Waste Manag . 2012;32:1575–82.

27. Cerrillo-Gonzalez M.M, , M. Villen-Guzman , C. Vereda-Alonso , C. Gomez-Lahoz, J. M. Rodriguez-Maroto and J.M. Paz-Garcia. Recovery of Li and Co from $LiCoO_2$ via Hydrometallurgical – Electrodialytic Treatment. Appl Sci. 2020;10:2367.

28. Liu C, Lin J, Cao H, Zhang Y, Sun Z. Recycling of spent lithium-ion batteries in view of lithium recovery: A critical review. J Clean Prod . 2019;228(1):801–13.

29. Mayyas A, Steward D, Mann M. The case for recycling: Overview and challenges in

the material supply chain for automotive li-ion batteries. Sustain Mater Technol . 2019;19:e00087.

30. Sha R, Durai L, Badhulika S, Materials A. Facile in-situ preparation of few-layered reduced graphene oxide – niobium pentoxide composite for non-enzymatic glucose monitoring. IEEE Int Conf Emerg Electron. 2018;1–4.

31. L. G. Bach, M. L. N. Thi, Q. B. Bui H-T. Nhac-Vu. Hierarchical cobalt nanorods shelled with nickel oxide vertically attached 3D architecture as non-binder and free-standing sensor for sensitive non-enzymatic glucose detection. Mater Res Bull . 2019;118:110504.

32. Saravanan Rajendran, Devaraj Manoj, Kumar Raju, Dionysios. D. Dionysiou, Mu. Naushad, F. Gracia, Lorena Cornejo, M.A. Gracia-Pinilla TA, PII: Influence of mesoporous defect induced mixed-valent NiO (Ni^{2+}/Ni^{3+})-TiO_2 nanocomposite for non-enzymatic glucose biosensors. Sensors Actuators B Chem . 2018;264:27–37.

33. Shabnam L, Nayeem Faisal S., Kumar Roy A, Haque E, Minett A, Gomes V G. Doped graphene/Cu nanocomposite : A high sensitivity non-enzymatic glucose sensor for food. Food Chem . 2017;221:751–9.

34. Baghayeri M, Amiri A, Alizadeh Z, Veisi H, Hasheminejad E. Non-enzymatic voltammetric glucose sensor made of ternary NiO/ Fe_3O_4 - SH/para-amino hippuric acid nanocomposite. J Electroanal Chem . 2018;810:69–77.

35. Min Ma, Taotao Zhe, Yiyue Ma, Zonghan Wang, Qiang Chen and Jianlong Wang. Highly sensitive and reproducible non-enzymatic glucose sensor fabricated by drop-casting novel nanocomposite with 3D architecture and tailorable properties prepared in controllable way. Talanta . 2018;180:133–43.

36. Reshma M, Manu R. Flexible Ag / FMWCNT electrode fabricated through benign reducing agent for sensor application. J ofThe Electrochem Soc. 2019;166(1):916–22.

37. Dighe AB, Dubal DP, Holze R. Screen printed asymmetric supercapacitors based on $LiCoO_2$ and graphene oxide. Z Anorg Allg Chem. 2014;640:2852–7.

38. Eslam A.A. Aboelazm, Gomaa A.M. Ali, Kwok Feng Chong. Cobalt oxide supercapacitor electrode recovered from spent lithium-ion battery. Chem Adv Mater. 2018;3:67–74.

39. Li L, Chen R, Sun F, Wu F, Liu J. Preparation of LiCoO2 films from spent lithium-ion batteries by a combined recycling process. Hydrometallurgy. 2011;108:220–5.

40. Xianhong He, Deming Li , Zhengyu Bai, Fangfang Chang, Jinli Qiao and Lin Yang. Multi-wall carbon nanotube-supported palladium–cobalt oxide nanoparticle as efficient catalyst for oxygen reduction reaction. Ionics (Kiel). 2019;25:5929–37.

41. Reshma M, Manu R. Fabrication of Cu-WO_3-functionalised multiwalled carbon nanotubes composite film electrode by direct deposition for sensing application. Thin Solid Films . 2021;737:138940.

42. Singh S, Ruey H, Abdullah H, Khan M R. Pd/CNT catalysts for glycerol electro-oxidation: Effect of Pd loading on production of valuable chemical products M. Electroanalysis. 2020;32:1139–47.

43. Farhadi S, Javanmard M, Nadri G. Characterization of Cobalt Oxide Nanoparticles Prepared by the Thermal Decomposition of $(Co (NH_3)_5 (H 2 O)) (NO_3)_3$ Complex and Study of Their Photocatalytic Activity. 336 Acta Chim Slov.

2016;63:335–43.

44. Fang Zhang, Changzhou Yuan, Xiangjun Lu, Luojiang Zhang, Qian Che and Xiaogang Zhang. Facile growth of mesoporous Co_3O_4 nanowire arrays on Ni foam for high performance electrochemical capacitors. J Power Sources . 2012;203:250–6.

45. Siyuan Zhou, Yingjie Zhang, Qi Meng b, Peng Dong, Zitong Fei and Qiangxiang Li. Recycling of $LiCoO_2$ cathode material from spent lithium ion batteries by ultrasonic enhanced leaching and one-step regeneration. J Environ Manage . 2021;277:111426.

46. Kalyani P, Kalaiselvi N, Muniyandi N. A new solution combustion route to synthesize $LiCoO_2$ and $LiMn_2O_4$. J Power Sources. 2002;111:232–8.

47. Fan X, Sun Y, Ohlckers P. Porous thin-wall hollow Co_3O_4 spheres for supercapacitors with high rate capability. Appl Sci. 2019;9:4672.

48. Giri S, Ghosh D, Malas A, Das CK. A Facile Synthesis of a Palladium-Doped Polyaniline-Modified Carbon Nanotube Composites for Supercapacitors. J Electron Mater. 2013;42:2595–605.

49. Masoumeh Pak, Ahmad Moshaii, Hossein Siampour SA and MN. Cobalt-copper bimetallic nanostructures prepared by glancing angle deposition for non-enzymatic voltammetric determination of glucose. Microchim Acta. 2020;187:276.

50. Mojtaba Mirzaeian, Nazym Akhanova , Maratbek Gabdullin , Zhanar Kalkozova, Aida Tulegenova, Abdullin Khabibulla and Shyryn Nurbolat. Improvement of the pseudocapacitive performance of cobalt oxide-based electrodes for energies. 2020;13:5228.

51. Arshid Numan, Navaneethan Duraisamy , Fatin Saiha Omar, Y. K. Mahipal, K. Ramesh SR, Centre. Enhanced electrochemical performance of cobalt oxide nanocubes intercalated reduced graphene oxide for supercapacitor application Arshid. RSC Adv. 2016;6:34894–902.

52. Jiao K, Jiang Y, Kang Z, Peng R, Jiao S and Hu Z. Three-dimensional Co_3O_4 @ MWNTs nanocomposite with enhanced electrochemical performance for nonenzymatic glucose biosensors and biofuel cells. R Soc open sci. 2017;4:170991.

53. Razium Ali Soomro, Aynam Nafady, Zafar Hussain Ibupoto S, Syed Tufail Hussain Sherazi , Magnus Willander and Muhammad Ishaq Abro. Development of sensitive non-enzymatic glucose sensor using complex nanostructures of cobalt oxide. Mater Sci Semicond Process . 2015;34:373–81.

54. Sicele A. Gonçalves, Eric M. Garcia, Hosane A. Taroco, Rodrigo G. Teixeira, Kassílio J. Guedes, Honória F. Gorgulho, Patrícia B. Martelli and Anyonio P.L. Fernandes. Development of non-enzymatic glucose sensor using recycled cobalt from cell phone Li-ion batteries. Waste Manag. 2015;46:497–502.

55. Li-Min Lu, Hong-Bo Li, Fengli Qub, Xiao-Bing Zhanga, Guo-Li Shen and Ru-Qin Yu. In situ synthesis of palladium nanoparticle–graphene nanohybrids and their application in nonenzymatic glucose biosensors. Biosens Bioelectron . 2011;26:3500–4.

56. Singh B, Bhardwaj N, Jain VK, Bhatia V. Palladium nanoparticles decorated electrostatically functionalized MWCNTs as a non enzymatic glucose sensor. Sensors Actuators A Phys . 2014;220:126–33.

57. Peng Liu, Min Zhang, Shilei Xie, Shoushan Wang, Wenxue Cheng and Faliang

Cheng. Non-enzymatic glucose biosensor based on Palladium-copper oxide nanocomposites synthesized via galvanic replacement reaction. Sensors Actuators B Chem . 2017;253:552–8.

58. Singh H, Bernabe J, Chern J, Nath M. Copper selenide as multifunctional non - enzymatic glucose and dopamine sensor. J Mater Res . 2021;36:1413–24.

59. Haghparas Z, Kordrostami Z, Sorouri M, Rajabzadeh M. Highly sensitive non - enzymatic electrochemical glucose sensor based on dumbbell-shaped double-shelled hollow nanoporous CuO / ZnO microstructures. Sci Rep . 2021;11:344.

60. Arumugam Manikandan, Vediyappan Veeramani, Shen-Ming Chen, Rajesh Madhu, Ling Lee, Henry Medina, Chia-Wei Chen, Wei-Hsuan Hung, Zhiming Wang, Guozhen Shen Yu-Lun Chugh. Low-temperature chemical synthesis of three-dimensional hierarchical $Ni(OH)_2$-coated ni microflowers for high-performance enzyme-free glucose sensor. J Phys Chem C. 2016;120:25752–9.

61. Li H, Zhang L, Mao Y, Wen C, Zhao P. A simple electrochemical route to access amorphous Co-Ni hydroxide for non-enzymatic glucose sensing. Nanoscale Res Lett. 2019;14:135.

62. Lili Wang, Yuying Yang, Bing Wang, Cunpeng Duan, Jiahui Li, Linlin Zheng, Jiahao Li and Zhen Yin. Bifunctional three-dimensional self-supporting multistage structure CC@MOF-74(NiO)@NiCo LDH electrode for supercapacitors and non-enzymatic glucose sensors. J Alloys Compd . 2021;885:160899.

63. Li Wang, Yaolin Zheng, Xingping Lu, Zhuang Li, Lanlan Sun and Yonghai Song. Dendritic copper-cobalt nanostructures / reduced graphene oxide-chitosan modified glassy carbon electrode for glucose sensing. Sensors Actuators B Chem . 2014;195:1–7.

64. Aysun Ş, Cellat K, Arikan K, Tezcan F, Gülbay S K, Kizildag S, Isgin E S and Sen F. Highly monodisperse Pd-Ni nanoparticles supported on rGO as a rapid , sensitive , reusable and selective enzyme-free glucose sensor. Sci Rep. 2019;9:19228.

CHAPTER 7

TERNARY COMPOSITE ELECTRODE BASED ON RuO_2/Fe_3O_4/MWCNT FOR SIMULTANEOUS DETECTION OF DOPAMINE AND ASCORBIC ACID

7.1. INTRODUCTION

One of the powerful antioxidants involved in human metabolism's physiological process is ascorbic acid. Ascorbic acid otherwise known as Vitamin C is used to treat cancer, scurvy, diarrhea etc. On the other hand, dopamine is one of the catecholamine neurotransmitters in the biological system [1,2]. Abnormal quantities of dopamine can lead to diseases like Parkinson's disease and other neurological diseases like Schizophrenia, Epilepsy, Restless Leg Syndrome (RLS) and drug addiction [3,4]. So monitoring such catecholamines is important. Ascorbic acid found in the mammalian brain is an important vitamin due to its excellent antioxidant and pH-regulating characteristics. This essential vitamin is mainly used in various fields including- the food processing industry and pharmaceutical products. The deficiency of this vitamin can lead to scurvy and cataracts [5,6]. Analytical methods like high-performance liquid chromatography, chemiluminescence [7,8] etc are employed for dopamine detection. But these methods are time-consuming, require expensive instruments and provide very low sensitivity. Both dopamine and ascorbic acid are found to be redox-active and hence they can be detected using electrochemical methods.

Electrochemical methods offer fast response, high sensitivity and minimal cost, making dopamine detection feasible. Ascorbic acid commonly interferes with dopamine during electrochemical studies since their oxidation potential is almost similar. Due to the overlap of oxidation potential of both biomolecules simultaneous detection of ascorbic acid and dopamine is found to be difficult [9,10]. Efficient nanocomposites capable of detecting both dopamine and ascorbic acid simultaneously are to be developed. In recent years modified electrodes with carbonaceous materials are developed which can detect a wide range of analytes. These carbon-based nanocomposites act as a supporting material for the development of hybrid nanocomposites. CNT-based nanocomposites are promising materials for such purposes [11,12]. When compared with other transition metal oxides, RuO_2 is very stable and hence applicable for various purposes including sensing, pseudocapacitor applications etc [12–14]. Even though transition metal oxides like ruthenium metal oxide and iridium metal oxide are found to be expensive, RuO_2 has been extensively studied due to its practical availability, thermal and chemical stability, environment-

benign nature, and lower cost compared to others. The stability of RuO_2 under physiological pH makes them efficient in sensing biological species. In the case of magnetite nanoparticles, these nanoparticles are less toxic and are found to be paramagnetic in nature. The unstable and easily oxidizable nature of Fe_3O_4 can be hindered by incorporating these nanoparticles into carbon nanotubules [14,15]. Thus MWCNT is capable of providing more active sites and also the individual properties of Fe_3O_4 and RuO_2 are enhanced by incorporating these oxides into MWCNT. Thus hybrid composite of MWCNT embedding Fe_3O_4 and RuO_2 can provide a synergistic effect for the electrochemical detection of biomolecules.

In the present study, CNT-modified composites embedding RuO_2 and Fe_3O_4 are fabricated by hydrothermal process. The RuO_2 and Fe_3O_4 are incorporated into MWCNTs so that modified electrodes with the enhanced properties of both RuO_2 and Fe_3O_4 are obtained. The modified electrode RuO_2/Fe_3O_4/MWCNT is found to detect dopamine and ascorbic acid simultaneously by electrochemical methods including cyclic voltammetry and differential pulse voltammetry. The hybrid nanocomposites behave as an electrochemical sensor and help in the rapid and simultaneous detection of dopamine and ascorbic acid. The sensor also possessed excellent stability and also gave satisfactory results on real sample analysis for the detection of both analyte molecules.

7.2. EXPERIMENTAL METHODS

7.2.1. Preparation of functionalised MWCNT dispersion

About 1 g of MWCNT (OD:30-50 nm, length:10-30 μm) was functionalized by refluxing with H_2SO_4 and HNO_3 in the ratio 3:1 for about 5 hrs at 70 °C. The obtained product was filtered, washed with doubly distilled water to make the pH neutral, and dried overnight at 50 °C in the oven. 0.05 g of FMWCNT is dispersed in 20ml deionized water and stirred for 6 hrs to obtain functionalized MWCNT dispersion.

7.2.2. Preparation of RuO_2 dispersion

0.01M aqueous solution of $RuCl_3$ was prepared from $RuCl_3.x\ H_2O$. To 10 ml of $RuCl_3$ solution, 10 ml of 0.2 M NaOH is added slowly under stirring conditions.

The solution is kept under continuous stirring for about 6 hours for the preparation of hydrous RuO_2 nanoparticles.

7.2.3. Preparation of Fe_3O_4 dispersion

0.01 M of ferrous sulphate solution is prepared from $FeSO_4.7H_2O$. To 10 ml of ferrous sulphate solution, 5 ml of 0.2 M NaOH is added and stirred for 2 hours. To this 0.2 g of urea is added which acts as a reducing agent and is kept under stirring for 1 hour which results in the formation of Fe_3O_4 nanoparticles.

7.2.4. Preparation of RuO_2/Fe_3O_4/MWCNT composites by hydrothermal method

The above-prepared solutions containing RuO_2 nanoparticles and Fe_3O_4 nanoparticles are transferred to the beaker containing FMWCNT dispersions and are kept under stirring for 2 hours, and finally transferred to an autoclave and kept at a temperature of 180 °C for 6 hours. The product obtained is filtered and washed thoroughly with deionized water and dried at 60 °C for about 4 hours. The obtained powder is further calcined at 400 °C for 2 hours which results in the formation of RuO_2/Fe_3O_4/MWCNT composites. The obtained powder was dispersed in deionized water for further use.

7.2.5. Preparation of modified Glassy carbon electrodes (GCE)

Glassy carbon electrodes were polished to a mirror-like finish using alumina powder. The GCE were thoroughly cleaned with water and to this 5 µL of a homogeneous solution of RuO_2/Fe_3O_4/MWCNT solution was drop cast and dried at room temperature for the preparation of modified electrodes. The synthesis of the RuO_2/Fe_3O_4/MWCNT and the sensing techniques for the biomolecules are shown in Scheme 7.1.

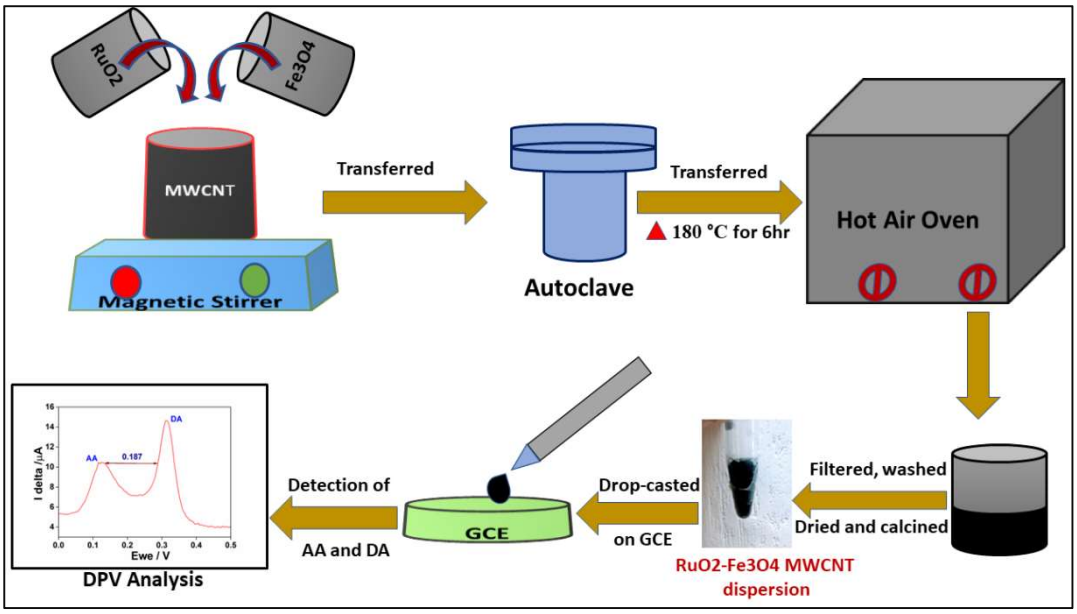

Scheme 7.1. Schematic representation showing the fabrication of RuO_2/Fe_3O_4/MWCNT composite and the electrochemical sensing of the composite towards ascorbic acid and dopamine.

7.2.6. Characterization techniques

The RuO_2/Fe_3O_4/MWCNT were characterized by various techniques. UV-Visible spectrophotometer (Jasco UV-750) in the range of 200-800nm was used to characterize the initially formed Fe_3O_4 and RuO_2. X-ray diffraction studies (Rigaku Ultima IV) were used to analyze the various planes of obtained Fe_3O_4 powder and RuO_2/ Fe_3O_4/MWCNT powder. Fourier transform infrared spectroscopy was used to analyze Ru-O and Fe-O bonds in RuO_2/ Fe_3O_4/MWCNT composite. Raman spectrum (Renishaw-confocal raman microscope 532nm laser) distinguished the RuO_2/Fe_3O_4/MWCNT composite from MWCNT by the Raman shift values. Scanning electron microscopy was employed to study the surface morphology and the various elements in the composite were analysed using energy dispersive X-ray analysis which is attached to the scanning electron microscope (SEM-Gemini 300). Electrochemical characterization including cyclic voltammetric studies of the fabricated composites and differential pulse voltammetric studies of the electrode towards sensing the analyte molecules were studied using an electrochemical work station (Biologic SP-200) which involves a three-electrode set up which include

saturated calomel electrode as reference electrode, platinum wire as counter electrode and RuO_2/Fe_3O_4/MWCNT/GCE as working electrode.

7.3. RESULTS AND DISCUSSION

7.3.1. UV-Visible Analysis

The nanoparticles of Fe_3O_4 and RuO_2 are analyzed by UV-Visible spectroscopy in the range of 200-800 nm. A broad absorption edge was noticed for Fe_3O_4 in the range of 360 nm. This is shown in Figure-7.1 (A). The magnetite nanoparticles formed are shown in the inset (left) of Figure-7.1 (A) and the attraction of these magnetic particles towards the magnet is also shown in the inset [right] of Figure-7.1 (A) [16–19]. An absorption around 710 nm is noticed for hydrous RuO_2 and is shown in Figure-7.1 (B). The hydrous RuO_2 dispersion is shown in the inset of Figure-7.1 (B) [20,21].

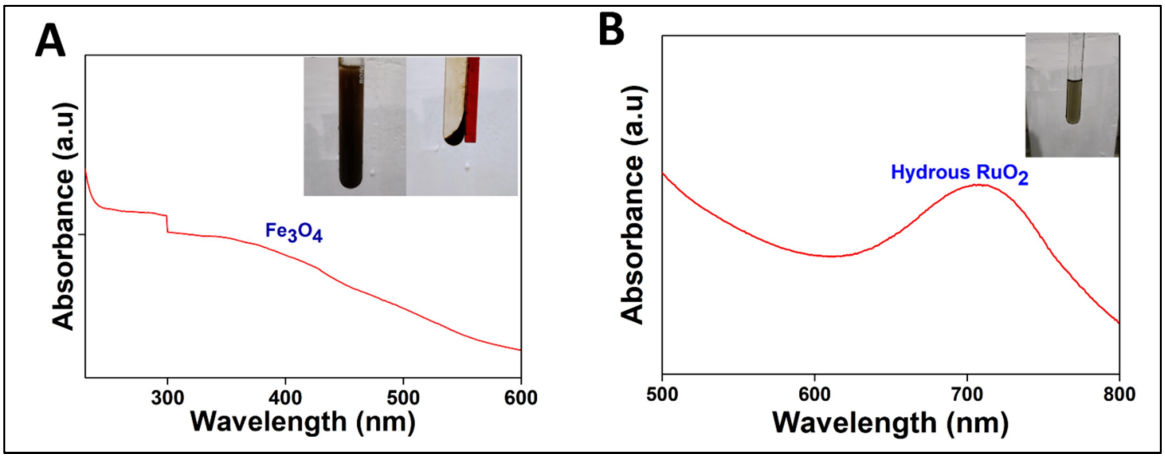

Figure-7.1. (A) UV-Visible spectra of Fe_3O_4. Inset (left) shows the formation of Fe_3O_4 dispersion and also (right inset) behavior of magnetite particles towards magnet (B) UV-visible spectra of hydrous RuO_2 and inset shows the formation of RuO_2 dispersion.

7.3.2. XRD of RuO_2/ Fe_3O_4/MWCNT Powder

The X-ray diffraction pattern of the as-prepared RuO_2/ Fe_3O_4/MWCNT powder is shown in Figure-7.2. MWCNT possesses two peaks at 26.2° and 43.2 ° corresponding to (002) and (100) planes [22]. Well-defined crystal faces of RuO_2 are noticed which corresponds to(110), (101) and (220) according to (JCPDS-21-1172) [23,24]. Besides the peaks of MWCNT and RuO_2 well-defined diffraction peaks of

Fe_3O_4 are also noticed in the XRD pattern which corresponds to the planes (220), (311), (400), (422), (511) and (440)which is in accordance with the (JCPDS 19-0629) [25,26]. The XRD of synthesized Fe_3O_4 [27,28] is shown in the inset of Figure-7.2.

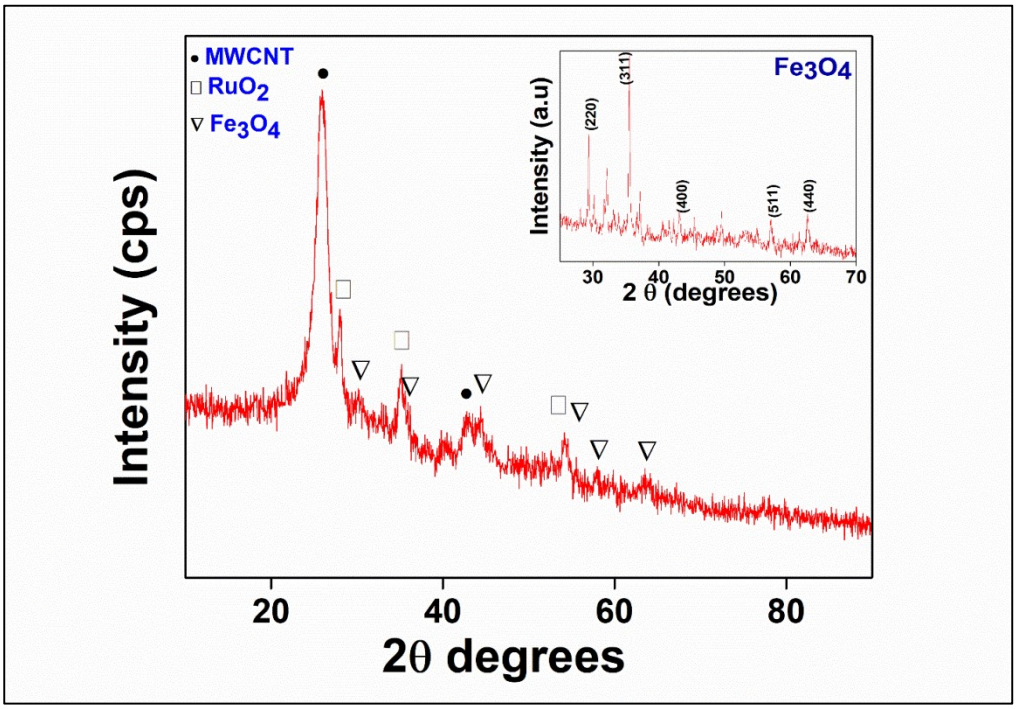

Figure-7.2. XRD pattern for the RuO_2/Fe_3O_4/MWCNT composite

7.3.3. FTIR of RuO_2/Fe_3O_4/MWCNT composite

FTIR spectrum of RuO_2/Fe_3O_4/MWCNT composites shows broad absorption bands in the range of 487-590 cm^{-1} which corresponds to the vibrations of Ru-O and Fe-O bonds. The functional groups present in MWCNT due to acid functionalization are revealed by the presence of peaks found at 1355 cm^{-1} (O-H bending), 1577 cm^{-1} (C=C stretching), 1731 cm^{-1} (C=O stretching), 2313 cm^{-1} (carboxyl group vibrations), 2920 cm^{-1} (methylene group stretching) and 3410 cm^{-1} (O-H stretching vibrations of hydroxyl group) [29–32]. Thus FTIR spectrum provided information regarding the various peaks arising due to the incorporation of RuO_2 and Fe_3O_4 on thefunctionalized MWCNT matrix and is shown in Figure-7.3.

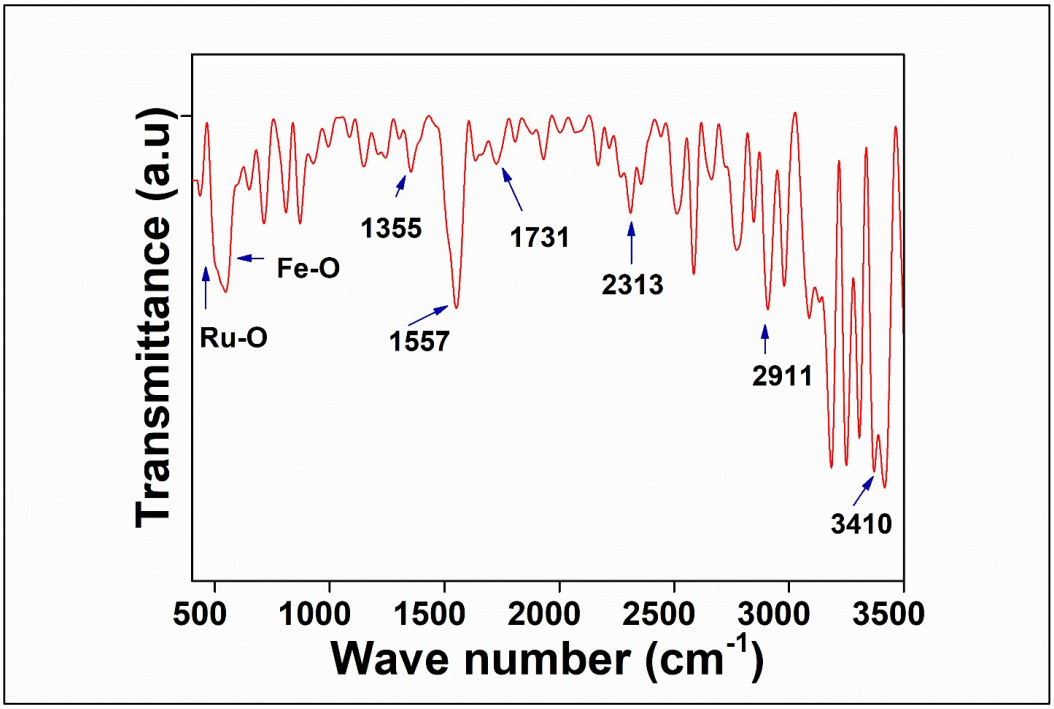

Figure-7.3. FTIR spectrum of RuO_2/Fe_3O_4/MWCNT composite.

7.3.4. Raman spectrum of RuO_2/Fe_3O_4/MWCNT composite

The presence of RuO_2 and Fe_3O_4 in the MWCNT matrix was further confirmed by Raman spectroscopy. The Raman spectrum of MWCNT consists of two peaks- one at 1352 cm^{-1} (D band) which signifies disordered carbon and the other one at 1585 cm^{-1} (G band) corresponding to well-ordered crystalline graphite.Apart from the peaks of MWCNT at 1352cm^{-1} and 1585 cm^{-1}, the modified composite exhibited peaks at wave numbers 217 cm^{-1}, 319 cm^{-1}, 404 cm^{-1}, 505 cm^{-1}, 601 cm^{-1} and 675 cm^{-1} corresponding to Fe_3O_4 and the peaks at 517 cm^{-1}, 637 cm^{-1} and 695 cm^{-1} are related to RuO_2 which corresponds to Eg, A1g and B2g modes of vibrations [33–37]. Raman spectrum of both MWCNT and RuO_2/Fe_3O_4/MWCNT are compared in Figure-7.4.

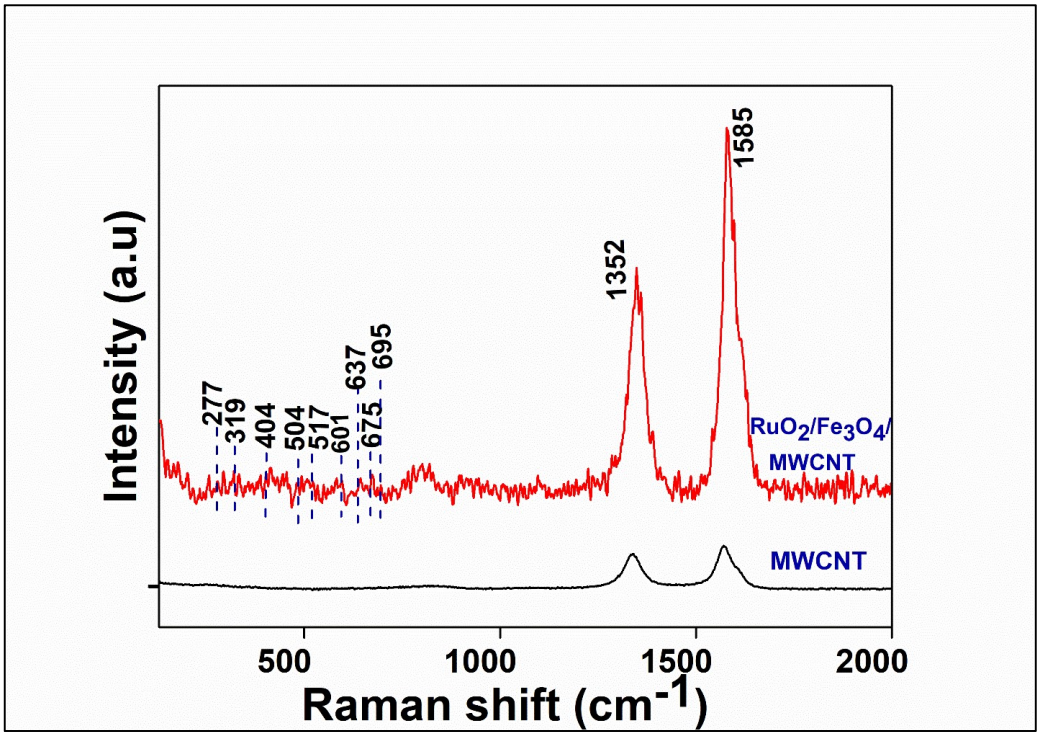

Figure-7.4. Raman spectrum of MWCNT and RuO_2/Fe_3O_4/MWCNT.

7.3.5. EDX-SEM Studies of RuO_2/Fe_3O_4/MWCNT composite

Elemental analysis of the synthesized RuO_2/Fe_3O_4/MWCNT composite showed the presence of carbon, oxygen, ruthenium, and iron as major elements, and the EDX spectrum is shown in Figure-7.5 (A). The surface morphology of deposited RuO_2/Fe_3O_4/MWCNT is shown in Figure-7.5 (B). An entangled network of MWCNTs coated with metal oxides of iron and ruthenium are very well distributed in the matrix. Thus MWCNTs served as favorable scaffolds for the incorporation ofthese metal oxides and as shown in Figure-7.5 (B).The Inset of 7.5 (B) shows the enlarged view of the circled area [25,29].

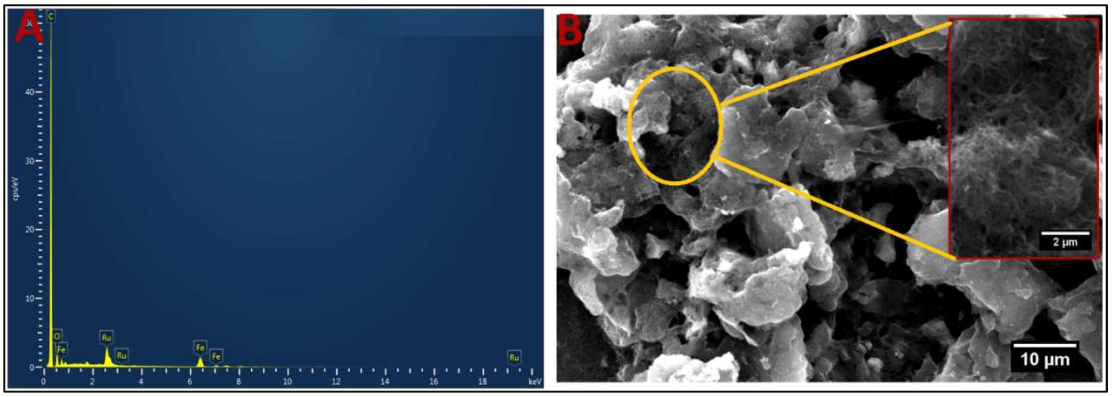

Figure-7.5. (A) EDX spectrum of RuO_2/Fe_3O_4/MWCNT composite (B) SEM images of RuO_2/Fe_3O_4/MWCNT film. Inset showing the enlarged view of the circled area.

7.3.6. Electrochemical Studies of RuO_2/ Fe_3O_4/MWCNTelectrode

The cyclic voltammetric behavior of RuO_2/Fe_3O_4/MWCNT/GCE composite is studied in PBS buffer solution with in a potential range of -0.5 to +0.5 V. The scan rates varied from 20 mV/s to 100 mV/s. Due to the faradaic reactions occurring at the electrode surface CV curves were not in an ideal rectangular shape [38]. It is also noted that the electrode maintained the same shapes as the CV curves with increasing scan rates as shown in Figure-7.6 (A). The electrode showed an irreversible oxidation peak on the individual addition of 1 mM of ascorbic acid and a reversible peak on the addition of 0.5 mM dopamine in PBS buffer at a scan rate of 50 mV/s. The electrode also exhibited response signals for both ascorbic acid (2 mM) and dopamine (1 mM) when these analytes are added simultaneously [39–43]. These all are shown in Figure-7.6 (B). To strenghthen the results obtained from CV curves, Differential pulse voltammograms (DPV) were also recorded for the individual as well as simultaneous determination of both dopamine and ascorbic acid. DPV curves of 200 µM ascorbic acid are shown in Figure-7.7 (A) and for 5 µM dopamine is shown in Figure-7.7 (B). Ascorbic acid exhibited an oxidation peak potential at 0.13 V whereas dopamine showed an oxidation peak at 0.31 V. The oxidation peak separation between dopamine and ascorbic acid is found to be 0.187V which is a good indication of RuO_2/Fe_3O_4/MWCNT composite to determine dopamine and ascorbic acid selectively and simultaneously [44] and is shown in Figure-7.7 (C).The changes in oxidation and reduction peak currents were investigated with varying scan rates ranging from 20 mV/s to 100 mV/s as shown in Figure 7.8 (A). The results provide information on the kinetics of the electrode reaction at RuO_2/Fe_3O_4/MWCNT/GCE composite on the

addition of 0.5 mM ascorbic acid and 0.5 mM dopamine. Dopamine exhibited both oxidation and reduction peaks whereas ascorbic acid exhibited only oxidation peaks. A linear relationship was obtained as peak currents were plotted against the square root of scan rates with R^2 values of 0.98 for both molecules and as shown in Figure-7.8 (B). This indicates a diffusion-controlled process occurring at the electrodes with the addition of analytes.

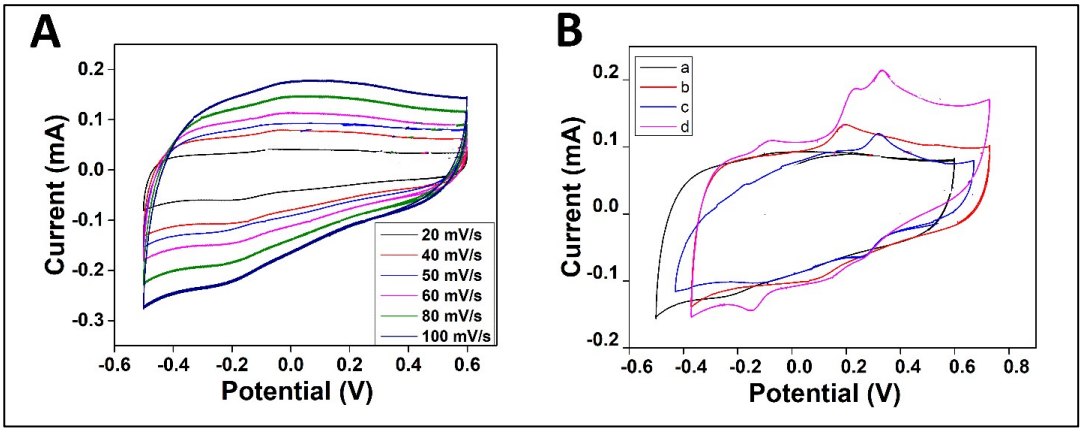

Figure-7.6. (A) CV curves of RuO_2/Fe_3O_4/MWCNT/GCE composite in PBS buffer at varying scan rates ranging from 20 mV/s to 100 mV/s. (B) Behaviour of CV curves of (a) RuO_2/Fe_3O_4/MWCNT/GCE composite (b) RuO_2/Fe_3O_4/MWCNT/GCE composite on the addition of 1 mM ascorbic acid alone (c) RuO_2/Fe_3O_4/MWCNT/GCE composite on the addition of 0.5 mM dopamine alone and (d) RuO_2/Fe_3O_4/MWCNT/GCE composite on the addition of 2 mM ascorbic acid and 1 mM dopamine simultaneously.

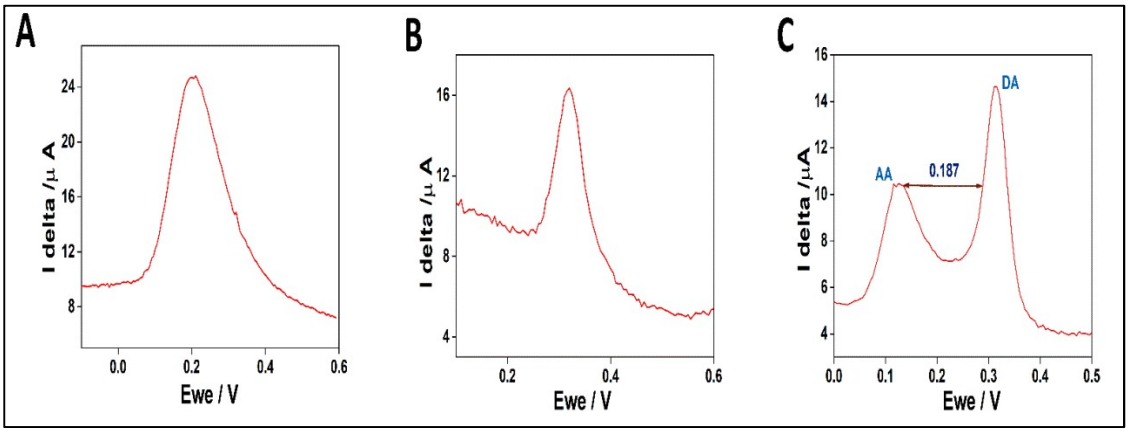

Figure-7.7. DPV curves of RuO_2/Fe_3O_4/MWCNT/GCE composite in 0.1M PBS containing (A) 200 µM ascorbic acid alone (B) 5 µM dopamine alone (C) both 50 µM ascorbic acid and 2 µM dopamine.

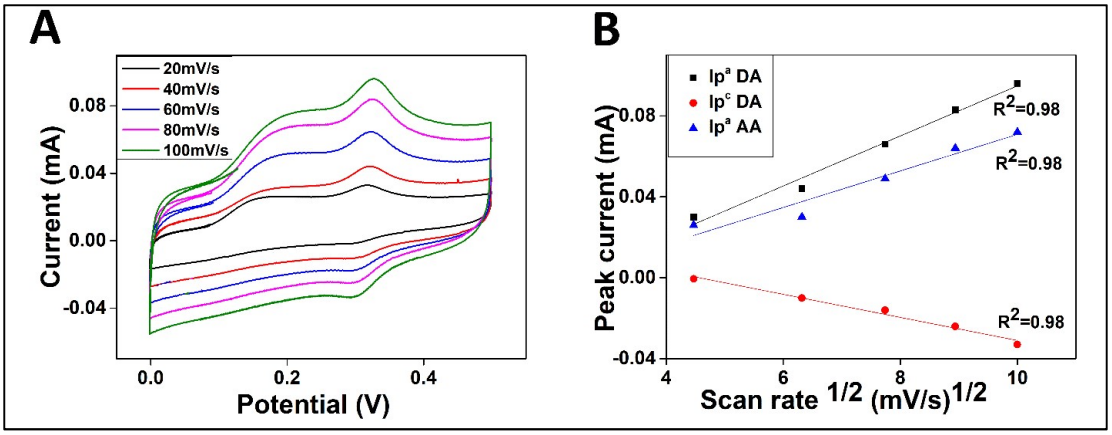

Figure-7.8. CV curves of RuO_2/Fe_3O_4/MWCNT/GCE composite in 0.1M PBS (A) in the presence of 0.5 mM ascorbic acid and 0.5 mM dopamine studied under different scan rates varying from 20 mV/s to 100 mV/s. (B) Calibration plot in which anodic and cathodic peak currents of both analytes dopamine and ascorbic acid are plotted against the square root of scan rate.

7.3.7. Individual and simultaneous determination of dopamine and ascorbic acid

The oxidation response of target analytes is studied using the DPV technique on RuO_2/Fe_3O_4/MWCNT@GCE in phosphate buffer. The modified electrode responded to the addition of ascorbic acid and dopamine. The individual detection of ascorbic acid was studied by varying the concentration of ascorbic acid and fixing the concentration of dopamine to 10 µM. Similarly for dopamine the individual detection was carried out by fixing the concentration of ascorbic acid to 150 µM and varying the concentration of dopamine. The concentration range studied for individual detection of ascorbic acid and dopamine is 50-290 µM and 2-42 µM respectively. The DPV curves are shown in Figure-7.9 (A) and 7.9 (C). With the increase in concentration peak currents of both ascorbic acid and dopamine were found to increase linearly and as shown in Figures- 7.9 (B) and 7.9 (D). The limit of detection of ascorbic acid and dopamine was found to be 1.12 µM and 0.11 µM (S/N=3). Further, DPV curves for simultaneous detection of both analytes were carried out by varying the concentration of ascorbic acid and dopamine simultaneously, in the range of 50-190 µM in the case of ascorbic acid and 2-25 µM for dopamine and is shown in Figure-7.10 [A]. The linear response of peak currents was noticed for both the analytes with their varying concentrations. This is shown in Figure-7.10 (B) and 7.10 (C). The limit of detection was found to be 1.19 µM for ascorbic acid and

0.16 µM for dopamine (S/N=3). Thus the composite was found to be an efficient sensor for the individual and simultaneous detection of ascorbic acid and dopamine [45–51]. Table 7.1 displays the LOD values of different modified sensors in detecting ascorbic acid and dopamine.

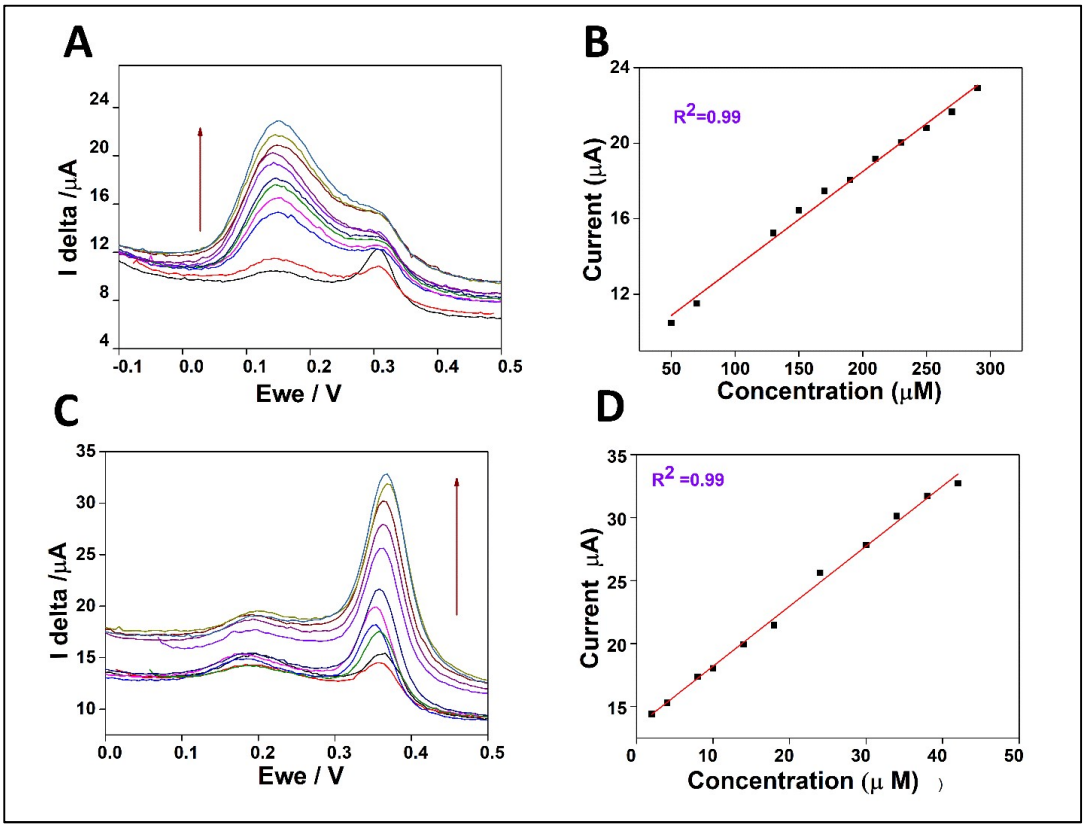

Figure-7.9. (A) DPV curves were obtained on varying the concentration of ascorbic acid from 50-290 µM and fixing the concentration of dopamine to 10 µM. (B) Linear plots of peak current vs concentration of ascorbic acid. (C) DPV curves were obtained on varying the concentration of dopamine from 2-42 µM and fixing the concentration of ascorbic acid to 150 µM. (D) Linear plots of peak current vs concentration for dopamine.

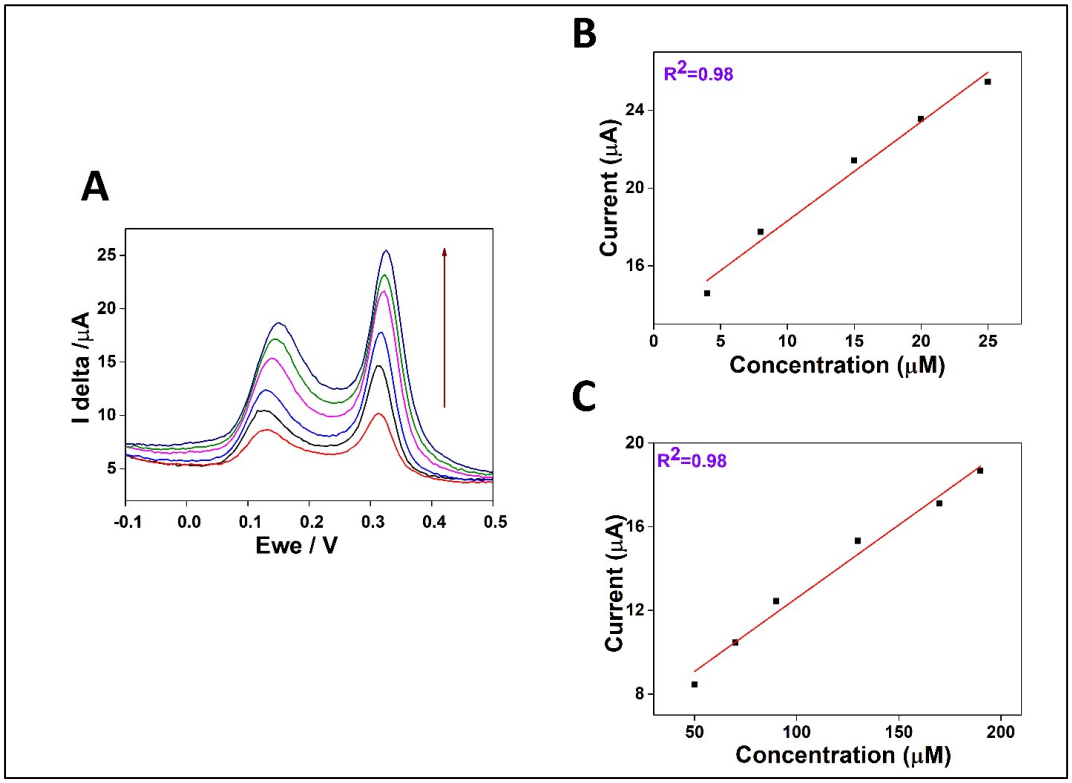

Figure-7.10. (A) DPV curves of ascorbic acid (50-190 μM) and dopamine (2-25 μM) at different concentrations. Calibration plots of oxidation peak current against the concentration of (B) dopamine (C) ascorbic acid.

TABLE- 7.1

A comparison of detection limits of different modified electrodes for sensing dopamine and ascorbic acid.

Electrode Materials	Linear range (μM)		Limit of Detection (μM)		References
	AA	DA	AA	DA	
CPC/ α -ZrP	40-1500	13-520	10	3.3	[41]
Fe_3O_4/rGO/GCE	1-9mM	0.5-100	0.42	0.12	[42]
Carbon nanotube-modified electrodes	0.08-1.36	0.5-10	0.02	0.1	[43]
PDbS–rGO/SPCE	10-1100	0.1-300	0.88	0.134	[44]
CeO2/rGO	50-500	10-150	10	2	[45]
PtNCs-MWCNTs-GNPs/GCE	100-1200	2-50	10	0.5	[46]
N-GA	100-1000	1-100	0.08	0.06	[47]
RuO_2/Fe_3O_4/MWCNT/GCE	50-290	2-42	1.12	0.11	This work

CPC/α -ZrP composite-cetyl pyridinium chloride/α-zirconium phosphate composite

PDbS - (poly (DMAEMA-b-styrene)

SPCE- Screen-printed carbon electrode

N-GA -Nitrogen-doped graphene aerogel

PtNCs-Platinum nano chains

GNPs -Graphene nanoparticles

rGO- reduced graphene oxide

7.3.8. Stability, Reproducibility, and Interference Study

The stability of the modified electrode was evaluated by measuring the current response on the first day and after 30 days of storage. The sensor retained 82% and 92% of the initial current response for ascorbic acid and dopamine (30 μM ascorbic acid and 8 μM dopamine simultaneously) as obtained from the DPV curves shown in Figure-7.11.This indicates the high stability of the modified electrode towards the detection of analytes. The reproducibility of the electrode was investigated by fabricating five similar modified electrodes and checking their current response tothe addition of ascorbic acid and dopamine. Almost all the electrodes exhibited similar behavior on the addition of analyte and the relative standard deviations of the peak currents were found to be 1.33 % and 1.38 % for ascorbic acid and dopamine. The modified electrode was found to be very much selective in the detection of ascorbic acid and dopamine since the electrode didn't exhibit any response to current on the addition of interferents like 2 mM glucose, sucrose, $Zn^{2+,}$ Mg^{2+}, Na^{+}, K^{+}, Cl^{-} etc. This reveals the anti-interference activity of the proposed sensor.

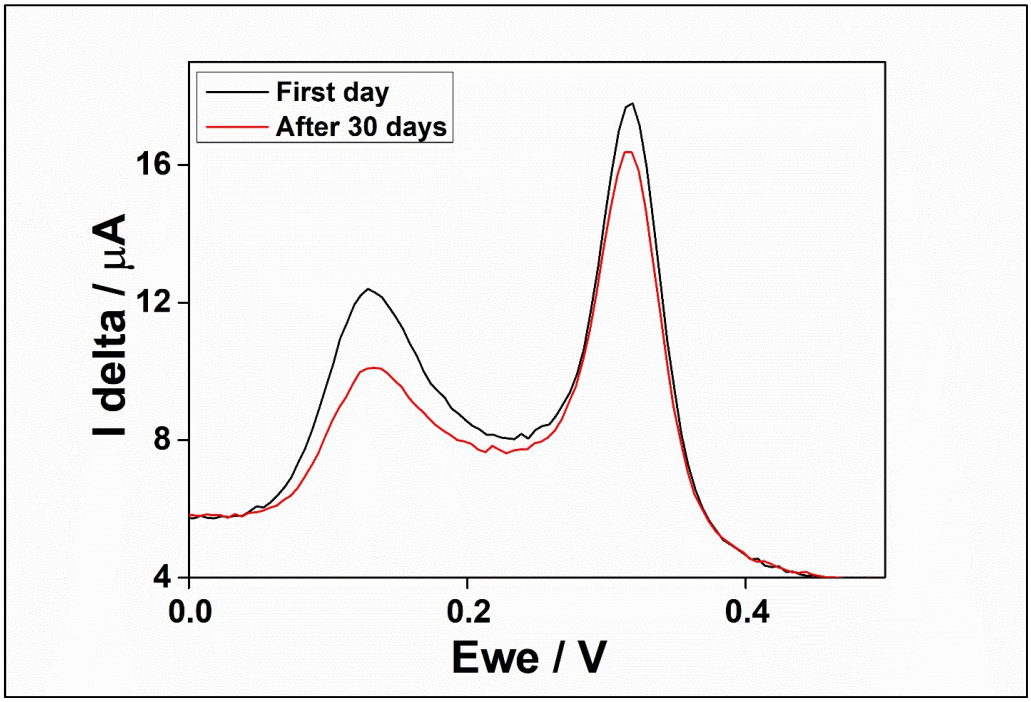

Figure-7.11. DPV curves of the electrode towards sensing analytes ascorbic acid and dopamine on the first day and after thirty days.

7.3.9. Real sample analysis

The real sample analysis was carried out using human blood serum to illustrate the practical applicability of the sensing material for the detection of ascorbic acid and dopamine. The serum samples were diluted with phosphate buffer and were spiked with known quantities of ascorbic acid and dopamine and finally, DPV curves were recorded. The results are listed in Table 7.2. The satisfactory recovery rates suggest that the proposed sensor can be availed for practical applications.

Table 7.2- Determination of Ascorbic acid and Dopamine in Serum samples.

Sample	Analyte	Added (µM)	Found (µM)	Recovery (%)
Serum 1	AA	80	79.43	99.28
	DA	25	24.61	98.44
Serum 2	AA	70	69.34	99
	DA	20	19.94	99.7

7.4. CONCLUSIONS

An electrochemically stable nanocomposite electrode was developed RuO_2/Fe_3O_4/MWCNT/GCE which provided an easy and fast response for the detection of dopamine along with ascorbic acid. The electrode material was fabricated through hydrothermal method. MWCNT provided numerous sites for the incorporation of metal oxides of iron and ruthenium. The fabricated composite material was characterized by various techniques involving UV-visible spectroscopy, XRD, FTIR, EDX, and Raman spectrum. The electrochemical reaction of the composite material was analysed using cyclic voltammetry. The sensing response of the electrode towards the analyte molecules, dopamine and ascorbic acid was very well studied using cyclic voltammetry and differential voltammetric technique. The limit of detection for ascorbic acid and dopamine was found to be 1.12 μM and 0.11 μM respectively. The sensor also gave a satisfactory response on real sample analysis. Thus the fabricated RuO_2/Fe_3O_4/MWCNT/GCE exhibited good sensing behavior towards the detection of ascorbic acid and dopamine.

7.5. REFERENCES

1. Jiang J, Du X. Sensitive electrochemical sensors for simultaneous determination of ascorbic acid, dopamine, and uric acid based on Au@Pd-reduced graphene oxide nanocomposites. Nanoscale . 2014;6:11303–11309.

2. Yang B, Wang H, Du J, Fu Y, Yang P, Du Y. Direct electrodeposition of reduced graphene oxide on carbon fiber electrode for simultaneous determination of ascorbic acid, dopamine and uric acid. Colloids Surfaces A Physicochem Eng Asp . 2014;456:146–52.

3. Aurora RN, Kristo DA, Bista SR, Rowley JA, Zak RS, Casey KR, M P H, Lamm C I, Tracy S L and Roseberg R S. The treatment of restless legs syndrome and periodic limb movement disorder in adults - An update for 2012: Practice parameters with an evidence-based systematic review and meta-analyses. Sleep. 2012;35 (8):1039–62.

4. Chen J, He P, Bai H, He S, Zhang T, Zhang X, et al. Poly (B-cyclodextrin)/carbon quantum dots modified glassy carbon electrode: Preparation, characterization and simultaneous electrochemical determination of dopamine, uric acid and tryptophan. Sensors Actuators, B Chem . 2017;252:9–16.

5. Fernandes DM, Costa M, Pereira C, Bachiller-Baeza B, Rodríguez-Ramos I, Guerrero-Ruiz A, et al. Novel electrochemical sensor based on N-doped carbon nanotubes and Fe3O4 nanoparticles: Simultaneous voltammetric determination of ascorbic acid, dopamine and uric acid. J Colloid Interface Sci.2014;432:207–13.

6. Du J, Tao Y, Zhang J, Xiong Z, Xie A, Luo S. Co_3O_4 -CuNi / reduced graphene composite for non- enzymatic detection of ascorbic acid. Mater Technol . 2019;34:665–73. 7.

7. Carrera V, Sabater E, Vilanova E, Sogorb MA. A simple and rapid HPLC-MS method for the simultaneous determination of epinephrine, norepinephrine, dopamine and 5-hydroxytryptamine: Application to the secretion of bovine chromaffin cell cultures. J Chromatogr B Anal Technol Biomed Life Sci. 2007;847 (2):88–94.

8. Xu X, Zhang H, Shi H, Ma C, Cong B, Kang W. Determination of three major catecholamines in human urine by capillary zone electrophoresis with chemiluminescence detection. Anal Biochem . 2012;427 (1):10–7.

9. Wei Y, Liu Y, Xu Z, Wang S, Chen B, Zhang D and Fang Y. Simultaneous detection of ascorbic acid, dopamine, and uric acid using a novel electrochemical sensor based on palladium nanoparticles/reduced graphene oxide nanocomposite. Int J Anal Chem. 2020;2020.

10. Moradpour H, Beitollahi H. Simultaneous electrochemical sensing of dopamine, ascorbic acid, and uric Acid using nitrogen-doped graphene sheet-modified glassy carbon electrode. J Carbon Res. 2022;8 (4):50.

11. Filik H, Avan AA, Aydar S. Simultaneous detection of ascorbic acid, dopamine, uric acid and tryptophan with Azure A-interlinked multi-walled carbon nanotube/gold nanoparticles composite modified electrode. Arab J Chem . 2016;9:471–80.

12. Samie HA, Arvand M. RuO2 nanowires on electrospun CeO_2-Au nanofibers/functionalized carbon nanotubes/graphite oxide nanocomposite modified screen-printed carbon electrode for simultaneous determination of serotonin, dopamine and ascorbic acid. J Alloys Compd . 2018;782:824.

13. Lee Y, Liao B, Weng Y. Ruthenium oxide modi fi ed nickel electrode for ascorbic acid detection. Chemosphere . 2017;173:512–9. Av

14. Dan Wu, Yuyang Li, Yong Zhang, Panpan Wang, Qin Wei B Du, Key. Sensitive electrochemical sensor for simultaneous determination of dopamine , ascorbic Acid and uric acid enhanced by amino-group functionalized mesoporous Fe_3O_4 @ graphene Sheets. Electrochim Acta . 2014;116:244–9.

15. Bagheri H, , Niyoosha Pajooheshpour , Bardia Jamali , Salimeh Amidi , Ali Hajian and Hosein Khoshsafar. A novel electrochemical platform for sensitive and simultaneous determination of dopamine , uric acid and ascorbic acid based on Fe_3O_4-SnO_2-Gr ternary nanocomposite. Microchem J . 2017;131:120–9.

16. Basavegowda N, Mishra K, Lee YR. Sonochemically synthesized ferromagnetic Fe_3O_4 nanoparticles as a recyclable catalyst for the preparation of pyrrolo(3,4-c)quinoline-1,3-dione derivatives. RSC Adv . 2014;4:61660–6.

17. Kumar GS, Adinarayana S, Chen Y, Chang C, Saeed SY, Mazhar K. Optical and Thermophysical Characterization of Fe_3O_4 nanoparticle Thermophysical Characterization of. Mater Sci Eng. 2020;956.

18. Seifi S, Ezzatzadeh E, Safarkar R. In vitro evaluation of its antimicrobial effect of the synthesized Fe_3O_4 nanoparticles using Persea Americana extract as a green approach on two standard strains. Asian J Green Chem. 2019;3:353–65.

19. Suriyaprabha R, Khan S H, Pathak B, Fulekar M H. Spherical Surfaced Magnetic (Fe_3O_4) Nanoparticles as Nano Adsorbent Material for Treatment of Industrial Dye Effluents. Int J Nanosci Nanotechnol. 2017;13 (2):169–75.

20. Xiao Z, Jiang X, Li B, Liu X, Huang X, Zhang Y, Li B, Ren Q, Luo J, Qin Z and Hu J. Hydrous RuO_2 nanoparticles as an efficient NIR-light induced photothermal agent for ablation of cancer cells in vitro and in vivo. : Nanoscale. 2015;7 :11962.

21. Ananth A, Gandhi M S, Mok Y S. A dielectric barrier discharge (DBD) plasma reactor : An efficient tool to prepare novel RuO_2 nanorods. J Phys D Appl Phys. 2013;46 .

22. Reshma M, Manu R. Fabrication of Cu-WO_3-functionalised multiwalled carbon nanotubes composite film electrode by direct deposition for sensing application. Thin Solid Films . 2021;737:138940.

23. Hosseini MG, Shahryari E. Anchoring RuO_2 nanoparticles on reduced graphene oxide-multi-walled carbon nanotubes as a high-performance supercapacitor. ionic. 2019;25:2383–2391.

24. Gopiraman M, Babu SG, Karvembu R, Kim IS. Nanostructured RuO_2 on MWCNTs : Efficient catalyst for transfer hydrogenation of carbonyl compounds and aerial oxidation of alcohols. Appl Catal A Gen 48484–96. 2014;484:84–96.

25. Guan D, Gao Z, Yang W, Wang J, Yuan Y, Wang B, Zhang M and Liu L. Hydrothermal synthesis of carbon nanotube/cubic Fe_3O_4 nanocomposite for enhanced performance supercapacitor electrode material. Mater Sci Eng B . 2013;178:736–43.

26. Sanjit Saha, Milan Jana, Pranab Samanta, Naresh Chandra Murmu, Nam Hoon Kim, Tapas Kuila and Joong Hee Lee. Hydrothermal synthesis of Fe_3O_4/RGO composites and investigation of electrochemical performances for energy storage applications. RSC Adv View. 2014;4:44777–44785.

27. Noval VE, Universitaria C. Fe_3O_4 -TiO_2 and Fe_3O_4 -SiO_2 Core-shell powders synthesized from industrially processed magnetite (Fe_3O_4) microparticles. Mater Res. 2019;22 (3).

28. Dheyab MA, Aziz AA, Jameel MS. Simple rapid stabilization method through citric acid modification for magnetite nanoparticles. Sci Rep . 2020;10:1–8.

29. Korkmaz S, Kariper İA, Karaman C, Karaman O. MWCNT / Ruthenium hydroxide aerogel supercapacitor production and investigation of electrochemical performances. Sci Rep. 2022;12.

30. Khorshidi A, Sadeghi N. Application of RuO_2 nanoparticles as catalyst in preparation of Indolo(3,2-a)Carbazoles. J Clust Sci. 2016;27:1923–32.

31. R Rahmawati, A Melati, A Taufiq, Sunaryono, M Diantoro, B Yuliarto, S Suyatman, N Nugraha and D Kurniadi. Preparation of MWCNT-Fe_3O_4 nanocomposites from iron sand using sonochemical route. IOP Conf Ser Mater Sci Eng. 2017;012013 (202).

32. Chaki SH, Malek TJ, Chaudhary MD, Tailor JP, Deshpande MP. Magnetite Fe_3O_4 nanoparticles synthesis by wet chemical reduction and their characterization. Adv Nat Sci Nanosci Nanotechnol. 2015;6:0–6.

33. Zhao K, Xu T, Cao J, Yang L, Wei M, Fan H, et al. Fabrication and adsorption properties of multiwall carbon nanotubes - coated / filled by various- Fe_3O_4 nanoparticles. J Mater Sci Mater Electron . 2019;30 (0123456789):18802–10.

34. P C Panta, C P Bergmann. Raman Spectroscopy of Iron Oxide of Nanoparticles (Fe_3O_4). J Mater Sci Eng. 2015;5 (1):4–6.

35. I. S. Zaine, N. A. M. Napiah, A. M. Yusof, A. N. Alias, A M M Ali and S H Khalid. Study on Dispersion and Characterization of Functionalized MWCNTs Prepared by Wet Oxidation. Appl Mech Mater. 2014;661:8-13.

36. Lin Y, Lee K, Chen K, Huang Y. Applied Surface Science Superior capacitive characteristics of RuO_2 nanorods grown on carbon nanotubes. Appl Surf Sci. 2009;256 (43):1042–5.

37. Chakraborty B, Joshi-imre A, Cogan SF.C harge injection characteristics of sputtered ruthenium oxide electrodes for neural stimulation and recording. j Biomed Mater Res B Appl Biomater. 2021;110:229–38.

38. Xiang D, Yin L, Wang C, Zhang L. High electrochemical performance of RuO_2-Fe_2O_3 nanoparticles embedded ordered mesoporous carbon as a supercapacitor electrode material. Energy . 2016;106:103–11.

39. Keerthi M, Boopathy G, Chen S, Chen T, Lou B. A core-shell molybdenum nanoparticles entrapped f - MWCNT s hybrid nanostructured material based non-enzymatic biosensor for electrochemical detection of dopamine neurotransmitter in biological samples. Sci Rep . 2019;9:13075.

40. Fernandes DM, Costa M, Pereira C, Bachiller-baeza B, Rodríguez-ramos I, Guerrero-ruiz A and Cristina Freire. Novel electrochemical sensor based on N-doped carbon nanotubes and Fe_3O_4 nanoparticles : Simultaneous voltammetric determination of ascorbic acid , dopamine and uric acid. Journal Colloid Interface Sci. 2014;432:207–13.

41. Kumar P, Soni I, Jayaprakash G.K and Flores-Moreno R. Studies of monoamine neurotransmitters at nanomolar levels using carbon material electrodes : A Review.

Materials (Basel). 2022;15:5782.

42. S. Ramakrishnana, K. R.Pradeep, A. Raghul, R. Senthilkumara, Murali Rangarajan and Nikhil K Kothurkar. One-step synthesis of Pt-decorated graphene- carbon nanotube for electrochemical sensing of dopamine, uric acid and ascorbic acid. Anal Methods. 2015;7:779–86.

43. Suhua Gao, Hongji Li, Mingji Li , Cuiping Li, Lirong Qian and BaoheYang. A gold-nanoparticle / horizontal-graphene electrode for the simultaneous detection of ascorbic acid , dopamine , uric acid , guanine , and adenine. J Solid State Electrochem. 2018;22:3245–54.

44. Zhao Y, Zhou J, Jia Z, Huo D, Liu Q, Zhong D, Hu Y and Yang Ml. In-situ growth of gold nanoparticles on a 3D-network consisting of a MoS_2 / rGO nanocomposite for simultaneous voltammetric determination of ascorbic acid , dopamine and uric acid. Microchim Acta. 2019;186:1–10.

45. Lin Liu , Yuting Ge , Xinlei Liu , Jianjun Ruan, Jiakai Cao, Chungxiang Wei, Pengjin Fang, Jiadong Zhou, Juanjuan Ma and Zhiwei Tong. One-pot ball-milling preparation of cetylpyridinium chloride/a- zirconium phosphate composite for simultaneous detection of ascorbic acid and dopamine. J Alloys Compd . 2021;860:157927.

46. Teo Peik-See , Alagarsamy Pandikumar, Huang Nay-Ming, Lim Hong-Ngee and Yusran Sulaiman. Simultaneous electrochemical detection of dopamine and ascorbic acid using an Iron oxide/Reduced graphene oxide modified Glassy Carbon Electrode. Sensors. 2014;14:15227–43.

47. Wang Z, Liu J, Liang Q, Luo G. Carbon nanotube-modified electrodes for the simultaneous determination of dopamine and ascorbic acid. Analyst. 2002;127:653–8.

48. Thirumalai D, Lee S, Kwon M, Paik H, Lee J, Chang S. Disposable Voltammetric Sensor Modified with Block Copolymer-Dispersed Graphene for Simultaneous Determination of Dopamine and Ascorbic Acid in Ex Vivo Mouse Brain Tissue. . Biosens. 2021;11:368.

49. Murali A, Lan Y P, Sarswat P K, Free M L. Synthesis of CeO_2 / reduced graphene oxide nanocomposite for electrochemical determination of ascorbic acid and dopamine and for photocatalytic applications. Mater Today Chem . 2019;12:222–32.

50. Huang Z N, Jiao Zou, Teng J, Liu Q, Yuan M M, Jiao FP, Jiang X Y and Yu J G . A novel electrochemical sensor based on self-assembled platinum nanochains - Multi-walled carbon nanotubes-graphene nanoparticles composite for simultaneous determination of dopamine and ascorbic acid. Ecotoxicol Environ Saf . 2019;172:167–75.

51. Beyene A G, Delevich K, Urbanová V. Nitrogen-doped graphene aerogel for simultaneous detection of dopamine and ascorbic acid in artificial cerebrospinal fluid. J Electrochem Soc. 2020;167:116521.

CHAPTER 8

SUMMARY AND CONCLUSIONS

8.1. SUMMARY OF THE PRESENT WORK

In the present work, functionalized MWCNT was anchored with various types of metal oxides and composites to form different types of modified electrodes, that can be applied for sensing and detection of various types of biomolecules and other materials. Functionalisation of MWCNTs has enabled carbon nanotubes and their hybrid composites to establish their uniqueness in various comprehensive areas. In the present work different facile, low cost and feasible techniques have been adopted to fabricate film as well as solid type composite based on MWCNTs. The developed electrode has gone through different analytical procedures and instrumental methods to know the efficacy under different operating conditions. Techniques such as electroless deposition, electro-deposition, dip coating, drop casting, hydrothermal method etc. have been used for the fabrication of these electrodes. Hybrid materials incorporating MWCNTs together with various metals and metal oxides have been synthesized. The following text makes a bee line approach of the major conclusions arrived from the present work.

8.2. MAJOR CONCLUSIONS

8.2.1. Major conclusions from the present work can be summarized as follows.

- Flexible Ag/fMWCNT electrodes were fabricated using benign reducing agent and the composite film developed are used as a sensor for sensing the analyte dopamine. The scope of the work lies in the fact that fabricated films possessed good pseudocapacitive behaviour as revealed from the electrochemical studies. The flexible electrodes of Ag/fMWCNT were used for sensing dopamine using chrono-amperometry and differential pulse voltammetry techniques. The limit of detection for dopamine was found to be 0.7 μM. The sensor also possessed good reproducibility and excellent stability.
- Flexible Cu-WO_3-MWCNT film was developed as a sensor for studying the ageing of lubricant oils. The fabricated film was used for the qualitative sensing of lubricant oils subjected to various heat treatment processes. The metal oxide-based MWCNT hybrid films was successfully employed for sensing various other components formed during the ageing process of

lubricant oils as revealed from electrochemical impedance studies. The fabricated electrode also possessed good energy storage characteristics.

- One other part of work deals with the importance of recovering valuable metals from spent lithium-ion batteries. In this work, Co_3O_4 used for the development of Pd@MWCNT-Co_3O_4 electrode was recovered from spent lithium-ion batteries through acid leaching process. The recovered cobalt was deposited onto the copper substrate by chronoamperometric technique. The developed Pd@MWCNT-Co_3O_4 electrode was used for glucose sensing applications. The results of the analysis revealed that Pd@MWCNT-Co_3O_4 electrodes exhibited superior sensing behaviour towards glucose over a wide range of concentrations and the limit of detection was found to be 0.6 μM.
- The last part of the work envisages the fabrication of ternary composites formed by RuO_2, Fe_3O_4 and MWCNT. The electrode was applied as an electrochemical sensor for rapid and simultaneous detection of both dopamine and ascorbic acid. The electrochemically stable nanocomposite RuO_2/Fe_3O_4/MWCNT/GCE gave a limit of detection of 1.12 μM and 0.11 μM for individual detection of ascorbic acid and dopamine. Simultaneous detection of ascorbic acid and dopamine also provided valid results.
- The crux of the present work emphasizes on development of efficient MWCNT-based nanocomposites for wide range of applications. Each MWCNT-based electrode precisely focused on electrochemical sensing of various analytes including dopamine, ascorbic acid and glucose. Facile and economic procedures were adopted for fabrication of such MWCNT composites. The developed nanocomposite electrodes served as superior sensors as revealed from the preciseness and LOD towards various analytes.

CHAPTER 9

RECOMMENDATIONS

9.1. FUTURE SCOPE OF THE WORK

Multifarious applications of fMWCNT based composite electrodes as sensors and other benevolent materials embedding various metals and metal oxides have been established in the present work. MWCNTs serve as an excellent scaffolding material for the incorporation of metals and metal oxides and such modified composites can be used for specified applications. The thesis focuses on fabrication of different MWCNT composites through various facile approaches which finds use in different electrochemical sensing platforms. The fabrication procedures adopted for the preparation of MWCNT-based electrode materials are simple and not laborious that can provide a new outlook for the development of more efficient materials.

The scope of the work lies in the modification of contemporary used methods and improving the efficiency of the process and applications of the materials used .Certain type of self-assembled monolayers can be created on the electroless copper substrates mentioned in the above work and the sensing behaviour of such fabricated films towards various analyte molecules can be considered.

As mentioned in Chapter 6, the metals and metal oxides are recovered from spent Li ion batteries are embedded to form MWCNT composite film. Rather than metals and metal oxides, non enzymatic electrochemical sensing studies could be conducted using suitable polymer materials. Moreover, the extraction techniques adopted for recovering the valuable metals can be further improved through suitable process modification for extraction.

Apart from sensor applications, these fabricated MWCNT hybrid electrodes can be strived for supplementary applications like supercapacitors, catalytic application and electronic applications.

9.2. LIST OF PUBLICATIONS AND PRESENTATIONS

LIST OF PUBLICATIONS

1. **Reshma.M**, R. Manu. Flexible Ag/fMWCNT Electrode Fabricated Through Benign Reducing Agent for Sensor Application. Journal of The Electrochemical Society, 166 (16) D1-D7 (2019). DOI: 10.1149/2.0381916jes
2. **M.Reshma**, R. Manu. Fabrication of Cu-WO_3-functionalised multiwalled carbon nanotubes composite film electrode by direct deposition for sensing application. Thin Solid Films 737 (2021) 138940 https://doi.org/10.1016/j.tsf.2021.138940
3. **M.Reshma**, R. Manu. Development of Pd@MWCNT-Co_3O_4 Electrode Sensors Using Cobalt Recovered from Spent Lithium Ion Batteries. Journal of the Electrochemical Society, 2023 170 077507 DOI: 10.1149/1945-7111/ace5e6
4. **M.Reshma**, R.Manu. Ternary Composite Electrode based on RuO_2/Fe_3O_4/MWCNT for simultaneous detection of Dopamine and Ascorbic acid. (Manuscript under communication)

LIST OF PRESENTATIONS

1. **Reshma.M**, R. Manu, Flexible Ag/fMWCNTFilm for sensing applications. International Conference on Advanced Materials (SCICON'19), 15-17 December2019, Amrita School of Engineering, Coimbatore.
2. **Reshma.M**, R. Manu, Development of self assembled monolayer on copper film for corrosion inhibition and protein immobilization. International Conference on Materials for Millenium (MATCON 2021), 15-19 March 2021, Cochin University of Science and Technology.
3. **Reshma.M**, R. Manu, Cu-WO_3-fMWCNT composite film electrodeas sensor for studying ageing of lubricant oils. World Sensor Congress (WSC-2022), 8-10March 2022, Centre for Materials for Electronics Technology, Thrissur.
4. **Reshma.M**, R. Manu, Development of high efficient bio-sensors; recovered from spent battery materials. Twenty Second National Convention of Electrochemists (NCE-22), 26-27 August 2022, PSG College of Arts and Science, Coimbatore.